Smart Grid Adaptive Volt-VAR Optimization in Distribution Networks

by

Moein Manbachi

M. Sc., Azad University, South Tehran Branch, 2009
B.Sc., Power and Water University of Technology, 2007

Thesis Submitted in Partial Fulfillment of the
Requirements for the Degree of
Doctor of Philosophy

in the
School of Mechatronic Systems Engineering
Faculty of Applied Sciences

SIMON FRASER UNIVERSITY

Fall 2015

Approval

Name:	**Moein Manbachi**
Degree:	**Doctor of Philosophy**
Title:	***Smart Grid Adaptive Volt-VAR Optimization in Distribution Networks***
Examining Committee:	**Chair:** Behraad Bahreyni Associate Professor

Siamak Arzanpour
Senior Supervisor
Associate Professor _____

Gary Wang
Supervisor
Professor _____

Jiacheng Wang
Supervisor
Assistant Professor _____

Kevin Oldknow
Internal Examiner
Lecturer & Faculty Teaching Fellow
School of Mechatronic Systems
Engineering _____

Hamidreza Zareipour
External Examiner
Professor
Department of Electrical & Computer
Engineering
University of Calgary _____

Date Defended/Approved: December 01, 2015

Abstract

The electrical distribution networks across the world are witnessing a steady infusion of smart grid technologies into every aspect of their infrastructure and operations. Technologies such as Energy Management Systems (EMS), Distribution Management Systems (DMS) and Advanced Metering Infrastructure (AMI) have partially addressed the needs of the distribution networks for automation, control, monitoring and optimization. Many utilities intend to explore the capabilities of advanced AMI systems for other functionalities within their grids. AMI systems produce an extensive amount of data that can be collected from termination points, for various optimization, control and energy conservation functions. Moreover, deployment of smart grid assets and smart system utilizations provide unprecedented opportunities for network operators and planners to adopt more efficient and reliable strategies for the technical/economic issues of their grids. Accordingly, new smart grid adaptive optimization and control techniques can be constituent components of future distribution grids.

The present thesis aims to propose a novel smart grid adaptive solution for one of the well-known techniques typically employed for distribution network voltage and reactive power optimization called Volt-VAR Optimization (VVO). Proposed VVO engine enables capturing AMI data to solve the VVO problem through its comprehensive objective function in quasi real-time intervals. Furthermore, this thesis investigates the impacts of disparate smart grid components such as Distributed Generation (DGs), Electric Vehicles (EVs) and Distributed Energy Resources (DERs) on proposed smart grid adaptive VVO. Solving maintenance scheduling problem of Volt-VAR Control Components (VVCCs), proposing a new solution for VVCC number of switching per day issue, offering a quasi-real-time load modeling approach to enhance the accuracy of energy conservation calculations, presenting a predictive VVO solution and considering Conservation Voltage Reduction (CVR) as a part of VVO objective to save the energy consumption of loads are some of the novel VVO studies presented in this thesis. This thesis examines proposed VVO performance and applicability through a real-time co-simulation platform using advanced communication protocols/standards such as DNP3 and IEC 61850. The results of thesis studies prove that applying proposed VVO engine could considerably enhance smart distribution system levels of accuracy, efficiency and reliability.

Keywords: Advanced Metering Infrastructure; Conservation Voltage Reduction; Co-Simulation; Distribution Network; Smart Grid; Volt-VAR Optimization

This Dissertation is lovingly dedicated to my parents and my sister whose passion, support and encouragement have inspired me to pursue and accomplish this research

Acknowledgements

Foremost, I would like to express my sincerest appreciation to my supervisor Dr. Hassan Farhangi for his perpetual support, wisdom and leadership who generously shares his immense knowledge with no hesitation during different times of the research. He continually and convincingly conveyed the spirit and the beauty of novelties that could be achieved in regard to this research.

Moreover, I would like to express my deepest gratitude to my supervisor Dr. Ali Palizban whose experience, vast knowledge and professional skills inspired me to understand the value of a practical research. I am sincerely thankful for his ongoing guidance, generous support, and for all technical discussions we had together.

Above all, I must express my warmest gratefulness to my senior supervisor Dr. Siamak Arzanpour for his exceptional supervision and encouragement. His invaluable advices and supports helped me as a PhD candidate and my research very much. It has been a pleasure having had the chance to study as a student of him.

I need to mention that without guidance and persistence advices of my supervisors, Dr. Hassan Farhangi, Dr. Ali Palizban and Dr. Siamak Arzanpour, this dissertation would not have been accomplished.

I would like to extend my sincere gratitude to Dr. Gary Wang and Dr. Jiacheng Wang for their great helps and advices in regards to this work.

I would like to gratefully acknowledge that this work was funded in part by Natural Sciences and Engineering Research Council of Canada (NSERC) Microgrid Network (NSMG-Net).

Last but not least, I am very thankful to Prof. Antonello Monti and Prof. Ferdinanda Ponci, for their technical supports and kind guidance. They superbly led a crucial part of this thesis during my research period at Automation for Complex Power Systems Laboratory, E.ON Energy Research Center, RWTH Aachen University, Germany.

Table of Contents

List of Tables

List of Figures

List of Acronyms

ACSI	Abstract Communication Service Interface
ADN	Active Distribution Network
AFE	Analogue Front End
AMI	Advanced Metering Infrastructure
ANN	Artificial Neural Network
ANSI	American National Standards Institute
BCBV	Branch Current to Bus Voltage
BCIT	British Columbia Institute of Technology
BES	Battery Energy Storage
BFS	Backward-Forward Sweep
BIBC	Bus Injection to Branch Current
BMS	Battery Management System
BPA	Bonneville Power Administration
BR	Breaker
BW	Bandwidth
CB	Capacitor Bank
CES	Community Energy Storage
CHP	Combined Heat and Power
CSA	Canadian Standard Association
CVR	Conservation Voltage Reduction
DA	Distribution Automation
DCC	Distributed Command and Control
DER	Distributed Energy Resources
DG	Distributed Generation
DISCO	Distribution Company
DMS	Distribution Management System
DNP	Distributed Network Protocol
DR	Demand Response
DS	Disconnector
DSO	Distribution System Operator
EMS	Energy Management System

EPRI	Electric Power Research Institute
EV	Electric Vehicle
FESS	Flywheel Energy Storage System
G2V	Grid to Vehicle
GA	Genetic Algorithm
GIS	Geographic Information System
GOOSE	Generic Object Oriented Substation Event
GTAO	Gigabit Transceiver Analogue Output
GTIO	Gigabit Transceiver Input Output
GTNET	Gigabit Transceiver Network
HAN	Home Area Network
HV	High Voltage
IA	Intelligent Agent
ICT	Information and Communication Technology
IEC	International Electro-technical Commission
IED	Intelligent Electronic Device
IEEE	Institute of Electrical and Electronics Engineers
IPR	In-line Power Regulator
IRR	Internal Rate of Return
JADE	Java Agent Development Framework
KCL	Kirchhoff's Current Law
KVL	Kirchhoff's Voltage Law
LAN	Local Area Network
LDC	Line Drop Compensator
LN	Logical Node
LTC	Line Tap Changer
LV	Low Voltage
MAPE	Mean Absolute Percentage Error
MAS	Multi Agent System
MCU	Master Control Unit
MDMS	Measuring Data Management System
MIP	Mixed Integer Programming
MINLP	Mixed Integer Non-Linear Programming

MINP	Mixed Integer Non-linear Programming
MLP	Multi-Layer Perceptron
MMS	Manufacturing Message Specification
MP	Master Problem
MSE	Maintenance Scheduling Engine
MU	Merging Unit
MV	Medium Voltage
NAN	Neighbor Area Network
NB-PLC	Narrow-Band Power Line Communication
NEEA	Northwest Energy Efficiency Alliance
NI	National Instrument
NLP	Non-Linear Programming
NN	Neural Network
O&M	Operation and Maintenance
OLTC	On-load Tap Changer
OPC	Open Platform Communication
PC	Personal Computer
PCC	Point of Common Connection (Coupling)
PEV	Plug-in Electric Vehicle
PF	Power Factor
PHEV	Plug-in Hybrid Electric Vehicle
PNNL	Pacific Northwest National Laboratory
PoC	Point of Connection
PSO	Particle Swarm Optimization
PV	Photovoltaic
QoS	Quality of Service
RMS	Root Mean Square
RP	Regulating Point
RT	Real Time
RTD	Round Trip Delay
RTDS	Real Time Digital Simulator
RTO	Real Time Operating
SA	Substation Automation

SCADA	Supervisory Control and Data Acquisition
SCL	Substation Configuration Language
SCUC	Security Constrained Unit Commitment
SIED	Switch IED
SLD	Single Line Diagram
SM	Smart Meter
SP	Sub-Problem
SV	Sampled Value
TCP/IP	Transmission Control Protocol/Internet Protocol
TD	Time Delay
V2G	Vehicle to Grid
VR	Voltage Regulator
VRLTC	Vacuum reactive LTC
VVC	Volt-VAR Control
VVCC	Volt-VAR Control Component
VVMS	Volt-VAR Management System
VVO	Volt-VAR Optimization
VVOE	Volt-VAR Optimization Engine
WAN	Wide Area Network
WANem	Wide Area Network emulator
WLAN	Wireless LAN
ZIP	Constant Impedance, Current and Power

Chapter 1.

Introduction

1.1. Preface

Maintaining voltage within desired level throughout the electric distribution network is one of the major challenges that electric power utilities have always grappled with. As customer electricity demand varies throughout the day, each customer forms a specific load profile. Hence, the power supplied by distribution network throughout a day has to vary to meet customer load profiles in general. This is one of the operating issues at the heart of modern grids that is not desirable for the system operators due to its higher expenditure and hard operational condition. The electric power utilities prefer to avoid the change in the supply through controlling the demand. In other words, they prefer a "generator-following approach", rather than a "load-following" approach. Thus, new strategies are emerging in order to control system demands and to optimize distribution grids. Typically, there are three main components employed inside distribution substation and/or along distribution feeder(s) to perform voltage regulation: On-Load Tap Changer of transformer (OLTC), Voltage Regulator (VR), and Capacitor Bank (CB). OLTCs and VRs are a type of transformer with variable turns ratios that are optimally placed in distribution networks to regulate voltage level of downstream nodes. CBs can control voltage by compensating reactive power of the grid as well. Generally, CBs are connected to the network with parallel configuration using specific switches. Closing these switches enables switchable shunt capacitors to compensate reactive power of the system to improve voltage drop at the Point of Connection (PoC).

The other important issue in distribution networks is “power loss”. There are different sources of losses in distribution system. As long as there is a feeder in a grid, line loss exists. Line loss imposes costs into the system by occupying the capacity of

transferring active power from supplier to consumer throughout the line. Applying reactive power control components such as CBs can assist network operators to control reactive power flow of the system which can lead to distribution network loss reduction. Theoretically, voltage and reactive power are related to each other. When reactive power flows over an inductive line, that line will face with a voltage drop.

For decades, the abovementioned components were the main tools for utilities to regulate voltage and reduce system loss. Most distribution networks employed these components which operated separately for voltage regulation and loss reduction aims. Further, by developments in optimization techniques, distribution utilities realized the fact that the efficiency of the system could be improved if voltage regulation and reactive power control are seen as an integrated optimization problem that can be called “Volt-VAR Optimization”, a.k.a. the “VVO”. Initial VVO techniques employed to statically minimize distribution network losses and to improve voltage profile of the system through semi-coordinated methods using static data. In brief, these VVO strategies present an integrated process of controlling voltage levels and reactive power (VAR) throughout distribution networks that could lead to system optimization in mid/long-term operating periods, e.g. monthly, seasonally and/or annually.

In order to respond to consumer’s demand within specific time-intervals, advanced VVO techniques emerged to track load changes. Other important needs of electric power utilities such as the energy consumption reduction and peak demand reduction emerged new conservation methods called “Conservation Voltage Regulation” or “Conservation Voltage Reduction (CVR)”. Generally speaking, CVR attempts to maintain customer’s voltage level in the lower limits of ANSI [1] or CSA [2] standard range, in order to achieve energy conservation without requiring changes in customer’s behavior. This could reduce the energy consumption and peak demand of the distribution network. In other words, CVR attempts to conserve energy by lowering voltage levels of termination points.

In recent decades, advancements in communication infrastructure, Information Technology (IT), optimization techniques and control technologies have made VVO techniques such as Volt-VAR Control systems (VVC) and Volt-VAR Management Systems (VVMS) more efficient. The main goals of these systems are to control and optimize

voltages and reactive power of distribution network in a coordinated way conforming to pre-determined aggregated feeder load profiles using Volt-VAR Control Components (VVCC), i.e. OLTCs, VRs and CBs inside distribution substations and/or along distribution feeder(s). Thus, VVO became a reliable tool to co-ordinately adjust voltage and reactive power levels of distribution network to address system needs.

In the last two decades, the mass electrification in most developed as well as developing countries has exposed the already frail distribution system to a wide variety of unpredictable load profiles with potentially negative and even unsafe levels of impact on the Quality of Service (QoS) delivered to customers. To counter such impacts, electric power utilities strive to employ new technologies to not only guarantee a certain level of QoS to their customers, but also save energy, reduce distribution losses and operational costs more. In order to reach the abovementioned aims, dynamic decisions have to be adopted according to real-time operation of distribution networks. Hence, the “automation” concept, design and implementation became essential for utilities. The emergence of smart grid has brought considerable opportunities for the automation of power distribution systems. Moreover, smart grid provided the electric utility companies with more visibility and pervasive control over their assets and services [3]. As explained, the driving factors behind utility companies’ investments in technologies such as: Distribution Automation (DA), Distributed Management System (DMS), Energy Management System (EMS), Substation Automation (SA) and Advanced Metering Infrastructure (AMI) were to make distribution networks more reliable, cost effective and efficient. In addition, applying smart grid technologies provide electric power utilities with multiple intelligence layers over their current and future assets [4].

DA provides distribution networks with flexible control that enhances reliability, efficiency and QoS. Moreover, it improves system visibility, asset management, fault detection and correction. On the other hand, controlling system voltage through advanced DA systems has made CVR more reliable. DMS designed to represent live view of the system close to real-time to the network operators. In brief, DMS comprises of various applications that are employed to monitor and control distribution network parameters in a reliable, efficient and secure platform. Nowadays, Volt-VAR Optimization or Volt-VAR Control is categorized as a part of DA and/or DMS.

AMI systems as another famed smart grid technology are able to capitalize on a two-way communication system between Smart Meters (SM) and control center to modify customers' service-level parameters. As AMI boosts the efficiency of utilities billing and revenue management systems [4], many utilities intend to explore the capabilities of advanced AMI systems for other functionalities within their grids. Smart meter installation programs at customers' premises produce an extensive amount of consumer data that can be collected from termination points, (typically every 15 minutes) for various optimization, control and energy conservation functions. Accordingly, new AMI-based optimization and control techniques can be essential components of future smart distribution grids. In order to extend DA benefits in future, AMI end-of-line sensors, a.k.a. smart meters are needed [5]. Hence, integrating DA with AMI seems essential for future grids. On the other hand, AMI provides a convenient environment to collect time-of-use rates, data and load-demand management that can be used in different applications such as energy conservation, reduction of nontechnical losses, outage management and unprecedented visibility to the edge of the network [6].

With the advent of AMI, a dynamic approach enables such systems to capture and control data close to real-time. This could lead to a more accurate VVO by bringing a real-time dynamic Volt-VAR Optimization from substation downstream to the edge of the feeders. Hence, it is more conceivable to upgrade the conventional static VVO and CVR systems into real-time, adaptive and dynamic VVO solutions via smart grid capabilities. The availability of smart metering technologies and their capabilities in transmitting real-time data of customers enables VVO Engines (VVOE) operate in real-time or quasi real-time. Therefore, one of the main targets of this work is to propose a novel smart grid-based Volt-VAR Optimization engine using quasi real-time AMI data.

Furthermore, the availability of dispatch-able energy sources in smart grid networks such as Electric Vehicles (EVs), Vehicle to Grid (V2G) systems, Community Energy Storage (CES) systems, smart inverter technologies and sustainable/renewable resources can make smart grid-based VVO more affordable and practical. In recent years, penetration of Distributed Energy Resources (DER) at customer's sides has changed the structure, operation and performance of smart distribution networks. DERs such as Distributed Generations (DG), Micro-Combined Heat and Power units (Micro-CHP) or

Photovoltaics (PV) have been employed for different operational needs in distribution grids. Hence, diversity in type and technology, as well as penetration of DERs could have considerable impacts on distribution network optimization and control. On the contrary, dynamic VVO approaches could speed up widespread deployment of DERs, DGs and other microgrid sources [7]. As such, this thesis aims to evaluate the impact of these technologies on proposed smart grid AMI-based VVO solution. Moreover, it tries to investigate if studied smart microgrid sources can assist VVO on performing its objectives or not as employing smart grid sources on performing VVO could lead to a more effective VVO solution.

On the other hand, as the roots of power system issues are typically found in the distribution system, the point of departure for grid overhaul is firmly placed at the bottom of the chain [4]. Additionally, it is clear that all voltage and reactive power control assets in distribution network have to go to maintenance after a specific number of operational cycles to preserve lifetime and quality of service. As advanced metering infrastructure-based Volt-VAR Optimization performs in quasi real-time, it is now important for network planners and/or operators to calculate the net benefit of the system for each quasi real-time operating stage. Moreover, the availabilities of Volt-VAR control components to perform AMI-based Volt-VAR Optimization have recently become very important as well. Hence, it is now vital for network planners and/or operators to know the benefit resulted from loss minimization and energy conservation of loads by AMI-based Volt-VAR Optimization in quasi real-time. At the same time, conventional maintenance scheduling techniques can have negative impact on the performance of new AMI-based Volt-VAR Optimization solutions as they have not considered VVO benefits in their objective function. Therefore, the necessity of new approaches for maintenance scheduling of voltage and reactive power control assets according to new AMI-based VVO features is felt more than before. The maintenance scheduling of voltage and reactive power control assets has to impose minimum negative impact on the quasi real-time Volt-VAR Optimization efficiency. Hence, if a Volt-VAR control component goes to maintenance for a short period, the value of lost benefit (because of the absence of that component) has to be minimized within that period. This thesis provides an efficient solution (that is employed in proposed VVO) to solve the maintenance scheduling issue of AMI-based VVO solutions.

Another important challenge is the fact that some of the main VVCCs such as switchable shunt CBs, VRs and OLTCs cannot be switched on and off more than pre-specified limits per day according to their lifetime. As real-time or quasi-real time VVO is capable of optimizing the network in its real/quasi-real time intervals, the number of VVCC switching per day could exceed the pre-determined limits. This may reduce the lifetime of Volt-VAR control assets which will not lead to a cost-effective VVO solution. In order to consider the abovementioned key factors, a predictive technique is designed that is able to predict distribution network day-ahead and/or time interval-ahead loads to optimize the network based on historical data of smart meters. Presenting such a method could solve the number of switching per day issue and perform an efficient VVO in advance.

As discussed, with the expansion of AMI infrastructure throughout distribution networks, this thesis proposes an advanced smart grid-based solution for VVO, using AMI quasi real-time data. Accurate, secure and reliable data, communication, system operation and their flows are the key factors of a successful VVO solution. Utilizing real-time approaches necessitates adequate real-time monitoring, operational and control platforms for further implementation. Thus, providing efficient co-simulation environment benefits electric power utilities and allow them to test the performance and study the impacts of such approaches before implementation. As such, this research presents real-time co-simulation platforms for proposed VVO engine in accordance with smart grid communication protocols/standards such as DNP3 and IEC 61850.

In brief, this thesis proposes a novel smart grid adaptive VVO engine using quasi real-time AMI data for smart distribution networks. Moreover, it investigates the impacts of different types of smart microgrid sources on proposed VVO. As a paradigm shift in transitioning from a centralized grid to a decentralized grid applying smart grid technologies [8] has been started, a feeder-based approach is chosen due to the fact that the decentralized approaches are well-matched with Distributed Command and Control (DCC) topology of smart microgrids. In a key part of this research, CVR considers as a part of the VVO objective. In addition, a new maintenance scheduling approach is presented for AMI-based VVO solution. To test the accuracy, the applicability and the performance of proposed VVO, real-time monitoring and control co-simulation platform is

designed and employed. The performance of proposed VVO is checked in the presence of various load conditions, microgrid sources and network reconfiguration condition.

Hence, the main advantages of proposed solution include but not limited to coordinated control between conventional VVCCs and new Volt-VAR control assets such as V2Gs, using quasi real-time AMI data that increases system visibility and efficiency, considering impacts of various microgrid sources in proposed VVO, providing a solution for maintenance scheduling of Volt-VAR control assets in the system, designing a day-ahead as well as time interval-ahead predictive VVO engine according to AMI historical data, solving number of VVCC's switching per day issue and providing a real-time co-simulation platform for testing the effectiveness of proposed approach.

1.2. Main Contribution and Novel Studies

As explained, the key contribution of this work is proposing a Volt-VAR Optimization engine using quasi real-time AMI data. Other important novel studies regarding proposed smart grid adaptive Volt-VAR Optimization engine are:

- VVO includes CVR based on quasi real-time AMI data
- An integrated VVO algorithm adaptable to distributed command & control architecture of smart microgrids
- Control strategies for VVO devices such as: OLTCs, VRs, and CBs inside distribution substation and along distribution feeder in quasi real-time
- The impact of various types of microgrid sources in VVO based on smart grid specifications
- The impact of load conditions on VVO design
- The impact of EVs with different charging and penetration levels on VVO
- Maintenance scheduling of Volt-VAR control devices and their impacts on proposed VVO
- Real-time/ semi real-time predictive algorithm based on load growth, historical and seasonal factors
- The impact of new VAR sources on proposed VVO
- Real-time co-simulation platform for proposed smart grid-based VVO
- Distribution network planning in the presence of smart grid adaptive VVO

The proposed approach intends to enable distribution utilities to operate/maintain systems with selective VVO in different operating scenarios such as increased renewable sources located at distribution feeders, new real-time switching schemes, system asset management, and electric vehicle charging infrastructure deployment.

1.3. Research Objectives

The main objective of this research is to design a novel Volt-VAR Optimization algorithm that enables distribution network to minimize power loss, optimize voltage profile and conserve energy in quasi real-time. The main deliverables are as follows:

- VVO algorithm or core engine: the system has to receive data from control system and optimize the grid based on the actual load profile (rather than static load profile) in quasi real-time.
- VVO System (core engine working with VVO assets): the algorithm should be integrated in terms of the core engine, VVO asset operation and other smart grid-based technologies located inside distribution substation and/or along distribution feeder(s).
- VVO System Integrated with Distributed Energy Resources (DER): various distributed generation and renewable resources are employed in VVO algorithm. DER unit impacts on VVO are discussed and the capability of each DER unit in VVO participation is studied. Moreover, with a new inverter technology, some of DER units are able to support reactive power.

The above objectives would have the following salient features:

- Coordinated control: the VVO engine can be operated in a coordinated control where all VVO assets such as CBs, OLTCs, VRs and DGs are participating in VVO without task confliction. Thus, priority levels of VVO control devices should be determined.
- VAR injection point allocation: the proposed VVO will be capable of finding the optimal size of VAR injection/absorption components. Finding the best location of switchable shunt CBs, and other predicted/unpredicted VAR injection/absorption points in the grid could help distribution network operators to avoid extra costs imposed by wrong or not well-optimized placements. This fact will be discussed in distribution network planning chapter of this research.
- Predictive algorithm: the study built a predictive VVO algorithm with various proportions of historical data vis-à-vis forward-looking prediction sliding window. This can be a novel approach that facilitates the operation of distribution network. The design is based on several key factors such as: load growth,

historical, seasonal and calendar factors. Designing a predicative algorithm may decrease VVO operating time which totally improves VVO performance.

- Studying EV effect on VVO: as electric vehicle deployment is one of the major concerns of distribution network operators, EV impact on proposed VVO is assessed. In addition, the capability of V2Gs on injecting reactive power to the grid is studied.
- Maintenance scheduling sub-problem: as each VVCCs and generating sources in distribution network has individual maintenance schedule, it is necessary to set the best maintenance time for each without having any operating issue. Thus, the research considers the maintenance scheduling issue as a sub-problem in VVO algorithm in order to find the best configuration of system at each operating time interval.
- Real-time co-simulation platform: To check the whole VVO system, this study presents a real-time co-simulation platform using smart grid features and standards such as IEC 61850.

1.4. Thesis Structure

This thesis is organized into the following fifteen chapters:

- Chapter 2 presents a comprehensive literature survey regarding Volt-VAR Optimization. It reviews Volt-VAR Optimization and Conservation Voltage Reduction histories, as well as modeling and optimization, smart grid functionalities, main projects of Canadian utilities, maintenance scheduling of Volt-VAR control components, predictive VVO, VVO with AMI, co-simulation platform, CVR integration with VVO previous studies
- Chapter 3 explains VVO main topology. First, it presents distribution network topology. Then, it describes Centralized and Decentralized VVO approaches. It investigates VVO data collection, communication needs, main features and topology considerations of proposed VVO.
- Chapter 4 reviews VVO main tool features. Voltage-regulating components as well as reactive power control components are fully investigated in this chapter.
- Chapter 5 presents VVO objective function and constraints in order to reach to a comprehensive objective function for smart grid adaptive VVO.
- Chapter 6 discusses microgrid sources in VVO problem. EVs, V2Gs, Micro-CHP/PVs and Community Energy Storage are some of the main sources this chapter study.
- Chapter 7 investigates Conservation Voltage Reduction from different aspects. Impact of VVO topology on CVR, CVR with AMI data, load modeling in new CVR solutions, VVCC switching events, CVR with smart grid technologies, economic factors, standards, regulations, and CVR role in short-term planning problems are some the topics covered in this chapter.

- Chapter 8 studies maintenance scheduling of VVCC problem. It proposes a new concept called Maintenance Scheduling Engine for solving AMI-based Volt-VAR control component maintenance scheduling issue.
- Chapter 9 explains the new concept of predictive VVO. It initially presents a day-ahead predictive VVO using neural network and then specifies online predictive VVO engine through online sliding window concept.
- Chapter 10 studies optimization techniques used in VVO problems of this thesis. First, it covers experimental and computational methodologies. Then, it explains Benders Decomposition, Genetic Algorithm (GA), improved GA and Particle Swarm Optimization (PSO) techniques.
- Chapter 11 introduces real-time co-simulation platforms for proposed smart grid-based VVO. Co-simulation platform, communication test-bench, test setup implementation, monitoring and control platform overview, IEC 61850 standard and real-time co-simulation of proposed VVO are some of the topics cover by this chapter.
- Chapter 12 gives studies, results and result analysis. Real-time adaptive VVO using Multi-Agent Systems (MAS), VVO with three levels of optimizations, impacts of EVs and V2Gs proposed VVO, day-ahead and live predictive VVO, novel approach for maintenance scheduling of VVCCs, smart grid VVO using PSO and Fuzzification, quasi real-time ZIP load modeling for CVR, real-time co-simulation platform using DNP3 protocol, communication parameter impacts on proposed VVO, the role of CES in VVO, impacts of Micro-CHP/PV and EV penetrations on proposed VVO, and real-time co-simulation platform using IEC 61850 MMS and GOOSE messaging are some of the studies this chapter covers.
- Chapter 13 presents the analysis abstract of chapter 12 in order to provide an overall view of the study results and conclusions.
- Chapter 14 investigates smart grid adaptive VVO roles in distribution network planning studies.
- Chapter 15 presents conclusions and future works following by references and appendices as last sections of this thesis.

Chapter 2.

Previous Studies

This section reviews literatures in regard to the history, research, growth and development of Volt-VAR Optimization as well as Conservation Voltage Reduction techniques through the years.

2.1. Volt-VAR Optimization History

Since distribution networks were first developed in the late 1800s, dispersed efforts have been devoted to study the impacts of voltage drop and reactive power resources on distribution grid. Figure 2.1 depicts the history of Volt-VAR Optimization and its development trend. The primary control method introduced to network was basic local control. Local controls, tried to use local measurements as their inputs to find the operating mode of OLTCs, VRs, and switchable shunt CBs. These measurements included incomplete inputs. In general, these locally measured inputs were used to determine approximation of distribution grid reactive current flow. In local control scheme, there was not any accurate centralized/decentralized Volt-VAR control in the system level, and CVR implementation was far from the optimal condition. In addition, trips and maneuverers that network operators should perform periodically on shunt CBs were not cost effective. Mostly, the CBs were not in their optimal operating modes or they were operating with wrong settings. Hence, from the optimization point of view, the voltage level was unacceptable, and the power factor was less than the appropriate value in most times. Moreover, the excessive reactive current flow of the grid created by incorrect setting was imposed additional power loss into the system.

In 1932, L. F. Brume [9] studied the characteristics of load ratio in local control circuits. It considered transformer tap and series reactor behaviors in his study. This research was one of the first notable studies related to Volt-VAR control concept. In 1970s, most studies focused on static optimization and control of reactive power sources in power systems [10]-[15]. Preliminary optimization of static capacitor installations in distribution

systems was presented in 1972 [13]. In 1980s, new centralized radio control systems were emerged in power systems. Centralized radio control systems were employed centralized-based monitoring systems, with the VAR measurement at distribution feeder breaker. A simple communication structure was designed between feeder devices. Mostly, a one-way communications to switchable shunt CBs were used and the only quantity under control was VAR flow at the feeder breaker. Thus, other backbones of distribution network such as customer loads and customer voltage were not considered. Moreover, if a network operator intended to reconfigure distribution feeders to isolate an occurred fault, or balance loads, such control logics were not able to track capacitor banks on feeders automatically. Some of the shortcomings of this control method were reliability, visibility and accuracy. Furthermore, the abovementioned control and optimization approach were made CVR inapplicable. These shortcomings were made a driving factor for electric power utilities to put one step forward and define Volt-VAR Optimization methods.

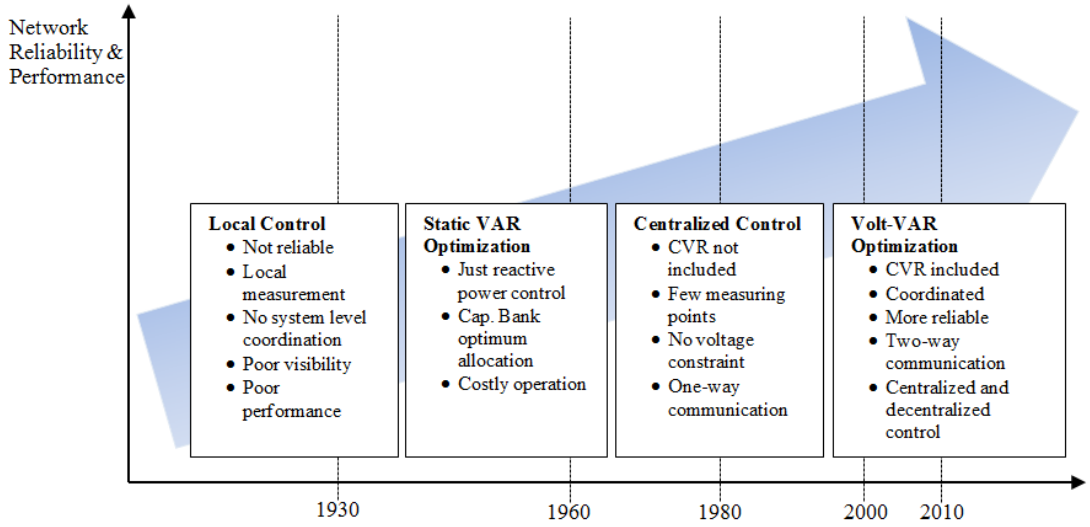

Figure 2.1. History of Volt-VAR Optimization

Generally speaking, the optimization and the allocation of reactive power sources for loss minimization [16] and the secondary Voltage-VAR control [17] are some of the issues that researchers were grappled with in the 80s. Valuable series articles about VVC in distribution systems published in 1985 by J. J. Grainger and S. Civanlar from North Carolina State University [18]-[19]. Initially, they studied the overall VVC problem and secondarily, they proposed applicable solutions for both control and design. It is quite possible to say that they were the first authors who used “Volt-VAR” notation for the

voltage and reactive power optimization and/or control issues. In 1990s, new distribution features such as Distribution Automation (DA) and Distribution Management Systems (DMS) have been developed. Roytelman and Shahidehpour were the first researchers who assessed the VVC issue for DMS [20]-[21]. Since 2000s, great efforts have been spent in designing and developing voltage and reactive power optimization solution for distribution networks in both academic and industrial settings [22]-[60]. The common view of most academic and industrial research studies is to segregate VVO and CVR [22]-[60].

2.2. Conservation Voltage Reduction History

Conservation Voltage Reduction concept on lowering voltage level of termination points has been applied in distribution networks for many years. A notable study regarding the impact of CVR on energy and demand was done by R. F. Preiss and V. J. Warnock in 1978 [61]. Preiss and Warnock studied 15 different feeders in the presence of 5 percent voltage reduction for a four-hour period in different weekdays and achieved almost 3 percent load reduction and less than one-half of one percent energy savings [61]. The second phase of that study published in 1986 showed that the average energy saving resulted from fixed 5 percent voltage reduction equalled to 0.71 per units during 24-hour CVR period in a day [62].

In 1987, D. M. Lauria investigated CVR at Northeast utilities that resulted in 1 percent energy consumption saving through 1 percent voltage reduction [63]. In brief, due to technical limitations and high costs, most CVR plans in the 70^{th} and 80^{th} decades were not pursued regularly by the utilities. In 1987, Bonneville Power Administration (BPA) signed a contract with Pacific Northwest Laboratories to test CVR conservation potential [64]. Subsequently, American electric power utilities in Pacific Northwest tested various CVR scenarios to check CVR capability on energy conservation. In 1990, D. Kishner's CVR implementation on Edison Commonwealth network demonstrated that CVR could provide about 1 percent energy saving thru 1.6 volts line voltage reduction [65]. In-line with disparate CVR research projects, new distribution network features such as DA and DMS emerged in 1990s [22]-[23], [66]. These new technologies brought great control and monitoring opportunities for distribution grids. Consequently, electric power utilities

preferred focusing more on DA, DMS and EMS development rather than investing in new CVR technologies.

In 2000s, new CVR technologies appeared again as the result of a need for voltage regulation of control components and DMS/SCADA (Supervisory Control and Data Acquisition) infrastructural technologies. T. L Wilson tried to investigate some of the main concerns caused by CVR implementations such as under-voltage problem and the amount of reduced energy consumption in two electric power utilities in the Pacific Northwest that had applied new communication and control technologies in their network [67]. On the other hand, other studies such as [68] focused on presenting economic analysis for CVR. Furthermore, Canadian utilities such as BC Hydro and Hydro Quebec began to perform CVR plans in 2008 and 2010 respectively [35], [44]. In 2008, a research survey conducted by the Northwest Energy Efficiency Alliance (NEEA) showed that 1 percent voltage reduction on average, will yield a drop of 0.7 to 0.8 percent in power consumption [69]. Moreover, this study derived that CVR could save 1 to 3 percent of total energy, 2 to 4 percent of kW demand, and 4 to 10 percent of kVAR demand [70]. According to a comprehensive research made by the Department of Energy's Pacific Northwest National Laboratory (PNNL) in August 2010, CVR could potentially provide peak demand reduction as well as annual energy reduction of approximately 0.5%-4% depending on feeder specifications [71]. Complete deployment of CVR on all distribution feeders would provide 3.04 percent reduction in annual energy consumption and if CVR was applied only on high value distribution feeders, the annual energy consumption could be reduced up to 2.4 percent [71]. This study also proved the necessity of accurate load modeling for new CVR techniques. In addition, other reputed research institutes, such as Electric Power Research Institute (EPRI) worked on CVR strategies for many years.

Study on the potential benefits of CVR by EPRI showed that by 3 percent voltage reduction it would be possible to typically achieve a 2.1% demand and energy reduction [72]. The abovementioned studies ascertained the fact that CVR could benefit distribution grid in a variety of different ways in full conformance with the grid specification. Today, CVR could be employed through conventional voltage control assets such as Load Tap Changer of Transformer (LTC) in distribution substation, VRs along distribution feeders, conventional reactive power control components such as switchable shunt CBs and new

VVCCs such as smart inverters, etc. Principal advantages of CVR include, but not limited to, demand reduction, energy consumption saving, reducing downstream substation and/or feeder overloading, increasing home appliance lifetimes, decreasing complaints on low-voltage and/or high-voltage events and lowering customer's electricity bill. Figure 2.2 presents the history of key CVR projects. From the abovementioned studies, it can be concluded that most CVR projects performed “pilot” and few distribution utilities implemented CVR in reality. Many of electric power utilities preferred to primarily perform CVR pilot projects as they could further perform cost-benefit analysis and get familiar with CVR benefits. Another reason was due to so called "Lost-Revenue" that electric power utilities may face while performing CVR. As reducing Medium Voltage (MV) side of distribution grid leads to lost-revenue for electric power utilities (i.e. utilities may sell less power to their consumers) some may consider this as an obstacle for CVR implementation and development.

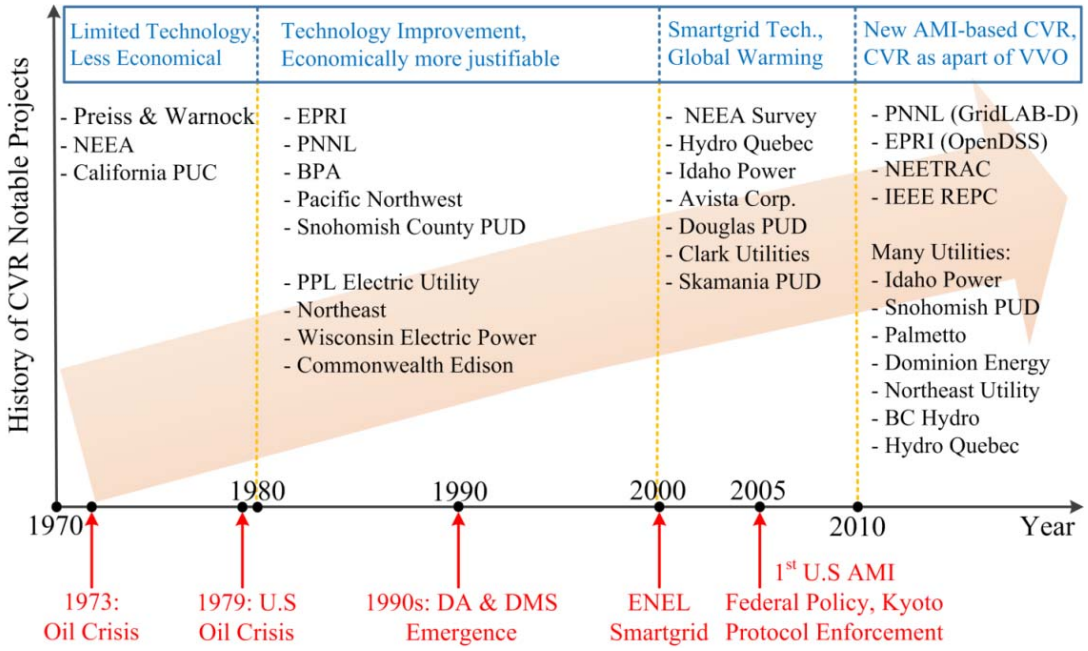

Figure 2.2. History of CVR plans

On the other hand, the electric service provider, i.e. a retail company, and distribution network owner are commonly different in electricity markets. Hence, regulations linked to CVR implementations in deregulated environments would be much more complicated. Even in several electricity retail markets such as New Zealand [73], generation companies are the owner of retail companies as well. This could raise CVR

regulatory issues as typically generation companies try to increase their revenue through selling more power to customers while duration of usage of distribution network is important for a retailer. Thus, the lack of comprehensive regulations for CVR is one of the barriers of CVR development especially in deregulated environments.

It is known that structure and characteristics of each distribution feeder is unique. Hence, benefits resulted by CVR plans could be different from one feeder to another. CVR approach could also be determined according to the availability of VVCCs and load characteristics of a feeder. In general, CVR approaches are getting more sophisticated as new technologies and components emerge. One of the simplest CVR approaches in blind feeders can be done in the presence of substation LTC and feeder VR that are set by Line Drop Compensator (LDC) for end-of-line voltages. Another basic CVR technique that is on-site involves voltage regulation in one specific location of a feeder. In more sophisticated techniques, distribution automation control is used to determine the operating strategies of OLTC, VR, or in some cases CBs. This technique can operate without consumer feedback, or it can utilize feedback from termination points depending on the availability of measurement units at the end of line. Another applicable CVR technique is rule-based CVR that includes independent operation of VVCCs based on pre-configured settings that could be updated frequently by control center through SCADA.

2.3. Modeling and Optimization Studies on VVO

Back to VVO approaches without considering CVR, studies have been done on various modelling approaches [22]-[27]. Table 2.1 presents a brief literature review of recent studies. Some research studies have focused on better problem definition and the optimization techniques such as Fuzzy [22]-[23], [27], Mixed Integer Linear/Nonlinear Programming [25] and Meta-heuristic [26].

Table 2.1. Volt-VAR Optimization Literature Review

Specifications	References
VVO-CVR	VVO [22-26, 29, 31-33, 47, 49,74-75, 77], CVR [43, 44, 76], Voltage Regulation [27, 30, 36, 37, 48, 50], VVO with CVR [27, 34, 35, 46, 51, 52]

Objective Function	Min. Loss [24-26, 47, 49, 51-52,], Min. Energy Loss [29, 47], Min. Voltage Deviation [23, 27, 36], Improving Voltage Profile [48], others: Max. DG active power [30], Max. fuzzy membership values [22]
Optimization Technique	Multi-objective Fuzzy [22, 24], Fuzzy [23, 27, 50], PSO [26, 29, 49-50], GA [47], SE [48], Bi-level optimization [30], Branch & Bound [52], Time-series [46], Benders Decomposition [25]
Innovation in algorithm	Using Intelligent systems [27, 36, 77], Bi-section search Algorithm [30], with open DSS [52], others [23, 25, 29, 50]
Smart grid adaptive	Conventional DG [29-31, 34-36, 49, 50, 75-78]
Real-time Study	[27, 36, 48, 51]
Explanatory Articles	[31-34, 35, 43-44, 46]

The predominant feature of this class of studies on improving VVO techniques is their focus on the algorithms and implementation techniques rather than focusing on initiatives smart grid features can provide. In total, aforementioned studies do not take advantage of the smart grid new capabilities and features. Hence, they could not be considered as smart grid-based approaches.

2.4. Smart Grid Functionalities in VVO

Few studies have just pursued the smart grid issues on VVO [28]-[31], [33]-[34]. Particle swarm-based optimization technique has been applied for optimal coordination of DGs, and other Volt-VAR control devices such as LTC and feeder capacitors in [29]. In [30], two optimization-based models have been proposed. Single-level optimization is employed for computing the maximum penetration level of DG and a bi-level optimization model is designed to evaluate the power value that a distribution system can transmit to network end-users. A study [33] has stipulated that the recent smart grid initiatives have created growing interest in the deployment of more advanced VVC systems for efficiency improvement, demand reduction, and better overall asset utilization [33]. Possible effects of smart grid actual functions on load tap changers of distribution transformer discussed in [34]. The abovementioned papers have focused on concepts such as: advantages, challenges and functional requirements of VVO in smart grids which could be considered as the early stages of smart grid-based VVO design. Thus, such reviews could assist in forming the basis for the smart grid-based Volt-VAR Optimization algorithms.

In September 2011, IEEE standard 2030 [79] was published. IEEE 2030 presents a comprehensive guide for smart grid interoperability. As explained, some research papers have tried to address different aspects of smart grid and their specifications [27]-[28], [30], [35]-[36], [43], [45]-[46], [48], [50], [80] before IEEE 2030 standard. Most such papers have focused on concepts, key challenges, and initial requirements of VVO in smart grids [3], [31]-[33], [38]-[39], [50] without considering interoperability issues. Some other works such as [81]-[82] have investigated the main issues new smart grid technologies, such as VVO, may face in complying with IEEE 2030 standard. From literature survey, it can be concluded that more theoretical work is required to explain and suggest new smart grid-based VVO techniques in compliance with IEEE 2030. In other words, there is a salient gap between conventional VVO and new innovative smart grid-based VVO in terms of efficiency, and optimization level.

Research into control strategies, such as [31], [36], [49], [56]-[60] have identified decentralized control strategies as suitable for future VVO engines, but have not discussed these in detail. A real-time simulation of multi-agent systems for decentralized secondary voltage control in distribution network is presented in [36]. It uses a real-time digital simulator (RT-Lab) with a Java Agent Development framework (JADE) applied to model distributed systems. Moreover, a decentralized architecture for optimal voltage regulation in smart grids has been assessed in [49]. The study strives to define a decentralized architecture to compute the actual value of cost functions and to propose distributed cooperative optimization strategies result in optimal asset of the voltage controllers. Given the fact that these studies [36], [49] have only considered voltage, a comprehensive decentralized integrated solution for VVO is needed.

As such, recent studies have designed an integrated VVO for distribution grid [24], [32], [51]-[52]. One of the articles [32] discussed the challenges of an integrated voltage and VAR optimization with the emerging high penetration of Advanced Metering Infrastructure, DER, Demand Response (DR) and Plug-In Electric Vehicles (PEV) in power distribution systems. The paper has just pointed out the integrated VVO impact on the operation of other power system domains, possible objectives, benefits, controllable variables, and information sources of an integrated VVO respectively but it has not proposed any applicable solution. Another research [24] explicated an integrated

voltage/reactive power control of radial distribution feeders just in planning issues. Employing new smart grid features such as real-time AMI, DGs and EVs have not taken into account in this paper as well. A coordinated optimization approach for Volt-VAR control of large power distribution networks has proposed in [44]. The study has proposed a conventional centralized approach without considering smart grid new features. An Integrated approach for control and optimization of system has presented in [51]. The paper has explained an approach to integrate and localize control of Volt-VAR control devices. This work has not employed new smart grid intelligent features as well. In addition to an integrated VVO, some efforts have been devoted to review the relation between VVO and Energy Management Systems [48]-[49], [74] but these studies have not given any integrated VVO solutions regarding to all Volt-VAR control devices.

The prospect of large penetration of dispatch-able customer side resources (co-generation loads), such as EV's, has also brought new challenges and opportunities to distribution networks. Although, system planners tend to demand new command and control strategies to accommodate and minimize the load impact of co-generations, others may regard the dispatch-able energy they provide as means to optimize the distribution service as a whole. Diverse research studies have reviewed the impact of EVs on distribution networks [83]-[84]. Some have mainly focused on G2V (Grid to Vehicle) loading effect on distribution network [85]-[87], while others have proposed coordinated EV charging strategies to optimize the grid by minimizing the active power loss of the network individually [88]-[90]. The foremost gap in research studies can be the shortcomings of studies encompassing the effects of EVs on a reliable VVO. Furthermore, new studies have proven the fact that new EV inverter technologies could provide reactive power injection (positive or negative injection (aka absorption)) opportunity for future grids [91]-[96]. This may impose extensive impacts on the optimization, VAR amount and the number of active distribution network switchable CBs. Thus, in near future, it may be possible to employ a small percentage of EVs as reliable reactive power generation sources in a V2G (Vehicle to Grid) mode in order to reduce active and/or reactive power loss of the grid. It has to be mentioned that large amounts of harmonics from EV charging stations may increase network line loss [97]. The result of [97] showed that for small-size EV charging stations, no harmonic mitigation measures are needed. However, for large and medium-size EV charging stations, the order of the harmonic current which may

exceed the standards has to be determined and then proper filters can be added to the EV charging station to avoid EV harmonic negative effects.

Various studies have assessed the impact of EV penetration on distribution networks [98]-[102] but it seems that new studies have to be performed to evaluate the impact of different EV penetration levels on the proposed AMI-based VVO solutions, which encompass CVR as a constituent component. EV penetration throughout distribution feeders could affect AMI-based VVO technologies in areas such as: loss minimization, control components, operating conditions and CVR performance, as VVO load characteristics and/or models could be changed in different EV penetration scenarios. Hence, the necessity of studying the impact of EV penetration on AMI-based VVO technology is now felt more than before.

In recent years, penetration of Distributed Energy Resources at customer's sides has changed the structure, operation and performance of smart distribution networks. DERs such as Micro-Combined Heat and Power units (Micro-CHP) or Photovoltaics (PV) have been employed for different operational needs at termination points. According to co-generation concept, Micro-CHP units are able to supply both heat and power for users. PV systems are also well-known for their clean power generated from sunlight. Hence, diversity in type and technology, as well as penetration level of the two abovementioned DERs could have considerable impact on distribution network optimization and control. Many recent studies have worked on Micro-CHP expansion in distribution networks. Some proposed residential microgrid scheduling based on smart meter data and Micro-CHP [103]. Some focused on the impact of Micro-CHP on the energy management [104] and demand response [105]. Studying the impacts of Micro-CHP penetrations on distribution network have been assessed by [106]-[108]. Regarding PV impact on distribution grid, several research studies [109]-[110] have focused on overvoltage issue caused by high penetration of PV's. Some investigated coordinated control of PV with Battery Energy Storage (BES) system [111]-[112] while some others attempted to see the impact of PV high penetration on low and medium voltage distribution network [113]-[115]. There are a few studies that considered Micro-CHP and PV penetrations together as micro-generation to assess their impact on distribution network performance [116]-[118]. From literatures, it can be concluded that as penetration of Micro-CHP and PV units within distribution

networks may potentially affect VVO, it is necessary to evaluate the impact of these micro-generation units on a new smart grid AMI-based VVO.

Various noteworthy works have been performed to study the impact of smart grid features, smart meter infrastructure, field demonstration, and energy efficiency on VVO [33], [78], [81], [119]. Some have focused on presenting new frameworks for Volt-VAR Control approaches [120]-[122]. Some have recently studied the advanced DMS function to handle EVs in distribution networks [123]. Other recent works studied VVO planning and management in the presence of DGs [124] and proposed simple new Volt-VAR Control for DGs [125]. In brief, VVO approaches are going to be smarter as they tend to adapt and upgrade their approach based on new capabilities brought about by smart grid technologies.

2.5. Canadian Utilities' Volt-VAR Optimization Projects

Different studies on Volt-VAR Optimization approaches have been pursued by some Canadian utilities such as BC Hydro [35], [127] and Hydro-Quebec [38], [43]-[44], [126], [128]. Reference [35], has shared BC Hydro's experience on Volt-VAR Optimization in distribution system. The first BC Hydro VVO project was completed in 1996 with the objective of minimizing the distribution substation peak load demand and relieving transmission capacity constraints [35]. During the five years of operation in winter periods, significant benefits were achieved as the winter energy was reduced by an average of 1.3 GWh/yr [35]. In 2006, the objective was changed from demand reduction into energy conservation and the system was operational through the whole year [35]. In 2007, the installed system provided around 7 GWh of energy savings or about 1% of the total energy throughput [35]. BC Hydro is implementing a state-of-the-art DMS to provide a platform to create opportunities to implement leading advanced distribution applications, such as VVO, network reconfiguration, fault location isolation and restoration [35]. This DMS will be able to model distribution systems and perform VVO close to real-time. Moreover, BC Hydro smart metering program started in 2011 [127]. It is expected that VVO using AMI infrastructure could save about 10 percent of energy in Gwh/yr [127]. Hydro-Québec smart grid VVC project is being conducted providing the utility with reasons to be excited about the benefits of the smart grid [38]. The VVC project is expected to reduce total energy

consumption in Quebec by approximately 2% or 2 TWh by 2015 [38]. The primary objective is to provide dynamic voltage control at a lower voltage (CVR) [38]. In addition, reference [43] has described a methodology used to assess the effectiveness of CVR in the Hydro-Québec distribution network. Hydro-Québec is counting on CVR and reactive power control, a combined method known as “CATVAR” [126], [128]. Implementing a dynamic Volt-VAR control is one of the targets of the 1st phase of smart grid project in Hydro-One Company [129]. In this project, VVO intends to use distribution-based power electronics to keep voltage and VAR of the system within desired operational limits [129]. One of the projects Varentec Company performs for Canada ministry of energy with five collaborators: Hydro One Networks Inc.; London Hydro Inc.; Entegrus Inc.; Enwin Utilities Ltd, and GE Digital aims to design distributed dynamic VVC and monitoring of distribution feeders in following Ontario regions: London, Chatham, Windsor, Toronto, and Markham [130].

2.6. Studies on Maintenance Scheduling of VVO

In recent years, different research studies have investigated maintenance scheduling of distribution network [131]-[147]. Some research work focused on the global maintenance scheduling problem [131]-[133] such that they define comprehensive objective functions for maintenance scheduling problem that can be used for maintenance scheduling of distribution networks as well. For instance, [133] proposes a comprehensive objective function for maintenance scheduling of generating units by defining an annual independent market called Maintenance Market. Moreover, some related studies considered electricity market impact on maintenance scheduling problem [131]-[135] and [138]. It has to be mentioned that many of maintenance scheduling of distribution network problems consider risk and/or risk management as their main approach [136]-[139]. These studies are vital for understanding the inherent characteristics of distribution network components as each of these assets has their own failure risk. Risk-based maintenance scheduling techniques are offering maintenance scenarios through calculating the risk of failure of distribution network assets.

On the contrary, some studies have assumed that the failure rate and the maintenance period of grid components are constant as they may not face with system

changes most of the time. Therefore, several papers studied Volt-VAR control asset features, operation and maintenance [140]-[142]. There are reference books [143]-[144] that also assessed maintenance of VVCCs such as CB, VR and OLTC separately in different chapters. There are several novel works that investigates maintenance scheduling problem in presence of smart distribution networks [145], and smart grid features such as Distributed Generation [135] and renewable energies [146] as well.

Generally, it can be observed from literature survey that there is a lack of a study on maintenance scheduling of VVCCs as a co-operating set. The reason lies in a fact that conventional VVO solutions statically optimized distribution networks. Hence, there was no need to ensure coordinated control between Volt-VAR control assets. Even when VVCC solutions emerged [74]-[75], [78], [81], [119], [148]-[149], the VVO core engine performed offline. As net benefit gained from static VVO solution has been calculated for large time period (e.g. annually), unavailability of a VVCC in the grid for a short period was not quite important in static VVO. Operation and Maintenance cost/benefits of a conventional VVO discussed in [150]. With the advent of new AMI-based VVO solutions, it is now vital for network planners and/or operators to know the benefit resulted from loss minimization and energy conservation of loads by AMI-based VVO in quasi real-time. Therefore, the necessity of new approaches for maintenance scheduling of VVCCs according to new AMI-based VVO solutions is felt more than before.

2.7. Review on Predictive VVO

The number of Volt-VAR control device switching per day is limited and could exceed from predetermined limit by a real-time or semi real-time approach. These VVO approaches could reduce the lifetime of VVCCs which practically might not be cost-effective solutions. In order to take the abovementioned key factors and concerns into account, predictive techniques can be proposed to primarily predict distribution network loads and then, optimize the network based on historical data of Smart Meters and global attributes collected from DMS/SCADA. Different research studies have presented different techniques to predict loads in distribution networks. Most of the studies aimed to focus on short-term/mid-term load forecasting of loads [151]-[154]. Few works have employed Neural Networks (NN) in optimization of distribution network [148], [155].

Hence, applying quasi real time data of smart meters for designing an online predictive VVO could be perceived as a novel approach.

2.8. VVO Studies using AMI Data

As explained in introduction, designing a real-time or semi real time VVO could optimize the network in real/semi-real time stage and could result in more accuracy in terms of loss reduction and voltage profile improvement. Few researches studied VVO in the presence of AMI data [156]-[161], while others investigate real-time solutions for VVO [162]-[165]. Regarding to the literatures, only few works such as [162] and [163] have been provided VVO system with practical real-time results. The reason lies in a fact that most conventional VVO approaches were performed offline. Hence, VVO approaches are going to be smarter as they tend to adapt and upgrade their approach based on new capabilities brought about by smart grid technologies. According to literatures, there is a gap between VVO offline design and VVO real-time implementation that can be solved by designing adequate real-time co-simulation platform for VVO solutions.

2.9. VVO Co-simulation Platform Studies

As discussed, with the expansion of AMI infrastructure throughout the distribution networks, it is now conceivable to propose advanced AMI-based solutions for the VVO, using AMI quasi real-time data. Recent studies have presented several AMI-based approaches for distribution network applications such as VVO [157]-[161], [166]-[167]. Utilizing real-time approaches necessitates adequate real-time monitoring, operational and control platforms for further implementation. Thus, providing efficient co-simulation environment benefits electric power utilities and allow them to test the performance and study the impacts of such approaches before implementation. Significant studies have been done on co-simulation of distribution networks and Information and Communications Technology (ICT) [162], [169]-[174]. For instance, [168] presented a co-simulation platform using GridLAB-D for network model, and ns-3 for the communication channel. Microgrid co-simulation framework ensured minimal synchronization errors in [169]. A new method of co-simulation of Active Distribution Networks (ADN) presented in [170] based

on Simulink and Ptolemy II. Regarding DMS co-simulation, [172] proposed a DMS with state estimator to decrease harmful effects of system. Additionally, [173] presents the design of co-simulation for distribution network frequency and noise analysis in time domain. Regarding VVC, [174] explains basics needs for real-time feeder monitoring of advanced Volt-VAR controls and proposed meter placement technique without presenting a co-simulation platform. On the other hand, [162] presents a co-simulation for VVC using EMTP-RV and Opnet. Other works have focused more on integrating intelligence into the system using simulation and/or co-simulation [175]-[177]. State-of-the-art development of Multi Agent Simulations illustrated in [175] for smart grids. Distributed intelligence and wireless communication applied in [176] to control CBs. GNU-Octave used in [177] to assess the performance of Volt-VAR control technique in the presence of ns-3 network simulator without testing real-time operation of VVO. For real-time operation of the system, [178] performed real-time observability analysis. Moreover, ref. [179] shares valuable experiences on deploying real-time state estimator in BC-Hydro DMS. A hybrid co-simulation is proposed in [180] for grids taking wide area monitoring and control, and standards such as IEC 61850 into account to evaluate real-time performance of wide area monitoring, protection and control applications. From the literatures, the necessity of designing a real-time co-simulation platform comprising of VVO engine, communication channel, and monitoring platform to provide a fully functional real-time system to check the performance of new AMI-based VVO solutions is felt more than before.

Hybrid solutions, comprising AMI and VVO functions, require real-time monitoring, operational and control platforms, such as a co-simulation platform, for testing and validation. Different studies have explored co-simulation for distribution networks [162], [168]-[169], [174], [176]-[177], [179]-[180]. IEC 61850 is a real-time peer-peer communication standard, initially designed for communication between different Intelligent Electronic Devices (IEDs) within substation. Given the popularity of IEC-61850, there is interest in extending this standard out of substation to support automation functions outside the substation [181]. Several works have studied different IEC 61850 smart grid and distribution network applications such as interoperability and interchangeability [182], adaptive protection [183], network simulation [184], feeder IED topology [185]-[186], Multi Agent Systems [187] and Energy Management Systems [188]. Very few researches have studied voltage control of smart grid using IEC 61850 concept [189]-[190]. The necessity

of proposing a real-time co-simulation platform consisting of smart grid-based VVO engine, communication channel, and monitoring platform to provide a fully functional real-time system is felt more than before as well. In addition, novel VVO solutions have to include automation system standards such as IEC 61850. The performances of these solutions have to be tested in different system configurations based on grid operational conditions and/or needs.

2.10. Integration of CVR as a Part of VVO Objective

Review of the existing literature that has investigated the performance of AMI-based VVO points to the fact that inclusion of the CVR sub-system could benefit utilities in their choice of control and optimization strategies. As CVR control actuators such as LTCs and VRs could be categorized as VVCC and as CVR and VVO objectives are well-matched, many researchers and/or utilities suggest considering CVR as a part of VVO. Therefore, it is conceivable to deem CVR as a major component of novel VVO solutions. Consequently, new VVO techniques would be able to perform energy saving and demand reduction besides performing loss and VVCC operating cost minimizations. Development of novel smart grid-based VVO solutions have become essential as electric power utilities and voltage regulation service companies are seeking more efficient techniques for VVO engine design.

2.11. Summary of Literature Survey

In summary, most of academic/industrial researches studied centralized VVO [22]-[26], [29], [31]-[33], [47], [49], [52], [74]-[75] and there were few studies that assess a new comprehensive decentralized VVO approach [36], [45], [50], [59]-[60], [80], [174], [176]-[177]. Centralized and decentralized VVO approaches are explained in next chapter of this thesis in detail. Moreover, notable gaps exist between offline VVO and smart grid-based VVO which requires real-time integrated approaches. Nevertheless, some works are in preliminary phases of a real-time VVO for future smart grids. Given the fact that the real-time adaptive VVO techniques have salient impacts on smart microgrids, studies of real-time adaptive VVO have become critically important. Thus, future investigations could

focus more on finding the optimal approaches based on the advantages of new smart grid and feeder-based technologies. Notwithstanding the value and novelty of the previous studies, it is conceivable to declare that the smart grids enable the feasibility and affordability of adaptive and close to real-time VVO engines. The systems could be more capable of achieving higher degrees of efficiency and reliability through employing a relatively sophisticated distributed command and control system.

The other gaps that have to be covered in new Volt-VAR Optimization solutions include but not limited to: considering dispatch-able sources such as vehicle to grid on Volt-VAR Optimization, availability of optimal strategies for maintenance scheduling of voltage and reactive power control assets in quasi real-time Volt-VAR Optimization, availability of predictive engine to solve voltage and reactive power control components number of switching per day issue, availability of Volt-VAR Optimization with comprehensive objective function includes conservation voltage reduction using advanced metering infrastructure data and the availability of a real-time co-simulation platform for testing the performance of smart grid-based VVO solution.

Chapter 3.

Volt-VAR Optimization Topology

3.1. Distribution Network Topology

Distribution network is a key part of power system that links bulk power source, e.g. transmission line, and customers. Typically, distribution networks in North America comprised of sub-transmission system, distribution substation(s), distribution feeder(s), distribution transformer(s), secondary feeder(s) and/or circuit(s) and service drops. Some power system experts introduce distribution networks between distribution substation and customer termination points. Figure 3.1 depicts Single Line Diagram (SLD) of a typical distribution network in North America.

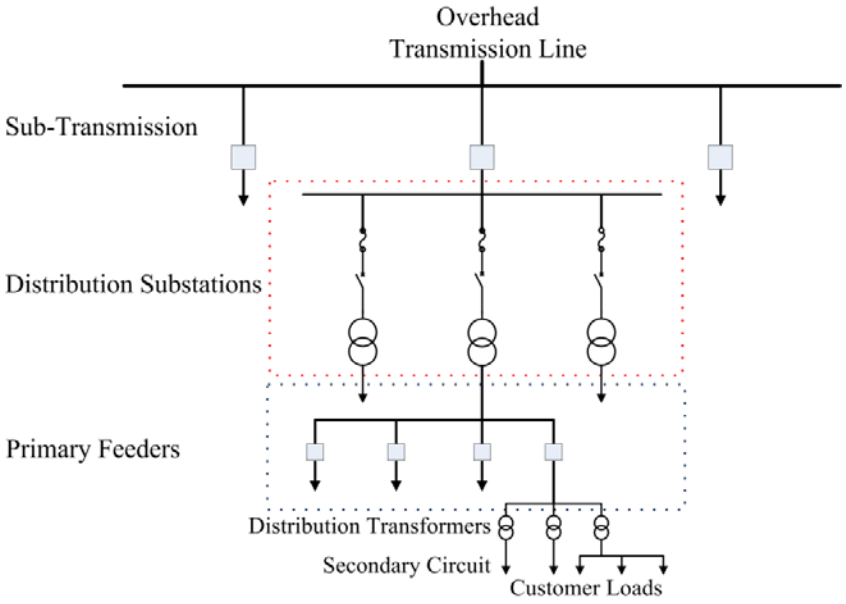

Figure 3.1. Single line diagram of a typical distribution network

Distribution substation that includes power transformer, station bus, switchgears, breakers and voltage regulating components such as tap changer and shunt capacitors, reduces voltage level of the system into primary feeder voltage that is normally between 4.16 kV and 34.5 kV. This three-phase primary feeder is responsible for feeding three-phase loads as well as single-phase laterals. Distribution transformer reduces primary

feeder voltage into secondary voltage called “utilization voltage”. At the end, secondary system components deliver power to customers through service drops.

Regarding control topology, SCADA are commonly used as a conventional tool for control and monitoring of remote stations, e.g. HV/MV substations, from a master control center. SCADA consists of monitoring and control equipment, sensing and measurement systems (telemetric) as well as two-way communication platform. Figure 3.2 shows SLD of a primary feeder with its main components. Shunt CBs are mainly used in primary feeder laterals. It is clear that using shunt CBs that are commonly connected near the load centers improve system voltage drop, loss and power factor. The rates of these CBs have to be selected cautiously to avoid overvoltage issues at low-load (light-load) conditions.

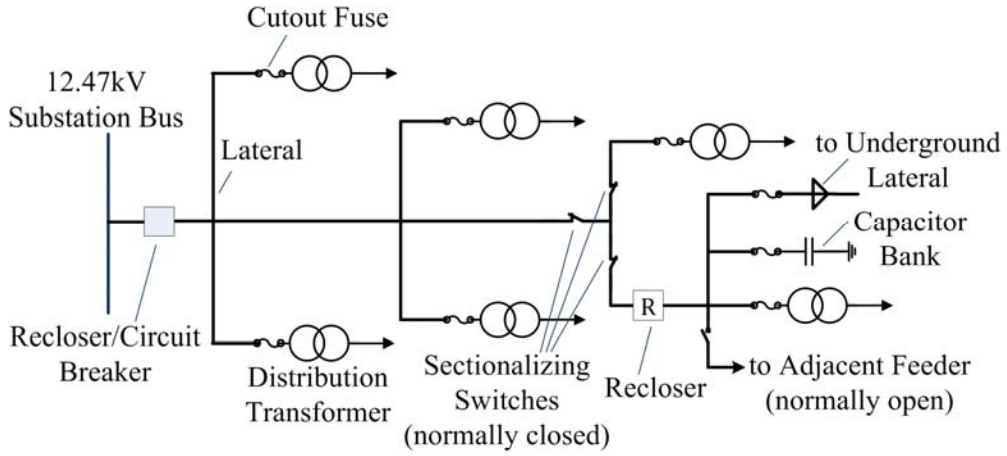

Figure 3.2. SLD of a typical North American primary feeder

The most simple, low cost and common type of primary feeder is “radial” primary feeder shown in Figure 3.3 .As seen in Figure 3.3, radial primary feeder can branch itself into several laterals that can be turned into sub-laterals indeed. As the reliability level of service of radial primary feeders are very low, disconnecting components such as sectionalizers, reclosers and disconnect switches are used to isolate the fault and to increase primary feeder reliability. Typically, primary voltage levels used in North America is 2.5 kV, 5 kV, 8.66 kV, 15 kV, 25 kV and 34.5 kV. Three-phase four-wired multi-grounded common neutral primary feeders such as 12.47Y/7.2 kV, 24.9Y/14.4 kV and 34.5Y/19.92 kV are widely used in North American distribution networks.

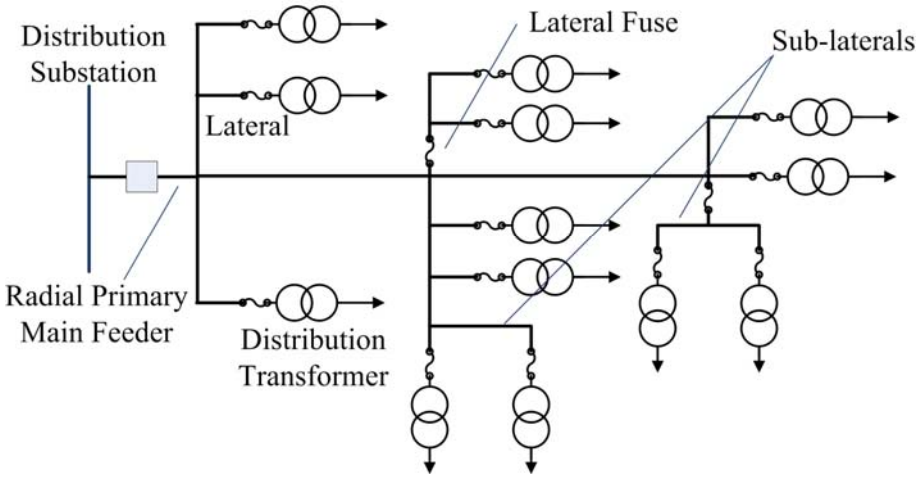

Figure 3.3. Typical radial primary feeder single line diagram

As explained, voltage levels of power systems are presented by ANSI C.84.1 “Voltage Ratings for Electric Power Systems & Equipment” [1]. According to this standard, voltage level for single-phase residential load is 120/240V that can be supplied by three-wire single-phase systems in 60 Hz. 120 V is for lighting and other small appliances and 240 V single-phase power connection is for large home appliances such as dryer, water heaters, etc. For commercial and high residential loads, the voltage level is 208Y/120 V with three-wire single-phase circuit. For industrial, super-high loads such as high-rises in downtown areas, and average-above commercials, 480Y/277 V systems are more common that are supplied from four-wire three-phase circuits.

Similar to the primary system, secondary systems are mostly radial. Figure 3.4 represents the single line diagram of a typical radial secondary system. On secondary grid, pole-mounted 3-phase or single-phase transformers, ranges from 75 kVA to 1000 kVA, are typically employed. Three-phase transformers with voltage rating of 216Y/125 V in ranges of 300 kVA, 500 kVA, 750 kVA and 1000 kVA are very common in North American distribution networks.

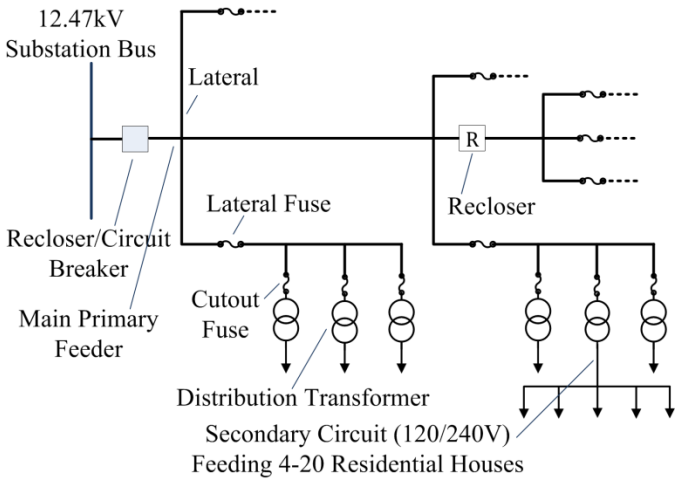

Figure 3.4. Typical North American radial secondary system

As most primary-secondary distribution feeders are radial, the main focus of this research is on radial topology in distribution systems. Grid topology and the specifications that each topology brings about, have considerable impact on Volt-VAR Optimization. The topology of each VVO approach intends to perform in a grid has to be in-line with the topology and control infrastructure of that grid. According to this fact, two main control topologies can be defined for recent VVO techniques explained in next section.

3.2. Centralized VVO vs. Decentralized VVO

Basically, one of the well-known VVO approaches recommended in recent years by different utilities and/or companies is “Centralized-VVO” (network-based) [22]-[26], [29], [31]-[33], [47], [49], [52], [74]-[75]. In centralized VVO, the processing system is placed in a central controller unit such as DMS in the so called “Utility Back-Office”. The DMS uses relevant measurements taken from termination points, i.e. utility subscribers, supplied to it from either field collectors or directly from Measuring Data Management System (MDMS), to determine the best possible settings for field-bound VVO assets to achieve the desired optimization and conservation targets. These settings are then off-loaded to such assets through existing downstream pipes, such as SCADA network.

However, the main challenge of centralized-VVO to meet integrated real-time and quasi real-time VVO solutions would be the huge amount of data that should be

transmitted from AMI to back-office and from VVO to control components throughout distribution network substations and feeders. This may lead to a “Data Tsunami”, SCADA blockage and/or failure. Moreover, capturing and transmitting huge amount of data can make the AMI very expensive. Although the optimization processing time issue can be solved by using fast computers and servers, the control system reliability is another important concern of this method that has to be considered. Failure in central control server could shut-down VVO in all distribution network feeders and substations. Moreover, Centralized VVO uses Geographic Information System (GIS) and network topology as the basis to determine the optimization targets for each tributary. However, due to the abovementioned challenges about access to real-time downstream sensory inputs, such functions rely on statistical load profile, rather than real-time load profiles.

On the contrary, decentralized-VVO technique employs local control to optimize the operation of VVO components on a feeder. That is why it is possible to call this approach “substation or feeder-based” approach. In this technique, VVO would be able to receive its required data from termination points to optimize specific distribution feeders. Different methods can be used for sending local data from AMI to the VVO engine that is discussed in next section of this chapter. Few studies have recently recommended decentralized VVO approach [36], [45], [50], [80], [174], [176]-[177]. This research proposes a “Decentralized-VVO” (feeder-based) approach based on new smart microgrid features such as pervasive control, Distribution Automation, real-time AMI and DMS as well. This Decentralized-VVO approach utilizes VVO engines which are located in the field, i.e. at medium voltage distribution substation, and in close-proximity to the relevant assets to improve voltage and conserve energy according to local attributes of the distribution network and global attributes from DMS/SCADA. Figure 3.5 compares centralized-VVO and proposed decentralized-VVO. As shown in Figure 3.5, real-time local measurements of AMI do not need to travel from the field to the back-office and the new settings for VVO assets are determined locally, rather than by a centralized controller.

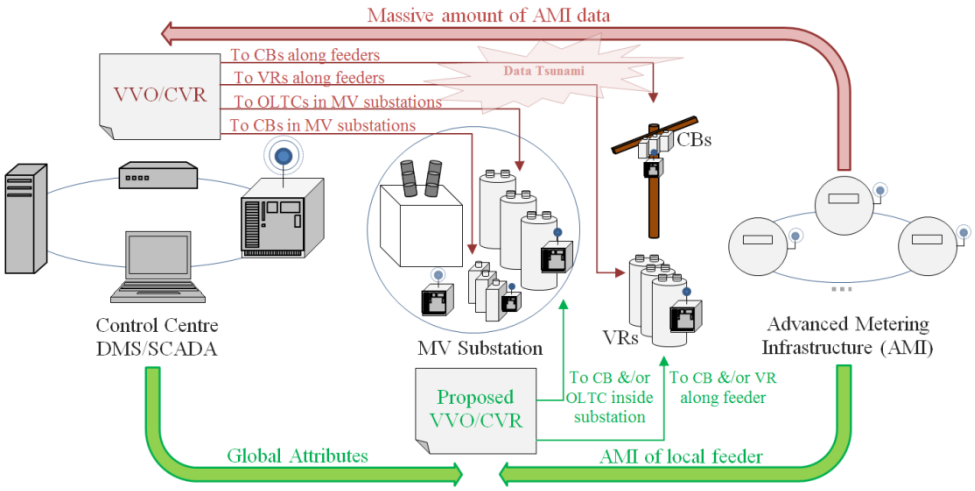

Figure 3.5. Centralized-VVO (Purple) versus Decentralized Proposed VVO (Green)

This approach may lead to less data transfer cost of AMI, better system reliability and faster optimization process but it can increase complexity of system as it increases number of local controllers that has to communicate with each other. Furthermore, this VVO strategy tries to apply local dispatch-able energy sources such as V2G systems, DERs, energy storages and smart inverter technologies which can make it more affordable and practical. Thus, the proposed research focuses on the feasibility of a quasi-real-time smart grid-based VVO engine that can readily control VVO in an integrated way through distributed command and control. It is expected that this technology would enable network operators to achieve higher levels of loss reduction, energy efficiency, energy conservation and reliability simultaneously.

Given the fact that the centralized VVO (network-based VVO) highly depend on network topology, a new approach which acts on feeder level can be an adequate solution. As stated, the main reason is the availability of real-time/quasi real-time local information that is able to emerge new class of optimization based on system local attributes. Achieving a real-time coordination of VVO and CVR (as a part of VVO) based on real-time data analysis with features such as: integrated VVO with distributed command & control architecture, coordinated optimization of VVO devices such as: OLTCs, VRs CBs, EVs and DGs inside distribution substation and along distribution feeder, and the ability to evaluate the impact of different load characteristics and real-time load profile over VVO

could bring lots of benefits to utility companies in terms of distribution network optimal operation and cost savings.

3.3. Proposed VVO Data Collection and Communication Needs

As mentioned in previous section, real-time values from smart meters could be employed to construct real-time load profiles for VVO engines. Smart meters in new distribution networks provide more accurate real-time measurements of service quality levels at termination points. Typically, smart meters are set to send customer's data every 15 minutes but most of them are capable of sending data even in 5 minutes time intervals. To capture, analyse and exchange data points related to feeder status, a system of data collection such as Measurement Aggregator, Intelligent Agents (IAs), etc., and a reliable bidirectional communication infrastructure are required. Communication infrastructure has to reliably and securely connect proposed VVO engine to data collection unit, VVCCs and to DMS/SCADA.

In first steps of this research, possibility of a reliable approach for constructing real-time load-profiles that has to be sent to integrated VVO engines through an agent-based distributed command and control architecture is studied. Intelligent Agents are tasked with applying appropriate configurations for relevant assets within a microgrid or utility's distribution network. Figure 3.6 depicts the primary structure of the proposed real-time intelligent agent-based VVO system. Two distribution feeders are paralleled with a tie-breaker (Breaker-1) to supply residential customers. Both feeders have Volt-VAR control devices at the Medium Voltage (MV) side of their transformers. Each feeder includes residential loads and each residential termination point equipped with a smart meter which captures load data (and if need be, other sample value data). Smart meters send data to other network nodes from the LV side to the MV side. Here, the distributed command and control scheme can be visualized as three Intelligent Agents controlling integrated VVO application. This classification is fully dependent on agent functionalities, tasks and location of the component within the distribution network. Thus, the required data for VVO is collected, analysed and processed by IAs implanted in the system. Such agents are tasked with processing smart metering data, determine probable events which have

produced that date and communicate their findings with the main VVO Intelligent Agent, who in turn can determine the new configuration settings for VVO components in the system.

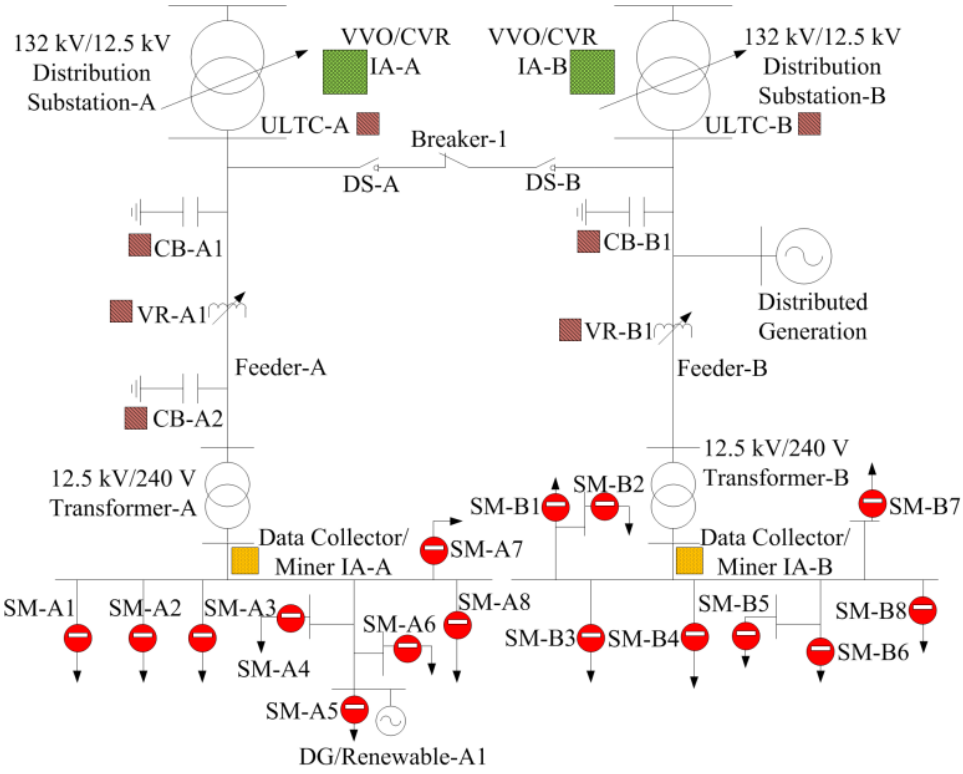

Figure 3.6. Intelligent Agent-based VVO topology in a distribution network
Note. IA: Intelligent Agent, OLTC: On-load Tap Changer, DS: Disconnector, CB: Capacitor Bank, VR: Voltage Regulator, SM: Smart Meter.

The ability to communicate the event, rather than the raw AMI data, will substantially reduce the bandwidth requirement of the communication system, and improves its performance. The main responsibility of VVO-IAs shown in Figure 3.6 is to provide an efficient adaptive VVO management in real-time. The central core of this VVO-IA is a VVOE that runs real-time optimization and control algorithms in order to maintain the voltage at the PCC (Point of Common Connection) with the residential consumers within ANSI C 84.1 standard [1] and CAN 3-C235-83 [2] limits (which is between 0.95 to 1.05 per units), and optimize system voltage, power loss and conserve energy simultaneously by applying voltage regulation and VAR injection devices within the substation and/or along distribution feeders in real-time.

After reaching the best online optimization solution for the distribution network, it reconfigures the network by sending control commands to VVCCs. These assets implement VVOE's commands in their task zone and if required, will send a new command to other IAs in the system. For instance, assume VVOE sends a command to a VAR injector CB-A1 agent (capacitor bank in feeder A) to inject 50 kVAR into the system in a specified real-time interval. CB-A1 can be considered as an agent who keeps records of its capacitor banks. Hence, it can decide which bank units have to be on/off to cover the 50 kVAR. This can be done based on capacitor bank positions and data. If the requested task could not be implemented, CB-A1 will inform the VVOE. The latter would then be responsible for finding an alternative solution for the network. It has to be mentioned that the design and implementation of required Intelligent Agents explained in this section were not included in targets of this research as the main focus of this research is on proposing a novel smart grid-based VVO engine. More details on main features, tasks and design of IAs for smart microgrid application such as proposed VVO can be seen in [191] and [192]. Regarding communication platform, this research investigates the applicability of famed communication protocols such as Distributed Network protocol (DNP3) as well as new smart grid communication protocols such as IEC 61850 on proposed VVO. The communication medium can be different according to system control infrastructure. In [193], Narrow-Band Power Line Communication (NB-PLC) studied for smart grid applications such as VVO.

3.4. Proposed VVO Topology Main Features and Classifications

Figure 3.7, Illustrates the main topology of proposed approach for VVO in a feeder. As it is typically shown, inside the substation and along distribution feeder, Volt-VAR control devices and DG units are located. The distribution network feeds feeder customers at LV side. In brief, smart meters are connected to a Master Control Unit (MCU) which sends smart meter data to the system data collector and/or Intelligent Agent (IA-IED). IA-IED sends required data of VVO Engine in quasi real-time. Then, the VVO Engine solves the optimization problem based on its objectives, constraints and data which has been

sent by smart meters. The optimal solution will be sent to the Volt-VAR control devices (they can also be IAs) to reconfigure distribution feeder in quasi real-time.

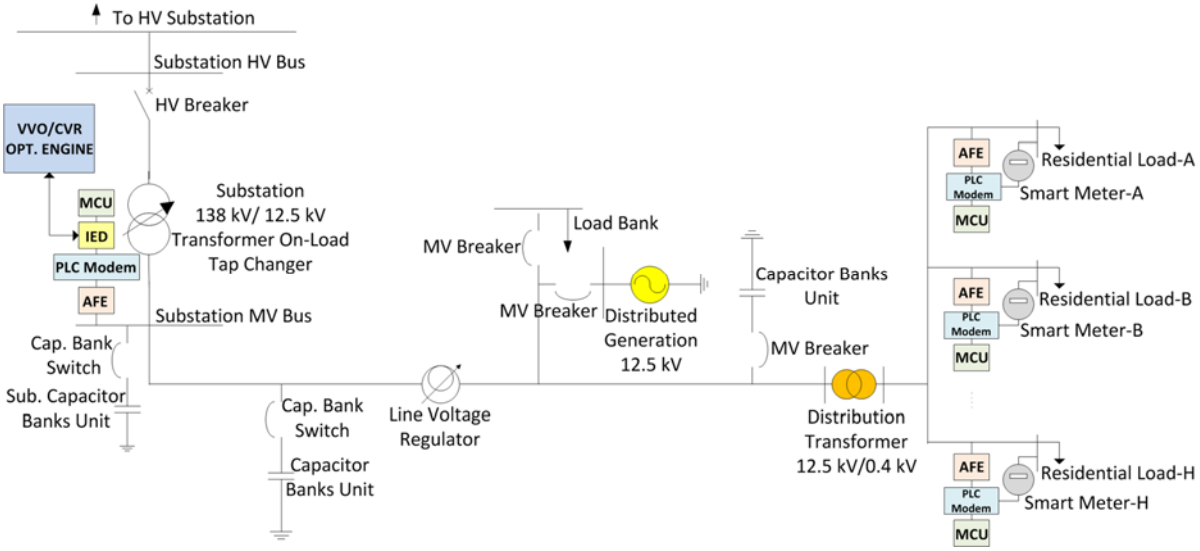

Figure 3.7. Main structure of proposed approach for VVO for a typical distribution feeder

Three optimization strategies can be adopted for the VVO algorithm according to grid planner or distribution feeder needs and/or objectives:

- VVO confined to distribution substation: First, the VVO algorithm confines VVO to the substation control devices such as OLTC and switchable shunt CB inside substation.
- VVO using VVCCs in substation and along distribution feeder: If the optimization objectives still not satisfied, the VVO engine uses VVCCs within distribution substation and along distribution feeder.
- VVO using other Volt-VAR control devices: In third step, the algorithm enables considering the role of DGs on voltage regulation and VAR injection. At each operating time interval, it checks the availability of DGs in microgrid in order to assist VVO according to DG priorities. The priorities are defined based on the effectiveness level of a DG in VVO application.

In future smart distribution networks, each node would be intelligent and would be able to control its system locally as a pre-emptive self-healing system. Hence, the adaptability of the VVO algorithm with future distributed control designs seems essential. Likewise distributed command and control topology, the proposed VVO is operates decentralized. Hence, the offered algorithm would be compatible with distributed

command and control structure of smart grids. Regarding other microgrid components such as EVs and V2Gs, Figure 3.8 illustrates the proposed VVO in the presence of EVs in distribution feeder. As smartening up of distribution network nodes are going to develop rapidly, designing a Distributed Command and Control topology for VVO in quasi real-time is conceivable. In a DCC structure, quasi real-time data are captured and filtered from termination points by data collectors and/or Multi Agent Systems. Then, the VVO engine optimizes the system and finds out the best configuration of the system at each quasi real-time interval. Configuration commands are being sent by VVO engine to VVCCs along distribution feeder. In a more complete view, this research proposes a VVO approach based on new smart microgrid features such as Distributed Command and Control and quasi real-time AMI.

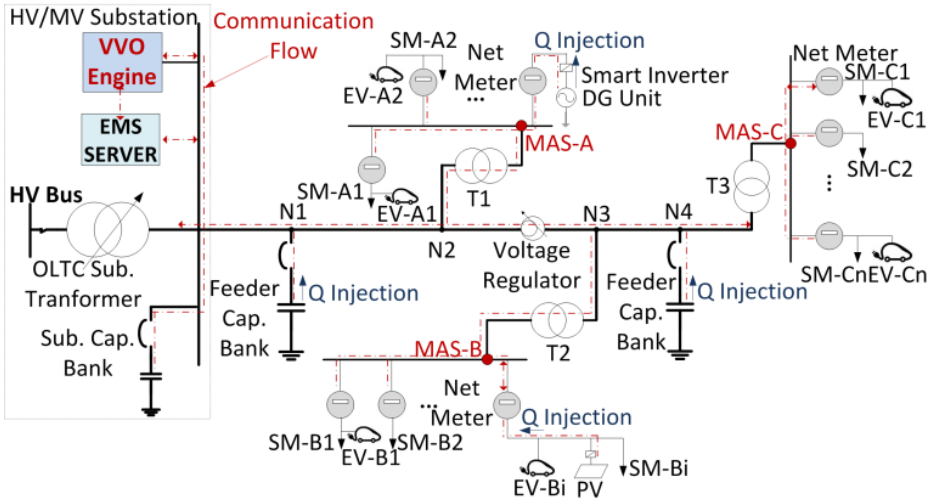

Figure 3.8. Topology of proposed VVO in a typical feeder with EVs

Figure 3.9 shows simplified topology of proposed VVO. Here, it is also assumed that distribution circuit is fed from an MV substation (as is mostly the case). As shown in Figure 3.9, quasi real-time local measurements do not need to travel from the field to the back-office and the new settings for VVO assets are determined locally, rather than by a centralized controller. This approach, might lead to less AMI cost, better system reliability and faster optimization process. Furthermore, this VVO strategy takes advantage of local dispatch-able energy sources such as V2G sources. Typically, local data that proposed VVO receives are active power, reactive power and voltages of system nodes. The global attributes that VVO engine receives from control center include, but not limited to weather forecast, calendar data, breaker's status, and feeder configuration. Thus, the proposed

technique consists of a quasi-real-time smart grid-based VVO engine that can readily control VVO in an integrated way through a DCC structure. Here, VVO engine tries to find the optimal setting of the abovementioned assets through system main variables. It performs power flow, calculates losses and follows load/energy consumption changes. The algorithm is also supported by selected measurements and different load profiles. It has to be mentioned that the operations of the smart distribution networks with high penetration of DERs significantly impact the operations of the transmission (and sometimes the generation) system.

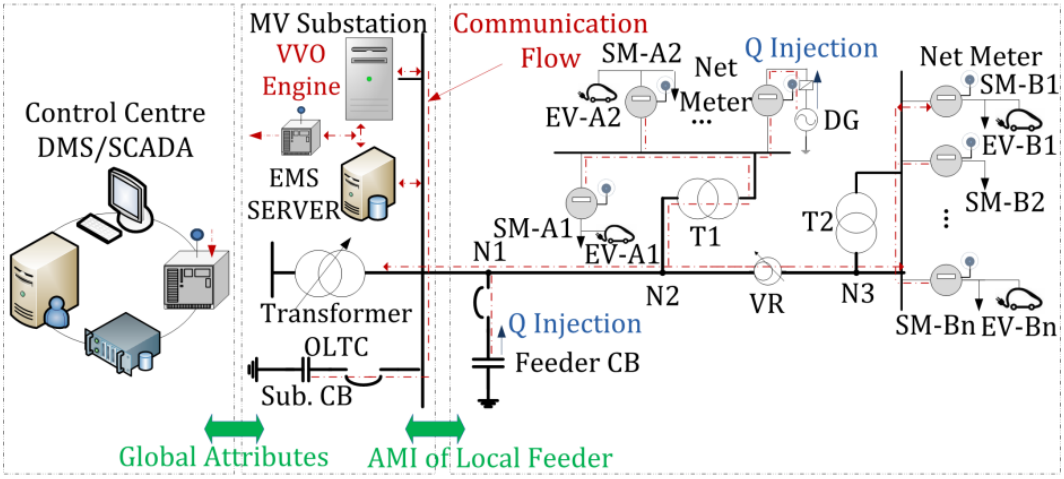

Figure 3.9. Basic Topology of Smartgrid adaptive VVO

Given the fact that the centralized VVO highly depends on network topology, a new approach which acts on feeder level could be an efficient alternative/additive solution. As discussed, the main differentiator between the two approaches is the availability of quasi-real-time local data that enables new class of optimization algorithms based on system local attributes. The proposed solution is able to track load changes using AMI data collected by smart meters at each operating time interval. Load changes could be calculated by the consumption data captured from meters. Moreover, the VVO engine is initially designed for a fixed distribution feeder, however it would be conceivable for the advanced VVO algorithm to observe feeder topology as global attributes that can be received from DMS/SCADA and/or breakers within the system and then, optimize the network with new configuration.

3.5. Predictive VVO Topology Considerations

Figure 3.10 depicts the main topology of the proposed predictive VVO in a typical distribution feeder from medium voltage substation down to the termination points. Data flow, as well as VVO command and probable VAR injection flows are shown in Figure 3.10. Three engines defined for proposed predictive VVO: VVO Engine, Prediction Engine and CVR Engine. VVO and CVR engines deal with system loss reduction and energy conservation respectively. The prediction engine that in here is Neural Network (NN) engine, aims to predict active/reactive consumptions of loads for the VVO engines.

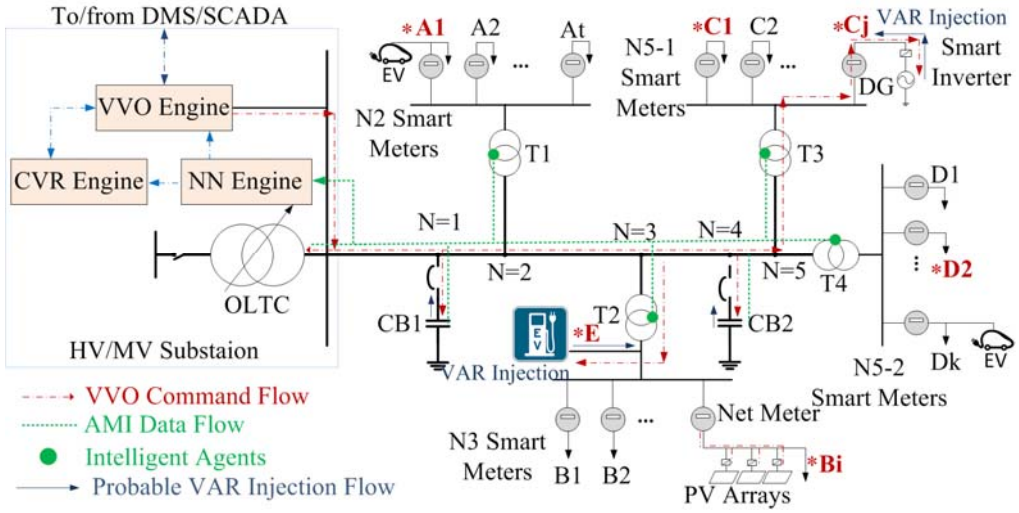

Figure 3.10. Main topology and data flows for presented predictive VVO

As proposed VVO, predictive VVO engine receives its required downstream data from data aggregators. It also obtains the required global attributes from DMS/SCADA and saves them to its database. Historical local AMI data has to be given to the system in order to predict the loads. The offline prediction engine initially predicts the active and reactive power loads of network load for each time stage of a day ahead. Then, VVO performs offline in order to find the optimal solution of distribution grid for day ahead. On targeted day, the VVO engine compares the result of predicted loads with real-time data measured by smart meters at each time interval. If the error rate is acceptable (typically, less than 5 percent) at specified time interval, the engine has already the optimal configuration of VVO assets to gain the optimal result. Hence, it sends control commands to VVCCs such as OLTCs, switchable CBs and VRs to optimize distribution network. If the error is high on that time stage, then a sliding window is going to be activated in order to

primarily find the optimal solution of system with new real-time data and secondarily update the following load prediction and VVO optimal configuration. Figure 3.11 shows the sliding window for predictive VVO solution.

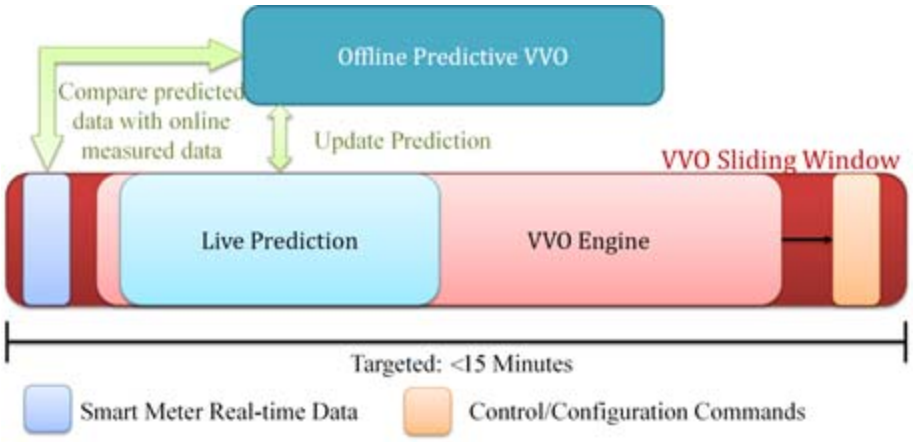

Figure 3.11. Predictive VVO solution using VVO sliding window

As shown in Fig. 8, a VVO sliding window will be activated when the predicted load is not following the real-time load accurately enough. The main task of the sliding window is to find the optimal solution of the grid in the time stage that high error happens and perform a live prediction for time stages ahead in order to update the results of offline prediction based on new collected real-time data. VVO online engine tries to find the best configuration of VVO assets within targeted frame (less than 15 minutes) based on new collected real-time data and the results of offline VVO. Then, it sends control commands to Volt-VAR control devices and updates the offline VVO after. Thus, the algorithm is designed in a way that could optimize smart grid and/or distribution networks locally through a dynamic prediction engine that is trained by different local factors such as active/reactive power of previous loads as well as some global attributes received from DMS/SCADA such as temperatures and dew points.

Chapter 4.

Volt-VAR Optimization Main Tool Features

As explained in previous section, one of the main targets of VVO solutions is to minimize distribution network losses. Typically, it is possible to classify network losses into technical and non-technical losses. Non-technical losses refer to losses that are independent from technical losses in the system. Electricity thefts, metering inaccuracies, component breakdown due to poor components maintenance or inaccurate calculation are examples of non-technical losses. The technical losses occur due to dissipation of energy in transmission, sub-transmission and distribution networks as well as transformer conductors. Transformer magnetic loss is considered as technical loss as well. As such, technical losses directly depend on system inherent characteristics and operational modes. The majority of technical losses occur in distribution networks. Hence, it is essential to initially understand technical losses in distribution networks and then try to minimize them through VVO techniques. Generally, there are two types of technical losses in distribution networks: fixed and variable. Fixed technical losses are typically shown themselves as constant heat or noise in energized distribution transformers. As this type of loss do not vary with current changes, it can be called “fixed”. Generally speaking, about 25 to 33 percent of technical losses are fixed [194]. Leakage current, dielectric, open-circuit, measurement and control device losses are some of the fixed losses in the system. Contrariwise, variable losses create 66 to 75 percent of technical losses [195]. They are proportional to the current squared.

As this type of loss is the most effective technical loss in distribution networks, this research main focus is on minimization of variable technical losses. Long distribution lines, distribution transformer placement far from load centers, low power/load factors of primary and secondary feeders, bad workmanships, inaccurate size selection of grid conductors and transformers inaccurate load balancing and phase balancing are some of the reasons of variable technical losses. From the abovementioned reasons, VVO techniques are mostly dealing with conductor, i.e. line/cable, loss as well as transformer loss directly. Moreover, VVO solution indirectly affects other reasons related to distribution network planning, such as conductor/transformer placement and size selection, fixed/switchable

capacitor and VR placements. Hence, this research tries to minimize distribution network line/transformer technical losses and investigates the impact of proposed VVO on planning problems of distribution networks.

As explained in previous sections, conventional VVCCs are the main tools of any VVO solution for loss reduction aim. Regarding VVCCs, voltage regulating components are typically installed in distribution feeders and at the main distribution substation. In some grids, substation transformer comprised of a tap changer that can regulate voltage of downstream feeder according to the load level condition. Voltage regulators are installed along distribution feeders to adjust voltage levels of specific nodes in the system. Reactive power control components such as CBs can be used in distribution substation and/or along distribution feeders to control reactive power flow of the system. As these conventional VVCCs have important role in distribution network VVO, studying their main features is indispensable.

4.1. Voltage Regulating Components

In order to maintain voltage level of system nodes within desired limits and to conserve energy according to CVR approach, voltage regulating tools such as OLTCs and VRs are used. Load tap changer of transformers and VRs are the most common voltage regulating tools in distribution grids. Step-type voltage regulating components are typically auto-transformers designed to adjust line voltage from -10 to +10 percent, i.e. per units, in 32 steps. In other words, each step has 5/8 percent of voltage regulation. If two internal coils of a voltage regulating tool be in series, it can adjust voltage up to/down to -10/+10 percent. When these coils are in parallel, the regulation range would be from -5 to +5 percent. Typically, each step-type voltage regulating device consists of two main parts: tap changing part and control part. Each voltage regulating device is equipped with required control system. Taps can be changed automatically under load condition through commands that are sending by voltage regulating device controller.

In general, controller regulates voltage levels as well as the Bandwidth (BW) according to the inputs that are received by potential and current transformers. This control system is comprised of three main settings: voltage set-point that shows desired output of

voltage regulating device, bandwidth that defines difference between the set voltage and measured voltage and Time Delay (TD) that presents the different between a time that voltage runs out of the bandwidth and the time that controller execute tap change. If the difference between measured and set voltages is more than half of the BW value, tap starts to change. Typically, TDs are in 10-20 seconds in conventional voltage regulating devices [196]. It has to be mentioned that some grids uses a type of voltage regulating device called “Auto-Booster” that is a kind of single-phase voltage regulating device with four tap steps. Each step of auto-booster has 1.5 to 2.5 percent voltage change that leads to 6 to 10 percent of regulation [196].

Voltage regulating devices such as VRs change the winding taps of their primary winding to regulate voltage of their secondary winding side, i.e. primary feeders. Distribution substation transformers can have off-load-type tap changer on the primary side and on-load tap changer on the secondary side to regulate voltage of downstream feeder(s). No-load tap changers also known as de-energized or off circuit tap changers, cannot be adjusted under load but Load or On-Load tap changers (LTCs/OLTCs) can operate without disconnection from the circuit. Hence, the availability of on-load tap changer for performing quasi real-time VVO is necessary. In OLTC design with high voltage rating, diverter switch and a tap selector design is used in general. For low voltage rating, selector switch mechanism is used. Voltage regulation in OLTCs with diverter switch and tap selector has two steps: first, a tap is pre-selected offline according to system voltage needs. Then, the diverter switch, changes switch OLTC to the new tap. Figure 4.1 shows an OLTC with diverter switch and tap selector structure. Nowadays, the switching time of diverter switch is between 40 and 60 milliseconds [198]. The total operational time of this type of OLTC is between 3 and 10 seconds [198]. Selector switch OLTCs, change the taps in only one step by rotating the main body of the switch. Figure 4.2 depicts these two OLTC mechanisms based on [198].

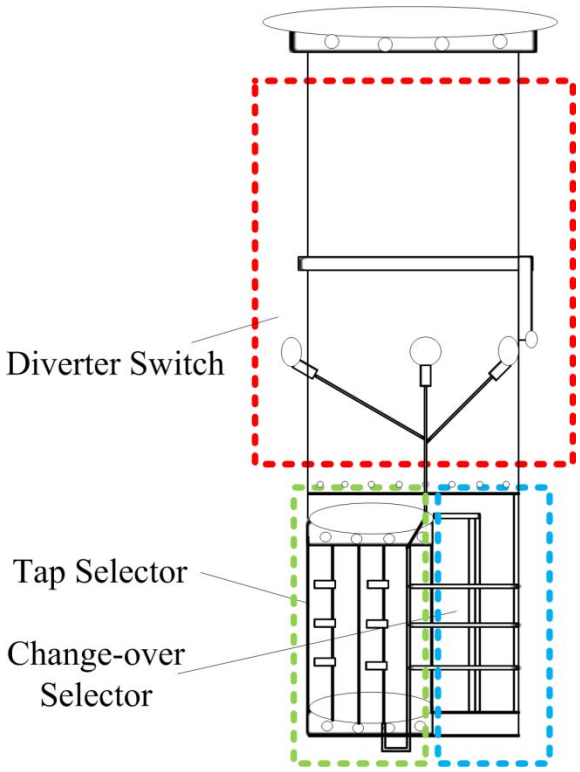

Figure 4.1. OLTC with diverter switch/tap selector structure

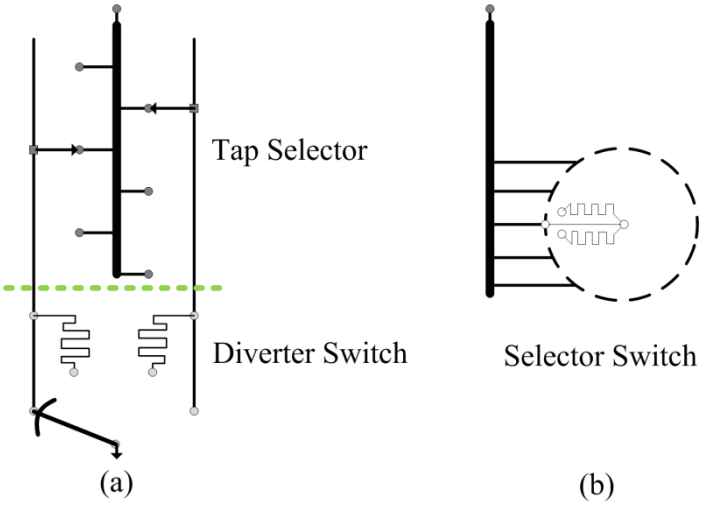

Figure 4.2. Diverter switch with tap selector OLTC (a) vs Selector Switch OLTC (b)

Conventional OLTCs are mainly resistive-based or reactive-based oil-type. According to their tap mechanism, both resistive-based and reactive-based OLTCs can be selector switch OLTC or diverter switch with tap selector OLTC. In recent years, new

vacuum type OLTCs that use vacuum switching technology. Nowadays, vacuum reactive LTCs (VRLTCs) are widely used in distribution substations.

Different types of voltage regulators are used in different locations along distribution feeder(s). Typically, 32-step single-phase VRs are widely used. Figure 4.3 represents a single-phase VR with its main parts.

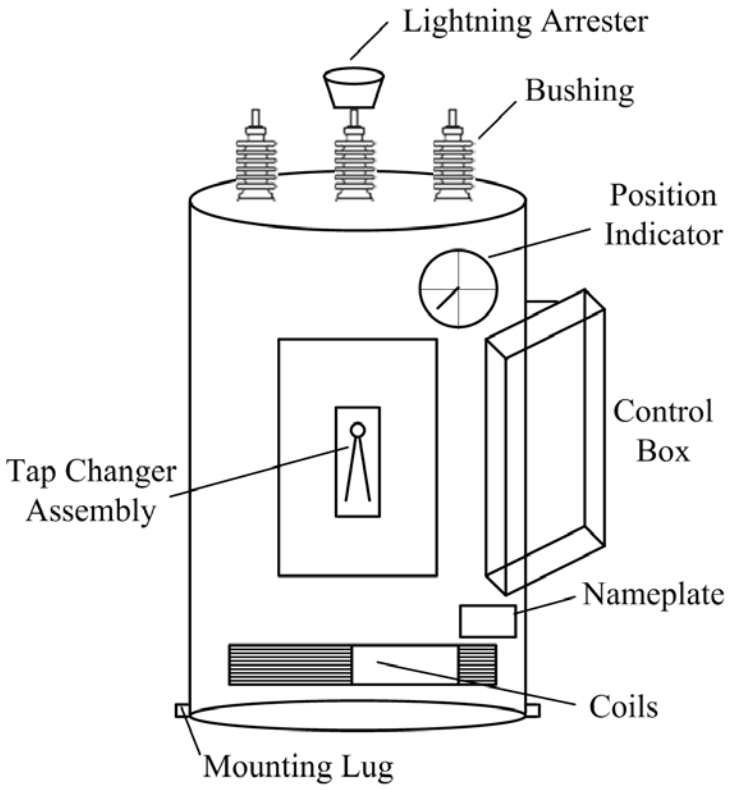

Figure 4.3. Single-phase VR different parts

Recent robust VRs can be operated for 20 years with about 2 million mechanical operations [200].The main types of VRs include but not limited to substation VRs and pole-mounted VRs. Three single phase VRs can be used to regulate voltage of a three phase system as well. Generally speaking, VRs try to maintain voltage at Regulating Point (RP) that is normally selected between VR and the end of the feeder. By performing CVR, VRs have to keep voltage of termination points within lower limits of ANSI band. Hence, the regulating point has to be intently selected. The automatic voltage control is typically obtained by adjusting resistance and reactance of VR control panel called “Line Drop Compensator” or “LDC”. Figure 4.4 shows the phasor diagram of control LDC of a VR

based on [196]. From Fig. 4 phasor, it is simply possible to find desired voltage at the load (V_L) by knowing the BW and TD values as well as knowing resistance (R_L) and reactance (X_L) values of LDC that are generally calibrated on control in volts (-24 V to +24 V). Resistance and reactance values for LDC can be found based on distribution feeder configuration.

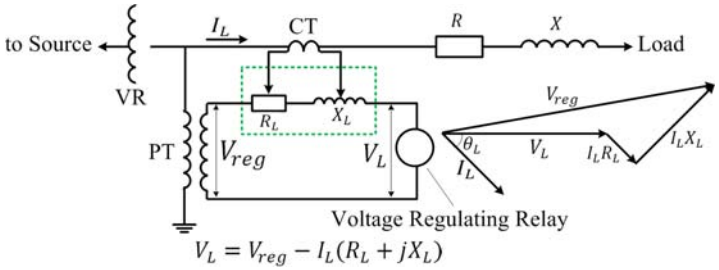

Figure 4.4. Phasor diagram of Line Drop Compensator of a Voltage Regulator

In VR without LDC, load voltage is highly affected by the load current magnitude. Using LDC help VR to define set-point regardless of load current magnitude. Figure 4.5 gives the difference between VR with LDC and VR without LDC. As it is shown in Figure 4.5, without LDC or a continuous control, voltage level of system will change to unwanted voltages during light-load conditions. It has to be stated that CVR tries to define load set-point in lower limits of ANSI standard, e.g. between 114 V and 120 V, to save the energy consumption. As rapid load changes may occur in distribution grids in real time, especially systems with high penetration of DERs, it seems essential to define a safety margin for lowering voltage of termination points through CVR to avoid voltage drop out of ANSI lower band.

4.2. Reactive Power Control Components

It is conceivable to say that shunt capacitors are the most installed reactive power control component in distribution systems. For many years, shunt capacitors have been used in distribution networks to regulate voltage and control reactive power flows of the grid. Nowadays, different shunt Capacitor Bank (CB) technologies are used for different smart grid optimization, and control aims such as VVO. Typically, shunt capacitor unit sizes are from 50 to 400 kVAR. Through banking process, they would be able to normally

supply 300 to 1800 kVAR in distribution systems [196]. Figure 4.6 shows a structure of a pole-mounted CB.

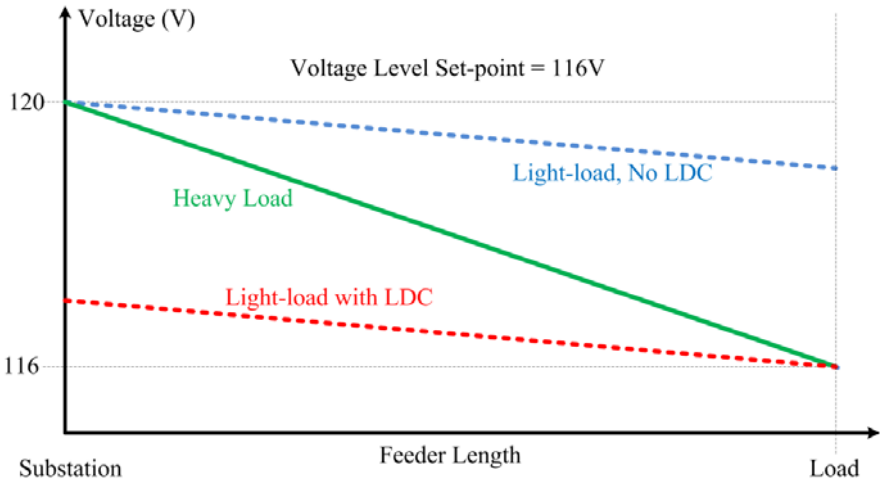

Figure 4.5. VR without LDC vs. VR with LDC Example

4.2.1. Capacitor Bank Types

In general, CBs are manufactured most in a single-phase structure. For three phase circuits, three single-phase CBs are connected to each other typically in Wye or Delta connection. There are three main types of CBs according to the configuration of CB fuses: fuse-less CB, CB with external fuses and CB with internal fuses. In fuse-less CBs, capacitor banks are initially connected as strings and then those strings are connected to each other in parallel. Figure 4.7 illustrates a fuse-less CB with two strings based on [202]. In this structure, if one of internal member of string fails, e.g. due to a short circuit, small current rise will occur on each capacitor unit. The reason lied in a fact that capacitor units at each string can be seen as series units connected to each other. The faulty unit can remain for a long period in the system as the faulty capacitor series group can operate in stable operating condition. Some of the key benefits of fuse-less CBs include but not limited to: need less substation space, less expensive and more resistive to external unpredicted outages. One disadvantages of this structure is that any bushing or internal fault lead CB to be switched off quickly because there is no fuse in the system. Moreover, CB should be turned off during loss of power of control relay.

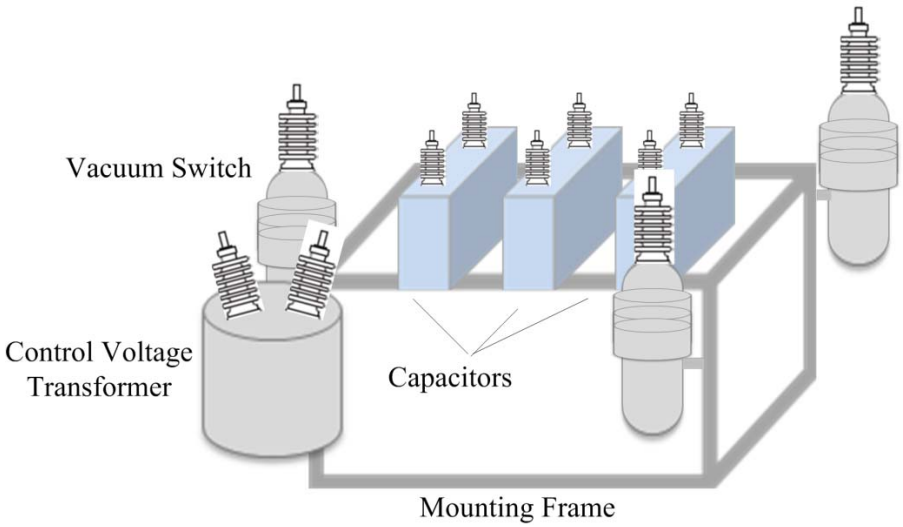

Figure 4.6. Pole-mounted Shunt Capacitor Bank

In CBs with external fuses, fuses are connected externally to capacitor. These fuses can isolate faulty capacitor unit in a bank. As such, other units can continuously operate in the system. Figure 4.8 shows structure of a CB with external fuse. This type of CB is commonly used in pole-mounted CBs of distribution grids. In three-phase system, when a capacitor unit fuse of a phase fails, voltages of other phases increase. In order to limit this overvoltage, limits for the kVAR size of capacitor units are defined in design of these CBs. The range size of these CBs is from 50 to 400 kVAR.

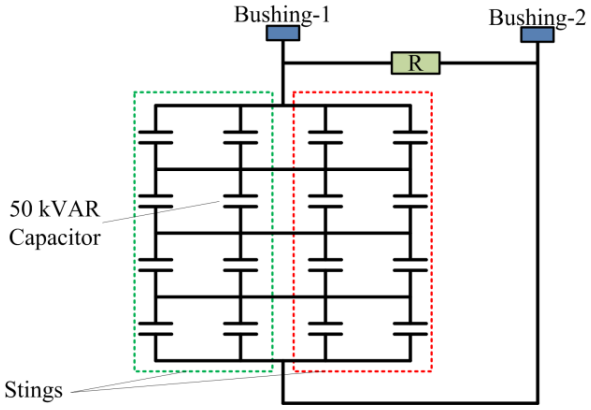

Figure 4.7. Fuse-less Capacitor Bank Structure

In CBs with internal fuses, the CB is built with parallel-series combination (Figure 4.8). Current limiting fuses are installed internally to isolate faulty capacitor unit. With this structure, the increasing voltage caused by faulty unit would be small. The main benefits of this CB type include but not limited to: CB and fuses are manufactured and tested

together, fuses are not affected by external factors, no harmful arcing in the system and proper working of other capacitor units when several units are short-circuited by an internal fault. The substantial problem of this CB type occurs when a couple of capacitor fuses fail. In this condition, the whole CB should be replaced.

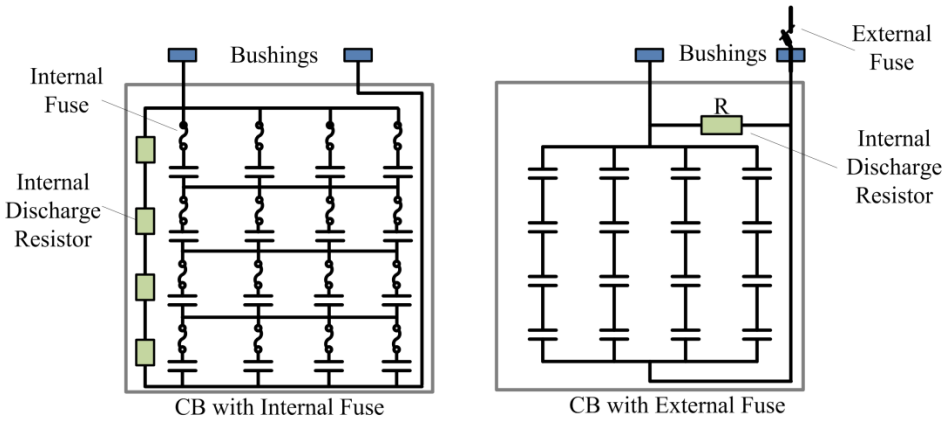

Figure 4.8. Capacitor Bank with Internal Fuse and External Fuse Structures

4.2.2. Capacitor Bank Specifications

The main specifications of CBs are given by standard [204]. Typically, CBs have to operate continuously without exceeding 120 percent of their Root Mean Square (RMS) voltage, 110 percent of their peak voltage, 180 percent of their RMS nominal current and 135 percent of their nameplate kVAR. Moreover, the kVAR of CB is proportional to system frequency. On the other hand, CBs are designed to operate continually without interruption in harsh environmental conditions. The acceptable 24 hours average and normal annual ambient temperatures are 40 and 25 degree of Celsius for metal enclosed or multiple row capacitors and 46 and 35 degree of Celsius for isolated or single row capacitors respectively. The bushing structure of single-phase CBs can typically be single or double bushing. Figure 4.9 shows single and double bushing structures of CBs based on [205]. In general single-phase CBs ranges from 20 to 1800 kVAR [196] use one or two bushing structures. Three-phase CBs typically have three-phase bushing design. Using shunt CBs in a feeder can reduce magnitude of source current which leads to improvement of voltage drop between source and load. Figure 4.10 gives the phasor diagram of a feeder with/without CB.

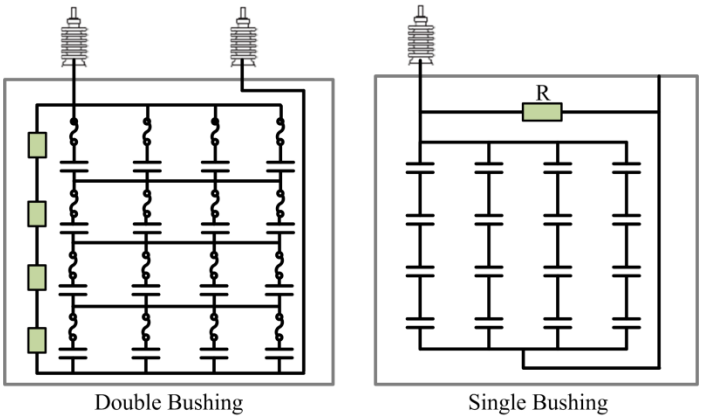

Figure 4.9. Capacitor Bank with Single and Double Bushing Structures

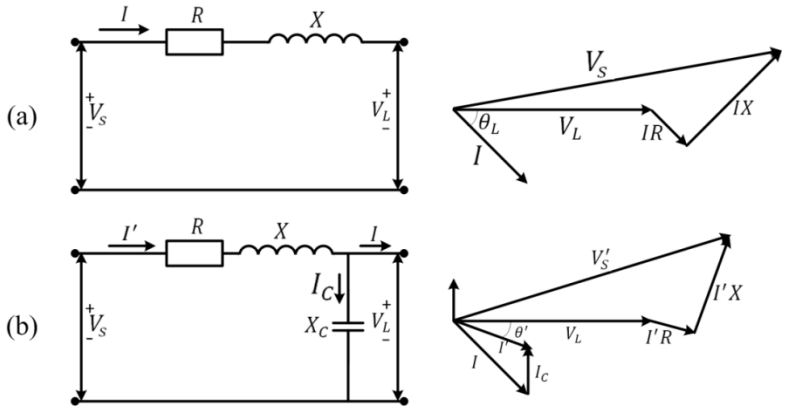

Figure 4.10. Phasor diagrams of system without capacitor (a) and with capacitor (b)

4.2.3. Shunt Capacitor Bank Location/Type Considerations

Generally, CB can be located in different part of a distribution feeder. It can regulate reactive power of a group of loads, a feeder branch or a local load. Hence, shunt CBs reduce maximum kVA demand, KVA demand, improve feeder voltage profile and reduce feeder loss. Pole-mounted CBs are the most applied shunt CBs in distribution networks. As shown in Figure 4.6, CB vacuum/oil switches, controller, and control transformer are the main parts of pole-mounted CBs. The voltage rating of pole-mounted CBs is typically from 460 V to 33 kV [196]. The available sizes are in wide range of 300-3000 kVAR [196]. Other shunt-CBs such as substation CBs are used in HV/MV substation as well. Metal-enclosed CBs are normally used in small substations or industrial fields. This type of CB has very high lifetime and less maintenance rather than other types of CBs as external environmental factors cannot affect their performances. Pad-mounted

CBs that are in metal enclosure are also common in North America. When system needs reactive power compensation, portable or mobile CBs that are typically mounted on a mobile truck are available in single and three-phase to decrease overloaded facilities and/or regions of a distribution grid.

4.2.4. Shunt Capacitor Bank Configuration

Shunt CBs have different configurations according to system design, protection and operation schemes. Figure 4.11 represents some of common shunt CB configurations such as Grounded Wye, Ungrounded Wye, Delta and Split-Wye.

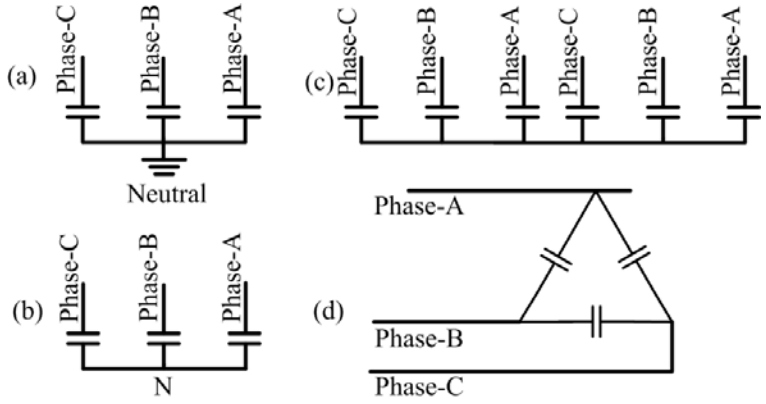

Figure 4.11. Shunt CB configurations

Note. (a) Grounded Wye, (b) Ungrounded Wye, (c) Split-Wye and (d) Delta Fixed Shunt Capacitor Bank vs. Switchable Shunt Capacitor Bank

Fixed shunt CBs are typically used for system base kVAR to inject certain amount of reactive power continuously throughout a long-term period of time. Fixed shunt CBs are applied in industries with constant/semi-constant loads as well. Figure 4.12 presents the effect of fixed CB on voltage of a distributed load feeder. It can be resulted from Figure 4.12 that using only fixed CBs in a system may result to overvoltage issues in light-load conditions.

Moreover, it would not be possible to follow reactive power needs of the system as load varies throughout a day. That is the reason switchable shunt CBs are used in distribution networks. Switchable shunt CBs can be switched on/off in different load conditions. As such, fixed CBs have to be used to support light-load condition while

switchable shunt CBs has to be used to control kVAR of the system in other operational times. Figure 4.13 shows an example of fixed and switchable shunt CB usage to meet reactive power demand. In switchable shunt CB, typical conventional control signals for the switch are voltage, current, kVAR demand, power factor and time [196].

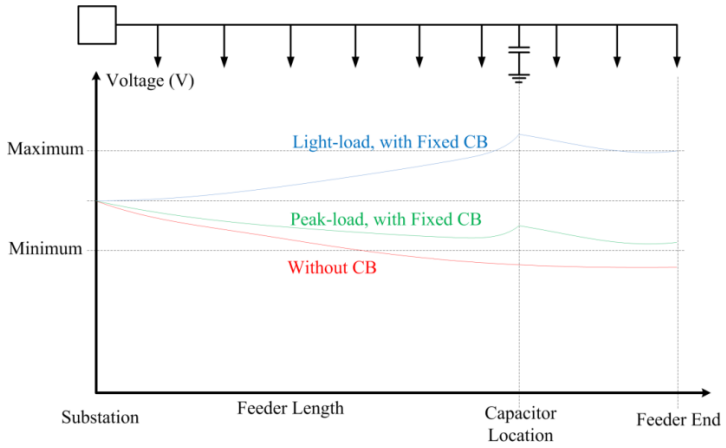

Figure 4.12. The effect of fixed CB on voltage of a distributed load feeder

Different switchable shunt CB configurations exist according to the switch, i.e. circuit breaker, design. Figure 4.14 represents some of the typical switchable CB configurations.

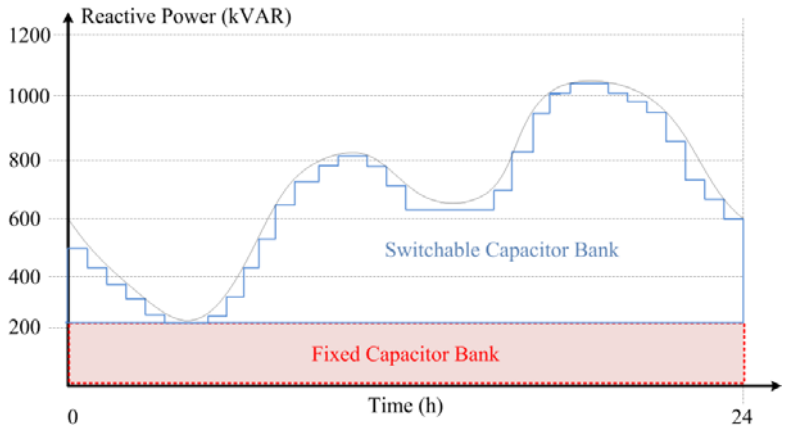

Figure 4.13. Fixed and switchable shunt CB operating areas

For Volt-VAR Optimization purposes, switchable shunt capacitor banks are used to regulate voltage and control reactive power of the system during different operating time intervals. Adequate control systems, i.e. controllers, have to be joined with switchable shunt CBs to send switching commands (opening or closing) to the banks.

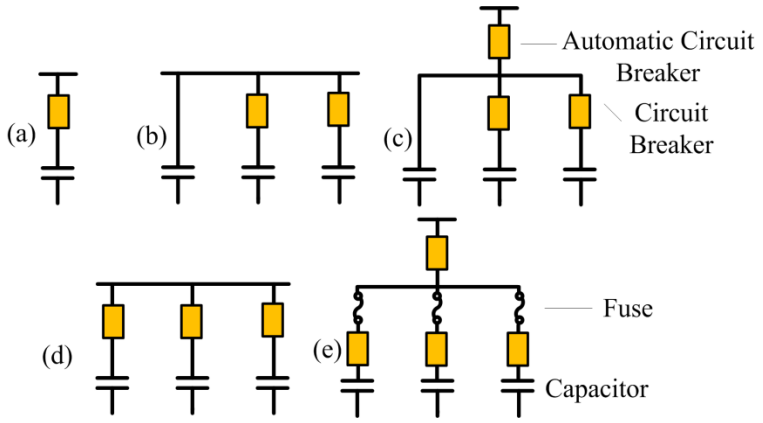

Figure 4.14. Switchable Shunt CB configurations

Note. (a) Simple bank, (b) bank with/without breaker, (c) bank with/without breaker by automatic circuit breaker (d) banks with breakers, and (e) banks with fuse, breakers and automatic circuit breaker

4.2.5. Switchable Shunt Capacitor Bank Controller

Typical switchable shunt CB control parameters include but not limited to: voltage (for voltage regulation), current (proportional to VAR demand), kVAR control (when load increases, demand increases in general), switch time (switch banks in different load conditions), and temperature (in some loads, kVAR demand raises by increasing temperature).

New automatic CB controllers have recently provided two-way communication structure for smart grid applications. These switchable shunt CBs can now be switched on/off locally and remotely. Remote control is available through SCADA where switching commands are sent from control center through famed communication protocols such as DNP3. Moreover, recent switchable shunt CBs provide extensive data logging (normally up-to 10000 events [207]-[208]) that can be downloaded such as temperature, voltage, current, power factor, kVAR, kW, neutral current and voltage, number of switching per cycle, time schedule. Data logging can typically be set from 1 to 60 minutes time intervals for 2 to 120 consecutive operating days [207]-[208]. Recent typical CB controllers are comprised of several important parts such as plate LCD to locally view real-time values, set-points and historical data, LED buttons that show live status of the CB control plan, USB and/or TCP/IP ports to receive and download CB memory data to an external computer and/or intelligent device, and memory that is the core of CB control which takes

responsibility of whole CB switching actions. Most recent CBs are capable of using IEC 61850 as their communication standard [209]-[210].

From the abovementioned studies, it is possible to define three main Volt-VAR control assets for performing novel smart grid-based Volt-VAR Optimization: OLTC, VR and switchable shunt CBs. As recent technologies of these VVCCs are able to receive control commands remotely from a DMS/SCADA, it would be possible to design a VVO engine to send control commands to these components in the system in quasi real time. Proper communication standard/protocol has to be defined and reliable and secure communication pipes have to be selected for implementing such a VVO that is operating with explained VVCCs.

Chapter 5.

VVO Objective Function and Constraints

As stated in previous section, the main objective of this research is to design an efficient real-time smart grid adaptive Volt-VAR Optimization algorithm to minimize distribution feeder losses, improve voltage profile and conserve energy intermittently. In order to construct a smart grid adaptive algorithm, it is necessary to study various types of distributed generations and renewable resources. Hence, natural and diesel gas engines, Flywheel Energy Storage Systems (FESS), EVs, Micro-CHPs and PVs are covered in different sections of this research. Moreover, other microgrid features such as V2G (vehicle to grid) and/or G2V (grid to vehicle) effects, data capturing from smart and/or revenue meters impact on VVO are taken into account. All abovementioned technologies consist of technical/economic constraints that may affect VVO objectives.

Another key factor in proposed VVO objective is to study available Volt-VAR control devices in distribution networks comprehensively. In order to design an integrated algorithm, on-load tap changer of distribution transformers, fixed and switchable shunt CBs, VRs and other VVO control devices studied thoroughly and their limitations considered as VVO problem constraints. Moreover, proposed VVO algorithm need to be matched with AMI data capturing time intervals. As explained before, typical smart metering infrastructures are set to capture data every 15 minutes although they are capable of sending data every 5 minutes. In this research, both AMI time intervals are used in different studies.

Generally speaking, a VVO algorithm strives to minimize network power loss and improve voltage profile of the system. This could be the basis of any VVO objective. Distribution network loss consists of two main parts: active and reactive. The active power loss (Ohmic loss) of the system mostly related to distribution lines and cables. As the active power consumed by customers' devices, most studies have focused on the active power loss minimization. On the contrary, the reactive power is a real concept employed to explain the backside energy flow in an AC system which is the production of electric and magnetic fields. Some of distribution system's reactive power resources include but

not limited to: synchronous generators/compensators, inductive/capacitive compensators, overhead lines, underground cables, transformers and inductive and/or capacitive loads. Reactive power in the system occupies the capacity of lines and prevents transferring pure active power from the sources to the network consumers. Moreover, the power flow study is an important tool for analysing distribution systems in steady-state operation. Power flow techniques try to find the optimal flow of the system and in some cases find a mode which gives the lowest cost per kilowatt-hour delivered to grid customers. The main goal of a power flow study is to obtain voltage, angle and magnitude of each bus in a power system in a specific power and voltage of system load and generator. Once these values are being found, real and reactive power flow on each branch of a feeder as well as generator reactive power output can be determined by power flow analytic approaches. Therefore, power flow study is one of the substantial parts of proposed VVO algorithm. Conventional three-phase power flow as well as Back-ward Forward Sweep (BFS) methods is used for different studies of this research. In a more comprehensive objective function, CVR would be a part of VVO engine. In order to build a CVR program as a part of VVO, it is necessary to initially characterize loads as various loads have different impacts on CVR performance. This research employed ZIP (Z: constant impedance, I: constant current, and P: constant power) load modeling in order to model different types of load in a distribution grid. Feeder load profiles can be derived in order to analyse feeder mixed load. Furthermore, CVR has to be defined in VVO objective to let the algorithm focus on energy consumption reduction, peak demand reduction or both.

As cited, most of the energy loss that occurs in a distribution system is Ohmic loss caused by the electric current flow through grid conductors but, the other loss which is worthy of consideration in VVO is transformer loss. Transformer loss consists of Ohmic (resistive/copper) and Core (iron) losses. Typically, the core loss in a transformer is larger (in magnitude) than the copper loss. Losses in transformers (excluding associated circuitry) vary with current of the load, which called "no-load" and/or "full-load" loss. Winding resistance is the key generator of transformer full-load load losses and more than 99% of the no-load loss is generated by hysteresis and eddy current losses. Moreover, transformer losses can be classified into two losses, one in the windings, called “copper loss”, and one in the magnetic circuit, called “core loss”. This research tries to consider transformer loss in its VVO objective in one of its studies. More details regarding

transformer loss calculations can be found in the Appendix C of this thesis. The main constraint of VVO problem could be summarized as: power flow constraints, generation limits, consumption limits, standard voltage limits, VVCC limits and smart grid-related constraints.

5.1. VVO Initial Objective Function

VVO engine is responsible for optimizing voltage, active and reactive power of the smart grid accordingly. Thus, the initial objective of the VVO engine can be the minimization of total apparent power loss (S) of distribution networks in quasi real-time intervals (kVA). This initial objective function can be seen in (5-1). $\forall t \in T$:

$$Min\{S_{f,t}^{i}\} = min\{({P_{loss,total}}^{2} + {Q_{loss,total}}^{2})^{0.5}\} \quad (5\text{-}1)$$

At each quasi real-time interval, total active and reactive power losses can be found by (5-2) and (5-3).

$$P_{loss,total} = \sum_{f=1}^{F} P_{loss,f,t} \quad (5\text{-}2)$$

$$Q_{loss,total} = \sum_{f=1}^{F} Q_{loss,f,t} \quad (5\text{-}3)$$

Here, $P_{loss,f,t}$, and $Q_{loss,f,t}$ are the active and reactive power losses of feeder line-*f* and time-interval-*t*. In addition, F denotes the last feeder line. If loss cost (C_{loss}) take into account, the main objective function can be written as (5-4).

$$Min\ S_{Loss} = Min\ (C_{loss} \times S) = Min\ (C_{loss}(\sqrt{P_{loss,total}^{2} + Q_{loss,total}^{2}})) \quad (5\text{-}4)$$

5.2. VVO Main Constraints

The active and the reactive power loss determination method based on power flow equations are given in (5-4) to (5-7). Proofs of these equations are shown in Appendix A.

$$\sum_{f=1}^{F} P_{loss,f,t} = \sum_{f=1}^{F} \begin{Bmatrix} G_{f,t}\begin{bmatrix}(\alpha_{ij,t}V_{i,t})^2 + (\alpha_{ji,t}V_{j,t})^2 - \\ 2\alpha_{ij,t}V_{i,t}\alpha_{ji,t}V_{j,t}\cos\theta_{ij,t}\end{bmatrix} \\ +G^0_{ij,t}(\alpha_{ij,t}V_{i,t})^2 + G^0_{ji,t}(\alpha_{ji,t}V_{j,t})^2 \end{Bmatrix} \quad (5\text{-}5)$$

Here, $f = i - j$

$$\sum_{f=1}^{F} Q_{loss,f,t} = \sum_{f=1}^{F} \begin{Bmatrix} -B_{f,t}\begin{bmatrix}(\alpha_{ij,t}V_{i,t})^2 + (\alpha_{ji,t}V_{j,t})^2 - \\ 2\alpha_{ij,t}V_{i,t}\alpha_{ji,t}V_{j,t}\cos\theta_{ij,t}\end{bmatrix} \\ -B^0_{ij,t}(\alpha_{ij,t}V_{i,t})^2 - B^0_{ji,t}(\alpha_{ji,t}V_{j,t})^2 \end{Bmatrix} \quad (5\text{-}6)$$

$$Y_{f,t} = G_{f,t} + jB_{f,t} \quad (5\text{-}7)$$

$$g_{ij,t} + jb_{ij,t} = \begin{cases} \sum_{j\in J} \alpha^2_{ij,t}\left(Y_{ij,t} + Y^0_{ij,t}\right) & i = j \\ -\alpha_{ij,t}\alpha_{ji,t}Y_{ij,t} & i \neq j \end{cases} \quad (5\text{-}8)$$

Here,V is the bus voltage magnitude, $G_{f,t}$is the Conductance vector of feeder line-*f* in per units [PU], $i, j$are neighbour buses, $\alpha_{ij,t}$is the acceleration factor, $\theta_{ij,t}$is the phase angle between bus-*i* and *j* in time-*t*, $B_{f,t}$ is Susceptance vector of feeder line-*f* in per units [PU], Susceptance matrix between bus-*i* and bus- *j,* $b_{ij,t}$ is Susceptance matrix between bus-*i* and bus- *j*, $g_{ij,t}$ is Conductance matrix between bus-*i* and bus- *j*, $Y_{f,t}$ is Admittance of feeder line-*f* at time-*t* [PU]. On the other hand, main required constraints for solving integrated VVO in quasi real-time intervals are as follows:

5.2.1. Bus voltage magnitude constraint

Constraint of (5-9) explains the fact that the voltage of each node of the system has to be between minimum and maximum desired values. ANSI-C84.1 [1] defines

standard minimum of 0.95 per units and maximum of 1.05 per units for distribution networks.

$$V_{i,t}^{min} \leq V_{i,t} \leq V_{i,t}^{max} \xrightarrow{ANSI-C\ 84.1} 0.95\ P.U \leq V_{ir,t} \leq 1.05\ P.U \quad (5\text{-}9)$$

5.2.2. Active/Reactive power output constraints

It is known that each node has to be within active and reactive powers of its limit. This fact creates operational limits for the nodes of the system. As such, (5-10) and (5-11) shows minimum and maximum active/reactive power limits of nodes.

$$P_t^{min} \leq P_t \leq P_t^{max} \quad (5\text{-}10)$$

$$Q_t^{min} \leq Q_t \leq Q_t^{max} \quad (5\text{-}11)$$

Here, $P$is the active power (kW), and $Q$is the reactive power (kVAR), The same concept can be used for nodes with generators (g) and DGs. Hence, (5-12) and (5-13) give the active/reactive power output constraints for nodes with DG. In (5-12) and (5-13), DG denotes Distributed Generation. These constraints show that the active and reactive power of nodes with DGs has to be within minimum and maximum limits.

$$P_{DGi,t}^{min} \leq P_{DGi,t} \leq P_{DGi,t}^{max} \quad (5\text{-}12)$$

$$Q_{DGi,t}^{min} \leq Q_{DGi,t} \leq Q_{DGi,t}^{max} \quad (5\text{-}13)$$

5.2.3. Power (thermal) limits of the feeder constraint

The maximum kVAs that can be transferred through grid branches, i.e. lines and cables, have to be considered due to the thermal limitation that branch material has. Exceeding above this limit would damage distribution network lines and/or cables.

$$S_{f,t} \leq S_{f,t}^{max} \quad (5\text{-}14)$$

Here, $S_{f,t}$ is feeder line-*f* kVA at time-*t*, $S_{f,t}^{max}$shows the maximum thermal limit of line-*f*.

5.2.4. Active/Reactive power balance constraint

Constraint (5-15) and (5-16) show that active/reactive powers have to be balanced at each node of the system due to the optimal power flow equations. In order to find the active ($P_{i,t}$) and the reactive power ($Q_{i,t}$) of system nodes, different methods can be used depends on optimal power flow method. A typical power flow uses (5-17) and (5-18) to obtain active and reactive power of system nodes.

$$P_{i,t} = P_{Gi,t} - P_{Li,t} \quad (5\text{-}15)$$

$$Q_{i,t} = Q_{Gi,t} - Q_{Li,t} + Q_{CB,c,t} \quad (5\text{-}16)$$

$$P_{i,t} = P_{Gi,t} - P_{Li,t} = \sum_{j}^{J} V_{i,t}V_{j,t}(g_{ij,t}\, cos\, \theta_{ij,t} + b_{ij,t}\, sin\, \theta_{ij,t}) \quad (5\text{-}17)$$

$$Q_{i,t} = Q_{Gi,t} - Q_{Li,t} = \sum_{j}^{J} V_{i,t}V_{j,t}(g_{ij,t}\, sin\, \theta_{ij,t} + b_{ij,t}\, cos\, \theta_{ij,t}) \quad (5\text{-}18)$$

Here, G is generator, L is load, $Q_{CB,c,t}$is reactive power injection of CB-*c* at time-*t*.

5.2.5. System Power Factor (PF) constraint

In some operational conditions, distribution network operator needs to maintain Power Factor of node of a system ($PF_{i,t}$) within desired limits (between $PF_{i,t}^{min}$ and$PF_{i,t}^{max}$). For this reason, (5-19) can be used.

$$PF_{i,t}^{min} \leq \left|PF_{i,t}\right| \leq PF_{i,t}^{max} \quad (5\text{-}19)$$

5.2.6. Transformer tap changer constraints

Transformer taps are limited. Hence, power flow should consider this limit as a constraint. Moreover, each transformer tap-step is able to level-up/level-down voltage in specific range ($\Delta V_{tr,t}$). As such, (5-20) and (5-21) has to be followed in the optimal power flow. Hence, the variables are OLTC taps.

$$\gamma_{tr,t} = 1 + tap_{tr,t}\frac{\Delta V_{tr,t}}{100} = \text{Turn ratio of OLTC} \quad (5\text{-}20)$$

$$tap_{tr,t} \in \left\{-{tap_{tr,t}}^{max}, \dots, -1, 0, 1, \dots, {tap_{tr,t}}^{max}\right\} \quad (5\text{-}21)$$

For OLTCs with 32 taps, tap-steps are equal to: $\Delta V_{tr,t} = 3125\%$. For offline studies, it is possible to consider maximum number of switching of OLTC per time interval, e.g. in a whole day. For this reason (5-22) can be used.

$$\sum_{t=1}^{T} N_{tr,t} \leq N_{max\,tr,t} \quad (5\text{-}22)$$

Here, $tap_{tr,t}$is transformer OLTC tap unit, $\gamma_{tr,t}$is the off-nominal turns ratio of OLTC, ${tap_{tr,t}}^{max}$is the maximum tap of OLTC, $N_{tr,t}$, is number of OLTC tap switching, and $N_{\max tr,t}$is the maximum number of OLTC tap switching from time interval-*t* to time interval-*T*.

5.2.7. Voltage regulator constraints

Similar to OLTC constraints, VR taps are limited as well. Moreover, each VR tap-step is able to increase/decrease voltage in specific range ($\Delta V_{tr,t}$). As such, (5-23) and (5-24) has to be followed in the power flow. Here, the variables are VR taps.

$$\gamma_{vr,t} = 1 + tap_{vr,t}\frac{\Delta V_{vr,t}}{100} = \text{Turn ratio of VR} \quad (5\text{-}23)$$

$$tap_{vr,t} \in \{-{tap_{vr,t}}^{max}, \dots, -1, 0, 1, \dots, {tap_{vr,t}}^{max}\} \quad (5\text{-}24)$$

For VRs with 32 taps, tap-step is equal to: $\Delta V_{tr,t} = 0.3125\%$ and for VRs with 16 taps, this value is equal to: $\Delta V_{tr,t} = \%0.625$. For offline studies, considering maximum number of switching of VR per time interval shown in (5-25) seems necessary.

$$\sum_{t=1}^{T} N_{vr,t}^{i} \leq N_{max\ vr,t}^{i} \quad (5\text{-}25)$$

Here, $tap_{vr,t}$is VR tap unit, $\gamma_{vr,t}$is the off-nominal turn ratio of VR, ${tap_{vr,t}}^{max}$is the maximum tap of VR, $N_{vr,t}$, is number of VR tap switching, and $N_{\max vr,t}$is the maximum number of VR tap switching located at bus-*i* from time interval-*t* to time interval-*T*.

5.2.8. Capacitor bank constraints

For Capacitor bank constraint, it is possible to consider each CB with $\beta_{c,t}^{max}$ banks such that each bank has $\Delta q_{c,t}^{i}$ kVAR capacity as shown in (5-26). Thus, CB total capacity ($Q_{c,t}^{i}$) can be obtained by (5-26). Here, $\beta_{c,t}^{max}$is the maximum bank of each CB. Moreover, (5-27) has to be followed in order to meet the reactive power demand such that the total reactive power provided by CBs does not exceed the required reactive power of the system. This could avoid overcompensation issue in the system, especially in light-load conditions. The maximum value ($Q_{max,t}^{i}$) are typically found by distribution network planners while finding optimal location and size of fixed and shunt CBs in the system. Here, Idenotes last bus with CB. If there is number of switching per day limit for CB, (5-28) can be used. In (5-28), $N_{CB,t}$is switching number and $SW_{cb}^{max}$is the maximum permitted number of switching of that CB in a day. Hence, the variables are banks of CB.

$$Q_{c,t}^{i} = \beta_{c,t}^{i} \Delta q_{c,t}^{i}, \quad \beta_{c,t}^{i} = \{0,1,2,\dots,\beta_{c,t}^{max}\} \tag{5-26}$$

$$\sum_{i=1}^{I} Q_{c,t}^{i} \leq \sum_{i=1}^{I} Q_{max,t}^{i} \tag{5-27}$$

$$SWcb = \sum_{t=1}^{T=96} {N_{CB,t}}^{i} \leq SW_{cb}^{max} \tag{5-28}$$

5.3. Moving Towards Comprehensive VVO Objective Function

In order to reach to a comprehensive VVO objective function, other VVO sub-parts as well as constraints have to be taken into account. Each VVO study requires its own objective and constraints due to network topology, available components and operational condition. In some studies, VVO needs to minimize voltage deviation of system nodes as well. This could lead system to reach to operator set-points with less voltage deviation. In other words, by putting this sub-part in VVO objective function, it is possible to force VVCCs in a system to keep voltages of system nodes around desired set-point. This can be written as (5-29).

$$Min\ O.F = \sum_{l=1}^{l=L} S_{LOSS,l} + \frac{1}{2} \times \sum_{i=1}^{i=I} |V_{base} - V_i|^2 \tag{5-29}$$

Here, $S_{LOSS,l}$is the apparent power loss of each line. In addition, Ldenotes last line of the system and $V_{base}$is voltage set-point and $V_i$is the voltage of node-*i*. In another case, while capacitor operating cost is as important as loss cost, it is possible for VVO to minimize the operating cost of CBs in the system by putting it as a VVO sub-part shown in (5-30). In V2G study, VVO can also consider the operating costs of V2Gs (C_{Q-V2G}) that can inject reactive power to the system in its objective function as (5-31). In (5-31), the first sub-part of the objective function shows energy loss cost of the system.

$$\forall t \epsilon T, \qquad Min\, O.F_f = min\left\{(C_l(\sum_{i=1}^{I} P_{loss,l})) + (C_{CB}(\sum_{i=1}^{I} Q_{CB,i}))\right\} \tag{5-30}$$

$$Min\, O.F_{f,t,new} = Min\left\{(C_l(\sum_{i=1}^{I} P_{loss,l}\Delta T)) + (C_{CB}(\sum_{i=1}^{I} Q_{CB,i})) + (C_{Q-V2G}(\sum_{i=1}^{I} Q_{V2G,i}))\right\} \tag{5-31}$$

Here, $O.F_f$is the objective function of studied feeder, $C_l$is the loss cost of line-*l* ($/kW), $C_{CB}$is the operating cost of CB located at bus-*i* ($/kVAR), $\Delta T$is the operating time interval, and $Q_{V2G,i}$is the reactive power injected by V2G at bus-*i*. As stated before, it is now conceivable to see CVR as a part of VVO objective. For this reason, different objective functions can be used for the VVO engine. First, a maximization problem can be defined for VVO engine as presented in (5-32). This objective function maximizes loss cost saving and CVR values.

$$O.F = Max\big((C_o - C_{lo}) + \Delta C_{CVR}\big) \tag{5-32}$$

Here, C_o is the initial loss cost of the system without VVO ($), $C_{lo}$is the loss and the operating costs of CBs and $\Delta C_{CVR}$is the value of saved energy by employing CVR method ($). As such, system loss costs (C_{lo}) can be found using (5-33).

$$C_{lo} = \sum_{t=1}^{T=96} \sum_{i=1}^{I} [\big(P_{loss\ i,t} \times C_{loss,t}\big) + (Q_{CB\ i,t} \times C_{CB,t})] + \sum_{t=1}^{T=96} C_{CVR-cost,t} \tag{5-33}$$

Here, $P_{loss\ i,t}$shows the active power loss of node-*i* at time stage-*t* (kW), $C_{loss,t}$gives the loss cost of the grid ($/kW), $Q_{CB\ i,t}$ is the kVAR of switchable CB (kVAR), $C_{CB,t}$ is the operating cost of CB at time interval-*t* ($/kVAR) and $C_{CVR-cost,t}$is the operating cost of CVR using OLTC or VR ($). Moreover, i denotes node numbers (*i*=1:*I*) and *t* denotes time intervals (*t*=1:*T*). Here, *T* can be equal to 96 time intervals if the study is for

a complete day and data capturing time intervals are set every15 minutes. Another VVO objective function considering CVR voltage constraint can be written as (5-34). In (5-34), the VVO engine tries to minimize distribution network line losses ($S_{LOSS,l}$), minimize voltage deviation of the system from the set-point and minimize the voltage difference between the last node of the system (V_{END}) and CVR voltage set-point (V_{CVR}) that typically is in lower limits of ANSI band. Moreover, (5-34) can minimize transformer loss (P_{Trans}) exists in the system.

$$O.F = \sum_{l=1}^{l=L} S_{LOSS,l} + \frac{1}{2} \times \sum_{i=1}^{i=I} |V_{base} - V_i|^2 + \sum_{e=1}^{e=E} |V_{END} - V_{CVR}| + (P_{Trans}) \quad (5\text{-}34)$$

In order to construct a more complete objective function, and in cases where operators intend to have a solution with fewer VVCC number of switching, it is possible to consider all VVCC operating costs in the objective function of proposed VVO. Typically, OLTC and VR Loss costs depend on the value of switching at each quasi real-time interval. This objective function can be written as (5-35) where VVO sub-parts can be obtained by (5-36) to (5-39).

$$Min\ O.F_{VVO,t} = Min\ (C_{loss,t} + C_{VR,t} + C_{OLTC,t} + C_{CB,t}) \quad (5\text{-}35)$$

$$C_{loss,t} = \sum_{l=1}^{l=L} (P_{loss,l,t} \times \pi_t) \quad (5\text{-}36)$$

$$C_{VR,t} = \sum_{r \epsilon R} C_{r,t} \times \left| X_{VR,r,t} - X_{VR,r,t-1} \right| \quad (5\text{-}37)$$

$$C_{OLTC,t} = \sum_{w \epsilon W} C_{w,t} \times \left| X_{OLTC,w,t} - X_{OLTC,w,t-1} \right| \quad (5\text{-}38)$$

$$C_{CB,t} = \sum_{c \epsilon C} C_{c,t} \times q_{inj,c,t} \times \rho_{c,t} \times \left| X_{CB,c,t} - X_{CB,c,t-1} \right| \quad (5\text{-}39)$$

In time interval-*t*, $C_{loss,t}$is the loss cost ($), $C_{VR,t}$is the VR operating cost ($), $C_{OLTC,t}$is the OLTC operating cost ($) and $C_{CB,t}$is CB operating cost ($).Moreover, $P_{loss,l,t}$is the active power loss of line-*l* at time-*t* (kW), $\pi_t$is the loss price ($/kW), $C_{r,t}$is the switching cost of VR-*r* at time-*t* ($/switch), $C_{w,t}$ is the switching cost of OLTC-*w* at time-*t* ($/switch), $X$is binary value (0: same tap, 1: new tap) in OLTC ($X_{OLTC,w,t}$) in VR ($X_{VR,r,t}$) and in CB ($X_{CB,c,t}$), $C_{c,t}$is the operating cost of CB-*c* at time-*t*, $\rho_{c,t}$is the number of CB bank, and $q_{inj,c,t}$is the size of each of CB-*c* bank. In more complete approach, CVR cost minimization is added to the above objective function. This objective function that is shown in (5-40) would be able to minimize distribution network loss, VVCC operational and CVR costs simultaneously. The first four sub-parts can be found through (5-36) to (5-39). The last VVO sub-part that is CVR cost can be found by using (5-41).

$$Min\ O.F_{VVO,t} = Min\ (C_{loss,l,t} + C_{VR,t} + C_{OLTC,t} + C_{CB,t} + C_{CVR,t}) \quad (5\text{-}40)$$

$$C_{CVR,t} = \sum_{n=1}^{n=N} C_{S.E,t} \times \frac{1}{\Delta E_{n,t}} = \sum_{n=1}^{n=N} C_{S.E,t} \times \frac{1}{CVR_{f,t} \times \Delta V_{n,t}} \quad (5\text{-}41)$$

In order,$C_{S.E}$, ΔE, $CVR_f$and $\Delta V$are cost of saved energy by CVR, energy load consumption through CVR, CVR Factor and Voltage Reduction in CVR. For any CVR study, it is necessary to model distribution network loads precisely. Hence, ZIP load modeling, shown in (5-42) and (5-43), is used in this research to calculate active and reactive power of loads at each operating time stage.

$$P = P_0(Z_p(\frac{V}{V_0})^2 + I_p\left(\frac{V}{V_0}\right) + P_p) \quad (5\text{-}42)$$

$$Q = Q_0(Z_q(\frac{V}{V_0})^2 + I_q\left(\frac{V}{V_0}\right) + P_q) \quad (5\text{-}43)$$

Here, $P_0$and $Q_0$are initial active (kW) and reactive power (kVAR) values. Moreover, V_0 is the initial voltage and Vis the voltage of the system. Z_p, I_p and P_p are active power ZIP coefficients and Z_q, I_q and P_q are reactive power ZIP coefficients. Changes in energy

consumption *(ΔE)* as well as voltage reduction (ΔV) can be found by (5-44) and (5-45). By dividing (5-45) and (5-45) CVR Factor (CVR_f) is gained which presents the ratio of energy consumption and voltage reduction (5-46).

$$\Delta E\% = (\frac{E_{base} - E_{CVR}}{E_{base}}) \times 100 \quad (5\text{-}44)$$

$$\Delta V\% = (\frac{V_{base} - V_{CVR}}{V_{base}}) \times 100 \quad (5\text{-}45)$$

$$CVR_f = \frac{\Delta E}{\Delta V} \quad (5\text{-}46)$$

Notwithstanding the abovementioned steps, it is possible to present a comprehensive objective function for proposed VVO engine. This comprehensive objective function is given in (5-40) but the method of finding each VVO sub-part can be defined through (5-47) to (5-51).

$$C_{loss,t} = \sum_{l=1}^{l=L} (\alpha_t \times P_{loss,l,t} \times \pi_t) \quad (5\text{-}47)$$

$$C_{VR,t} = \sum_{r \epsilon R} \beta_t \times C_{r,t} \times \left| X_{VR,r,t} - X_{VR,r,t-1} \right| \quad (5\text{-}48)$$

$$C_{OLTC,t} = \sum_{w \epsilon W} \gamma_t \times C_{w,t} \times \left| X_{OLTC,w,t} - X_{OLTC,w,t-1} \right| \quad (5\text{-}49)$$

$$C_{CB,t} = \sum_{c \epsilon C} \delta_t \times C_{c,t} \times q_{inj,c,t} \times \rho_{c,t} \left| X_{CB,c,t} - X_{CB,c,t-1} \right| \quad (5\text{-}50)$$

$$C_{CVR,t} = \sum_{n=1}^{n=N} \mu_t \times C_{S.E,t} \times \frac{1}{\Delta E_{n,t}} \quad (5\text{-}51)$$

In (5-47) to (5-51), $\alpha, \beta, \gamma, \delta$ & ε are VVO sub-part's weighting factors. These factors enable the VVO engine to weight each sub-part according to its importance level, i.e. effectiveness, at each operating time-interval in distribution network. It is possible to assume that these values are known for network operators as they need to find the value and effectiveness of each VVO sub-parts before any optimization. However, this research proposed a Fuzzification technique to compute the effectiveness of each VVO sub-part according to distribution network operator desired settings within VVO engine algorithm. Hence, VVO sub-part's weighting factors can be found through Fuzzification. For instance, (5-52) explains the Fuzzification algorithm for loss cost minimization sub-part.

$$\begin{aligned} &if: \ f_{Loss} \leq f_{Loss,dmin,t} \ \rightarrow \ \alpha_t = 10 \\ &elseif: \ \alpha_t > f_{Loss,dmin,t} \ \& \ \alpha_t < f_{Loss,dmax,t} \\ &\rightarrow \ \alpha_t = \frac{\left| f_{Loss} - f_{Loss,dmin,t} \right|}{f_{Loss,dmax,t} - f_{Loss,dmin,t}} \times 10 \\ &else: \ f_{Loss} \geq f_{Loss,dmax,t} \ \rightarrow \ \alpha_t = 0 \end{aligned} \quad (5\text{-}52)$$

If the loss (f_{Loss}) found by the VVO engine is less than the minimum desired value of loss ($f_{Loss,dmin}$) the weighting factor would be equal to 10 but, if the weighting factor is more than the maximum desired value of loss ($f_{Loss,dmax}$) the weighting factor would be equal to 0. If the loss is between desired minimum and maximum range, the system will find a weighting factor between 0 and 10 according to (5-51). Minimum and maximum desired values for other VVO subparts such as: f_{CVR}, f_{CB}, f_{VR} and f_{OLTC} have to be defined in the VVO engine by the operator to allow the engine finding the optimal weighting factors of each objective function subpart, according to system operational needs for each operating time interval. In other words, this VVO sub-algorithm ensures that the value of power loss minimization is set correctly in compliance with network operator desired values and/or distribution network needs.

In brief, the comprehensive objective function subparts attempt to minimize the loss, VVCC operational and CVR costs of the grid according to network constraints at each quasi real-time interval. In BFS power flow method, current injection ($I_{n,t}^{k}$) of each node of the system at each quasi real-time interval can be found using (5-52).

Here, $k$denotes iteration number. The relationship [B] and the bus-injection to branch-current [BIBC] matrices can be solved by Kirchhoff's Current Law (KCL) in Backward-Forward Sweep (BFS) distribution load flow technique. Furthermore, the branch-current to bus-voltage matrix [BCBV] can be obtained by Kirchhoff's Voltage Law (KVL). By initial estimate for node voltages, BFS finds load and line currents and by calculating current, voltages of all nodes of system, i.e. solution of BFS load flow, can be found using (5-53) to (5-56) through iterative steps till convergence. Here, 0 denotes initial value. BFS converges when the difference of voltages between two consecutive iterations would be less than epsilon (typically less than 10^{-3} or 10^{-4}). The active and reactive power losses can be found by knowing voltages of nodes and currents of branches. More details regarding BFS load flow method can be found in Appendix II.

$$I_{n,t}^{k} = \left(\frac{S_{n,t}}{V_{n,t}^{k}}\right)^{*} = \left(\frac{P_{n,t} + jQ_{n,t}}{V_{n,t}^{k}}\right)^{*} \quad (5\text{-}53)$$

$$[B] = [BIBC][I] \quad (5\text{-}54)$$

$$[\Delta V^{k+1}] = [BCBV][B] = [BCBV][BIBC][I^{k}] = [DLF][I^{k}] \quad (5\text{-}55)$$

$$[V^{k+1}] = [V^{0}] + [\Delta V^{k+1}] \quad (5\text{-}56)$$

5.4. Other VVO Constraints

Regarding EV studies, it has to be stated that the voltage of nodes with EV charging stations and EVs ($V_{EVi,t}$) have to be between minimum and maximum voltages ($V_{EVi,t}^{min}$ and$V_{EVi,t}^{max}$) according to [89]. Moreover, the active power of EV ($P_{EVi,t}$) should be less than maximum charging limit of EV ($P_{EVi,t}^{max}$). In other words, the active power of EV cannot exceed maximum charging limit of EV due to physical constraint [179]. These constraints are shown in (5-57) and (5-58) respectively.

$$V_{EVi,t}^{min} \leq V_{EVi,t} \leq V_{EVi,t}^{max} \text{ [89]} \quad (5\text{-}57)$$

$$0 \leq P_{EVi,t} \leq P_{EVi,t}^{max} \text{ [179]} \quad (5\text{-}58)$$

Moreover, in case of reactive power injection by EVs, (5-59) and (5-60) can be used. Thus, the reactive power injection to the grid, that has negative value by itself ($Q_{EVi,t}$), should be less than the capacity of maximum inverter reactive power generation ($Q_{EVi,t}^{max}$).

$$0 \leq -Q_{EVi,t} \leq -Q_{EVi,t}^{max} \quad (5\text{-}59)$$

$$\forall i = 1, \dots, I \quad Q_{i,t} = ((Q_{EVi,t} + Q_{CBi,t}) - Q_{L,i,t}) \leq \sqrt{S_{i,t}^2 - P_{i,t}^2} = Q_{i,t}^{max} \quad (5\text{-}60)$$

For economical/operational constraints for EV studies, constraint shown in (5-61) limits the operating expenses of CBs to a budget ($C_{Op-Budget}$) defined by distribution network planners ($). As an operational constraint, (5-62) is used to limit the CB and EV charging station expenses.

$$\left\{(C_{CB}(\sum_{t=1}^{T}\sum_{i=1}^{I} Q_{CB,i,t}))\right\} \leq C_{Op-Budget} \quad (5\text{-}61)$$

$$\left\{(C_{CB}(\sum_{t=1}^{T}\sum_{i=1}^{I} Q_{CB,i,t})) + (C_{Q-V2G}(\sum_{t=1}^{T}\sum_{i=1}^{I} Q_{V2G,i,t}))\right\} \leq C_{Op-Budget} \quad (5\text{-}62)$$

As stated before in (5-12) and (5-13), active and reactive power of system nodes with DERs have to be between defined maximum/minimum range in DER studies, such as Micro-CHP/PV penetration study. Moreover, the voltage of system nodes (*n*) with DERs ($V_{DER,n,t}$) have to be within pre-defined minimum ($V_{DER,n,t}^{min}$) and maximum ($V_{DER,n,t}^{max}$) range as shown in (5-63).

$$V_{DER,n,t}^{min} \leq V_{DER,n,t} \leq V_{DER,n,t}^{max} \quad (5\text{-}63)$$

As mentioned before, by receiving data from AMI, the VVO engine runs its algorithm and performs load flow within each optimization cycle to avoid constraint violations. The algorithm seeks the optimal solution of Volt-VAR control assets at each iteration step. Other DER considerations for VVO studies are explained in the next chapter of this thesis.

Chapter 6.

Microgrid Sources in Volt-VAR Optimization

In recent years, environmental and economic concerns as well as power quality, and reliability issues in conventional distribution networks, have led evolutionary changes to generation/load interactions of distribution networks. Recent distribution grids tend to rely on Distributed Energy Resource (DER) generations to meet growing needs of demand with more emphasis on efficiency, reliability and quality of service. In general, DERs are small electricity and/or heat generating units that can be installed close to loads in order to supply a part of load electricity/heat needs. Most types of DER technologies include generator, energy storage and load control. In microgrids, loads and DERs are aggregated as a system to provide electricity and heat through a distributed command and control infrastructure.

Typically, microgrids are connected to the traditional grid (Macro-grid) but they are able to be disconnected from traditional grid autonomously and operate in island mode to supply a part of grid without interruption to increase system reliability and resiliency. Microgrids can be comprised of various renewable resources such as solar (PV), wind, distributed generation (DG) such as micro-turbine, natural gas-engines, and DERs such as Micro-Combined Heat and Power (Micro-CHP) and energy storage systems. Figure 6.1 shows microgrid different levels in a typical distribution network. Moreover, employing local energy sources to supply local loads lead to loss reduction and efficiency improvement in distribution grids. In brief, the availability of reliable distributed command and control, communication infrastructure, local generation, power electronics, energy manager and protection are the key factors that let microgrids to operate semi-autonomously. Although there is still a long way to reach to a pre-emptive self-healing grid, as a long-term target of microgrids, advancements in microgrid component technologies have made new energy optimization and conservation possible.

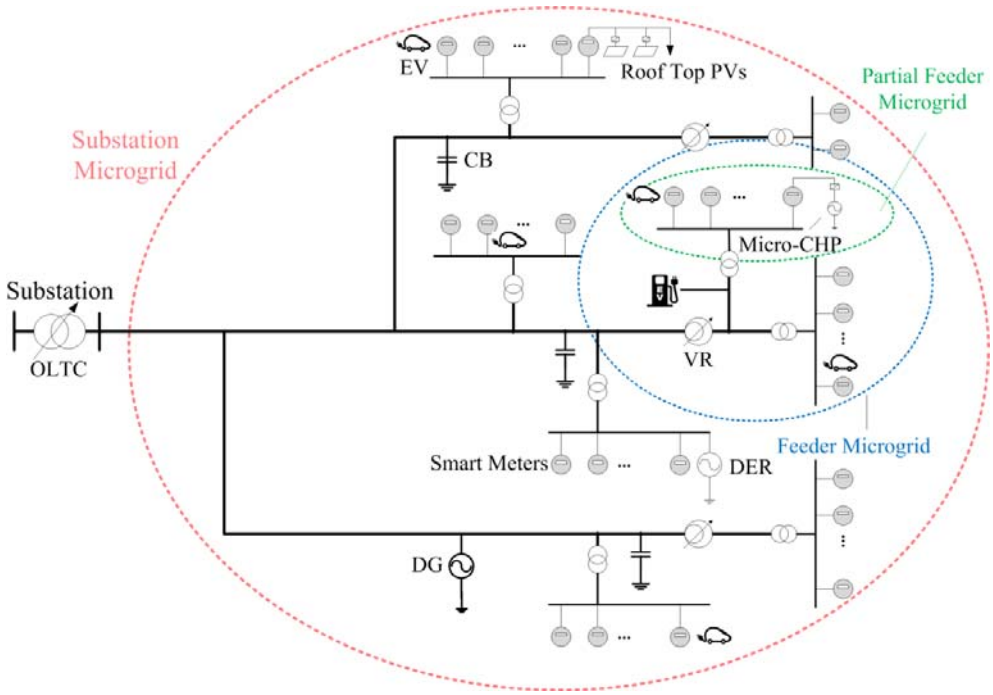

Figure 6.1. Microgrid levels of operation in a typical distribution network

VVO, as a part of smart distribution network optimization solution has to operate in-line with microgrid key features. As such, new VVO techniques require to be integrated with microgrid sources and loads. Moreover, they need to function in compliance with microgrid control and communication topologies using recent protocols and/or standards. The main aim of microgrid control is to provide control over network and ease grid with autonomous components. Microgrid control enables interface switch of the system to island microgrid during fault, power quality and other network unintentional events. By clearing fault and/or event, microgrid control has to re-connect microgrid to the macro-grid autonomously. Moreover, each DER is able to control power in different microgrid operating modes. For instance, DERs employ power vs. frequency droop controls to follow required demand during microgrid island mode of operation. This control provides frequency load-shedding when there is not adequate generation in the system. In addition, each DER has voltage control to ensure system stability. Microgrid voltage control aims to ascertain that there is no large circulating reactive power flowing between DERs, especially in microgrid with high penetration of DERs. For this reason, voltages vs. reactive power droop controllers are employed. Voltage set-point can be defined based on the reactive powers generated by DERs. As kVARs become capacitive, local voltage set-point decreased but inductive kVARs provide voltage rise in set-point.

It has to be stated that microgrid components are following peer-to-peer, plug-and-play architectures to ease system usage, increase the efficiency of the grid as well as increase grid power quality. As such, DERs can be connected through a peer-to-peer structure to their local control systems. This distribution control topology lead system to a higher level of reliability compared with centralized control or master-slave topologies. On the other hand, microgrid component's plug and play structures let microgrid expansion without re-structuring the network. Moreover, reliability and maintenance of a grid with plug and play components are much higher than other grid components with rigid structures. In order to smarten-up distribution networks, it is possible to control different microgrids that are connected to each other through real-time data of DERs and loads. AMI infrastructure provides the opportunity to capture required data of DERs and loads for control and optimization purposes. Nowadays, microgrid dispatch is no longer based on the number and type of DER units. In conventional control, a control center or dispatching center, dispatches all generating unit active and reactive power outputs to follow system demand. This approach may not be doable in distribution networks with high penetration of generating units. In a distribution system with microgrids, each microgrid can be seen as a unique source with known active/reactive power generation or consumption.

In microgrids with high penetration of sources such as PVs, intermittent generation may cause stability issues. Using DERs can decrease power fluctuations that might be created by these types of sources. Moreover, storage systems are needed for reserve energy when there is no solar radiation. As such, a microgrid including high penetration of PVs is mostly integrated with local generations and storage. The DER in microgrid with high penetration of PVs can control active and reactive power flows between microgrid and distribution grid. Moreover, it can supply power when PVs are not available. On the contrary, the inverter-based energy storage enables generation to be connected as quickly as possible to the microgrid without inverter interference as generation needs fast response of inverter. In microgrid island mode, high penetration of PVs may cause different issues. For instance, microgrid may face with power generation more than the amount that system requires. Energy storage integrated with PVs can help microgrid to store extra power generated by PVs. Another method is using power vs. frequency control to reduce the power output of PVs in light-load islanding operating scenarios. A proper

power vs. frequency controller, enables automatic generation reduction of PVs when frequency of the system increases in microgrid light-load island modes. Moreover, it sends commands to the storage to be charged to control PV outputs effectively. In brief, distributed command and control is widely used in microgrids to perform local control over system components and dispatch distribution grids according to microgrid operational requirements.

Reliable and secure bi-directional communication infrastructure is another major feature of successful implementation of smart microgrids. Typically, three communication layers are used in microgrids. Wide Area Network (WAN) that can be based on 3G/4G, Ethernet, Fiber Optics, etc. supports transmission grids. For distribution networks, Neighbor Area Network (NAN) and/or Local Area Networks (LAN) are typically used. For customer side, i.e. termination points, Home Area Network (HAN) is used. IEC 61970 which focuses on common information model and energy management, IEC 61968 which focuses on distribution management, and IEC 61850 that is for power automation are some of the standard of WAN networks. ANSI C12.22 and IEEE 802 are some of the well-known standards of LAN networks and ZigBee is the most applicable protocol of HANs. The main standard of microgrids is IEEE 1547 that is Standard for Interconnecting Distributed Resources with Electric Power Systems [211]. IEEE 1547 covers standards of different microgrid aspects such as design, interconnection, monitoring and operation of microgrids in normal and island modes. Moreover, IEEE 2030 provides a guide for smart grid interoperability of energy technology and information technology operation with the power system, and end-use applications and loads [79]. The IEC 61850 standard [181] is one of the famed standards for automation of substations through Ethernet LANs in smart grids. IEEE 802.11 [211] shows that with the recent advancement in wireless communication technologies through Wireless LAN (WLAN) or Ethernet LAN, it is now conceivable to employ IEC 61850 standard in distribution level. IEC 61850-7-420 is a part of IEC 61850 standards that intends to give complete object models that are required for DERs [181]. It applies communication services mapped to MMS under IEC 61850-8-1 standard [181].

Therefore, the compatibility of the communication standard/protocol of smart grid-based VVO solution with communication standards/protocols of microgrid technologies

and components is necessary. As explained, proposed VVO topology is compatible with smart microgrid distributed command and control topology. Moreover, the control of voltage and reactive powers of smart distribution grids through conventional and new VVCCs can make VVO more efficient. In brief, this research tries to study the impacts of new smart grid-based VVO technology on smart distribution grid as well as the impacts of smart microgrid components on smart grid-based VVO. For this reason, different microgrid sources such as DG, FESS, Energy Storage, Micro-CHP/PV, EV and V2G are considered as grid components and the impact of them on proposed VVO engine is investigated in different studies. Moreover, proposed VVO engine tries to assess if microgrid sources are able to increase VVO efficiency or not.

6.1. EVs in Electrical Distribution Networks

Generally speaking, penetration of dispatch-able resources on customer side or co-generation loads such as EV has brought new opportunities as well as challenges to distribution networks. EV as one of microgrid sources has rapid growth in North America. Although distribution planners intend to provide command and controls strategies to adjust co-generation impacts on loads but dispatch-able energy sources can be a tool for system service optimization. As such, new studies have shown the fact that new inverter technologies could provide reactive power injection/ absorption opportunity for microgrids [91]-[96]. Using these types of technologies such as Vehicle to Grids (V2Gs) with reactive power support capabilities have considerable impacts on the optimization, reactive power need, the size and the number of switchable shunt CBs in distribution networks as it will be possible to employ a percentage of EVs as reliable reactive power generating sources in V2G mode to reduce active and/or reactive power loss and conserve the energy consumption in the system.

In general, EVs could be classified based on three main charging levels [83] as well as on their technology shown in Table 6.1. Large penetration of EVs at different consumption levels and within various locations (house, workplace, shopping centers) could lead to salient changes in distribution network demand and daily load profile.

Table 6.1. EV Charging Levels based on [216]

AC Level 1	AC Level 2	AC Level 3	DC Level 1	DC Level 2	DC Level 3
120V, 1.4 Kw (12 A) 120V, 1.9 kW (16 A)	240V, up to 19.2 kW (80 A)	>20 kW, single and 3 phase	200-450 V DC, up to 36 kW (80 A)	200-450 V DC, up to 90 kW (200 A)	200-600 V DC, up to 240 kW (400 A)

Many research studies have tried to evaluate the profile and the trajectory of these changes based on different EV penetration levels [87]-[89] which could be an expedient measuring factor. Generally speaking, when an EV injects reactive power into the grid, it may raise distribution feeder capacity. It may improve voltage profile and power loss if there is no overcompensation of the reactive load. It may also lead to an increase in voltage, which results in an increase in loads. This increase in load may be either greater, or smaller than the reduction of losses. Hence, the overall input of kW in the system may either increase, or decrease. Power flow, that is run within VVO algorithm covers these following points such as system overcompensation, load rise and overall input of kW. EV charging stations may follow different operating modes [84]-[88]. Figure 6.2 illustrates different operating points of AC/DC inverter of an EV. The most common EV operating scenario is P>0, Q = 0 (on the border between Quadrant I and IV) which shows that EV consumes only the active power of the grid. Another possible operating mode of EV inverter enables EVs to inject reactive power into the grid (Quadrant IV) while still consuming active power of the grid for charging [91]-[94], [96]. This leads to the rise in distribution feeder capacity, improvement in voltage profile and power loss reduction.

The topology of the bidirectional charger needs minimal changes in order for it to be suitable for reactive support [95]. Single phase inverters have been tested for their ability to inject reactive power into the network in [212]-[213]. According to these research studies, if the voltage rate of the dc-link capacitor of the inverter increased at least 3% it would be possible to inject VAR. Moreover, the current ripple rate of the dc-link capacitor is strong enough for inverters to operate in capacitive mode. It should be mentioned that the total losses of the AC/DC converter could be slightly increased by reactive power support in normal operation of the charger [95] but the EV battery and the input inductor current are not affected by capacitive operation at all [92].

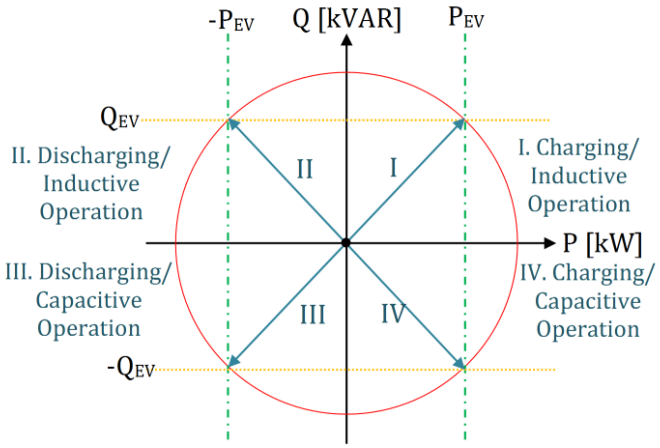

Figure 6.2. Active and reactive power generation quadrants of an EV

Moreover, studies have shown that the DC-link capacitor could be capable of supplying reactive power into the grid without engaging the EV battery [95]. Thus, VAR injection by EV inverters will not cause any degradation on EVs battery life [93]. This important study shows that EV charging stations could be one of the future candidates for reactive power injection into the grid even when electric car is not connected to the charging station. As shown in Figure 6.2, the amount of reactive power that an EV charging station can inject in the charging mode is confined by the charger power limit and the active power drawn from the grid. It is clear that if an EV is using the maximum active power from a charging station, this station cannot generate reactive power but as the charging stations are in idle mode most of the time, they could inject reactive power into the grid when required. Moreover, the charger can be rated at 10% to 20% higher power than the maximum real power drawn during charging to make the charger capable of injecting VAR during all operating conditions [95]. Therefore, one might need to acknowledge this feature as one of EV's potential advantages. This research tries to assess EV reactive power generation effect on VVO and more specifically, on the VAR injection amount and cost of CBs in one of its studies. Additionally, the proposed VVO attempts to find the optimal VAR injection of CBs and EV charging stations with VAR injection capability. Hence, the research ignores the economics and/or regulatory issues in terms of desirability or willingness of stakeholders (Grid Operators, EV Car Manufacturers and Drivers) to enable V2G as a mainstream technology and/or solution.

6.2. Micro-CHP/PV in Smart Distribution Network

Penetration of DERs throughout smart grids and/or distribution feeders has raised grid complexities as well as uncertainties that affect conventional monitoring, optimization and control systems. Hence, electric power utilities are trying to verify the impact of DER penetrations on their monitoring, control and optimization systems. As mentioned before, DERs such as Micro-CHPs or PVs are used for different operational aims. PV modules supply residential buildings with clean active power while Micro-CHP units can provide both heat and electricity. Prior to investigating the impact of different Micro-CHP/PV penetration levels on different VVO sub-parts, it is necessary to initialize Micro-CHP and PV types and penetration levels.

In one of the studies of this research, two different types of Micro-CHP units: Heat Led with electricity rejection and Electricity Led with heat rejection are considered. The range of Micro-CHP is considered between 1 and 3 kWe. As most Micro-CHPs are heat led, the ratio between heat led Micro-CHP and an electricity led Micro-CHP assumed to be 2.5 in Micro-CHP/PV study of this thesis in Chapter 12. Moreover, present percentages of PV, Electricity Led Micro-CHP and Heat Led Micro-CHP along studied distribution feeder assumed to be equal to 30, 20 and 50 percent respectively. Different penetration levels is considered to check the impact of Micro-CHP/PV units on presented smart grid-based VVO: Normal, High and Very High. At each penetration level, VVO engine strives for optimizing the grid and finding the optimal response of each VVCC. The active power generation profile of micro-generation comprised of PVs, heat led and electricity led Micro-CHP units in the case study for all quasi real-time intervals resulting from the AMI data.

6.3. Community Energy Storage (CES) in Smart Grids

Community Energy Storage (CES) is one of the recent advanced smart grid technologies that provide distribution grids with lots of benefits in terms of stability, reliability, quality and control. As it benefits both costumers and utilities, this technology has become a crucial element of recent microgrids. CES is typically located at the edge of the grid (rather than distribution substation), close to customers and DERs to smooth the impacts of intermittent DERs such as PVs or other smart grid components such as

EVs and help integration of these sources to the smart grid. The main concept of CES initially used in HV/MV substations equipped with a community energy storage batteries that can give advantages much more than conventional substation batteries. This type of CES could provide regional control benefits at transformer/feeder levels. New types of substation CES units could provide voltage regulation though their four quadrant inverters without need to have OLTC in substation anymore. In recent years, this concept became more applicable in customer side and DERs. The main tasks of CES in distribution networks can be summarized as peak-shaving, smooth DER's intermittencies (output shifting/leveling), power quality improvements (voltage and reactive power supports), islanding during outages, frequency regulation and etc. Typically, a CES consists of a battery (mostly lithium ion in a battery box), a four-quadrant inverter (in grid inverter panel), and a measurement/control system (in meter and breaker panel) that includes Battery Management System (BMS) and inverter monitoring/control. The main difference between CES and DGs lies in the fact that CES has a fully dispatch-able four-quadrant inverter that enables it to bi-directionally exchange active and reactive powers. In other words, CES is able to regulate voltage, frequency and inject/absorb reactive power to/from the grid. Figure 6.3 present the main structure of CES inspired from [214].

The operation of CES is very simple. CES systems store energy in their batteries and supply active or reactive power due to system active/reactive demand(s). CES can be considered as a backup power of a certain group of residential houses as it can supply power for a short period while discharging. Typically, the voltage rates of CES at LV side is 240/120 V AC. Moreover, the rated power is typically 25 to 50 kW [215], and the rated energy for 25 kW is from 25 to 75 kWh and for 50 is from 50 to 150 kWh. In other words, the discharge time of most CES system are from one to three hours at each operating cycle. Typically, the discharge power is equal to the rated power but charging power has to be less than or equal to the rated power. By dividing rated energy and rated power, discharge time is obtained. Typically, the charge time has to be less than two times of the discharge time [214].

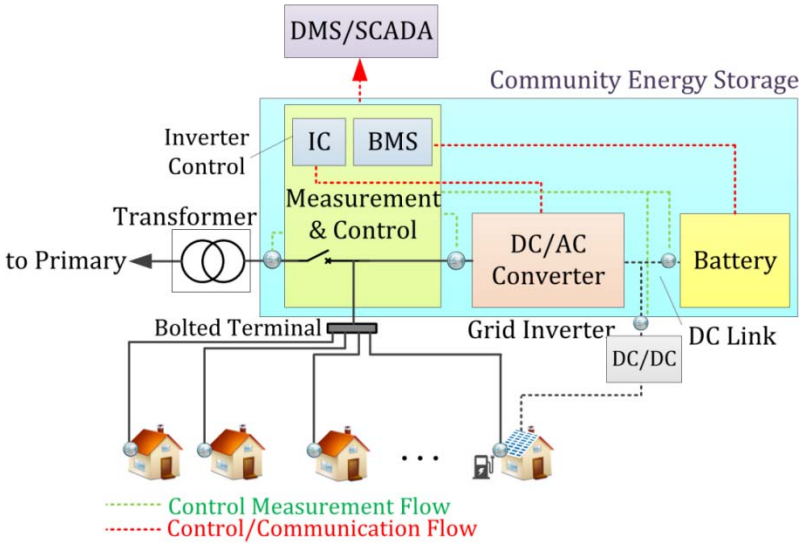

Figure 6.3. The main structure of Community Energy Storage System

Generally, CES such as any battery energy storage systems has three modes of operation: discharge, standby and charge. According to the four-quadrant inverter capability, CES discharge can be fully active power, active/reactive (inductive) and active/reactive (capacitive). VVO prefers CES systems more than switchable CBs as they are able to supply the active power. In addition, VVO prefers CES systems more than DGs as well because, CES systems provide reactive power supports and other benefits to the grid. As one of the most important tasks of CES can be peak shaving, VVO can help CES to discharge during peak quasi real-time intervals. This could definitely benefit VVO as well. The second mode of operation of CES systems is standby mode. In this operating mode, the CES systems are generally disconnected from the grid but they are in standby and ready to be integrated to the grid while system needs them. Due to the concept of four-quadrant inverters explained in section 6.1, it is possible to say that these inverters may inject/absorb reactive power into the system while they are in standby mode (P=0, Q<0 or Q>0). This could create a new mode of operation for CES in future. For instance, VVO could send a control command to a standby CES to be connected to the grid and inject reactive power. This suggested mode of operation needs further technical/economic investigations.

The last CES mode of operation is charge mode. Typically, CES system charge in very light load conditions. VVO can help CES to charge in light load quasi real-time intervals as well. As explained, the charge time has to be typically less than two times of

discharge time. From VVO power loss minimization point of view, as CES consumes active power in charge mode, active power loss increases slightly but as power loss level is very low in light load condition, the total impact of CES charge mode to the system is not significant. From CVR point of view, fewer active power consumption leads to more energy conservation. As such, one may argue that extending CES charge time very close to two times of discharge time and setting four-quadrant inverter to consume the fewest possible active power to charge batteries that comes with reactive power support can be more beneficial to smart grid-based VVO during light loads. Regarding this argument, one has to be reminded that the value of VVO objective function is at its lowest rate during very light load condition. Hence, this won't be much beneficial to the whole system if operating cost of CES take into account as well. Moreover, the impact of time-consuming charge on CESS battery efficiencies has to be investigated.

In brief, CES systems provide different intelligent layers in terms of energy management, feeder optimization and local control to the grids. This could definitely help VVO objectives. Moreover, as most of new CES communication technologies are based on DNP3 and IEC 61850 protocols/standards, proposed VVO engine in this research can be integrated with CES control system. For instance, VVO would be able to find CES discharging control commands for peak shaving during peak time intervals.

Chapter 7.

Conservation Voltage Reduction (CVR)

Nowadays, the advent and the expansion of smart grid technologies have facilitated the adoption of energy efficiency technologies in electric distribution networks. The organic growth of this well-designed layer of intelligence over utility assets enables a range of smart grid's fundamental applications to emerge [3]. Faced with diverse technological, organizational, and business issues that adversely affect the bottom line, electric power utilities are contemplating immediate changes and/or upgrades of their technologies, business processes, and organization [4]. As explained before, many electric power utilities have begun upgrading and improving the operation of their distribution grids using smart grid technologies such as EMS, DMS, SA, and AMI in recent years. Others intend to overhaul and/or upgrade their grids using the aforementioned technologies. In general, electric power utilities seem eager to continue integrating novel smart grid functionalities based on their priorities and road maps.

However, applying smart grid components and technologies necessitate electric power utilities to seek new optimization and energy saving techniques in-line with the yet-to-be-integrated smart grid technologies. The primary concern of electric power utilities is to find cost-effective solutions for optimal operation of their existing grids and then, to specify the best short-term and long-term plans to update and expand distribution networks according to their smart grid technology development plans. As explained before, one of the well-known energy saving techniques that has been taken into consideration by many utilities in the last two decades is "Conservation Voltage Regulation", "Conservation Voltage Reduction" or "CVR". ANSI C 84.1 standard [1] has defined the acceptable ranges of voltage at termination points (e.g. 114-126 V in North America). Based on that, CVR tries to decrease consumer's voltage level into the lower limits of ANSI range, i.e. 114-120 Volts, to reduce energy consumption. CVR is not a new concept as it had been used for many years by electric power utilities for load reduction purposes especially in peak times. It had been common to lower voltage of high consumption loads such as industrial machines to decrease aggregated load of the system during peak hours. Despite that fact, CVR revived in another form when utilities

realized that many of their distribution network feeders in United States supplied a higher voltage level to termination points, i.e. consumers receive 120.5 V power on average [217]. The main reason for that phenomenon was electric power utility's obsession with supplying flawless power to their customers, as well as significant limitations in their monitoring technologies. Moreover, it was revealed that many other distribution utility feeders were working at upper levels of ANSI band, i.e. 120-126 V [218]. Hence, electric power utilities contemplated again the option of lowering the voltage level of consumption in order to achieve energy conservation as well as demand reduction. Figure 7.1 depicts CVR voltage reduction compared with conventional voltage regulation.

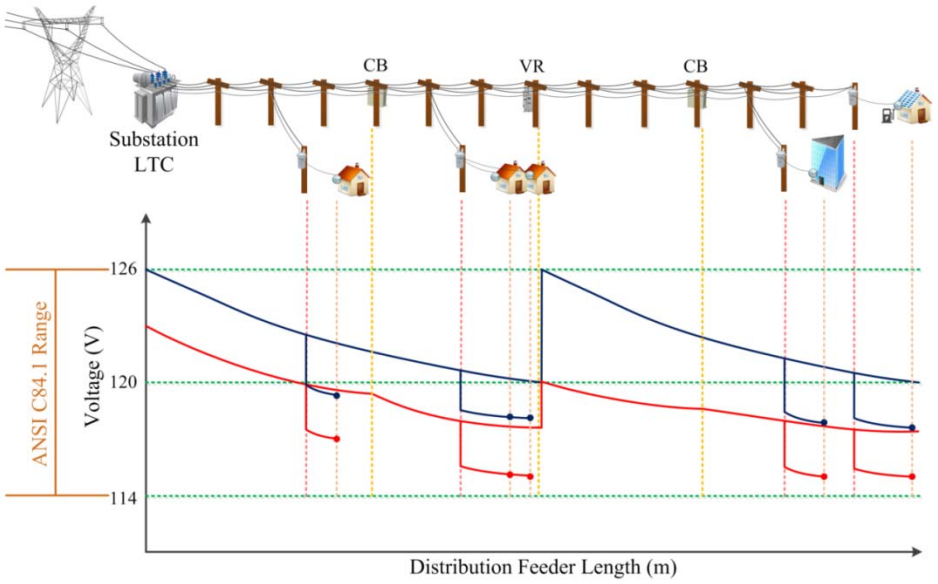

Figure 7.1. Conservation Voltage Reduction (red) vs. conventional voltage regulation (blue)

As future CVR techniques acknowledge CVR as an inseparable part of VVO technologies, it would be necessary to investigate the requirements and challenges, as well as pros and cons of these novel CVR approaches for future distribution networks. This chapter aims to assess novel smart grid-based CVR technique benefits and challenges from design to implementation step.

7.1. Impact of VVO Topology on CVR

As part of VVO engine, new CVR techniques need to follow VVO topology. In that regard, it is possible to classify new VVO approaches as Centralized VVO [32], [52], [74]-[75], [81], [119], [149] or Decentralized VVO [36], [45], [77], [80], illustrated in Figure 7.2. As explained before, the processing system is placed in a central controller unit such as DMS in centralized VVO. The DMS uses related measurements taken from utility subscribers supplied to it from either field collectors or directly from MDMS, to determine the best possible settings for VVCCs to achieve the desired optimization and conservation targets. These settings are then off-loaded to such assets through existing downstream pipes, such as SCADA network. It can be interpreted from [219] that centralized VVO approach is in accordance with coordinated control and monitoring of EMS/SCADA of distribution networks that is mostly centralized in nature. Hence, it seems that the infrastructure of utilizing centralized VVO is available in many distribution networks.

In contrast, decentralized VVO utilizes VVO engines which are located in the field and close to the relevant VVCCs to perform optimization based on local attributes of the distribution network. In this case, local measurements do not need to transfer from the field to the back-office, and the new settings for VVCCs are determined locally, rather than by a centralized controller. Moreover, utilizing intelligent systems such as Intelligent Agents enable such systems to avoid sending excessive data to the VVO engine [191]. As decentralized VVO approach follows microgrid DCC topology, some may believe that this approach could be developed in-line with microgrid expansion plans within distribution networks. Here, there is no need to transfer huge amounts of data from smart meters located at customer premises to the VVO engine. Thus, this approach may lead to less VVO-related AMI cost compared with centralized approach. In both explained VVO topologies, CVR tries to cover missing regulation zone that is LV secondary side of transformer through existing VVCCs in the MV primary side of transformer and/or probable VVCCs in the LV secondary employed in some new studies [220]. Algorithm-based CVR techniques such as model-based, or heuristics-based, could be applied for both centralized and decentralized VVO.

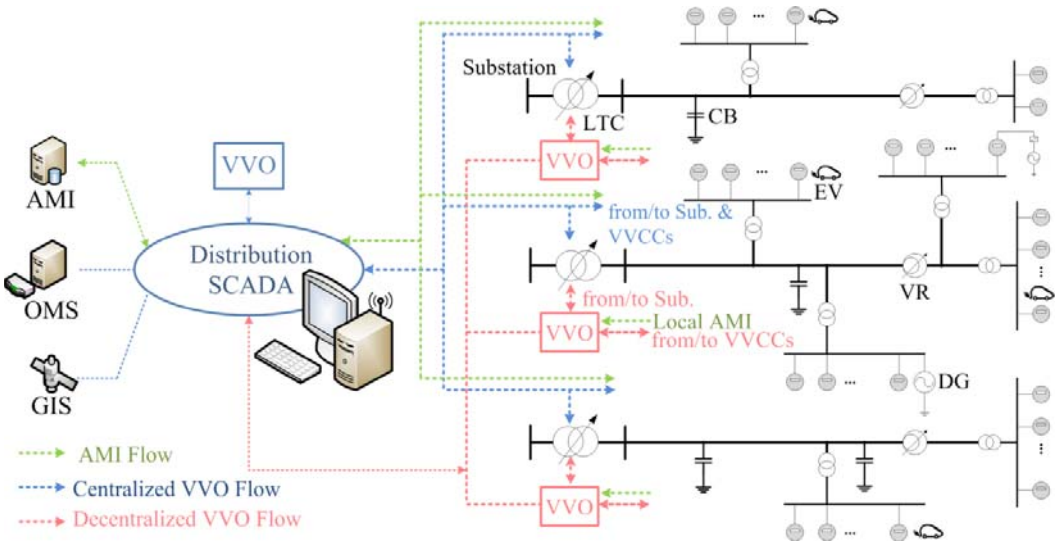

Figure 7.2. Centralized and Decentralized Volt-VAR Optimization approaches

In centralized VVO, huge amounts of consumer's data are sent to VVO engine located in the control center. Hence, the necessity of using data filtering approaches in order to avoid SCADA blockage or data tsunami is felt more in centralized VVO rather than decentralized VVO. In general, CVR could be accomplished through both aforementioned topologies in two different parts of distribution network. In the first method, CVR uses VVCCs located at the MV side. In the second method, In-line Power Regulators (IPRs) are used at the LV side of transformer to reduce the voltage level of consumption. As this method requires IPR installations, it would be necessary to perform detailed cost-benefit analysis and compare the benefits of this method with the first common technique in future. As a result, a comprehensive cost-benefit analysis is needed in order to select centralized or decentralized approach. However, decision has to be taken according to control command topology and future roadmap regarding smart grid and/or DER development [221].

7.2. AMI-based Conservation Voltage Reduction

AMI provides electric power utilities with a two-way communication system to the meter, as well as the ability to modify customers' service-level parameters [3]. The expansion of AMI technologies and developments of smart meter installations through smart metering programs provide distribution grids as well as CVR with a great opportunity

to capture voltage feedback of termination points. Here, one important question is how many measurement nodes CVR requires. Depending on grid operating condition, smart meter data availability & accessibility and the type of optimization algorithm, the required measurement points could differ from one CVR approach to another. As mentioned before, it is possible to use data capturing/filtering techniques to lower AMI costs related to VVO especially for centralized VVO. In decentralized VVO, IAs could process the required data of VVO engine according to their pre-defined tasks. Another advantage of AMI-based VVO is the possibility of monitoring termination points, i.e. the targeted location of voltage reduction, online or in quasi real-time. As most recent smart meters are pre-configured to send consumer data every 15 minutes (or 5 minutes in some cases) [222], it would be conceivable to optimize the distribution grid through AMI-based VVO-CVR for each quasi real-time stage.

Another fact on using AMI data that deserves to be mentioned here is data fluctuations that may occur due to load variations in quasi real-time. It is clear that there is a time gap between data capture and the operation time of Volt-VAR Control Components commanded by the VVO engine. Load variations during and after this time gap could cause inaccurate CVR. Speeding up the process through predictive algorithms for load forecasting could be a future solution. In addition, load variations impose a safety margin at the lowest limit of ANSI for AMI-based CVRs that has to be considered as a constraint in CVR problem. For instance, CVR cannot reduce consumer voltages into 115 V or less due to safety reasons and in order to cover load variations.

7.3. Load Modeling in New CVR Approaches

The efficiency of a CVR plan depends on load type and mix. Hence, load modeling is an integral part of any CVR. Basic conventional load modeling techniques are regression and load composition models. In regression technique, load model is considered as a regression model, but in load composition technique, the CVR is being performed through load mix information. In the first technique, regression error could bias CVR and in the second technique, composition of loads for all operating time stages is not constant. Therefore, new methods are required to accurately model loads. One of the most common load modeling techniques is ZIP load modeling. In this model, load is

considered as a combination of three constants; constant power (P-constant), constant current (I-constant) and constant Impedance (Z-constant) loads. Many notable research studies such as [71] have used ZIP technique to model loads for CVR analysis. As long as load model is not fully constant power, CVR would be able to conserve energy at customer's premises. In order to determine the impact of each load model, it would be necessary to study each of them:

- Constant Power (*P*): In constant-P, load demand would be constant regardless of voltage. Hence, if the load is fully constant power, by decreasing the voltage, the network loss will increase. In this scenario, CVR will not lead to energy conservation but rather increases the power loss of the grid, and therefore has negative impact on VVO engine sub-parts. Some Examples of constant-P loads are electric motors, heat pumps, air conditioner, etc.
- Constant Impedance (*Z*): Here, the demand would be proportional to voltage squared. Thus, by maintaining the voltage within the lower limits of ANSI band, the network loss would slightly be increased by CVR sub-part, although VVO engine would be able to mitigate the impact and conserve energy. Some important Constant-Z loads are incandescent light, resistive water heater, stovetop, oven, etc.
- Constant Current (*I*): Here, the demand would be proportional to the voltage. Therefore, by reducing the voltage level, CVR sub-part could conserve energy. Losses could even be decreased slightly. There are few constant-I devices such as welding units, smelting, florescent, some power electronics, etc.

Different combination of the abovementioned loads can be observed in different times of a day for each and every consumer. Moreover, by dividing changes in energy consumption (ΔE) by changes in voltage reduction (ΔV), CVR factor (CVR_f) is gained. CVR_f , that is typically between 0.5 and 1.5 [218], is one of the foremost factors to check CVR effectiveness according to consumer type and mix in a feeder. As mentioned before, load data is received in quasi real-time in AMI-based CVR. Hence, considering a fixed ZIP load model for all time stages of a day as well as all days of a year leads to inaccurate load modeling and imprecise energy saving calculation of CVR. At each quasi real-time stage, different appliances with different ZIP penetration percentages operate in a distribution feeder. Hence, load model could be unique or at least different for each quasi real-time stage. Load disaggregation techniques can be utilized to present a more accurate ZIP model of loads for each quasi real-time stage. Using load disaggregation techniques bring opportunity for CVRs to find ZIP of each quasi real-time stage separately that increase CVR load model accuracy and improve CVR energy conservation calculation

accuracy. Another issue on finding accurate ZIP model is the lack of sufficient research on reactive power model of ZIP. In other words, very few works have been done to evaluate accurate reactive power of CVR factor. As such, more studies have to be done on finding reactive power model of loads in order to perform precise quasi real-time CVR in near future.

7.4. CVR Objectives as a Part of VVO Engine

Generally, the main targets of a smart grid-based VVO can be summarized as minimizing distribution network losses, minimizing the operating costs of VVCCs and maximizing the benefits achieved by CVR through energy saving and demand reduction. Typically, loss minimization is fulfilled using reactive power control components such as switchable shunt Capacitor Banks. In plenty of operating scenarios, VAR injection by CBs could lead to voltage increment in distribution grid due to load mix and type. In this operating scenario, VVO objective is to minimize loss while trying to reduce the line voltage to perform CVR. If there is no compromise solution applied for these conflicting sub-parts of VVO, the algorithm may slow down or even diverge which may cause VVO to fail. Therefore, trade-off approach by weighting each VVO sub-parts of VVO objective function could be an appropriate solution for this operating issue. In order to detect accurate weighting factors of each VVO sub-parts, Fuzzification techniques can be employed. To make Fuzzification technique fully functioned, VVCC operating costs, VVO-CVR costs as well as revenue gained from energy saving and loss reduction have to be known. Then, the weighting factors of each sub-part will be determined according to the given cost-values.

7.5. Volt-VAR Control Component Switching Events

With the advent of real-time CVR techniques, one concern is to keep the lifetime of CVR components such as VRs and LTCs as per normal. Using AMI gives CVR an opportunity to conserve energy in quasi real-time. As LTCs and VRs operate in quasi real-time in AMI-based CVR, they could be switched on/off much more than before. Due to the fact that each Volt-VAR control component operates within distribution network has

limitation on its number of switching per day, a solution has to be made to settle this issue. It has to be stated that new advancement in VVCC technologies have decreased this concern as new maintenance free VR and/or LTCs have entered the market with 2-million allowable switching events over a life cycle of 20 to 25 years. In other words, allowable switching events could be between 219 and 274 switches per day that are quiet adequate switching numbers in comparison with quasi real-time stages per day of VVO (every 15 minutes: 96; every 5 minutes: 288), but this concern still remains in grids comprised of older operating VRs and LTCs.

Predictive techniques could also be used to solve this issue as well. Predictive techniques enables detecting the best VVCC switching times through load forecasting according to VVCC's switching constraints, and the value of VVCC switching at each specific time stage to decrease VVCC switching events. Another solution could be giving high weights to VVCC switching costs in specific operating time stages in VVO objective function. The high costs of switching at those time stages lead to less switching events although accurate determination of switching numbers would be tough in this technique.

7.6. CVR and Smart Grid Technologies

New smart grid technologies could impact the distribution network and CVR efficiencies. Generally speaking, the expansion of technologies such as smart inverters in DGs, BES systems, CESS systems and EV charging stations are gradually changing the characteristics of the distribution networks and consequently the CVR solutions. From VVO point of view, the abovementioned technologies could be considered as new VAR injection sources for VVO engines to achieve higher levels of accuracy and optimization in the near future. Therefore, new smart grid-based VVO techniques would be able to request VAR from smart grid sources and/or technologies.

Moreover, penetration of smart grid technologies such as EVs, Micro-CHPs and PVs could change the load model. Thus, it is necessary for future CVRs to present a more accurate real-time load model according to the existing smart grid components in the system. From CVR point of view, a good feeder is a feeder for which "flattening voltage" can be carried out comfortably. However, the emergence of smart grid power electronics

raises load variations in the distribution networks which consequently lead to excessive operation of VVCCs such as VRs and LTCs. On the other hand, the impact of DERs operation on VVCCs could produce voltages, which could be higher or lower than the values CVR expected. Predicting these load variations and monitoring the impact of DERs are key tasks of future VVO engines to precisely model loads in real-time according to the characteristics of load as well as smart grid DERs. Another issue can be load imbalancies of phases that may occur in the presence of single-phase DERs. In this operating scenario, the availability of single-phase VRs and/or CBs could be pivotal in proposing a CVR plan. In addition, when reverse power flow occurs in the presence of DERs, there is more possibility for voltage to run out of ANSI range. Hence, considering CVR as a sub-part of VVO could be more meaningful when VVO observes the mentioned impacts of DERs in the system.

7.7. Economic Factors for Future CVR Plans

In order to prepare a successful CVR plan, it is compulsory to consider economic factors alongside technical factors. As new CVR plans are being considered as a sub-part of VVO engines, VVO economic factors affect CVR plans as well. First and foremost, VVO implementation costs have to be compared with the value of "Negawatt" [223], e.g. the value of saved energy achieved by VVO. Moreover, if the Internal Rate of Return (IRR) matches with electric power utility targets, CVR plan could be workable. VVO implementation costs include but not limited to:

- VVO AMI costs (AMI system, End-of-Line metering if not available)
- VVO-CVR Engine cost, existing VVCC operating costs, required VVCC costs (replacement or new installation)
- VVCC switching value cost
- Feeder related costs (re-conductoring, balancing, re-configuration)
- Communication infrastructure costs
- Maintenance scheduling of VVCC costs and;
- Crew costs

On the other hand, earned revenue as an outcome of VVO-CVR plan comprises of the revenue earned through loss reduction, the revenue earned through energy consumption saving and the value of demand reduction. Here, the main concern is still the value of lost-revenue that some utilities consider as part of their expenses even when some studies have shown that CVR costs are less than the generation cost of most common generating units in the system. Taking lost-revenue into account, could decrease the outcome value and raise the IRR of CVR plans.

7.8. Standard and Regulations for Future CVR Plans

By proposing new, or by expanding existing regulations and protocols, it will be possible to bring future CVRs to higher levels of accuracy and efficiency. As mentioned before, proposing CVR regulations in accordance with market rules is essential in deregulated distribution networks. If we assume that CVR implementation could lead to better electricity price offers for consumers, retailers could encourage Distribution Companies (DISCOs) to perform CVR. As DISCOs may not be eager to increase their expenses caused by CVR, retailers could provide adequate incentives for distribution network operator according to cost-benefit analysis.

On the other hand, standards such as IEEE 1547-2003 [224] impose limitations on CVR plans in distribution networks with DERs. Hence, new procedures are required for CVR implementation in microgrids with DERs. Furthermore, it is essential to use reliable and secure communication protocols in order to perform coordinated control, and build a reliable two-way communication system from termination points to VVO engine and from VVO engine to VVCCs. DNP3 is one of the well-known applicable standards for this aim. Moreover, IEC 61850 [181], [225], used in substation automation and smart grid applications, can also be applied for CVR implementation. IEC 61850-7-420 defines standards for DERs in the system. IEC 61850 90-1 helps substations to communicate with each other. IEC 61850 90-2 supports communications between control center (that is VVO engine in centralized VVO) and substations. IEC 61850 90-6 provides the required standards for distribution feeder automation systems and IEC 61850 90-7 supports smart grid technologies such as storage, PV and smart inverters. As VVO engine sits in the MV substation in decentralized VVO, IEC 61850's main standard could also be used.

7.9. CVR Impact on Short-Term Planning of Distribution Networks

New CVR approaches could affect short-term planning of distribution networks in different manners. As the location of VVCCs, such as VRs along the distribution feeder highly depend on the end-of-the-line load and feeder length, VR placement is done according to the value of voltage drop at the end of the feeder. Emergence of new CVR approaches shall impact the VR placement in short-term planning, considering CVR benefits. It seems that in the near future, VRs could be located much closer to load consumption centers, i.e. end of lines in order to save more consumed energy through CVR. Moreover, using single-phase IRPs at the LV secondary side of the transformer could also be a future candidate for CVR approaches that might be taken into account by distribution network planners.

According to methods determined for VVCC operations by VVO engine, maintenance scheduling plans of VVCCs could also be modified. Distribution network planners have to assess VVCC switching costs besides maintenance scheduling costs of VVCCs to achieve a more accurate estimation of expenses caused by CVR and to properly compare expenses with revenues gained from CVR energy saving in order to reach to a more appropriate strategy for VVCC operations. For fixed and switchable shunt CB placements, benefits gained by new real-time VVO have to be considered in distribution network's short-term plans. For future EV charging station placements, the capability of EVs for injecting reactive power into the system has to be put in VVO objective function. In addition, reaching more accurate approximation of load amount and types could help both CVR and short-term planning to execute more effectively in future distribution networks. At the end, Figure 7.3 summarizes future CVR challenges and probable solutions.

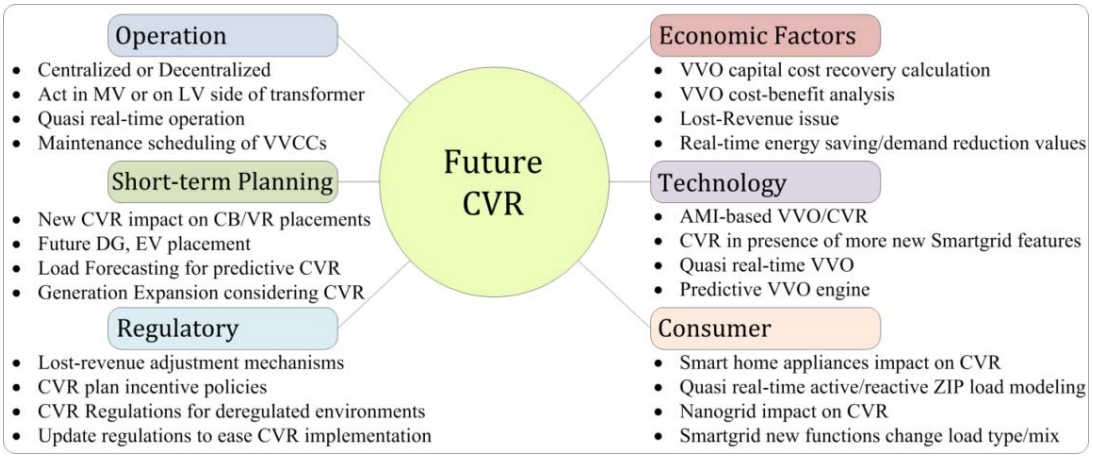

Figure 7.3. Future CVR challenges and probable solutions

7.10. Summary

The growth and the expansion of smart grid technologies and/or functionalities could accelerate the emergence of a new generation of CVR approaches that could operate as a key part of Volt-VAR Optimization engines to increase the Negawatts (kW that can be saved through energy conservation and energy efficiency approaches) throughout the distribution networks. Applying AMI data could improve CVR operation by providing it the opportunity to save energy at each quasi real-time stage. In AMI-based CVR approach, quasi real-time load modeling is indispensable. Finding quasi real-time ZIP load models increases the accuracy of CVR operation and energy consumption saving calculations. Due to the load variations in quasi real-time, it would be essential to employ weighting factors for VVO engine objective function sub-parts such as VVCC operating costs, loss minimization costs and CVR benefit maximization for each real-time stage to find optimal VVCC strategies of each quasi real-time operating stages. Applying predictive algorithms in the future could lower the impact of load variations on CVR and could robustly solve the number of switching operation issue of VVCC.

Developments of smart grid technologies such as PV, BESS, CESS and EV could bring opportunities and/or challenges to CVR. VVO could benefit from smart grid technologies with new reactive power control source. On the other hand, intermittent operation of aforementioned sources forces more variations in the distribution grids that lead to excessive operation of several VVCCs. As generation and load variation

predictions can be fully done by Artificial Intelligence techniques, it seems that using artificial intelligence could be one of the greatest solution candidates for solving this issue in future real-time CVRs. Significant economic factors such as VVO AMI costs, VVO-CVR Engine cost, existing VVCC operating costs, the required VVCC costs, VVCC switching value cost, communication facility costs, revenue earned by loss reduction, revenue earned through energy consumption saving and the value of demand reduction have to be taken into account in CVR plan cost-benefit analysis. Lost-revenue value is still a major concern of some electric power utilities for CVR implementation while some studies showed that CVR cost are typically less than the generation cost. Standards and protocols such as IEC 61850 could provide a reliable bi-directional communication between different parts of VVO.

Ultimately, as new CVR approaches could affect different parts of the distribution network short-term planning such as CB, VR, DG and EV charging station placements, CVR energy saving in future short-term planning of distribution networks could improve the accuracy of short-term planning. It could reduce CVR costs that could indeed smooth the path of smart grid-based CVR development in the future of electrical distribution networks.

Chapter 8.

Maintenance Scheduling of Volt-VAR Control Components

As explained in introduction section, the roots of power system issues are typically found in the electrical distribution systems and the point of departure for grid overhaul is firmly placed at the bottom of the chain [3]. As such, maintenance scheduling of distribution network assets is one of the challenges of distribution network planners. Various distribution network assets such as transformer, capacitors and distributed resources are going to be inspected and/or going to maintenance annually. As quasi real-time VVO solutions are going to be utilized more to minimize distribution network loss and increase energy conservation of termination points in near future, applying a reliable Maintenance Scheduling Engine (explained in this chapter as MSE) in-line with recent smart grid VVO technologies (e.g. new AMI-based VVO solutions) as well as distribution network other requirements can help distribution network to be optimized more effectively. Therefore, maintenance scheduling of Volt-VAR Control Components has become very important. VVCCs of a distribution network are now able to save the energy consumption as well as improve system loss in quasi real-time intervals through AMI-based VVO approaches. As proposed smart grid-based VVO performs in quasi real-time, finding a proper maintenance scheduling approach to match with this VVO approach seems necessary.

Hence, this chapter proposes a novel approach for maintenance scheduling of Volt-VAR control assets for new AMI-based VVO solutions through Maintenance Scheduling Engine (MSE) concept. MSE is responsible for solving maintenance scheduling of VVCC's problem in coordinated time frames with AMI-based VVO. MSE has to send final maintenance scheduling optimal strategies and/or results to VVO Engine (VVOE) in order to keep maximization of VVO operational benefits when VVCCs are gradually going to maintenance in different time periods. Thus, this novel approach could solve maintenance scheduling of Volt-VAR control asset's issue, improve AMI-based VVO performance without any interference or failure, and optimize distribution network effectively.

8.1. Maintenance Scheduling Engine (MSE) Concept

This section studies maintenance scheduling problem of VVCCs in presence of the proposed AMI-based VVO approach. As it is mentioned in previous section, different Volt-VAR control assets such as CBs, VRs and OLTC exist in distribution networks. According to VVCC principal characteristics and their specific roles in AMI-based VVO, and according to field investigations by contacting different utilities, required maintenance period and specifications for each Volt-VAR control component is found and shown in Table 8.1. As it is represents in Table 8.1, maintenance scheduling time period for most VVCCs is considered annually. Contrariwise, AMI-based VVO engine performs every 15 minutes. Hence, there should be time coordination between maintenance scheduling problem and Volt-VAR Optimization problem. This study proposes a MSE demonstrated in Figure 8.1 to solve this issue.

Table 8.1. Maintenance Features for Volt-VAR Control Components

VVCC /Grid Component	Maintenance Duration (hours)	Most Maintenance Duration (hours)	Maintenance times per year/Maintenance Procedures
Switchable Shunt Capacitor Bank	4-8	6	1/ Capacitance balance, capacitor switching device, find hot spots, loose connections; visual inspections, removal of birds' nests, etc.
Voltage Regulator	Single phase: 5 Three-phase: 8-10	9	1/Inspect /change contacts, oil level/quality, pressure gauge, driving mechanism, operational tests, record counter operations
On-load Tap Changer of Transformer	10-12	12	1/1/Inspect /change contacts, oil level/quality, pressure gauge, driving mechanism, operational tests, record counter operations
XMFR	-	-	no maintenance process

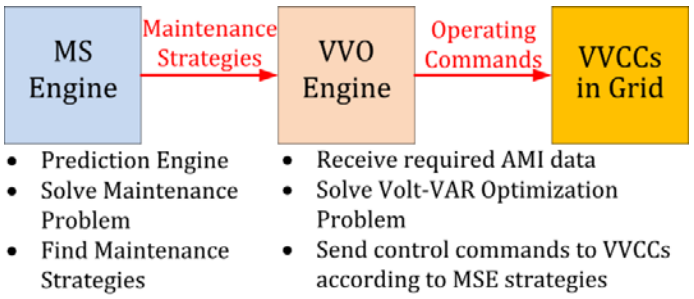

Figure 8.1. General task flows of Maintenance Scheduling and VVO Engines

MSE is responsible to predict the best maintenance time of each VVCC within one-year horizon by its Artificial Neural Network (ANN) prediction engine. Basically, the horizon of maintenance scheduling that network planners provide is for a complete year as each VVCC has to be checked annually. In other words, network planners have to optimally determine when VVCCs have to go to maintenance in a year. Hence, network planners are dealing with annual load forecasting to find which days of a year are more suitable for the maintenance of VVCCs. Fundamental factors required by MSE to solve maintenance scheduling problem include but not limited to maximum maintenance period for each VVCC, crew costs, maintenance costs and the value of benefit gained from VVO operation. Therefore, the objective function of maintenance scheduling problem for AMI-based VVO could be as (8-1).

$$Max\ MS.O.F = \sum_{t=1}^{T}\left(V_{VVO,t} - C_{VVO,t}\right) \times (1 - x_e) - \sum_{t=1}^{T}((FC \times \frac{1000}{8760} \times x_e) + (VC \times x_e \times h_e)) \quad (8\text{-}1)$$

FC and VC respectively show fixed maintenance costs (for CBs: \$/kVAR/year, for OLTC/VRs: \$/switching/year) and variable maintenance costs (for CBs: \$/kVARh, for OLTC/VRs: \$/switch×h). *X* is the Maintenance binary value (1: under maintenance & 0 otherwise) and *h* is the maintenance time. Key constraints for explained maintenance scheduling problem are as follows:

- One-time Maintenance: each VVCC has to go to maintenance only one time in horizon year
- Maintenance Window: each VVCC should not go to maintenance early or late
- Maintenance continuity: maintenance hours of each VVCC should respect time continuity
- Maintenance Duration: maximum maintenance duration of each VVCC should be respected
- Maintenance/VVO constraint: All VVCCs in a system cannot go to maintenance at a same time as it may cause VVO failure

Thus, MSE primarily commences its prediction engine regarding to specific annual historical data such as loads, electricity price and value of VVO sub-parts in general. Then, it finds hours and days of prediction year that each VVCC can optimally go to maintenance. At the end, it sends maintenance problem results to the VVO Engine. The main advantages of this approach includes but not limited to: AMI-based VVO can optimize distribution network online without any interruption, VVCCs are going to maintenance in optimal sequence and this approach keeps the well-performance of both AMI-based VVO and distribution network. In brief, MSE could suggest different optimal scheduling for each Volt-VAR control asset. It is known that loss minimization can be done through reactive power injections of switchable shunt CBs and through increasing voltage level of nodes by VRs and/or OLTC. On the other hand, CVR can be utilized by lowering voltage level of termination points by VRs and/or OLTC. Hence, finding trade-offs between these two parts of AMI-based VVO (i.e. loss minimization and CVR) in some time periods is probable.

This could lead the optimization engine to converge to the optimal solution very slowly or even lead to optimization divergence. In order to solve this issue, MSE provides AMI-based VVO sub-parts with intelligent weighting factors that could be defined for each VVO operating time stage (i.e. every 15 minutes). Hence, the whole system is guaranteed to operate efficiently and to find optimal results for both maintenance scheduling and VVO problems.

8.2. Summary

This chapter proposed a novel approach for maintenance scheduling of Volt-VAR Control Components in quasi real-time AMI-based Volt-VAR Optimization of distribution networks by a coordinated command and control system between VVO Engine and MSE. Hence, MSE of this chapter has been solved according to historical data such as previous year's loads, weighting factors, and/or value of loss minimization to find optimal maintenance periods for different types of Volt-VAR control assets within distribution network. In next step, VVO engine received MSE optimal results. Then, VVO engine regulated itself according to maintenance strategies sent by MSE. Thus, quasi real-time AMI-based VVO performed online without any interruption or interference that could be caused by maintenance scheduling problem.

Proposed MSE approach has to find optimal maintenance periods within a horizon year in such a way that VVO engine would face with minimum losses during VVCC maintenance periods. Therefore, the best maintenance strategies according to the VVO engine and other main maintenance problem requirements could be found with proposed solution. In conclusion, this approach could be utilized as an "additive" part of existed AMI-based VVO solutions or as a part of future quasi real-time VVO techniques to lead future distribution networks to higher levels of optimality, accuracy and efficiency.

Chapter 9.

Predictive Volt-VAR Optimization

This chapter aims to discuss the possibility of designing a predictive VVO engine in compliance with smart grid features. As explained in previous chapters, the AMI data is collected by the measurement aggregators in the system in a time-interval manner, i.e. every 15 minutes. Hence, there is a time lag between data collection and VVO command executions. In other words, the result of VVO for time interval *t* is based on load data captured in time interval *t-1*. As active/reactive load profile changes from an operating time interval to the next time interval is not much in most time of a day for a feeder, it is possible to perform VVO commands in present time interval based on data captured in the previous time interval with acceptable approximation, but in order to become more precise, VVO can employ predictive techniques to forecast data of the next time interval according to feeder configuration and historical data. Therefore, predictive VVO engine can bring great opportunity for AMI-based VVOs to become more efficient in near future. In order to design a prediction engine, four different prediction steps have to be followed: Inputs, Prediction Model, Prediction Algorithm, and system outputs. These steps are followed in this study in two different approaches:

- Day-ahead predictive VVO: According to system historical data and other feeder attributes, VVO tries to forecast day-ahead load profile for system nodes for quasi real-time intervals of the next day. This approach can also be called Offline Predictive VVO. The main advantage of this approach is on having a super-fast performance in the grid as VVO finds the optimal solution of the system for each quasi real-time interval in a day-before. Hence, control commands will be sent to the VVCCs right after the operating time stage begins. As the prediction can be improved by the previous time interval data, live prediction could lead system to a higher level of accuracy.
- Live Predictive VVO: In this approach, the VVO engine primarily finds the optimal settings of VVCCs for a day ahead. Then, at each quasi real-time interval, it improves its prediction using the previous time interval data. This improvement is done through a live prediction part of the VVO engine. This could help system to find active and reactive consumption/generation of distribution network loads/generations in a more precise method. Moreover, in distribution grids with high penetration of distributed generation, renewable resources, power electronics and variable loads, that might have salient load-variations, this approach can be more applicable rather than the day-ahead approach.

In recent years, many researches have worked on electric load forecasting using Artificial Neural Networks. The reason most literatures use ANNs lies in a fact that ANN has an appealing ability to model the non-linear relationship between distribution system loads and weather parameters. That is the reason why this technique is mostly applied for short-term load forecasting of distribution networks as well. Although predicting all system nodes separately could be more time consuming than predicting total load of the feeder or distribution grid (in short-term load forecasting), it seems that ANN could be candidate for live prediction as its prediction model is also simple, efficient and cost-effective. In next sections of this chapter, the inputs, prediction models, the algorithms and the outputs of both VVO predictive approaches are discussed.

9.1. Neural Network Engine for Day-ahead Predictive VVO

Generally, it is known that next day's load correlates the loads of previous days and other factors such as temperature, dew points and calendar dates. Hence, Multi-Layer Perceptron (MLP) Neural Network is applied in order to find the abovementioned dependencies. As system inputs in this study were captured from substations and as acceptable error was about 5 percent, MLP was an appealing method. The structure of MLP network is similar to a nonlinear system recognition problem. Some of the exclusive features of MLP method such as its nonlinearity and its considerable versatility provide a great environment to employ specific inputs such as time stage, type of a day (working day, holiday), and number of days in a week in Neural Network engine. MLP tries to combine neurons in a way that the output be a linear combination of inputs. The relation between inputs and the output of a Neural Network can be shown by (9-1).

$$y_{out} = \rho \sum_{i=1}^{I} (w_i x_i - \theta) \tag{9-1}$$

Here, $y_{out}$is the output, $x_i$are the inputs, $w_i$are the neuron weights, θis the bias and ρis the activation function that could be a linear function, logistic function and/or hyperbolic tangent function. The MLP used in this study consists of three layers: Input,

Mid-layer (hidden layer) and Output. Figure 9.1 shows three different layers of considered MLP-NN.

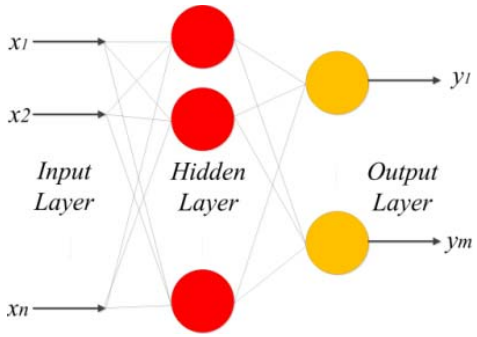

Figure 9.1. Three different layers of a MLP Neural Network

The Neural Network structure applied in this study is a Universal Function Approximator that proves the fact that in the existence of correct number of neurons in the mid-layer, the Neural Network is able to approximate a continuous function in R^ntoR^m. In order to minimize the difference between predicted output and the real output of the system, the network has to be trained well. Each epoch gives the repetition of the training algorithm for all input data. The training method used in this study is Back-Propagation in MATLAB. In this method, the gradient of least squared errors is estimated by back-propagation of the error and then, the weights of the system can be optimized by it. The inputs of the Neural Network engine for training for each smart meter are as follows:

- Active/Reactive Load of previous day at that time stage
- Active/Reactive Load of previous week at that time stage
- The average of previous day active/reactive load at that time stage
- Time stage numerator (1 to 96: each time stage=15 minutes)
- Types of day (Binary: 1=work day, 0=holiday)
- Week numerator (1 to 7)
- Temperature (°C) at that time stage
- Dew Point (°C) at that time stage

Therefore, the Neural Network engine trains the network based on the abovementioned data and predicts the active and reactive power of loads for all time stages of a day ahead at each node of the system. Then, the resulted data will be sent to the VVO engine for network optimization.

9.2. Predictive Engine Algorithm for Online Predictive VVO

In order to design a predictive algorithm for VVO, offline prediction and VVO engines have to primarily find and save system optimal results for day-ahead based on system historical data. At targeted day and at each time interval, the system compares real data with predicted data. If the error is not acceptable, the VVO engine sliding window finds the optimal solution of the system for that time interval and updates previous offline results. This structure could lead to a more fast and accurate results. Moreover, it can solve the VVO asset switching per day issue through combining offline and live VVO. Figure 9.2 presents the flowchart of proposed predictive VVO.

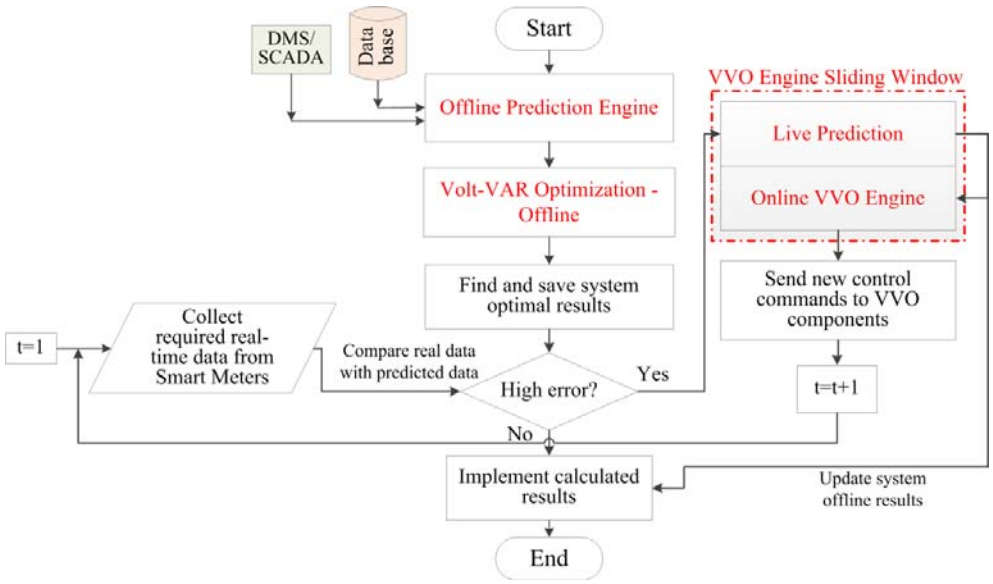

Figure 9.2. Basic flowchart of proposed predictive VVO

VVO knows the result of time intervals from a day before. Hence, at each time interval it compares offline prediction with real measurement. If it is satisfactory, it will send optimal commands to VVCCs. Otherwise, it runs live prediction in order to correct prediction error using a feedback from real-time measured load. It is simply known that VVO asset switching per day issue can be solved in offline VVO ((5-22), (5-25) and (5-28)). It is possible to consider this issue as a constraint in VVO engine. In proposed real-time predictive VVO, live sliding window will find the new optimal configuration of network using this constraint. Moreover, it already knows how many times CBs or VRs were being switched on or off before that time stage. Hence, it will provide a new optimal configuration based on previous situation of VVO control components and predicted (updated

prediction) data of upcoming time stages. It has to be mentioned that the prediction ahead, gives the algorithm a great chance to perform faster and solve the problem within considered time-frame. Otherwise, only online VVO approaches may fail to find the optimal solution within required time-frame or may fail to provide a technique to solve VVO asset switching per day issue. As explained, a constraint in offline VVO considers this issue and online VVO decision will be based on offline VVO switching scenarios (that has already solved the issue) and collected real-time data that can be used for updating predictions for time interval ahead.

9.3. Live Prediction Engine Design

Basically, day-ahead load prediction highly depends on the loads of previous days and other factors such as temperature, dew points and calendar. Hence, Multi-Layer Perceptron (MLP) Neural Network is used to find the dependencies among mentioned factors. MLP combines neurons in a way that the output be a linear combination of inputs. The inputs and the output relation in a Neural Network can be presented by (9-2).

$$X_j = \sum_i \omega_{ij} Y_i + \theta_j \qquad (9\text{-}2)$$

Here, Y_i is the output of *i*, X_j is the input of *j*, $\omega_{ij}$is the neuron weight from *i* to *j* and $\theta_j$is the bias on *j*. There is an activation function that could be a linear function, logistic function and/or hyperbolic tangent function within NN engine. This study used Back-Propagation algorithm for NN training in order to predictive loads of the system. Figure 9.3 shows different layers of NN engine using back-propagation technique. First, the NN engine initializes all biases and weights in networks. Second, it propagates the inputs forward. For each hidden or output layer unit *j* it computes the net input of unit *j* through (9-2). Then, it computes the output of each unit *j* by (9-3).

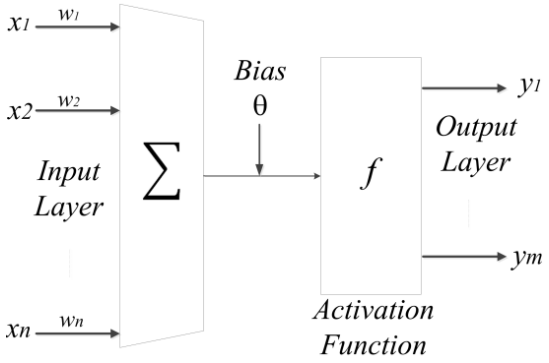

Figure 9.3. Different layers of Neural Network Engine

$$Y_j = \frac{1}{1 + e^{X_j}} \tag{9-3}$$

Here $Y_j$is the output of unit *j* and X_j is the input of unit *j.* Then, the algorithm tries to back-propagate the errors for each training sample. First, it computes the error for the output layers using (9-4) and then finds the error for hidden layers through (9-5).

$$err_j = Y_j(1 - Y_j)(\tau_j - Y_j) \tag{9-4}$$

$$err_j = Y_j\big(1 - Y_j\big)\sum_k err_k\,\omega_{jk} \tag{9-5}$$

Here, $\tau_j$is the real output value for unit *j*, $err_k$is the error of *k* and the ω_{jk} is the weight from unit *j* to unit *k*. For each weight in the network, there is a weight increment (9-6) and weight update (9-7). Similarly, for each bias in the network, there is a bias increment (9-8) and bias update (9-9).

$$\Delta\omega_{ij} = \propto err_j Y_i \tag{9-6}$$

$$\omega_{ij} = \omega_{ij} + \Delta\omega_{ij} \tag{9-7}$$

$$\Delta\theta_i = \propto err_j \tag{9-8}$$

$$\theta_j = \theta_j + \Delta\theta_j \tag{9-9}$$

Where, $\Delta\omega_{ij}$ is the change in weight from *i* to *j*, $\Delta\theta_i$ is change in bias and $\propto$ is learning rate that is between zero to one. The algorithm will be trained until reaching to the convergence rate. Hence, the algorithm tries to reduce prediction error by updating its weights within learning procedure. The NN engine provided for this study is in MATLAB environment. The inputs of the Neural Network engine for training for each smart meter are as follows:

- Active/Reactive Load of previous day at that time stage
- Active/Reactive Load of previous week at that time stage
- The average of previous day active/reactive load at that time stage
- Time stage numerator (1 to 96: each time stage=15 minutes)
- Types of day (Binary: 1=work day, 0=holiday)
- Week numerator (1 to 7)
- Temperature (^{o}C) at that time stage
- Dew Point (^{o}C) at that time stage

Hence, the prediction engine trains the network based on the abovementioned data and predicts the active/reactive power of loads for all time stages for every node of the system. Then, the resulted data will be sent to the VVO engine for the optimization of network.

Chapter 10.

Optimization Technique for Volt-VAR Optimization Problem

10.1. Experimental/Computational Methodology

Different optimization techniques can be used for Volt-VAR Optimization problem. Depending on variables, parameters and complicacy of the system, VVO problem can be determined as:

- Multi Objective Optimization: VVO needs to simultaneously optimize two or more conflicting objectives subject to certain levels of constraints.
- Mixed Integer Nonlinear Programming: VVO deals with non-linear systems in which some variables are constrained to take integer values such as capacitors banks (on/off), voltage regulators and tap changer steps (on/off) and some may have nonlinearities as system intends to minimize grid loss and conserve the energy consumption. Hence, the VVO objective function and constraints may contain nonlinearities.

As explained, many optimization techniques could be employed for proposed VVO problem. As it is not possible to cover all VVO optimization methods in a research, the effort of the research is to find an efficient algorithm for proposed VVO with acceptable accuracy and reliability with short-enough convergence time.

10.1.1. Initial Choices

As Heuristics & Meta-heuristic techniques impose few or no unreal assumptions on the problem, they are able to optimize distribution network precisely in most times. Moreover, they may have very large search space for candidate solutions. This can lead to precise solution but can affect computational time as well. Genetic Algorithm (GA) (meta-heuristic approach) is one of the techniques that are widely used in distribution network applications such as VVO. Moreover, Bender's Decomposition technique (heuristic approach) is another interesting technique for VVO application as it is able to divide the large-scale optimization problem into smaller Master and Slave sub-problems. Technique such as Particle Swarm Optimizations (PSO), as a stochastic optimization, is

another convenient approach. Therefore, the techniques that are covered in this research are:

- Genetic Algorithm (GA): Improved genetic algorithm can solve the optimization problem precisely with adequate convergence time. Crossover and mutation step determinations are very important in terms of the optimization accuracy. Local optimums should be avoided. Initial populations should be in rational range. Applying huge initial population leads to a time-consuming optimization.
- Benders Decomposition: Benders technique decomposes optimization problems with lots of constraints into several sub-problems with fewer constraints. As VVO problem consists of disparate objectives and constraints, Benders decomposition technique could be a candidate for the optimization problem especially in large distribution networks.
- Particle Swarm Optimization (PSO): As a stochastic optimization, PSO is able to optimize distribution networks very fast. The simplicity of the structure, accuracy and fastness of this optimization technique are some of the reasons that most researchers intend to work with PSO.

10.1.2. Matching VVO technique with Real-Time Operating (RTO) systems

Real-Time Operating (RTO) systems are online tools tailored for checking the performance of optimization process. RTO in VVO can be a complex model-based system that resides in, and optimizes system operations. This research matches its final VVO technique with co-simulated RTOs in next chapter.

10.1.3. Initial Flowchart of VVO

The conceptual VVO algorithm is presented in Figure 10.1. As shown in Figure 10.1, required data of VVO is captured by measurement aggregator and/or IAs. If receiving data are as same as previous time-interval data, the engine imposes previous optimal solution to the present time interval. Otherwise, it begins to find the optimal solution of present time interval in three operating steps. First, the VVO engine tries to confine the solution into distribution substation. Then, it expands the optimization space along distribution feeder. In third step, it tries to check if any of the present DGs and/or DERs in the system are available on helping VVO with reactive power support or not. If for any reason, the system finds no optimal solution during specified computation time, the engine may try to offer closest feasible solution. Otherwise, it has to report algorithm divergence.

The corrective actions have to be followed by the divergence report to avoid incorrect settings of VVCCs in the system.

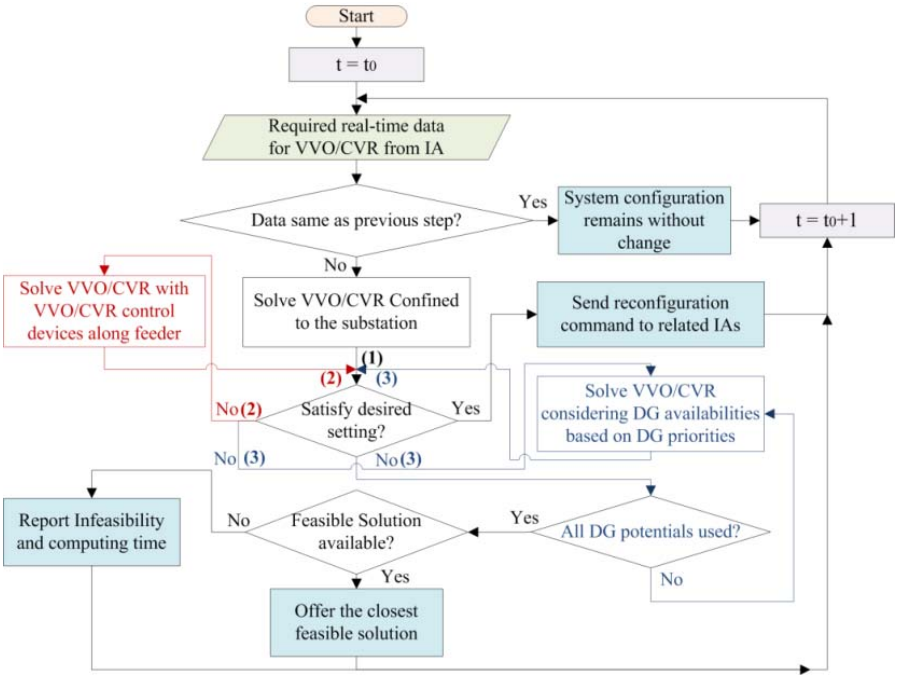

Figure 10.1. Conceptual flowchart of proposed VVO

10.2. Benders Decomposition Technique

10.2.1. Introduction

In 1962, J. F. Benders [226] proposed a technique for solving a mixed-integer programming problems by partitioning these types of problems into two parts:

- Integer Part
- Continuous Part

It uses the branch-and-bound method on the integer part and linear programming on the continuous part. Benders technique is described in many sources on large-scale optimization and stochastic programming. It is an approach for solving mathematical programming with complicated variables. It searches over values of these variables that, when fixed, result to a much simpler sub-problem. The search learns from past experience by employing “Benders Cuts”. In 1972, A. Geoffrion [227] said: “J.F. Benders devised a

clever approach for exploiting the structure of mathematical programming problems with complicating variables (variables which, when temporarily fixed, render the remaining optimization problem considerably more tractable).” He generalized this technique to a broader class of programs in which the parameterized sub-problems need no longer to be a linear program. Nonlinear convex duality theory applied in Geoffrion’s work to derive the cuts. Hence, Geofrrion’s work plays a key role in extending benders approach.

10.2.2. Benders Decomposition Advantage

Benders decomposition decomposes along time intervals. There exists other technique that decomposes along time intervals that are faster than benders decomposition but this approach is the learn-to-walk-before-you-can-run method in reaching to optimal solution of an optimization problem. That makes this technique valuable compared with other decomposition/relaxation techniques.

10.2.3. Brief View of Benders Decomposition Method

- Problem is decomposed to a Master Problem (MP) and several Sub-Problems (SPs).
- Generally, master problem is an integer problem and sub-problems are some linear / nonlinear programs.
- Typically the lower bound solution of the master problem involves fewer constraints.
- The sub-problems test the solution of the master problem to check if the solution satisfies the remaining constraints or not.
- If the sub-problems are feasible, the upper bound solution of the original problem will be calculated while forming a new objective function for further optimization of the master problem solution.
- If any of the sub-problems is infeasible, an “Infeasibility Cut” that represents the least satisfies constraint will be introduced to the master problem.
- Then, a new lower bound solution of the original problem will be obtained by re-calculating the master problem with more constraints.
- The final solution of benders decomposition algorithm may need several iterations between the master problem and sub-problems.
- When the upper bound and the lower bound are sufficiently close, the optimal solution of the original problem will be achieved.

10.2.4. Benders Decomposition Applications

Benders Decomposition Algorithm is very helpful in solving large-scale MIP problems. Some of successful applications of it are [228]: electrical power systems, operation and planning in management, electronic packaging, network & communication design, transportation, logistics, manufacturing, military and warfare strategies.

10.2.5. Basic Formulations of Benders Decomposition [229]-[234]

*Problem-1 (P-1)

Objective Function

$$Min\ Z = c^T x + d^T y \tag{10-1}$$

Subject to

$$Ay \geq b, \quad Ex + Fy \geq h, \quad x \geq 0, \quad y \in S \tag{10-2}$$

$A \rightarrow m \times n, \quad E \rightarrow q \times p, \quad F \rightarrow q \times n$

$x, c: p\ vector$

$y, d: n\ Integer\ Vectors$

$b \rightarrow m\ vector,\ h \rightarrow q\ vector$

$S = Arbitrary\ Subset\ of\ E^P with\ integral - valued\ components$

Since *x* is continuous & *y* is integer: *P-1 is a Mixed-Integer Problem & If *y* values are fixed, then * P-1 is linear in *x*.

$$Min\left\{d^T y \middle| Ay \geq b + min\left\{c^T x \middle| Ex \geq h - Fy,\ x \geq 0\right\}\right\} \tag{10-3}$$

Master Problem (MP-1)

$$Min \;\; Z_{lower} \tag{10-4}$$

Subject to:

$$Z_{lower} \geq d^T y, \qquad Ay \geq b, \qquad y \in S \tag{10-5}$$

Sub-Problem (SP-1)

$$Min \;\; c^T x \tag{10-6}$$

$$Ex \geq h - F\hat{y}, \qquad x \geq 0 \tag{10-7}$$

$\hat{y}$: Solution of the Master problem

Subproblem-2 (Dual of SP-1)

$$Max \; (h - F\hat{y})^T u \tag{10-8}$$

$$E^T u \leq c, \qquad u \geq 0 \tag{10-9}$$

10.2.6. Benders Decomposition Algorithm

Benders Algorithm is based on the linear duality theorem that guarantees the solution of the primal problem to be equal to the solution of the dual problem. The idea behind benders algorithm is “Learn from one’s mistakes”. It distinguishes primary variables from secondary variables. Then, it searches over primary variables in master problem. For each value of primary variables, it solves problem over secondary variables i.e. sub-problems. If the solution is suboptimal, it will find out the reason and then, it presents a constraint that eliminates not only the solution but a large class of solutions that are suboptimal for the same reason i.e. benders cut. Finally, it adds this cut to the master

problem and re-solve the problem. Figure 10.2 fully describes benders decomposition algorithm.

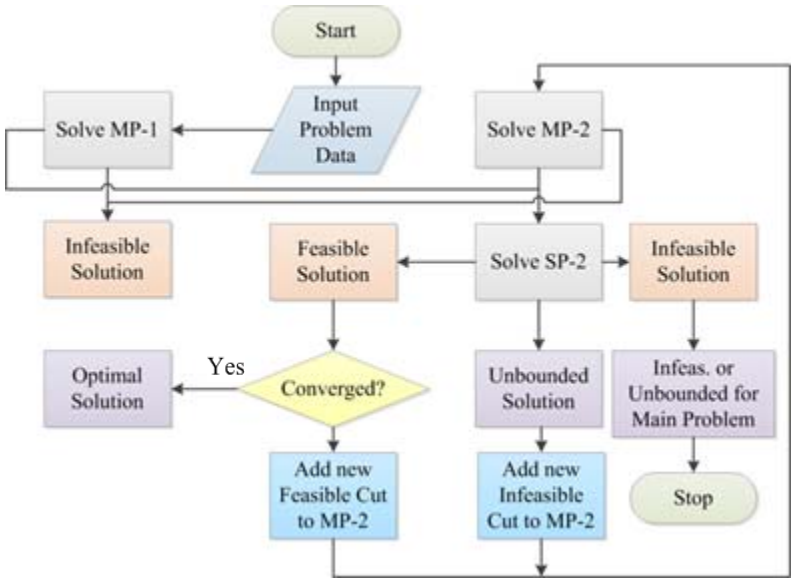

Figure 10.2. Benders Decomposition Algorithm

Benders Decomposition Algorithm Steps:

Step-1:

Solve MP-1 → Initial Lower bound solution

If feasible → Check Convergence Criterion → If yes, Optimal Solution

→ If no, add a Benders Cut to MP-2

If Infeasible → Infeasible for original problem (*P-1)

If Unbounded → Let, $\hat{Z}_{lower} = \infty$ for $\hat{y}$ in *S* and then → go to Second Step (SP-2)

Step-2:

Solve SP (SP-2 or SP-1)

For SP-2:

$$\hat{Z}_{upper} = d^T \hat{y} + (h - F\hat{y})^T \hat{u} \qquad (10\text{-}10)$$

$\hat{u}$: Optimal dual solution

$\hat{Z}_{upper}$: Upper bound solution of the original problem (*P-1) for $\hat{u}$

For SP-1:

$$\hat{Z}_{upper} = d^T\hat{y} + c^T\hat{x} \tag{10-11}$$

$\hat{Z}_{upper}$: Upper bound solution of the original problem (*P-1) for $\hat{x}$

Convergence Condition

If

$$\left|\hat{Z}_{upper} - Z_{lower}\right| < \varepsilon \tag{10-12}$$

Then,

Stop

Otherwise,

Generate Feasibility Cut:

$$Z_{lower} \geq d^T y + (h - F\hat{y})^T\hat{u} \tag{10-13}$$

Then,

Go to Step-3.

If SP-2 is Unbounded (i.e. SP-1 is infeasible) → Generate Infeasibility Cut for Solving MP-2:

$$(h - F\hat{y})^T\hat{u}^r \leq 0 \tag{10-14}$$

It is needed to calculate $\hat{u}^r$ first:

$$min\ 1^T s \tag{10-15}$$

$$x \geq 0,\ s \geq 0, \quad Ex + Is \geq h - F\hat{y} \tag{10-16}$$

1^T: Unit Vector

I: Identity Matrix

If SP-2 is Infeasible→ Original Problem (*P-1) has either no feasible solution or an unbounded solution.→ $Stop$

Step-3:

In order to obtain new lower bound solution ($\hat{Z}_{lower}$) with respect to $\hat{y}$ for original problem (*P-1)

Solve MP-2

In MP-2 we may employ either Feasibility Cut or Infeasibility Cut:

$Min \ \ Z_{lower} \ \ s.t. \quad Ay \geq b$

Feasibility Cut:

$$Z_{lower} \geq d^T y + (h - Fy)^T u_i^P, \ \ i = 1,2, \dots, n_P \tag{10-17}$$

Infeasibility Cut:

$$(h - Fy)^T u_i^r \leq 0, \ i = 1,2, \dots, n_r, \ \ y \in S \tag{10-18}$$

Then, go back to Step-2 (Solving SP again)

If MP-2 is Unbounded→ $\text{Let } \hat{Z}_{lower} = \infty for\ \hat{y} \rightarrow \text{Return to Step} - 2$

If MP-2 is $\text{Infeasible} \rightarrow$ so will be the original problem P-1 → Stop the process.

10.2.7. Alternative forms of Benders Cuts:

Feasibility Cut:

$$Z \geq d^T y + (h - Fy)^T u_i^P \overset{1}{\rightarrow} Z \geq d^T y + w(\hat{y})_i - (y - \hat{y})^T F^T u_i^P, \quad i = 1,2, \dots, n_P \qquad (10\text{-}19)$$

$w(\hat{y})_i$: Optimal Solution for SP-1

u_i^P: Incremental change in optimal objective

*Decreasing the objective value of the original problem by updating y from $\hat{y}$ to a new value.

Infeasibility Cut:

$$(h - Fy)^T u_i^r \leq 0 \overset{2}{\rightarrow} v(\hat{y})_i - (y - \hat{y})^T F^T u_i^r \leq 0, \; i = 1,2, \dots, n_r \qquad (10\text{-}20)$$

$v(\hat{y})_i$: Optimal solution of the Feasibility check Sub-problem

*Updating y to a new value to eliminate constraint violations in SP-1 based on given in the master problem.

10.2.8. Benders Decomposition Applications in Power Systems

G. Cote and M Laughton [235] were pioneers in using Benders technique in power systems. In 1979, they published a paper (decomposition techniques in power system planning: the Benders partitioning method) at International Journal of Electrical Power Energy Systems which received great feedback from power system experts. In 1980, L. F. B. Baptistella and J. C. Geromel [236] presented a decomposition approach to problem of Unit Commitment schedule for hydrothermal systems. They were first researchers to employ Benders for SCUC (Security Constrained Unit Commitment) problems in power systems. A. Monticelli [237], A. J. Conejo [238] and M. Shahidehpour [239], were some of the famous researchers who extended Benders decomposition to power system large-scale problems.

Nowadays, benders decomposition technique is used in various types of power system applications such as: SCUC of power systems, distributed networks loss reduction, feeder reconfiguration in distribution networks, smart grid operations,

generating unit planning, transmission planning, optimal generation bidding and valuation, optimal power flow, hydro-thermal scheduling, generation maintenance scheduling, transmission maintenance scheduling, long-term fuel budgeting or scheduling and long-term generating unit scheduling and valuation [228].

10.2.9. Benders Decomposition for Volt-VAR Optimization Problem

For the VVO problem, benders decomposition can be comprised of two objective function sub-parts (K_1^t andK_2^t). The first sub-part ensures system active power loss minimization and Conservation Voltage Reduction.

$$K_1^t = (P_{loss}^t \times \pi^t) + C_{CVR}^t \tag{10-21}$$

The second sub-part of the objective function minimizes VVCC (here, OLTC, VR and Shunt CBs) switching operation costs.

$$K_2^t = \pi_{OLTC}^t \times |tap^{t-1} - tap^t| + \pi_{VR}^t \times |vrtap^{t-1} - vrtap^t| + \pi_{CB}^t \times |{cstep_i}^{t-1} - {cstep_i}^t| \tag{10-22}$$

Hence, the main objective function can be written as follows:

$$O.F_{VVO}^t = min(K_1^t + K_2^t) \tag{10-23}$$

The main constraints of this objective function are power balancing equality constraints as well as constraints (5-9) to (5-19) in Chapter 5 and the following VVCC inequalities:

$$tap_{min}^t \leq tap^t \leq tap_{max}^t \tag{10-24}$$

$$vrtap_{min}^t \leq vrtap^t \leq vrtap_{max}^t \tag{10-25}$$

$$cstep_{i_{min}}^{t} \leq {cstep_i}^{t} \leq cstep_{i_{max}}^{t} \quad (10\text{-}26)$$

As it is seen, the VVO objective function is a Mixed Integer Non-Linear Programming problem (MINLP). As solving MINLP problems are typically complex, Benders' Decomposition Technique can be used in order to break down the optimization problem into a Master problem that solves Mixed Integer Programming (MIP) part and a Slave problem that solves the Nonlinear Programming (NLP) part of the problem.

VVO Master Problem:

The master problem is responsible for finding optimal taps of OLTC and VR as well as finding optimal banks of CBs to minimize the costs of VVCC switching operations. As such, the integer variables are included in the master problem.

$$O.F_{Master}^{t} = K_2^t + \delta \quad (10\text{-}27)$$

The above formulation is subject to the (10-24) to (10-26) constraints. The benders' cut for the master problem can be written as:

$$\delta \geq O.F_{Slave}^{t} + \left\{ \begin{array}{c} \sum_{l=1}^{l=L} \lambda^{t(w)}\left(tap^t - tap^{t(w)}\right) \\ +\mu^{t(w)}\left(vrtap^t - vrtap^{t(w)}\right) + \xi^{t(w)}\left({cstep_i}^t - {cstep_i}^{t(w)}\right) \end{array} \right\} \quad (10\text{-}28)$$

Here: $w = 1,2,\dots,r-1$. In master problem, $\delta$is the under-estimation of the slave problem cost that has infeasibility cost. The main task of the master cut is to integrate master and slave problems. This cut is updated at each iteration based on slave objective function value.

VVO Slave Problem

In slave problem, all integer variables are fixed (that are found by master problem) as slave has to deal with system nonlinearities. In some operating cases, it is probable

that the master solution lead to an infeasible slave problem. In order to avoid infeasibility of slave due to master solution, two variables (α_i^tandβ) are added to the slave problem objective and constraints. Therefore, the slave minimizes NLP as well as technical infeasibilities.

$$O.F_{Slave}^t = K_1^t + W\sum_{l=1}^{l=L}\alpha_i^t + \beta \tag{10-29}$$

Here W is very large positive constant, α_i^t and β are defined variables. The constraints of the slave problem are constraints (5-9) to (5-19) shown in Chapter 5 as well as the following constraints:

$$Q_{G,i}^t - Q_{L,i}^t + Q_{sh,i}^t = \left|V_i^t\right|\sum_{j=1}^{j=J}\left|V_j^t\right|\left|Y_{ij}\right| sin(\theta_i^t + \theta_j^t - \varphi_{ij}^t) \tag{10-30}$$

$$Q_{sh,i}^t = \begin{cases}\alpha_i^t - \beta & i \in CB \\ 0 & Otherwise\end{cases} \tag{10-31}$$

The dual variables associated with the discrete variables ($\lambda^{t(w)}$, $\mu^{t(w)}$and $\xi_i{}^{t(w)}$) that previously determined by the master problem are shown below:

$$tap^t = tap^{t(r-1)} \quad : \lambda^{t(w)} \tag{10-32}$$

$$vrtap^t = vrtap^{t(r-1)} \quad : \mu^{t(w)} \tag{10-33}$$

$$cstep_i{}^t = cstep_i{}^{t(r-1)} \quad : \xi_i{}^{t(w)} \tag{10-34}$$

Convergence Criterion

The benders decomposition algorithm converged to the optimal values when two conditions satisfy: (1) The solution of the master problem is feasible, (2) The slave problem

(upper bound) and lower bound variable (δ) obtained by the master problem are very close to each other (less than epsilon). The benders decomposition flowchart of the VVO problem is shown in Figure 10.3. For each iterate (*w*), the algorithm solves the master problem and finds integer variable values based on master problem solution of that step. In next step, the algorithm solves the slave problem in compliance with the master problem solution. Here, the algorithm gets the objective function of the slave problem, defined infeasibilities and dual variables. In last step, the algorithm checks the convergence criterion. If the abovementioned convergence criterion satisfied, the VVO reached to its optimal VVO solution. Otherwise, the algorithm will generate a new bender's cut based on duality variables and begins solving master problem again. This iterative process continues until system reaches to the optimal solution.

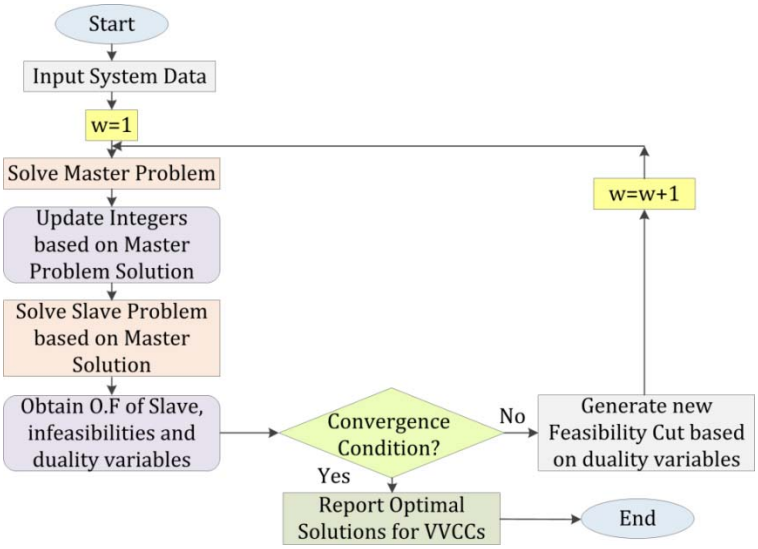

Figure 10.3. Flowchart of the VVO problem using Benders Decomposition algorithm

10.3. Optimization method: Genetic Algorithm

In this section, an efficient Genetic Algorithm (GA) algorithm is presented for the Volt-VAR Optimization problem. GA is a search heuristic optimization method based on natural evolution [240]. It consists of four important steps to reach to the optimized solution. The first step is "Initialization". In initialization, initial population is generated randomly which typically represents hundreds or thousands of possible solutions in search space. The population size depends on problem nature. The second step is "Selection"

where a proportion of initial population is selected in order to form new generation. Most likely solutions are selected according to the fitness function of the problem. As such, the fitness function measures the quality of solutions. The third step is “Genetic Operator” section that generates the second population of solutions from selected set using two operators: Crossover and Mutation. The last step is convergence criterion where GA generation process is repeated until convergence condition has been satisfied. The convergence conditions can be different from one problem to another. Typically when successive iterations are not producing better results anymore, the algorithm converges to the optimum. The main steps of an improved GA technique used for proposed VVO are explained in this section of this chapter.

10.3.1. Coding

For GA-based VVO algorithm, it is necessary to introduce switchable shunt CB, OLTC and VR codes primarily. It can be assumed that the size of each bank of a CB is “q_{sh}” kVAR. As such, each CB in GA can have integer values from 0 (no CB) to ρwhich is the maximum bank number of each CB. For OLTC as well as VRs, the integer values can be from 0 (no tap) to R or W that are last taps of VR and OLTC respectively. Table 10.1 shows the coding for CB, OLTC and VR. In order to construct chromosome, VVCCs of the grid nodes has to be defined in a matrix called surface chromosome. Each generated surface chromosome is comprised of rows that show grid nodes and columns that show VVCC of the system such as CB, OLTC and VR. Table 10.2 depicts surface chromosome structure.

Table 10.1. Coding table of VVCCs in GA technique

CB-1, OLTC-1, VR-1	...	CB-k, OLTC-w, VR-r	...	CB-$\boldsymbol{\rho}$, OLTC-W, VR-R
x_1, y_1, z_1	...	x_k, y_w, z_r	...	x_ρ, y_W, z_R

10.3.2. Initialization

As stated, a random number between 0 andρ is generated for CBs. Random number from 0 to *W* and from 0 to *R*, are generated for OLTC and VRs as well for each gene. By repeating random production, an initial population is gained.

Table 10.2. Surface Chromosome structure

	Node-1	Node-2		Node-*j*		Node-*n*
CB	x_{11}	x_{12}	…	x_{1j}	…	x_{1n}
OLTC	y_{11}	y_{12}	…	y_{1j}	…	y_{1n}
VR	z_{11}	z_{12}	…	z_{1j}	…	z_{1n}

10.3.3. Crossover Operator

The crossover operator is typically employed for reproduction of selected generation. In this research two types of crossover are proposed.

- Crossover-1: here, two chromosomes are considered as a parent. These parents are then crossed-over to substitute two rows of chromosomes of same VVCC.
- Crossover-2: In this crossover type, some genes are randomly selected from two chromosomes and the data of them is exchanged as well.

Figure 10.4 depicts two-crossover approach of this research using both crossover-1 and crossover-2 for the VVO.

10.3.4. Mutation Operator

The aim of the mutation step is to diversify the solution search and prevent solution from falling into local optimum peaks/valleys. Two different types of mutation are used in this research.

- Mutation-1: In this mutation type, a row of chromosome is selected in a random way initially. Then all elements of that row are changed to other solutions with P_mProbability.
- Mutation type-2: In this type of mutation, some of the genes are selected randomly and the values of them are changed totally with P_{m2}Probability. Fig. 5 shows

Figure 10.5 shows two-mutation approach of this research using both mutation-1 and mutation-2 for the VVO.

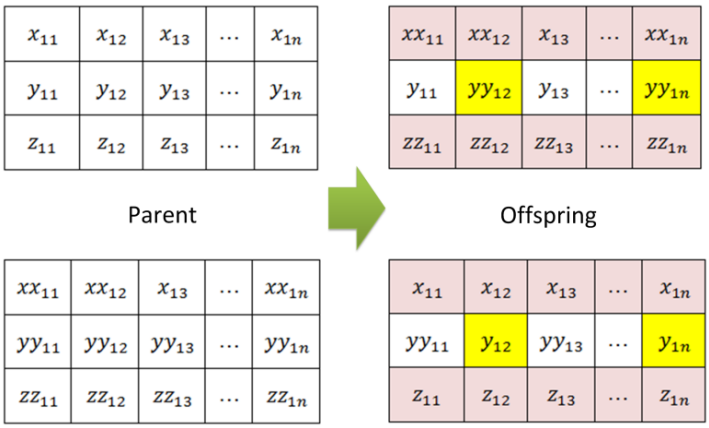

Figure 10.4. Two crossover technique for VVO using improved GA

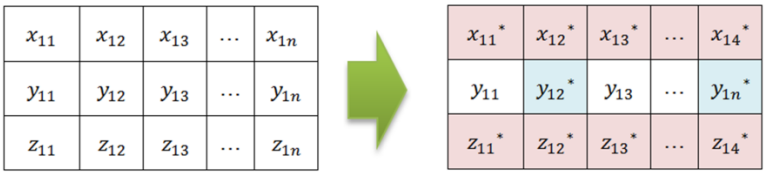

Figure 10.5. Two mutation structure for VVO using improved GA

10.3.5. Fitness Function

Typically the fitness function is gained from the objective function. For the VVO problem, the fitness function can be defined as:

$$Fitness\ Function = (\frac{1}{O.F_{VVO}}) \tag{10-35}$$

10.3.6. Steps of the proposed algorithm

Based on the abovementioned steps, the VVO algorithm can be consisted of the following steps:

- Data Collection: Loads/ Generation, CB, OLTC and VR data
- Coding, Initial Population Generation and Chromosome Generation
- Selection
- Crossover-1/Mutation-1
- Crossover-2/Mutation-2

- Load Flow to check constraints, update reactive power injections and voltage regulations
- Evaluation of the objective function as well as the fitness function for each chromosome
- Sort chromosomes based on fitness functions and select high quality population
- Check convergence condition: If convergence condition is not satisfied, algorithm selects new population. In order to avoid local optimum, if convergence is gained for the first time P_m and P_{mm} mutation probabilities are changed and shift the algorithm to new population selection step.

These iterative steps are repeated until convergence. Therefore, this type of GA used two steps of crossover and two steps of mutation to perform faster and to avoid local optimum. As the AMI data of previous time interval is used for the optimization of the present time interval, the VVO optimization engine results might not be accurate especially in cases where there are load uncertainties in the system. As such, the GA can find three solutions for each quasi real-time interval: solution for exact given load, solution for higher load condition and solution for lower load condition. For instance, when total load of the system in present time interval is higher than system load in previous time interval, the VVO can find a more accurate solution for present load as it find three optimal solutions for each quasi real-time interval. At each quasi real-time interval, the engine considered upper load condition 5 percent more and lower load condition 5 percent less than normal load condition. Therefore, the VVO engine could have solutions for each quasi real-time interval conditions. Figure 10.6 gives two-crossover of surface chromosomes in this approach.

10.4. Particle Swarm Optimization (PSO)

This section elucidates Particle Swarm Optimization (PSO) as proposed VVO engine optimization algorithm. PSO is a meta-heuristic optimization approach inspired by bird flocking and swarms of social organisms [29]. In PSO, each solution is modeled as a particle comprised of a value and a fitness value. Each particle seeks optimal point and for this reason, it has movement and velocity. Moreover, PSO operates based on the relocation and intelligence of particles using social interaction concept.

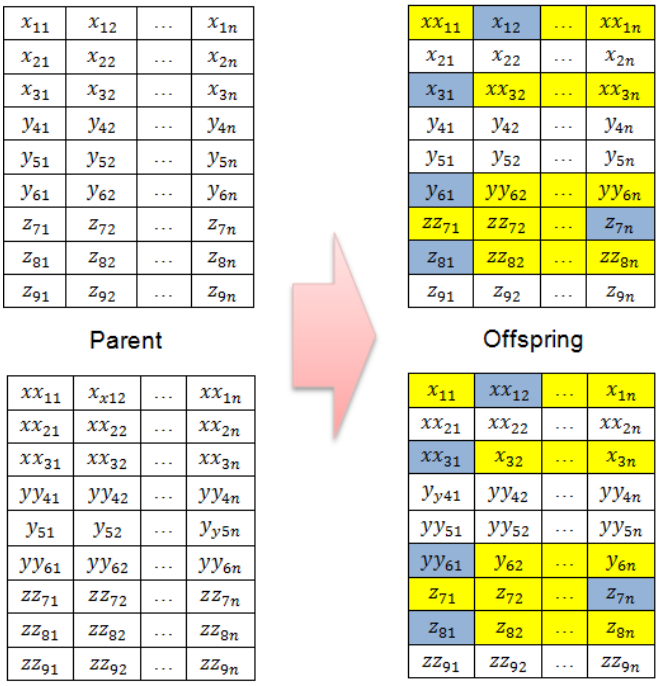

Figure 10.6. Two crossover technique for surface chromosomes with three load levels

Each particle, i.e. solution response, moves in search space. At each step, each particle saves the best position that had the best result on that position. This is called *Pbest*. In other word, *Pbes*t is the best position of a particle compared to it. Moreover, particles are working together and share information about their position. Hence, the movement of a particle depends on three main factors: present position of that particle, the best position that particle has experienced till now (*Pbest*) and the best position that all particles have had till now (*Gbest*). Therefore, after random initial population, *Pbest, Gbest*, position and velocity of particle are being updated to lead *Gbest* to final optimum value. New position of a particle can be determined by (10-36).

$$X_i^{t+1} = X_i^t + V_{vel,i}^{t+1} \tag{10-36}$$

Here,V_{vel} specifies changes in position of particle that can be defined by (10-37). As shown in (10-37), velocity consists of inertia, cognitive and social component sub-parts. The random values (r_1, r_2) produces a random number between 0 and 1. $\varphi_1$and φ_2 are

acceleration constants, the summation of which are experimentally chosen to be less than or equal to four.

$$V_{vel,i}^{t+1} = V_{vel,i}^{t} + \varphi_1 . r_1 \left(Pbest_i - X_i^t \right) + \varphi_2 . r_2 \left(Gbest_i - X_i^t \right) \quad (10\text{-}37)$$

Substantial advantages of PSO approach can be summarized as: PSO is a zero-order approach without heavy complex mathematical computations such as gradient approaches. It has acceptable computational load and it has quite rapid convergence. It has to be mentioned that PSO algorithm does not have Selection approach. In other words, no particle can be removed, although the value of each particle can be changed in PSO. In addition, PSO does not use Mutation or Crossover steps like GA. PSO uses local and global search and the ratio of these searches can be defined by weights. Figure 10.7 illustrates the proposed VVO engine flowchart. As explained, the required data from AMI is collected.

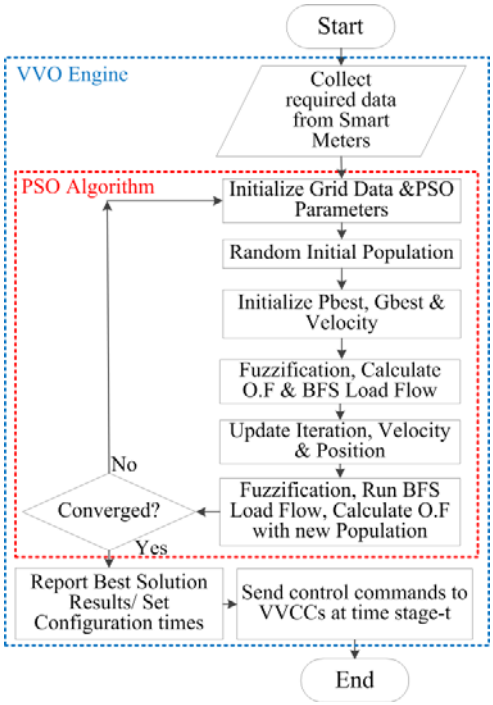

Figure 10.7. Flowchart of proposed Volt-VAR Optimization Engine using PSO

Network and PSO parameters are set initially and then, initial random population is generated. Moreover, initial *Pbest, Gbest* and velocity are computed as well as the objective function and constraints for the first iteration. In next iterations, position and

velocity of each particle are updated till *Gbest* converges to the optimum value. The results of PSO are sent to VVCCs within distribution substation and or along distribution feeder to update configuration of the grid according to new VVCC's optimal values. Hence, proposed VVO of this research could optimize distribution grid through PSO and Fuzzification technique could determine weighting factors of each VVO objective sub-parts within PSO algorithm.

10.5. Summary

This chapter studied three main optimization technique used in this research for Volt-VAR Optimization problem. Each optimization technique has its pros and cons based on distribution grid topology, condition as well as level of accuracy and speed that network operator needs. This chapter explained benders decomposition as one of the most applicable optimization techniques in distribution network planning. This approach can solve VVO optimization problem with desirable speed and accuracy. However, generating weak benders cuts can affect benders decomposition performance. Moreover, the complicacy of this technique has made its users to apply it more for large optimization problems where it is more necessary to decompose the problem into master and slaves. That is the reason this research has not used this technique much despite studying it in detail. It is possible to say that Genetic Algorithm is the most applied optimization technique in power systems. The reason lies in several facts. First, GA concept is very easy to understand and it does not need much knowledge of mathematics. Second, as many power system applications can be described as chromosomes and as fitness function can be defined well, the GA performs adequately in these applications. At last but not least, GA can be easily transferred from one system model or simulation to another level of that model or simulation. GA has couple of disadvantages. There is no guarantee that GA could find global optimum within specified optimization time especially when the convergence rate is defined very high. Moreover, GA may fall into local optimums. In order to boost algorithm response time and to avoid GA to fall into local optimum, this study assessed improved GA with two levels of crossover and mutation. As proposed VVO application performs in quasi real-time (typically every 15 minutes), presented improved GA could provide system with the optimal solution with adequate optimization time.

Particle Swarm Optimization is another optimization technique that is widely used in distribution network optimizations. The main benefits of PSO can be summarized as: easy concept, simple implementation, derivative-free, insensitive to scaling of design variables, works with very few parameters and effective global search algorithm. The main disadvantage of this method is its tendency to converge fast and immature in partial optimums. PSO also used for proposed VVO engine. The results of VVO studies show successful performance of these optimization techniques for proposed VVO.

As proposed VVO performs in quasi real-time and as the VVO approach is feeder-based with few integer variables (not a large scale problem), these optimization techniques performed adequately. In other words, proposed approach shows the fact that it does not need sophisticated optimization algorithm to perform. Another important benefit is that the proposed VVO can give operator a chance to choose its own optimization technique (among studied optimization solutions) according to system number of variables and operational needs such as accuracy and optimization time. Definitely, investigations regarding more efficient optimization solutions would be necessary if the aim is to find suitable optimization solutions to be very close to real-time. Approximate-based techniques such as Meta Modeling could be a great solution candidate for this future study.

Chapter 11.

Real-time Co-Simulation Platform for Smart Grid VVO

As explained in literature review chapter, the necessity of designing a real-time co-simulation platform comprising of VVO engine, communication network, and monitoring platform to provide a fully functional real-time system to check the performance of new smart grid adaptive VVO solutions is felt more than before. This chapter presents different real-time co-simulation platforms for smart grid-based VVO applications in smart distribution networks. In first application, VVO is tested over a real-time co-simulation platform using Real Time Digital Simulator (RTDS) as system simulator, DNP3 protocol as reliable communication platform and OPC server as control command sender. The main focus of this study is to create a reliable co-simulated environment for VVO to be checked in quasi real-time operation through a real-time system. In next study, the performance of the whole system is tested by imposing delays and packet losses into the platform through Wide Area Network emulator (WANem). The third study investigates a reliable control and monitoring platform for the VVO engine. In other words, it completes the first study that used RTDS, DNP3 and OPC server for real-time co-simulation platform with more focus on the monitoring and control parts. The last study investigates a real-time co-simulation platform using RTDS, DNP3 and IEC 61850 MMS and GOOSE protocols. It presents how IEC 61850 MMS and GOOSE would assist VVO engine, performing reliably on different grid operating scenarios such as normal, faulty and grid reconfiguration modes.

11.1. Overview of the Test Platform

The platform for testing, monitoring and control applications is built wherein the different components constituting the monitoring and control systems are either emulated or integrated in a plug and play fashion. These different components are generally the measurement acquisition channel, different measurement protocols, communication networks, measurement aggregators and monitoring and control applications. The testing platform is principally designed to quantify the effects introduced by these components.

The structure of the platform can be functionally divided into three main parts namely the Real Time Simulation of Power Systems, Measurement Acquisition System and the Software Platform that enables the development of monitoring and control applications.

The general scheme of the structure is given in the Figure 11.1. The power system simulation is performed in Real time Digital Simulator (RTDS) as shown in Figure 11.1. The RTDS is a powerful computer designed to accurately and reliably simulate power system phenomena in the range of 0 to 3 kHz [241]. It is comprised of both specially designed hardware and software. It can simulate power systems and also provide real time measurements through its specialized output boards in such a way that they emulate real world measurement devices. In the proposed VVO application the Gigabit Transceiver Network (GTNET) board is used that emulates remote measuring units that can send measurements in Distributed Network Protocol (DNP3), that is one of Substation Automation well-known protocols [242], to the control center through the Ethernet connection. The measurement aggregator used is the OPC server that collects the DNP3 measurements from RTDS that were sent through Ethernet network. The third part is the software platform wherein the measurement aggregator is realized that collects data from different sources and provides it to the control applications. The RTDS simulates the grid in real time providing the GTNET board with the real time measurements via the optic fiber.

The GTNET board then encapsulates them into a specific message format, in this case into DNP3 format, and sends it to the measurement aggregator in our case the OPC server which then makes these measurements available to the VVO application developed in MATLAB via the OPC toolbox of MATLAB. Measurements from RTDS are received from RTDS into MATLAB and the control signals are sent back to RTDS via OPC server in DNP3 format. DNP3 is based on a Master Slave mode of operation where GTNET board or the measuring devices are the Slaves and the OPC server which is the measurement aggregator functions as a Master that polls for slaves and asks measurements and writes control messages to them. Figure 11.2 depicts basic flowchart of the VVO engine using real-time co-simulation platform.

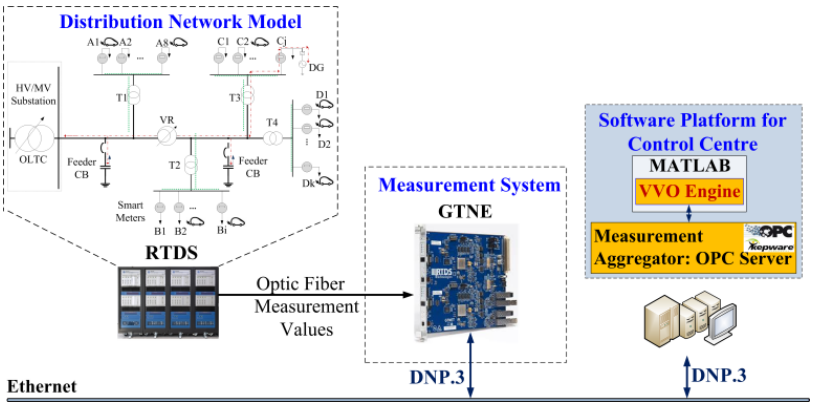

Figure 11.1. Overview of the test platform

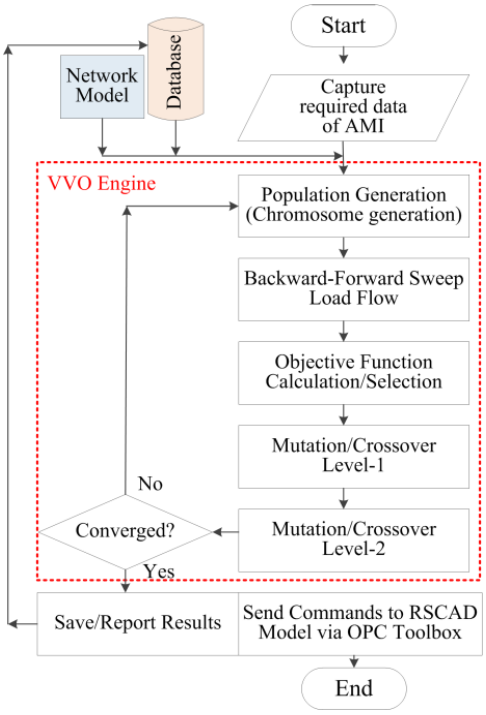

Figure 11.2. Basic flowchart of proposed VVO

11.2. Co-Simulation Platform with Communication Test-bench

As explained in previous section, the platform is built in order to test and asses the influence of different components included in the monitoring and control systems of distribution networks namely the sensors, measurement units, communication infrastructure, time synchronization units, data concentrators and most importantly, the

monitoring and control applications for operation and control of distribution grids. This section intends to use the real-time co-simulation platform to check the robustness of the monitoring and control application for communication network delays. The structure of the platform can be functionally divided into five main parts namely; the Real Time Simulation of Power Systems (here distribution network), Measurement Acquisition System, Communication network interface, Communication test platform and Software Platform that enables development of monitoring and control applications. General scheme of co-simulation platform is given in Figure 11.3.

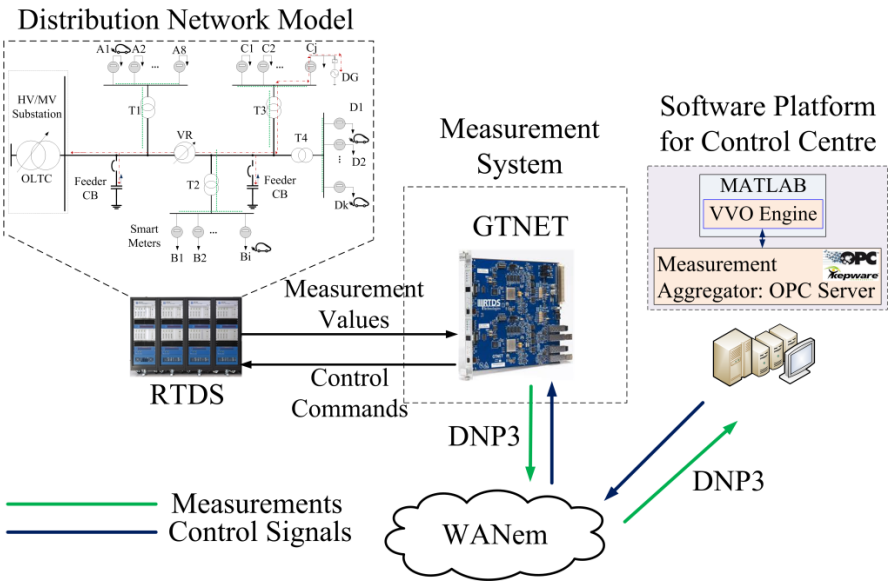

Figure 11.3. Real-time Co-simulation platform setup

11.3. Implementation of the test setup

Primarily, distribution network model is simulated in real-time using the RTDS. Then, the measurement acquisition system of this test setup is realized with specialized output boards, the GTNET, where they function as a smart meter that sends measurement data and also as an Intelligent Electronic Devices (IEDs) that receive control signals from control center to switch CBs, change the tap settings of OLTC and/or VRs using DNP3. The RTDS simulates distribution system in real-time and then, appropriate measurement values are sent to the GTNET board via fiber optic cables which are encapsulated in DNP3 format and sent to the Master which in this co-simulation platform is DMS/SCADA at control center. Likewise, control signals are sent via DMS/SCADA to the GTNET that

performs as an IED receives control commands and passes them to the simulation environment. The software platform is responsible to aggregate measurements from different devices and facilitate them to the monitoring and control applications. For presented test platform, the Kepware OPC server is used as DMS/SCADA that aggregates DNP3 data.

As mentioned before, control application of VVO is developed in MATLAB which interacts with the OPC server via the OPC toolbox of MATLAB to receive DNP3 measurements from smart meters and to write control commands back (which are the output of the VVO optimization engine) to IEDs throughout the same OPC interface in DNP3 format. The communication platform between the IEDs and smart meters is achieved through Ethernet connections. To emulate real distribution network operating conditions so as to assess the influence of the communication network delays and packet losses on the functioning of the monitoring and control of VVO engine, a virtual Wide Area Network Emulator (WANem) is used [243]. WANem is a Wide Area Network Emulator, meant to provide a real experience of a Wide Area Network/Internet, during application development and/or testing over a LAN environment. Typically application developers provide applications on a LAN while intended purpose for the same could be clients accessing the same over the WAN or even the Internet [243]. Figure 11.4 illustrates the routing of packets if WANem is employed. Without WANem, the packets would reach to destination through the switch depicted as the normal packet flow and if WANem is used, then packets follow the emulated packet flow as shown in Figure 11.4.

Network emulation is the act of introducing a device to a test network (typically in a laboratory environment) that alters packet flow in such a way as to mimic the behavior of a production, or live network such as a LAN or WAN. Manually network characteristics such as delay, jitter, packet loss and distribution characteristics of the delay could be set by WANem. For presented co-simulation platform in this section, communication network that introduces delays of normal distribution as well as packet losses are emulated by WANem.

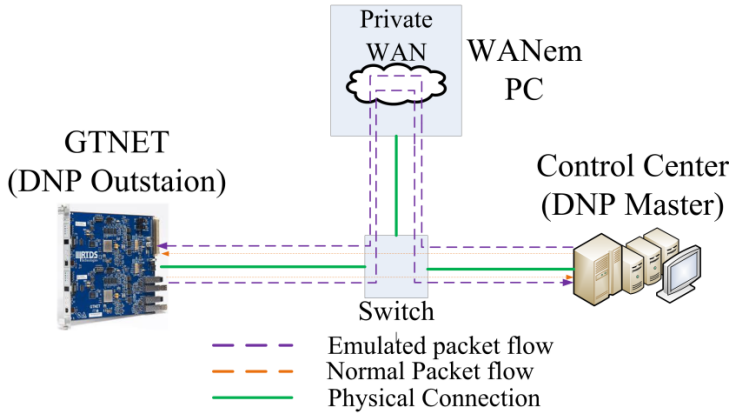

Figure 11.4. Routing of packets with WANem

Four different network conditions that introduce delays of 50ms, 100ms, 200ms and 1 second are emulated in the presence of a 10% packet loss each respectively. The delay conditions of communication network are set in such a way that delay is introduced between the source of the measurement/control signal and the destination. Hence, the delay is introduced between the GTNET (smart meter) and the PC where the VVO runs, and between the PC and the GTNET (IED) to test the control signal. Wireshark is run on the PC where control applications are run to see the Round Trip Delay (RTD) and throughput of the measurement/control signals (in DNP3) received and sent to the GTNET of RTDS respectively. Thus, when round trip delay plotted with the Wireshark it actually shows end to end delay. More details regarding the result of this study is presented in next chapter of this thesis.

In brief, the key benefits of presented co-simulation platform includes but not limited to its adaptability with new smart grid based VVO solutions, its coordination with smart grid technologies such as DMS and AMI, its simplicity and comprehensibility using MATLAB programming for VVO engine design and its communication platform using real substation automation protocol (DNP3).

11.4. Monitoring and Control Platform Overview

This section explains co-simulation monitoring and control platform overview, design and main setup. Basically, co-simulation platforms for monitoring and control applications are designed utilizing various monitoring and control components that are

emulated or integrated in plug and play modes. These assets are mainly the measurement acquisition units, communication networks, measurement protocols, monitoring and control actuators. The general overview of the designed co-simulation platform for the proposed AMI-based VVO engine is presented in Figure 11.5. As illustrated in Figure 11.5, similar to 1st co-simulation study, distribution network assets are modeled in RTDS that is capable of real-time simulation of distribution grids. Moreover, it can utilize real-time measurements through its interface boards to emulate real measurement devices. In the proposed AMI-based VVO engine, two GTNET boards are used to emulate smart meters or measurement field collectors. RTDS GTNET cards are able to send measurements in DNP3 to the VVO engine placed in MATLAB via optic fiber Ethernet connection. The Kepware OPC server is used as measurement aggregator that collects DNP3 measurements from RTDS model.

Here, the software platforms, such as RSCAD run-time, provide system with monitoring and control among all data collected from loads, VVO engine control commands to VVCCs and measurements after optimal reconfiguration of the system at each quasi real-time operating stage. The GTNET boards change AMI data into DNP3 format, and send data to the measurement aggregator that is the OPC server that provides required quasi real-time measurement values for the VVO engine in MATLAB. After finding the optimal solution of the grid by the VVO engine, control signals are sent back from VVO engine to RTDS via OPC server in DNP3 format to impose new optimal settings to distribution network VVCCs.

RSCAD runtime shown in Figure 11.6 enables monitoring the status and values/taps of VVCCs as well as other measurements in real time. Any changes in active and reactive power consumptions of customers, as well as distribution network parameters, such as node voltages, branch currents and phase angles, can be observed in real-time via monitoring platform depicted in Figure 11.6. Moreover, the aforementioned data and parameters are saved to system database for further analysis and study purposes.

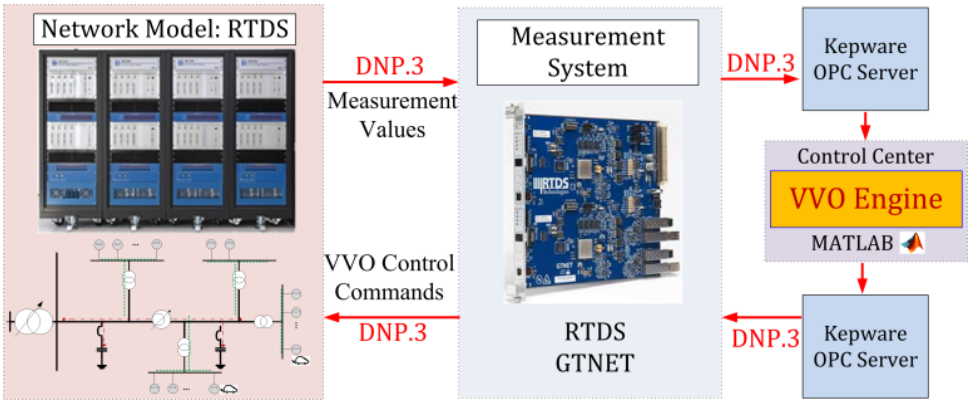

Figure 11.5. Main structure of real-time co-simulation platform for AMI-based VVO

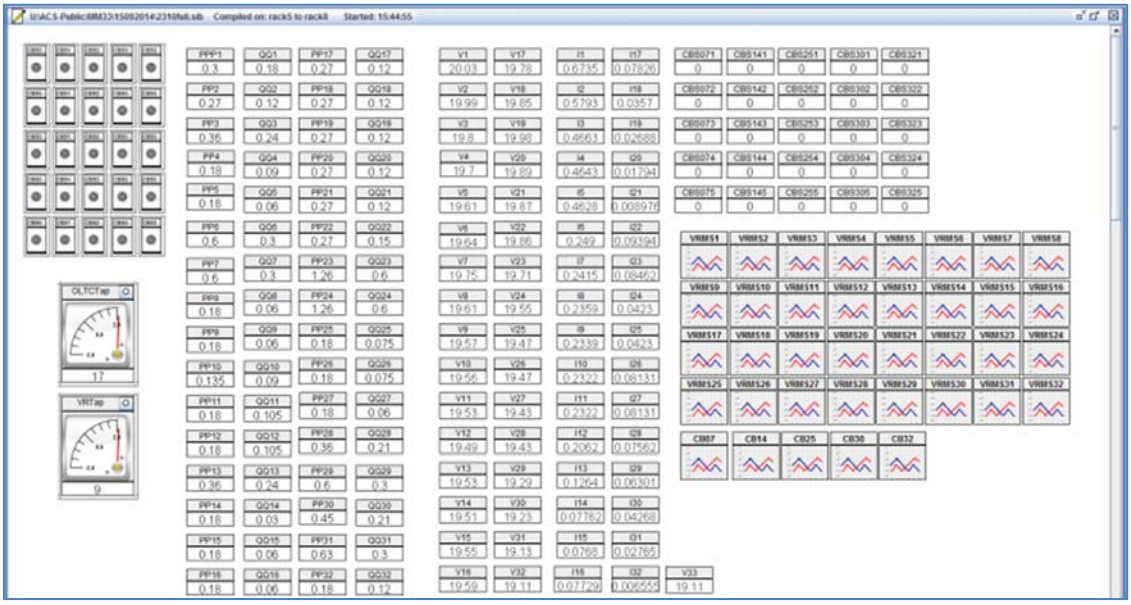

Figure 11.6. Monitoring platform for real-time co-simulation of AMI-based VVO

11.5. IEC 61850 Standard in Automation Systems

Technology improvements in electronics, communication and information technology have enabled unprecedented opportunities in the automation of substations. Devices deployed in power systems generally follow proprietary standards. It becomes a daunting task to design an automation system with devices from different manufacturers. Thus IEC 61850 was developed to make automation system components interoperable and interchangeable. This standard defines an object oriented hierarchical data model with semantics that enables data abstraction and provides information on the data to be

exchanged as well as the mechanisms of data exchange. The data models are application independent and the scope was originally within substation but the standard is extended to incorporate data models of distributed energy resources [181]. As the standard divides the domain related model for both communication services and data from the communication protocols, namely the OSI layers, any automation system that is based on IEC 61850 would achieve long term interoperability even under constant advancements in the communication technologies and evolving functionalities of the substation. Furthermore, mapping data models and services to the real communication protocols is standardized in IEC 61850 that ensures interoperability.

Application functions up to the data interfaces of the primary equipment are broken down into the smallest possible sections that may be implemented separately in Intelligent Electronic Devices (IEDs). The standard defines these basic pieces of functionality as Logical Nodes (LNs). The data objects within a LN contain attributes which could be values or detailed properties of the data object [244]. This hierarchical model is depicted in Figure 11.7. The semantics of the information exchange within the scope of IEC 61850 is formalized only because the LNs are standardized. The IEC 61850 provides standardized Abstract Communication Service Interface (ACSI) where a set of services such as: read, write, control, reporting, logging, get directory, file transfer, and response to those services are defined. These services enable IEDs to behave identically from a network behavior perspective [245]. These abstract services and object models need to be mapped on to the services and object models of real communication protocols that could be practically implemented, which can operate in real computing environments. IEC 61850 maps these models and services to the Manufacturing Message Specification (MMS) [246]. Theoretically the abstract models of IEC 61850 could be mapped on to any communication protocol but MMS was chosen as it supports complex named objects and a set of flexible services that enables a straight forward mapping of data models and services defined in IEC 61850. For the proposed work the LN “XCBR” was used to realize all the functionalities of a circuit breaker. The status changes of the circuit breakers are reported to the control center using the MMS protocol. Apart from the core ACSI services, IEC 61850 defines services such as the Generic Object Oriented System Event (GOOSE) [49] and Sampled Values (SV) [247] as well.

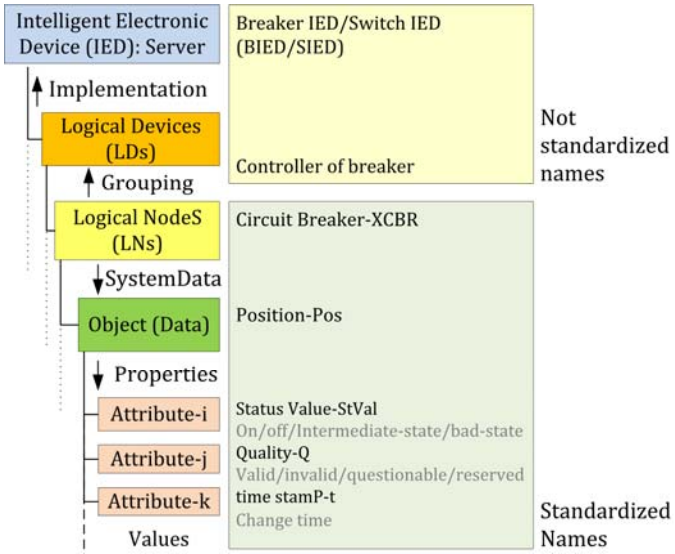

Figure 11.7. Hierarchical data model proposed by IEC 61850

GOOSE service is generally used to transmit time critical information, e.g. the status changes between the IEDs, when faults happen in the grid, and SV is used for transmitting time synchronized stream of samples of currents and voltages. An overview of the mapping of the services to the communication stack is provided in Figure 11.8. Apart from data models and the services, IEC 61850 provides performance requirements on communication technology as well.

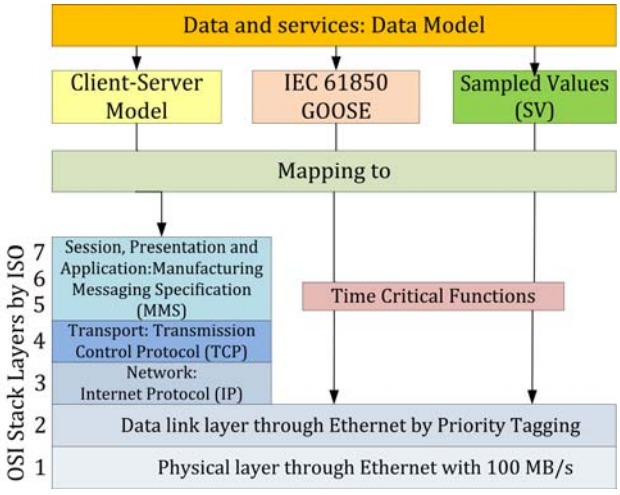

Figure 11.8. IEC 61850: Mapping to communication stack

Typically, the maximum transfer time, depending on requirements of the automation function, that is allowed for sending and receiving of messages between the IEDs is also provided [248]. IEC 61850 uses Substation Configuration description

Language (SCL) for the configuration of substation devices [249]. Data representation as SCL enables different IED to exchange data in an interoperable environment. Six performance classes are defined, mapping typical allowable transfer times for different types of applications where tripping and protection applications require less than 3 milliseconds. The standard proposes 2-bus Ethernet architecture for the substation presented in Figure 11.9.

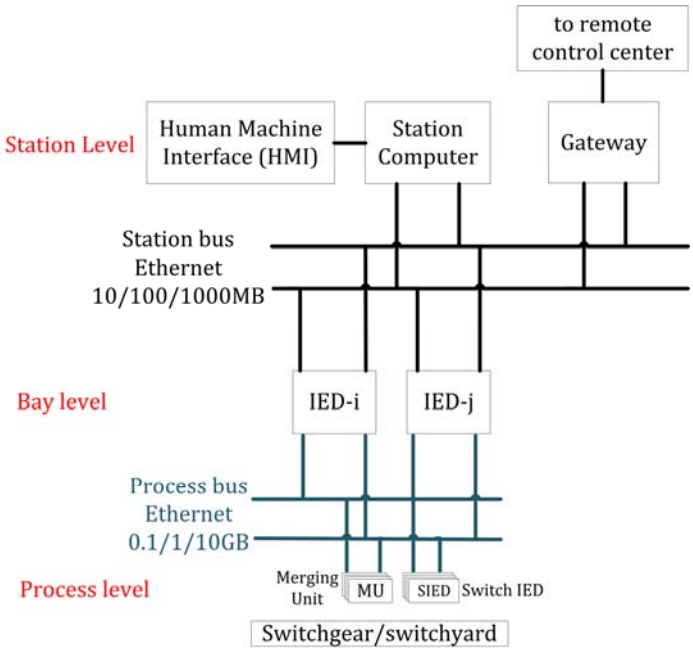

Figure 11.9. Ethernet bus architecture

The Merging Unit (MU) digitizes transducer outputs and publishes them as SV into the Ethernet-based high speed process bus. Breaker IED/Switch IED (SIED) sends GOOSE messages indicating changes in the status of breakers or switches. All MUs and SIEDs are synchronized to a single time reference. A station bus is setup at substation level to provide primary communication between IEDs that are responsible for station monitoring, control and protection.

The communication could be either with client server based IEC 61850 MMS protocol or with a publisher subscriber based GOOSE services. Typically, the local HMI, the station computer and the station gateway are connected to the station bus. Remote control center via the Wide Area Networks (WAN) can access the data from the IEDs of this particular substation through the network gateway using services provided by IEC

61850 MMS protocol. Both process bus and station bus are proposed to have two Ethernet buses to achieve higher redundancy and reliability.

11.6. Co-Simulation Platform for Smart Grid-based VVO

11.6.1. Co-Simulation Platform Configuration

In the co-simulation platform discussed here, the VVO engine runs on a PC representing the automation unit at a high to medium voltage substation. IEC 61850 MMS protocol is used to gather the status of different switching devices, e.g. circuit breakers, in order to be able to impose the necessary changes in grid configuration in real-time according to the topology of the system. The VVO receives measurements and sends control commands to remote VVCCs using DNP3 protocol. DNP3 is used to show a case that the platform supports multiple kinds of protocols along with IEC 61850 protocols. Moreover DNP3 is a very popular communication protocol, used by major utilities for wide area monitoring and control in US and Canada. In reality a complete revamp of the communication infrastructure would always be carried out in stages and therefore in the transition phases the power systems would be operated partially with the old communication infrastructure (including communication protocols) and partially with the new. In this work a possible method of introduction of IEC 61850 communication protocols is investigated. IEC 61850 communication services are used for automatic service restoration after a fault and update the VVO engine with real time changes in network topology. Whereas the measurement acquisition from remote measurement units and sending control commands to VVCCs is done through the old communication infrastructure through DNP3 protocol.

The distribution feeders are assumed to be equipped with switchgears which are IEC 61850 compatible. This means that each switching device is configured as a SIED and exchanges GOOSE messages with the other switching devices to automatically isolate faults and restore service by closing appropriate circuit breaker(s). Different SIEDs are pre-configured to take a set of actions when they receive GOOSE messages from other SIEDs. As grid topology is important for the VVO engine, it periodically reads the status of the breakers using IEC 61850 MMS protocol. This enables it to receive updated

data regarding any changes in the topology of the system, which may require a new batch of optimal set points of VVCCs to be calculated. This automation platform using IEC 61850 enables the VVO algorithm to operate robustly for any configuration changes the system may assume.

11.6.2. Co-Simulation platform Realization

The real-time co-simulation platform is functionally divided into three sections. The first section is real time distribution network simulation in RSCAD shown in Figure 11.10. The second section consists of measurement, control and monitoring systems and the third section includes software platform for control and monitoring. As depicted in Figure 11.10, the distribution network is modeled using RTDS. As explained before, RTDS enables simulating power system dynamics up to 3 kHz [241]. Different distribution network scenarios, i.e. fault / normal conditions, could be emulated using RTDS. RTDS is equipped with specialized boards named "Gigabit Transceiver Input Output" (GTIO) that emulate the outputs of a real transducer. The transducer outputs from RTDS are provided to the measurement, control, monitoring and protection devices that constitute the second section. These devices are realized by Gigabit Transceiver Network boards and National Instruments-Compact Reconfigurable Input Output (NI-cRIO). The GTNETs support DNP3, as well as IEC 61850 GOOSE protocols, whereas the NI-cRIO is configured as an IED that supports IEC 61850 MMS protocol. This platform uses four GTNET boards, two of which are configured for DNP3 protocol, as DNP3 Slave, and two support IEC 61850 GOOSE protocol. Each GTNET card is configured to emulate multiple SIEDs. One of the two GTNETs configured for DNP3 is responsible for sending measurements to the VVO engine and the other receives control command signals, i.e. the outputs of the VVO engine, notifying new setting of VVCCs. One of the two GTNETs supporting GOOSE protocol is configured as a publisher and the other as a subscriber.

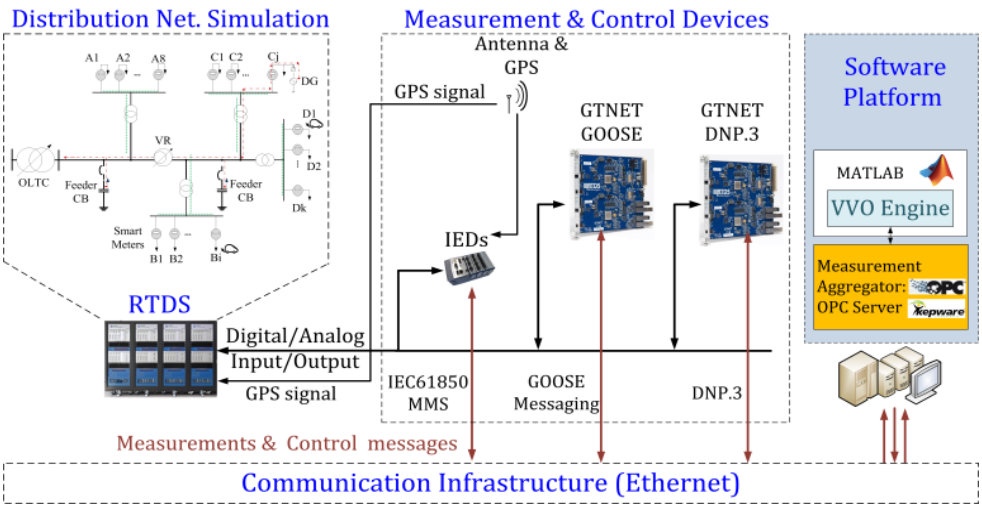

Figure 11.10. Designed real-time co-simulation platform

When a fault occurs in the system, the relays emulated in RTDS detect an over current and initiate tripping of appropriate circuit breaker(s). Subsequently, as the status of the switching device(s) changes, the GTNET board which is configured as a publisher publishes GOOSE message notifying this change in the status. Upon receiving these GOOSE messages by the subscribing GTNET, appropriate SIEDs emulated by this GTNET, takes action for service restoration. These status changes are made available to the NI-cRIO-based IED that supports MMS server via the analogue output boards of the RTDS (GTAO) in real time. RTDS runtime is employed as monitoring platform of co-simulation where different grid variables, such as voltage, current, active/reactive power injections as well as VVCC online status and/or values are monitored in real-time.

Finally, the Software Platform principally emulates the functions of a remote control center. Measurement of different formats are aggregated and made available to the control applications, and control commands are sent to the remote control units emulated in RTDS. The Kepware OPC server is used to emulate both as the DNP3 Master and MMS client. It aggregates measurements sent with DNP3 protocol and sends back control commands to VVCCs emulated in RTDS. The MMS client requests the status information of the different switching devices from the NI-cRIO based-IED. Such measurements and status changes, indicative of the present topology of the grid, are made available to the VVO engine implemented in MATLAB via the OPC tool box of MATLAB. The VVO engine runs in quasi real-time, and the optimal control settings it produces are sent back via OPC

toolbox to OPC server, which translates the control command values to DNP3 control messages to be sent to remote VVCCs emulated in RTDS. Figure 11.11 illustrates the co-simulated system levels for the proposed smart grid-based VVO engine.

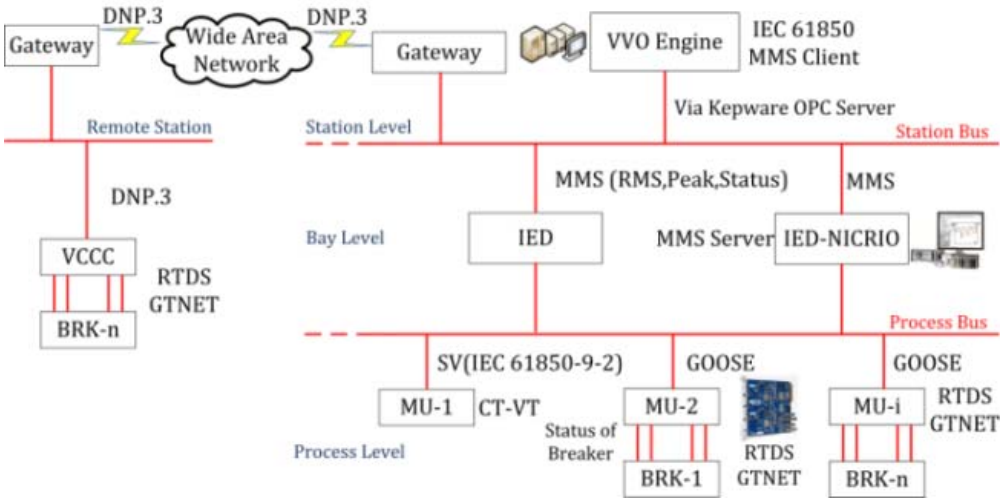

Figure 11.11. IEC 61850 architecture for proposed smart grid-based VVO

Chapter 12.

Studies, Results and Result Analyses

This chapter presents different studies for proposed smart grid adaptive VVO. The result analysis of each study are given after each case study simulation and results. These studies cover the following VVO aims/topics:

- Real-time adaptive VVO using IA and IEC 61850 protocol
- Design VVO engine with different levels of operation as well as DGs
- Impacts of V2G on performance of the VVO engine
- Design a VVO engine using Vehicle to Grid Dispatch
- Design a day-ahead predictive VVO
- Design an online predictive VVO using VVO real-time sliding window
- A solution for VVO maintenance scheduling issue using Maintenance Scheduling Engine concept
- Smart grid adaptive VVO using Particle Swarm Optimization and Fuzzification
- ZIP load modeling for Conservation Voltage Reduction using disaggregated AMI data
- Real-time Co-simulation platform for Volt-VAR control (no CVR)
- Real-time Co-Simulated Platform for Energy Conservation
- Real-time Communication platform study for AMI-based VVO
- Monitoring and Control real-time co-simulated platform for proposed VVO (CVR included)
- Impacts of Micro-CHP/PV penetrations on smart grid VVO using AMI data
- Community Energy Storage VVO Study
- Impacts of EV penetration on proposed VVO using real-time co-simulation monitoring platform
- Real-time Co-simulation platform for smart grid adaptive VVO using IEC 61850 MMS and GOOSE

12.1. Real-Time Adaptive VVO Topology Using Multi Agent System and IEC 61850-Based Communication Protocol

12.1.1. Case Study

In this section, modified IEEE 34 node distribution test system [250] is used for testing the accuracy and the applicability of proposed VVO engine. This study uses the network topology shown in Figure 3.6 of Chapter 3.4.The modified test system consists of 34 residential nodes with 34 metering points (smart meters). The power is supplied from the HV side and transmitted by a radial distribution network. The system is modified to have two 50 kW microgrid DG units. In this study, active and reactive powers of the DGs are controllable. Hence, the power factor can be controlled within the desired range. Figure 12.1 presents single line diagram of the case study. A 2500 kVA transformer is placed inside the HV/MV substation at the first feeder. It has 34 tap steps. Each tap can increase/decrease the voltage by 0.3125 percent. Along distribution feeder, 34 points are assumed as VAR injection points. The system has two VRs between nodes 8-9 (VR-1) and 19-20 (VR-2) respectively. They can increase/decrease the voltage by 0.625 % in 17 taps (from 0.95 to 1.05 per units).

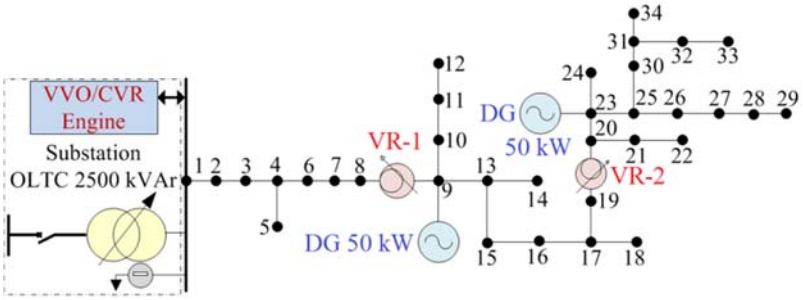

Figure 12.1. Modified IEEE 34-Node Test Feeder

The system study is based on Per Units (P.U.) and the equations mentioned in Chapter 5. For the objective function, (5-1) to (5-3) and (5-4) to (5-8) is used. Constraints of this study are (5-9) to (5-27). The basic information of feeder lines such as line lengths and line reactance and impedances are given in [250]. The information of nodes is given in Table 12.1. Three types of residential consumption profiles for 34 nodes are considered (type-1, type-3: residential and type-2: light commercial). The reason is that the loads can show different characteristics in different operating conditions. In this case, the real-time

data acquisition intervals from smart meters are set to 15 minutes to be in line with current practice prevalent in AMI and distribution automation systems. The simulation is performed for 96 time stages (a complete day in winter). Figure 12.2 illustrates the detected residential loads in the 96 time stages.

Table 12.1. General Data of Nodes (Load Curve Types, Active and Reactive Power)

No.	Load Type	P kW	Q kVAR	No.	Load Type	P kW	Q kVAR
1	1	20	10	18	3	1.2	0.8
2	2	30	15	19	2	1.2	0.5
3	3	10	5	20	2	2	1.5
4	1	10	5	21	2	2	1.5
5	2	2	1	22	2	1.1	0.5
6	1	5	2.5	23	1	17	8
7	2	2	1	24	2	5	2.5
8	2	5	2.5	25	1	110	55
9	2	5	2	26	1	9	5
10	1	34	17	27	1	25	12
11	3	135	70	28	2	23	1
12	3	3	1.5	29	2	3	1.5
13	1	40	20	30	2	38	19
14	2	1.2	0.5	31	2	11	5.5
15	2	6	3.5	32	2	24	12
16	2	2	1	33	2	3	1.5
17	2	2	1	34	2	3	1.5

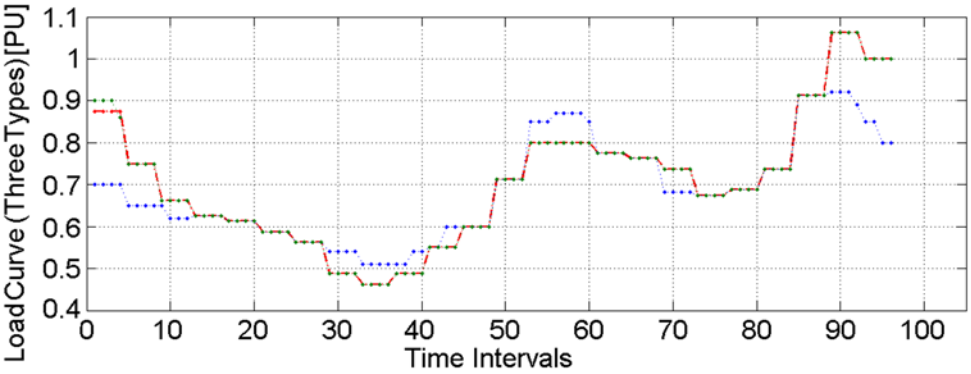

Figure 12.2. Residential loads in 96 time stages (Red: type-1, Blue: type-2, Green: type-3).

Thus, VVO engine uses quasi real-time VVO data from IAs (acquired from smart meters) to determine new settings for VVO assets (e.g. voltage regulators and/or VAR injecting components) to re-optimize the voltage, active and reactive power of the smart distribution network every 15 minutes. The algorithm for VVOE is an improved Genetic

Algorithm (GA) which works based on natural selection method. Chromosome matrix has candidate rows for VAR injection point values and VR tap positions. The column of this matrix is the candidate nodes for VAR injections. The simulation was run in the MATLAB environment.

12.1.2. Case Study Results and Result Analysis

Here, different scenarios are presented and compared. The first scenario is the blind distribution network without any near real-time distributed command and control for VVO. Figure 12.3 represents the power loss curve in different scenarios and Figure 12.4 shows the voltage curve for the end-feeder node (node-34). In Figure 12.3 and Figure 12.4, the blue curves show the blind distribution network result. As illustrated, the blind feeder is faced with different problems such as voltage of the buses under the standard limit and large system loss. The results of this scenario are compared to the following scenarios:

- OLTC effect: Transformer tap changer is added to the distribution network with its maximum tap by VVO engine.
- CB's effect: In addition to OLTC, VVO engine defines the VAR amount and locates the VAR injection points. The green curve in Figure 12.3 and Figure 12.4 represents the effect of VAR injection system in the network. By implementing this scenario, the voltage of the buses is increased and the power loss is decreased. Lack of an optimal strategy for VVO is felt because the voltage of the network is still less than ANSI-band.
- VR effect: In this scenario, one of the VRs (VR-2) is added to the network with its maximum tap. The red curve in Figure 12.3 and Figure 12.4 represents this scenario. As seen, the scenario improves the voltage and the active and the reactive power of the system but still, the system has voltage problems.
- Implementing near real-time VVO optimization through VVO engine: In this scenario, the VVO engine determines the amount and the location of VAR injections in addition to changing the tap steps of existing VRs and OLTC in the distribution network. Thus, the system reconfigures itself by applying an agent-based distributed command and control in 15 minutes intervals.

In Figure 12.3 and Figure 12.4, the magenta curves show the impact of OLTC in the network. As observed, the voltage and the power loss of the system can be improved but the system would still have numerous problems.

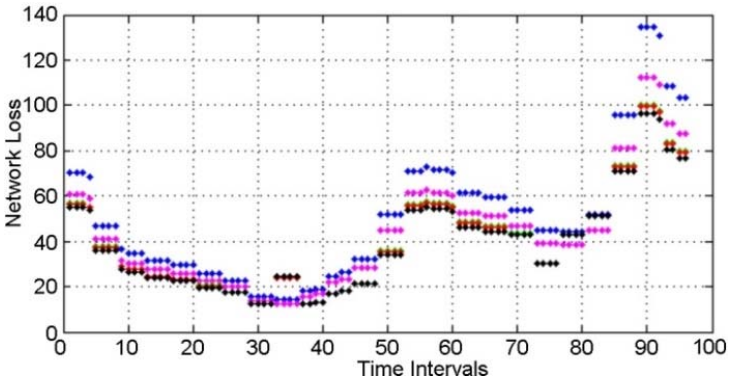

Figure 12.3. Loss Curve in different scenarios (Blue: no VVO, Magenta: OLTC effect, Red: VR effect, Black: Complete VVO).

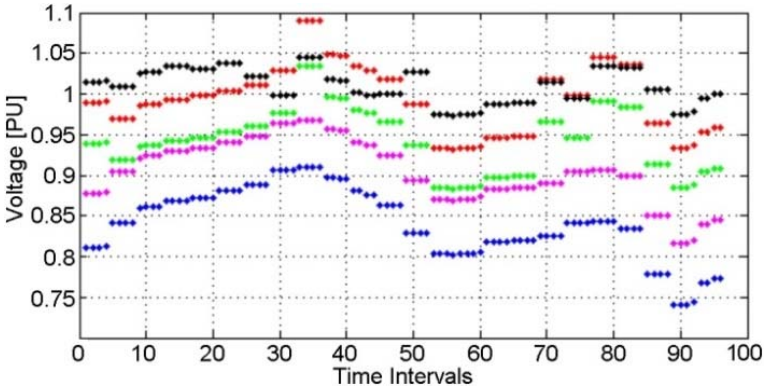

Figure 12.4. Voltage Profile of Node-34 in different scenarios.

The VVO engine runs an integrated VVO algorithm in order to find tap positions and system required reactive powers. The black curves in Figure 12.3 and Figure 12.4 depicts the impact of the proposed system. Here, the optimal solution leads to fixed taps for OLTC (% tap = 0.953125) and VR-2 (% tap = 0.9625) and different taps in time stages for VR-1. The reason is that the system has limitations in changing taps. Therefore, it is better for the system to decrease the number of tap changes during its operation. Moreover, the optimal solution suggests various VAR injection points during near real-time intervals (15 minutes). This implies that the load of the system varies with the time stages and VVO engine has to adapt the system to load variations. Figure 12.5 presents chosen VAR injection points and Figure 12.6 gives the VR-1 tap positions which are obtained by VVO engine during time intervals. Furthermore, CVR task of the algorithm has kept the voltage of the nodes within ANSI-band. Figure 12.7 clearly shows the voltage of all 34 nodes which are kept within ANSI standard limit.

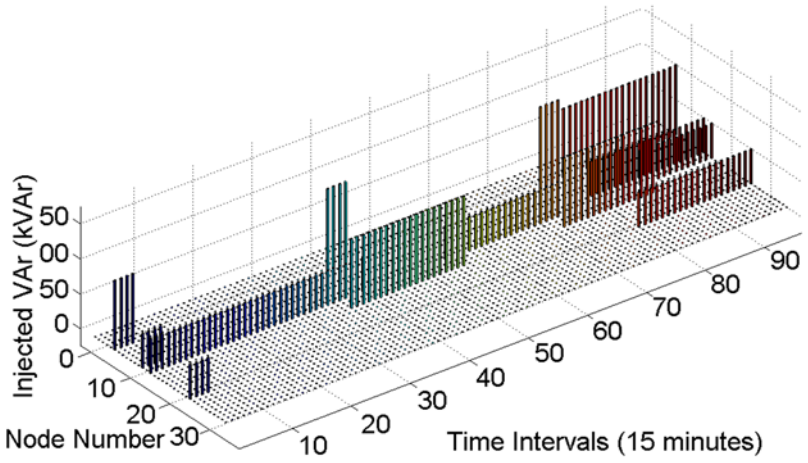

Figure 12.5. VAR injection points during time stages based VVO engine calculations

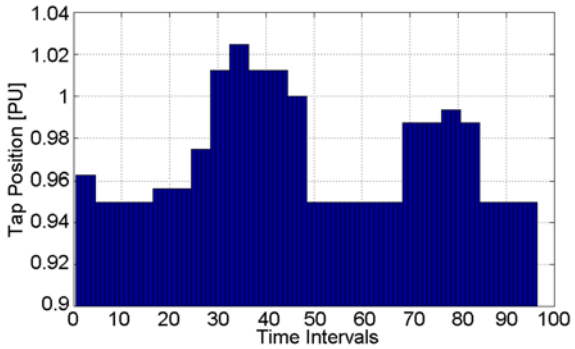

Figure 12.6. Tap positions of VR-1 obtained by VVO engine

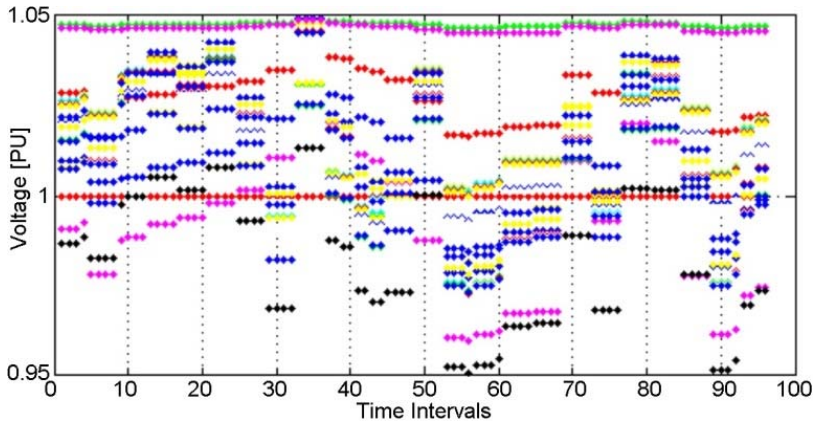

Figure 12.7. Voltage result for all nodes based on ANSI Band.

As a result, the voltage of the system is well-regulated by the VVO engine algorithm and the power loss of the system reduced significantly. In this case study, the reduction loss percentage from the first scenario up to the last scenario was 40.625 % and the

voltage drop regulation of last node (node-34) in peak is equal to 31.75 %. Additionally, the power factors of all nodes are well-raised at each time interval. Table 12.2 shows the power factor values of all 34 nodes in the peak load. In conclusion, the VVO engine can optimize the distribution network in a distributed command and control platform by applying IAs.

Table 12.2. Power Factor of All nodes Calculated by VVO Engine

No.	*PF*	No.	*PF*	No.	*PF*
1	0.9771	12	0.9997	23	0.9797
2	0.9928	13	0.9771	24	0.9928
3	0.9997	14	0.9928	25	0.9771
4	0.9771	15	0.9903	26	0.972
5	0.9928	16	0.9928	27	0.9789
6	0.9771	17	0.9928	28	0.9999
7	0.9928	18	0.9993	29	0.9928
8	0.9928	19	0.9928	30	0.9928
9	0.9954	20	0.9841	31	0.9928
10	0.9771	21	0.9841	32	0.9928
11	0.9997	22	0.9928	33	0.9928
				34	0.9928

12.1.3. Conclusion

This study proposed a quasi-real-time adaptive approach for an integrated VVO in smart grid applying a distributed command and control platform. The study explains different types of control schemes and proposes distributed command and control as the most adaptive scheme for the future smart grid. Moreover, as VVOE is responsible for distribution network reconfiguration, the algorithm objectives and constraints are given in the study. In addition, modified IEEE 34 node distribution network has been applied in order to test the effectiveness of the VVO optimization engine. The test is simulated in MATLAB environment. Hence, the optimal configuration of the distribution network is obtained for a full day and the system configuration is updated every 15 minutes. The VVO engine determined the amount of each VAR injection points and found the optimal tap positions of OLTC of the substation and existing voltage regulators for each time interval. The simulation results illustrated that the system can be controlled adequately in terms of voltage, active and reactive power regulations by the proposed integrated VVO approach.

As a result, this study can be the basis for future studies in smart grid adaptive VVO techniques. Such studies should determine the required type and frequency of the AMI data vis-à-vis the structural, topological and computational complexity and efficiency of VVO algorithms. Furthermore, such studies would produce the required benchmarks to determine the impact of network topology on the efficiency of VVO algorithms. At last but not least, the importance of building a comprehensive quasi real-time VVO-CVR is that it saves energy which can be gained from network loss reduction, while improving voltage profile and conserving energy.

12.2. Real-Time Adaptive Optimization Engine Algorithm for Integrated VVO and CVR of Smart Microgrids

12.2.1. The Effects of Proposed VVO in British Columbia Institute of Technology (BCIT) Case Study

In this section, a BCIT case study is fully assessed. The main topology of the VVO of this study is as same as Figure 3.7 of Chapter 3.4. Considered BCIT distribution network consists of 21 nodes, two main substations (Sub-F and Sub-E) and various types of loads. Moreover, the network has different distributed generation sources such as: Micro-turbine, Roof-top PVs and Flywheel Energy Storage System (FESS). Figure 12.8 presents the single line diagram of the BCIT case study. Here in this study, the objective function calculated based on (5-2) to (5-4) and the constraints are (5-9) to (5-19), (5-22), (5-25) and (5-28). As it is shown in Figure 12.8, both substations have a 2000 kVA transformer. Sub-E has a CB unit with 150 kVA capacity (3*50 kVA). It is assumed that both transformers have tap-changers with 17 tap-steps that can regulate the voltage between -%5 to +%5. Hence, each tap step can regulate the voltage plus or minus % 0.625.In addition, 1300 kW total load which is located at the MV side of Sub-E is considered in the simulation. The proposed VVO is performed in 15-minutes time intervals for a complete day (96 time stages). The captured values of active and reactive power of nodes as well as load types are presented in Table 12.3. At the low voltage side of Sub-F, a micro-turbine (220 kW, 275 kVAR) is placed which operates in parallel with the network.

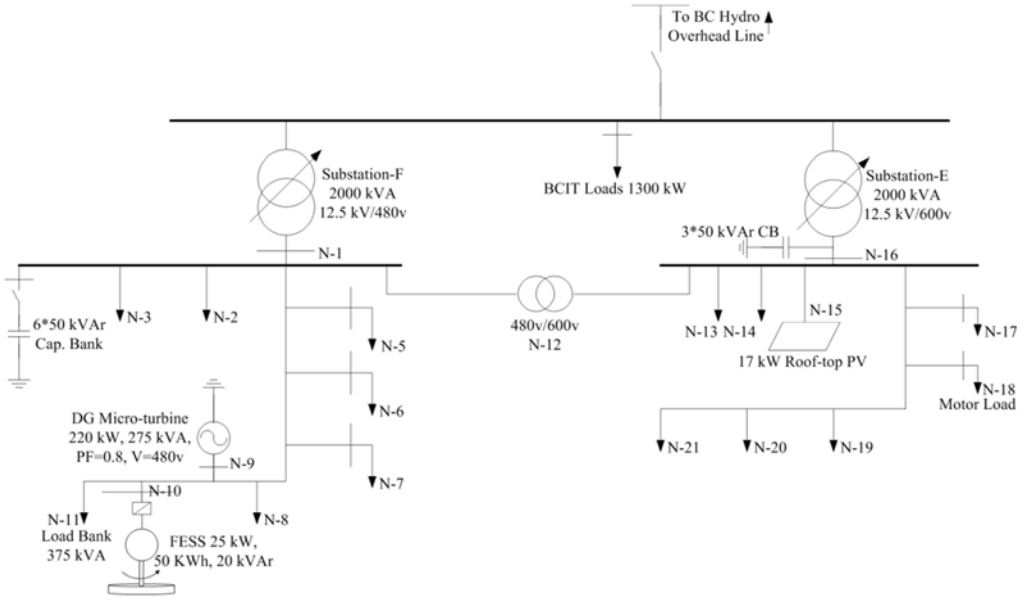

Figure 12.8. Single Line Diagram of Considered Case Study

In addition, the feasibility of installing a 25 kW, 50 kWh FESS with 20 kVAR injecting power on node-10 is under study. At the LV side of Sub-E, a roof-top PV with 17 kW total generation is placed. According to the geographical position of BCIT campus (Burnaby: -123.02E, 49.26 N), the operational hours of a solar PV in average is around 3.8 hours/day/year. According to the previous records, generating capacity of the roof-top PV in the best insolation condition will be equal to 11.2 kW which is considered in simulation.

Table 12.3. Curve Types, Active and Reactive Powers of Loads in BCIT Case Study

Node Number	Load Type	P (kW)	Q (kVAR)	Node Number	Load Type	P (kW)	Q (kVAR)
N-2	1 Com.	0.03	0.015	N-13	3 Com.	0.065	0.032
N-3	1 Com.	0.025	0.012	N-14	3 Com.	0.015	0.008
N-5	1 Com.	0.08	0.040	N-17	3 Com.	0.015	0.008
N-6	1 Com.	0.065	0.032	N-18	5 Motor Load	0.015	0.009
N-7	2 Com.	0.015	0.007	N-19	3 Com.	0.015	0.008
N-8	2 Com.	0.015	0.007	N-20	3 Com.	0.01	0.005
N-11	4 Load bank	0.72	0.375	N-21	3 Com.	0.015	0.008

The studied network consists of different load types. Figure 12.9 depicts different load profiles of BCIT loads which is obtained from measured data. As it is presented in Figure 12.9 and Table 12.3, network typical loads have three different types which are

mainly commercial loads (load types: 1, 2, 3). Moreover, the load curve of the existed load bank (load type-4) at node-11 is different with other typical loads. For the load bank, it is shown that it has been switched on at the beginning of working hours of laboratory (10 A.M) and it has been switched off at 6:30 P.M. Additionally, an inductive motor load exists at node-8 of the system. This three phase motor has 20hp (15 kW) rated power with 1800r.p.m. It has 0.86 Power Factor (reactive power is equal to 8.9 kVAR) at ¾ full load. The load curve of the motor load (load type-5) is as follows: It has been switched on at 10 A.M and operates at 0.92 of its nominal mode and it has been switched off at 7 P.M.

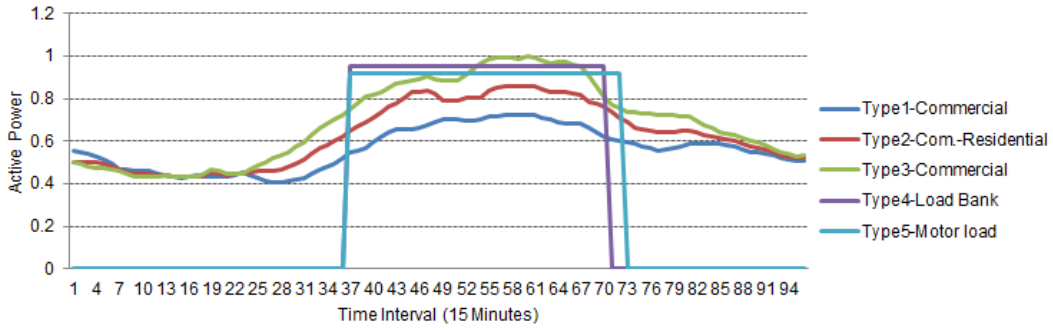

Figure 12.9. Load profile types of the Case Study

The effect of proposed quasi real-time VVO algorithm is evaluated. First, the initial condition (dumb mode) of BCIT distribution network without VVO implementation is presented and then, the quasi real-time VVOVR is studied in two modes (confining to the substations and distributing along the feeder). The applied optimization technique for the VVO engine is improved GA. Figure 12.10 presents the system loss curve in three different scenarios: a) without VVO, b) VVO confines to the substations and c) VVO options within substations and along distribution feeder. As it is pointed out in previous section, VVO engine can optimize the network based on system operator desired settings. In the first case, the desired setting for loss minimization at peak is considered to be equal to 120 kW. Hence, the algorithm is found the VVO results confined to the system substations. In second scenario, the desired setting for the system loss at peak is changed to 100 kW. Thus, the algorithm used other VAR injection candidates along BCIT feeder as well as substation Volt-VAR control devices. On the other hand, VVO algorithm regulates the voltage profile of the network. Figure 12.11 illustrates the voltage profile of all BCIT nodes in four cases: a) dumb system without VVO, b) VVO inside substations, c) VVO with only VAR injection CB candidates and d) Integrated quasi real-time VVO.

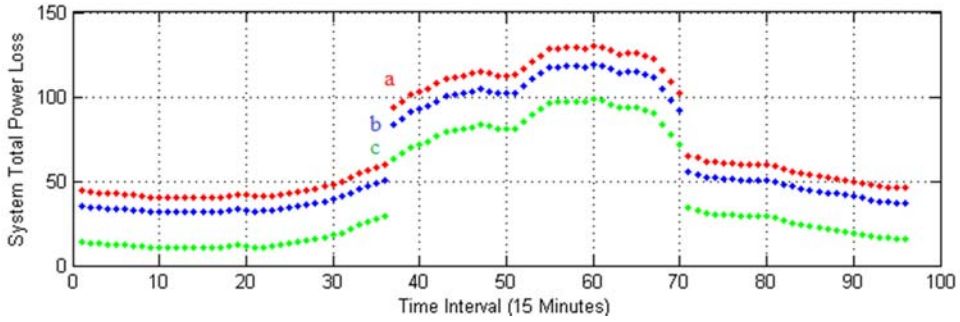

Figure 12.10. System Loss Curve for Different Scenarios: a) without VVO, b) VVO confines to the substations and c) VVO implementation within substations and along distribution feeder

As it is observed in Figure 12.11, some of the voltage nodes are out of ANSI standard in the first case.

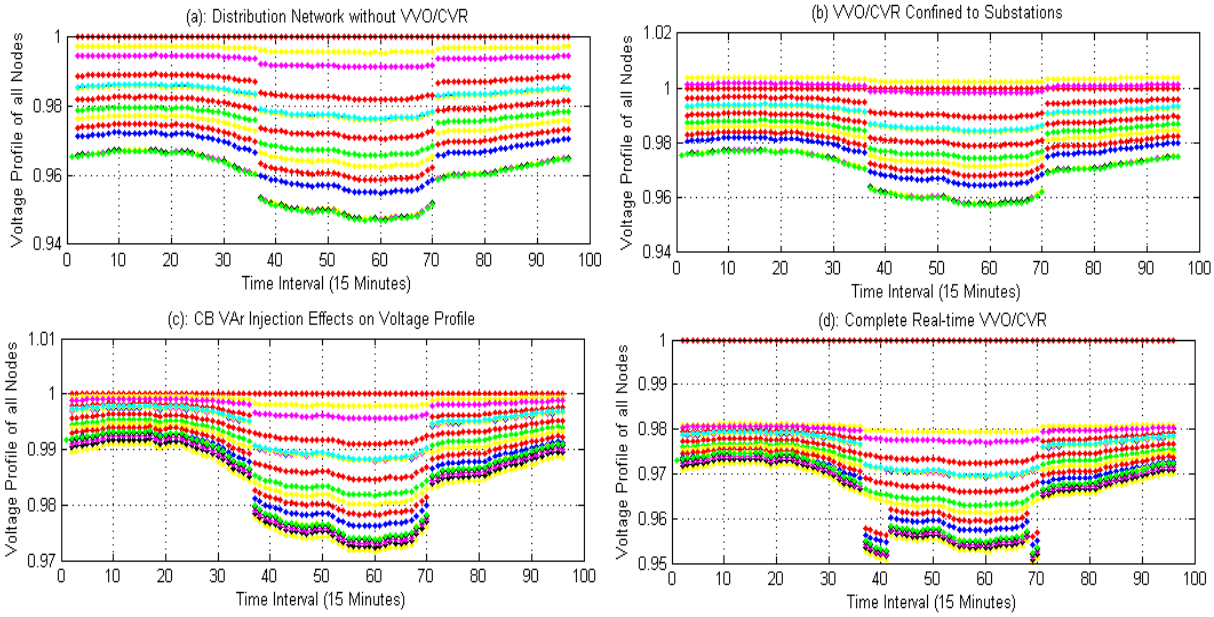

Figure 12.11. Voltage Profile of All Nodes of the Case Study in Different Scenarios

In case (b), this issue is solved by VVO engine. In this case, the Tap position of Transformer-1 is equal to 0.99375 and the capacitor bank of Sub-E is employed in full capacity (150 kVAR). In presence of capacitor banks along distribution feeder, system voltage profile improves significantly. In this step, CVR tries to reduce the voltage of some nodes by applying OLTCs and existed VRs in order to conserve energy. This condition is shown in case (d). In this case, VVO algorithm set the Transformer-1 tap position at 1.01875 and set the Transformer-2 tap position at 1. Moreover, it recommends a VR close

to node-12. The tap changes of this VR are shown in Figure 12.12. Furthermore, Figure 12.13 presents the VAR injection point candidates at each quasi real-time interval.

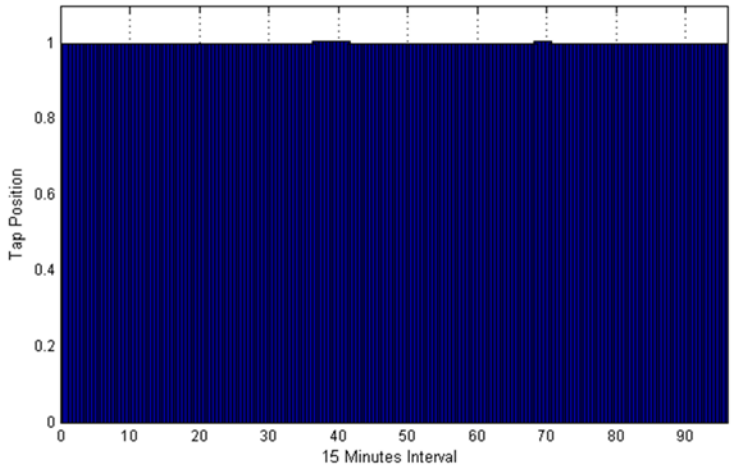

Figure 12.12. Tap changes of the VR during a full day operation

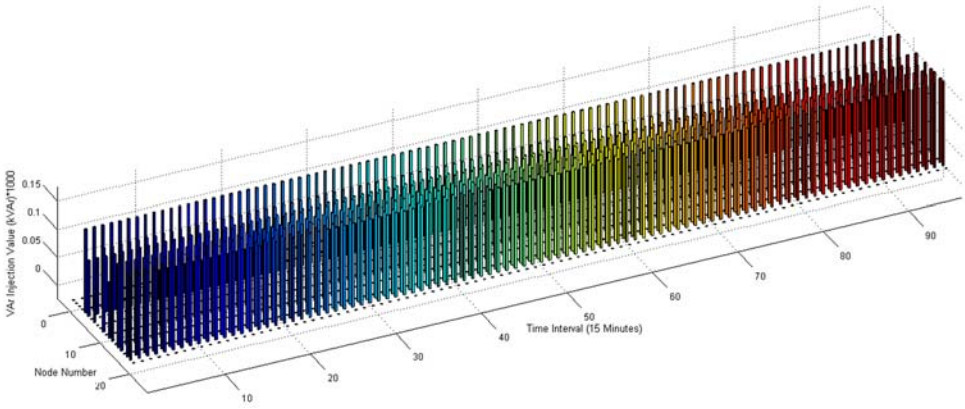

Figure 12.13. CB VAR injection point candidates at each quasi real-time interval

12.2.2. The Effect of Flywheel Energy Storage System on the System VVO

In this sub-section the effect of FESS on system Volt-VAR Optimization is studied. It has to be mentioned that the effect of other existed DG sources such as Micro-turbine (as a generating unit which operates in parallel with distribution network) and roof-top PV are considered in the main VVO. Thus, the Flywheel role in quasi real-time VVO cycles is assessed. As it is noted, the system has a Flywheel Energy Storage System which is able to inject 25 kW active and 20 kW reactive powers to the grid every two hours (50 kWh, 40 kVAh). After discharging and transmitting power to the grid, FESS will be back to the

charge mode. One of the substantial features of new flywheel energy storage technology is that it let operators to regulate and control the charge and discharge cycles of a FESS. Therefore, Figure 12.14 illustrates the effect of FESS in VVO loss reduction and assumed charge/discharge cycles of it. As it is shown in Figure 12.14, FESS is available for VVO in several time stages based on its regulated cycles and assist VVO to reduce the system loss considerably. Based on determined priority, VVO engine asks FESS to participate in VVO at each quasi real-time stage. It checks FESS availability every 15 minutes. If FESS is available, the VVO algorithm will choose FESS as one of the Volt-VAR control devices in its problem.

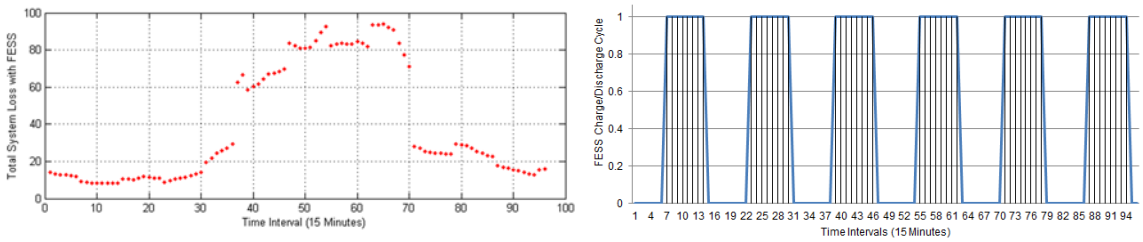

Figure 12.14. The Effect of FESS on VVO and its Charge/Discharge Cycle

As a result, the offered VVO approach optimized the BCIT network in a complete reliable and efficient way in quasi real-time. Table 12.4 gives the total and comparable results of the proposed VVO engine. Considering the results of Table 12.4 and the fact that the mean approximated energy cost for BCIT campus is equal to 6 Cents per kWh, VVO can save lots of costs for BCIT. If VVO is being limited to the substations, it is possible to save 926.8182 kW-15minutes of energy and CAD 13.90227 per day as energy conservation. If the VVO algorithm is being implemented along distribution feeder, the values will be raised (2929.465 kW-15minutes of energy and CAD 43.94197 as energy conservation). Finally, if the flywheel storage system effect is being considered, the conservation values will be 3266.567 kW-15minutes of energy and CAD 48.99851. By simple approximations, it can be concluded that it is possible to conserve huge amount of energy and save lots of costs in BCIT campus by applying proposed quasi real-time smart grid adaptive VVO approach. It is clear that this approach can help campus economy as well as utility to conserve more energy.

Table 12.4. Results of the VVO for the Case Study

	Network without VVO	VVO Confined to Substations	VVO	FESS
Total daily loss (kWh)	1750.0007	1518.29625	1017.63475	816.64175
Cost Saving (CAD)	0	13.90227	43.94197	48.99851

12.2.3. Conclusion

This study presented a quasi-real-time smart grid adaptive VVO approach based on distributed command and control structure that can minimise distribution network loss and improve voltage profile of nodes. The offered algorithm has numerous abilities such as considering existed Volt-VAR control components based on operator desired settings, ability to determine VAR injection points along the feeder, optimizing VVO problem in quasi real-time, extendibility of the algorithm to be predictive and smart grid adaptable structure based on the availability of distributed generation sources. BCIT distribution network is used to study the applicability and the accuracy of the VVO algorithm. The results are shown that the presented VVO is able to optimize system in different levels and it is completely adaptable with distributed generations in smart microgrids. Hence, at each quasi real-time stage, the algorithm could improve system loss as well as voltage profile and implemented an integrated VVO in a reliable and efficient approach.

Given the fact that each distribution network node will be able to be smart with self-healing structure in the future, the offered algorithm is adaptable with both now and future frameworks. This can help distribution networks to achieve higher degrees of energy conservation and voltage regulation at each quasi real-time interval through an integrated VVO technique. Therefore, both customer and utility can get advantageous from a quasi-real-time VVO. Consumer can reach to a more reliable network with less expenses and utility can conserve more energy from implementing the explained VVO approach.

12.3. Impact of V2G on Real-time Adaptive VVO of Distribution Networks Case Study and Result Analysis

12.3.1. Case Study: IEEE-37 Bus Test Feeder

In this section, a revised IEEE-37 node test feeder [251] is applied as the case study. The feeder has two DG units and a substation with a 2500 kVA transformer. The OLTC of the transformer has 17 tap steps which regulates the voltage from -5% to 5%. Different types of switchable CB (25 to 200 kVAR) are employed in the study. Figure 12.15 and Table 12.5 depict revised IEEE-37 node test feeder single line diagram and load regions. Furthermore, different loads are used in the study (Figure 12.16). In this study, the main objective function equations are (5-1) to (5-3), (5-5) to (5-8) and the constraints are (5-9) to (5-28) and (5-57) to (5-60). Figure 3.8 of Chapter 3.4 shows system topology. Moreover, this study uses Chapter 6.1 theories.

12.3.2. VVO Implementation without EV

So far, it is assumed that there is no VVO in the network. In the next step, VVO optimizes the network (still without EV) in 15 minute time intervals for a complete day (96 time stages). The VVO optimization technique is an improved genetic algorithm (GA) with new two crossover and two mutation steps in order to achieve high precision.

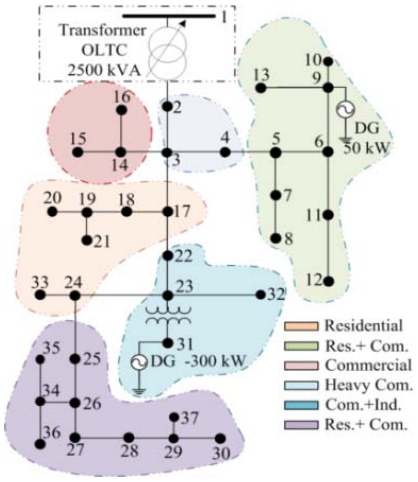

Figure 12.15. IEEE-37 node test feeder single line diagram

12.3.3. VVO in Presence of EVs

Table 12.6 shows the initial result of the feeder. In order to study EV effects, disparate users with different consumption levels are applied as shown in Figure 12.16. The study considered EV charging Level I, Level II and the combination of them for different locations (residential, workplace, commercial (shopping malls) and industrial.

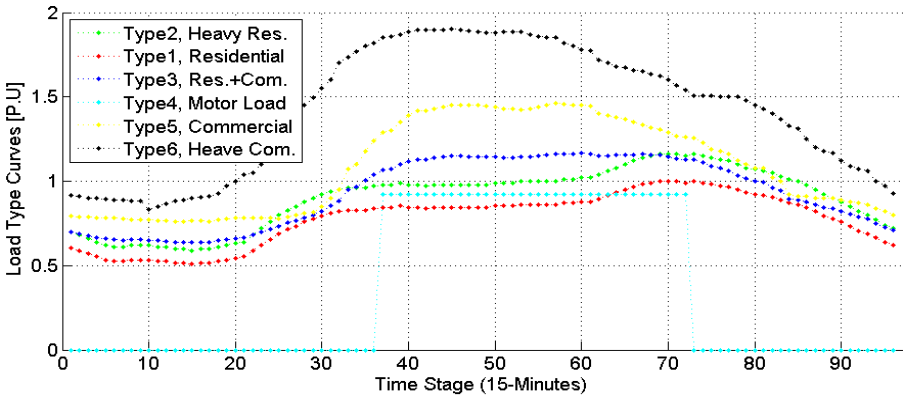

Figure 12.16. Different Daily Load Curves of Customers

Table 12.5. IEEE-37 node test Feeder General Load Data

Node No.	Load Type	P kW	Q kVAR	Node No.	Load Type	P kW	Q kVAR
2	6	0.35	0.175	22	5	0.085	0.040
4	5	0.085	0.040	25	1	0.085	0.040
6	3	0.085	0.040	26	2	0.042	0.021
8	3	0.085	0.040	27	3	0.14	0.070
10	1	0.042	0.021	28	3	0.126	0.062
12	2	0.042	0.021	30	2	0.042	0.021
13	4	0.14	0.070	31	6	0.5	0.250
15	5	0.085	0.040	32	6	0.085	0.040
16	5	0.085	0.040	33	2	0.042	0.021
18	2	0.042	0.021	35	2	0.042	0.021
19	2	0.042	0.021	36	1	0.085	0.040
20	2	0.042	0.021	37	1	0.085	0.040
21	2	0.042	0.021				

In addition, it assessed EV impacts on the system in two penetration levels (Normal and High) for different customers. For residential customers, normal penetration level

means 2 EV per 10 houses and high penetration means 4 EV per 10 houses. Moreover, normal and high penetration levels (First H and N are high and normal residential penetrations, second H and N are high and normal penetrations of other EV charging locations) for work, commercial and industrial locations are the existence of 2 and 4 charging stations at each location respectively.

Table 12.6. VVO Initial Results (without EV)

Operating Scenario	Apparent Power (kVA)	Active Power (kW)
Dumb (No-VVO)	8664.6	6414.4
Volt/VAR Optimization	8175	6053.2
Loss Reduction	489.6	361.2

Figure 12.17 illustrates EV regions in the case study. Therefore, VVO optimizes distribution feeder in presence of EVs with different charging levels and scenarios (level I, level II, 50% level I and 50% level II, 30% level I and 70% level II, 70% level I and 30% level II) and finds the grid losses and CB switching numbers which are given in Table 12.7. It is foreseeable that the grid losses rise significantly because of the active power consumed by EVs that impose Ohmic loss to the grid.

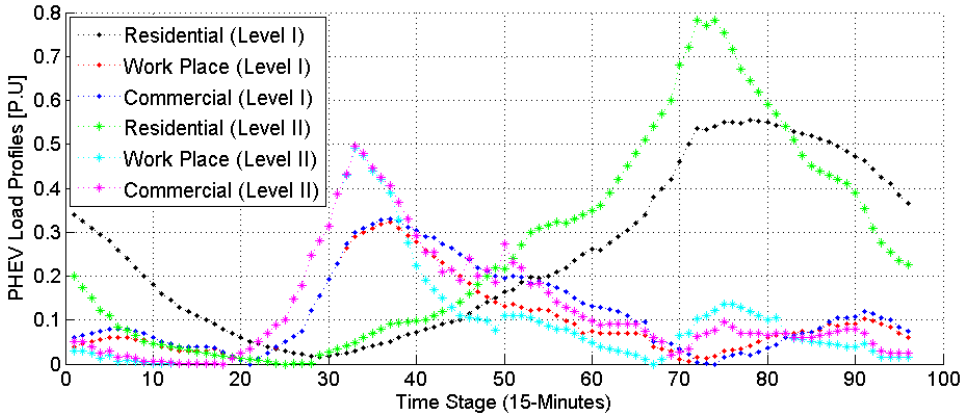

Figure 12.17. EV Load Curves for different consumers

12.3.4. VVO in Presence of EVs as Reactive Power Injectors

Here in this study, EV charging station Level I, is capable of generating reactive power around 35 % of its active power [93] and the EV charging station Level II is able to inject VAR to the grid with a rate around 50% to its active power [94]. This study studies

EV effects when 10% of them are able to inject VAR to the network. Different operating scenario results are given in Table 12.7. The most decisive point lies in the fact that the engine minimizes the system apparent power loss with less capacitor bank amounts (kVARs). The reason is that the VAR sources of the network are increased by EVs so that the system has reached to a lower loss with lower switchable capacitor bank amounts.

Table 12.7. VVO Results in Different EV Charging and Penetration Levels

Charging/ Penetration Levels		S (kVA) No VVO	S No EVQ Inj.	S EV QInj.	SW# EV No Q	SW# EV Q Inj.
1.44 kW	NH	8777.8	8302	8283.5	18	30
	NN	8770.3	8270.6	8266.8	22	16
	HH	8834.3	8348.4	8325.7	16	47
	HN	8826.8	8326.2	8319	14	30
3.88 kW	NH	8787.2	8280	8278.3	26	30
	NN	8779.1	8275	8274	16	20
	HH	8852	8351.4	8343.8	32	30
	HN	8843.9	8341	8338.8	20	20
50/ 50	NH	8782.7	8297.6	8290.3	28	22
	NN	8774.9	8287.8	8272.4	16	24
	HH	8843.4	8386.9	8350.3	18	18
	HN	8835.6	8358.6	8340.4	12	14
30/ 70	NH	8784.7	8297.6	8294.0	12	16
	NN	8776.8	8281.8	8274.4	32	20
	HH	8847.1	8376.9	8345.6	16	24
	HN	8839.1	8361.6	8337.9	22	30
70/ 30	NH	8780.7	8322.0	8285.3	16	18
	NN	8773	8290.4	8277.8	12	16
	HH	8839.8	8344.6	8333	16	24
	HN	8832.1	8327.5	8320.7	18	26

Table 12.8 presents peak power losses and total reactive power injection of CBs in two simulated steps (step-1: EV with no VAR injection, step-2: EV with VAR injection). Although EVs increase distribution network ohmic losses but, they might be employed as a reactive power sources which let network operators reduce system losses. For more

clarification, the VVO engine calculates the operating cost of feeder switchable capacitor banks based on (12-1), which is presented in Table 12.8.

$$C_{OP} = \left(C_p . S_{Loss}^{Peak} + C_e \sum_{t=1}^{T} \sum_{i=1}^{I} S_{loss,i,t} . \Delta T_t + C_{vs} \sum_{t=1}^{T} \sum_{i=1}^{I} Q_{SCBi,t} \right) \quad (12\text{-}1)$$

Where $C_p \cong 0.3287$, $C_e \cong 1.6$ and $C_{vs} \cong 0.0137$ are cost of daily peak power loss ($/kVA), energy loss cost ($/kVAh), and daily per kVAr cost of switchable CBs ($/kVAR-day) respectively. $S_{Loss}^{Peak}$is the apparent peak power loss and $Q_{SCBi,t}$ is the VAR amount of capacitors (kVAR).

Table 12.8. VVO Switchable Capacitor Bank Results (Q: Total Injected reactive Power in Step1 and Step 2)

Scenarios		Peak Loss-1	Peak Loss-2	Q-1 (kVA)	Q-2 (kVA)	Saving ($)
1.44 kW	NH	14204.2	14023.84	60700	52875	136.87
	NN	14191.59	14071.72	62650	58325	65.28
	HH	14295.35	14046.89	60050	49625	179.26
	HN	14282.85	14073.09	58400	52325	94.74
3.88 kW	NH	14218.8	14018.54	57600	53100	64.35
	NN	14205.72	14036.9	62350	54950	103.01
	HH	14323.73	14106.46	56975	51875	82.38
	HN	14310.53	14121.43	57250	53525	54.45
50/50	NH	14211.93	13971.97	64400	48300	232.30
	NN	14198.95	14060.82	58075	56900	40.97
	HH	14309.88	14148.64	54950	54200	69.09
	HN	14297.13	14198.47	59925	59000	42.06
30/70	NH	14215.01	14056.58	59050	54050	74.32
	NN	14202.02	14017.07	60250	53475	104.84
	HH	14315.75	14139.81	60600	54075	139.41
	HN	14302.82	14122.57	54050	53725	42.43
70/30	NH	14209.09	13963.33	50000	48250	82.84
	NN	14196.05	14024.95	55275	53625	42.69
	HH	14304.06	14106.18	57250	53100	75.51
	HN	14291.35	14087.78	55750	53200	45.84

It is concluded that the daily operating cost of CBs has reduced. Figure 12.18 to Figure 12.22 illustrate the result of the weakest node of the feeder (Node-37) in level II-HH scenario. Figure 12.20 represents the CB configuration of Node-37 in first step of simulation.

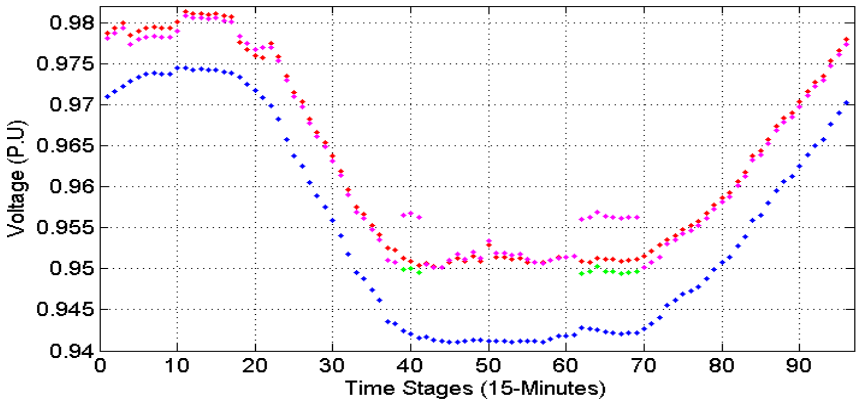

Figure 12.18. Voltage Profile of Node-37 in the case study (Blue: No VVO, Green: VVO with EV, Magenta: VVO with EV and OLTC Action, Red: VVO with EV capable of inject VAR

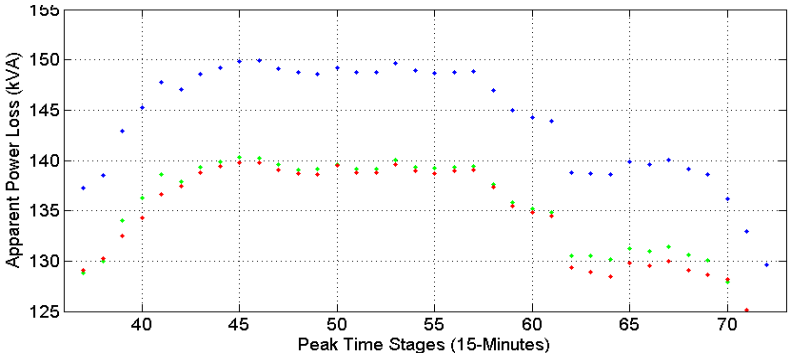

Figure 12.19. Node-37 loss around peak times (Blue: No VVO, Green: VVO with EV, Red: VVO with EV capable of inject VAR)

Thus, with less CB amounts, VVO has reduced network loss more. As a result, the proposed algorithm could optimize distribution network feeder with/without EVs in quasi real-time based on current and future Smartgrid prerequisites and presents EV potential on supplying a small portion of distribution network reactive power that give rise to a system with less losses and CB operating costs.

12.3.5. Conclusion

This study assessed the effect of EVs with different charging (I and II) and penetration levels (Normal and High) on quasi real-time VVO of distribution networks.

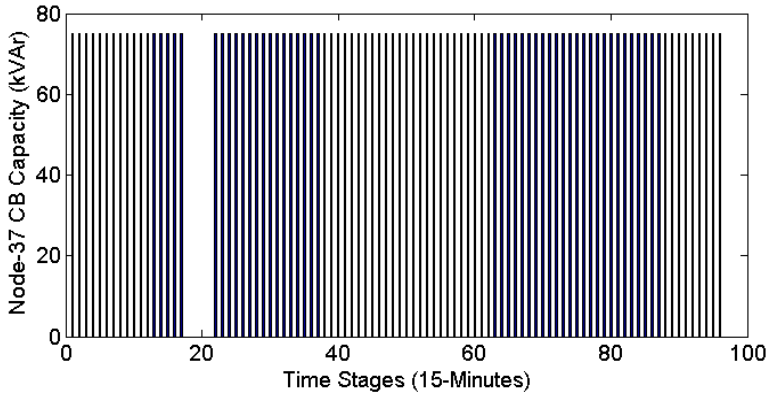

Figure 12.20. Capacitor Bank Switching Strategy of Node-37 for step-1

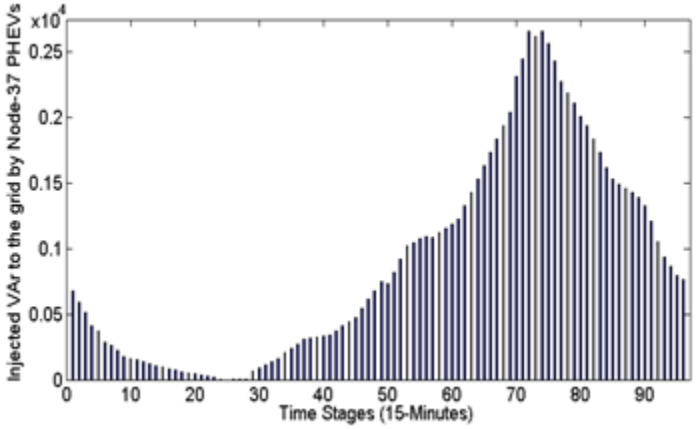

Figure 12.21. Quasi real-time VAR injection of Node-37 EVs to the grid

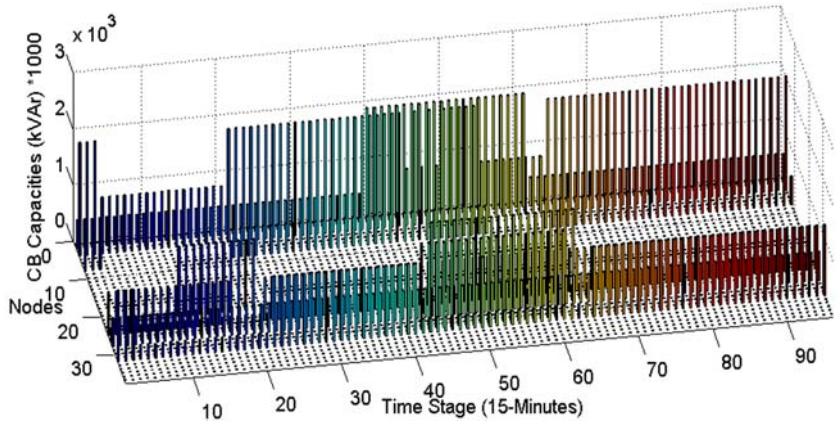

Figure 12.22. Capacitor Banks strategies for all nodes in Level II, HH Scenario

The results have proven the possibility of supplying part of distribution network required reactive power from EVs by changing the operating mode of their inverters. This potentially bring upon a network with less reactive power compensation issue. Moreover, it could reduce the operation costs of switchable capacitor banks which are located along distribution feeder. Regardless of the economic factors that should be taken into account in future studies, EV reactive power injection seems to be an appealing approach especially in cases that EVs are close to weak points of the network and/or the locations where consumes more reactive powers. In order to test the accuracy of the proposed technique, a revised IEEE-37 node test feeder is applied with different consumption regions for EVs. Finally, it is concluded that EV's role in future distribution networks cause new challenges and opportunities that distribution network short term/ long term planners have to take into account to conserve distribution network energy and costs effectively.

12.4. A Novel VVO Engine for Smart Distribution Networks utilizing Vehicle to Grid Dispatch

12.4.1. Case Study Definition

As a case study, a revised IEEE-123 node test feeder [252] is utilized in this section. The medium voltage substation of the feeder consists of a 5000 kVA transformer. The OLTC of the transformer has 17 tap steps which is able to regulate the voltage from -5% to 5%. Moreover, three VRs exist along distribution feeder. Based on distribution network operator required setting, each VR are able to regulate the voltage in 5 tap steps. When there is a common voltage regulation device such as OLTC and the objective is load reduction or energy conservation, the sum of feeder minimum Objective Function (OFs) is not equal to minimum OF for the common bus, which provides the same voltage to the heads of all connected feeders. In IEEE 123 Node Test Feeder, there is only one connected feeder to the MV substation. Hence, VVO problem is not dealing with this issue here. The network has four fixed CBs in different location of the feeder and different types of switchable CB (100, 150, 200, 250 and 300 kVAR) are employed by VVO engine in the study. Table 12.9 depicts revised IEEE-123 node test feeder main data and Figure 12.23

represents the single line diagram and load regions of the case study. As depicted in [252], some nodes do not have any active and reactive power consumption/generation. Hence, Table 12.9 only shows the loads of the system. As given in Table 12.9, the loads of the system have been classified into six different regions (1: Residential, 2: Heavy Residential, 3: Commercial, 4: Heavy commercial, 5: Motor Load (considered as a specific industrial), and 6: Industrial) based on their type. Different types of loads are presented in Figure 12.24. Furthermore, each region of the network has specific combination of loads that is shown in Figure 12.23. The VVO engine designed and programmed in MATLAB. Figure 3.9 of Chapter 3.4 presents system topology of this study. Moreover, Chapter 6.1 theories are used in this study as well. Here in this study, the objective function calculated by (5-30), and constraints of the problem are from (5-9) to (5-28) and from (5-57) to (5-62).

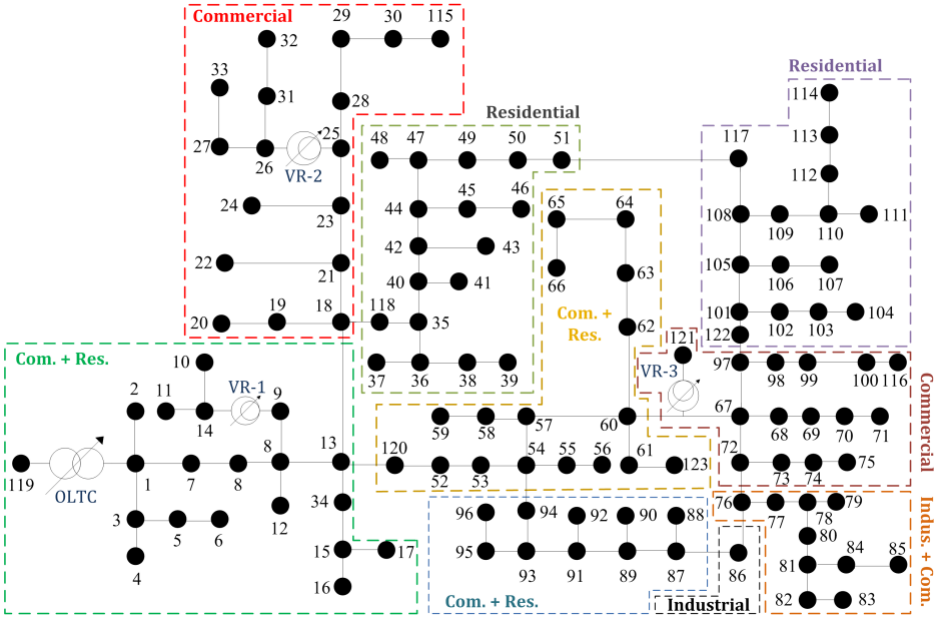

Figure 12.23. IEEE-123 node test feeder single line diagram

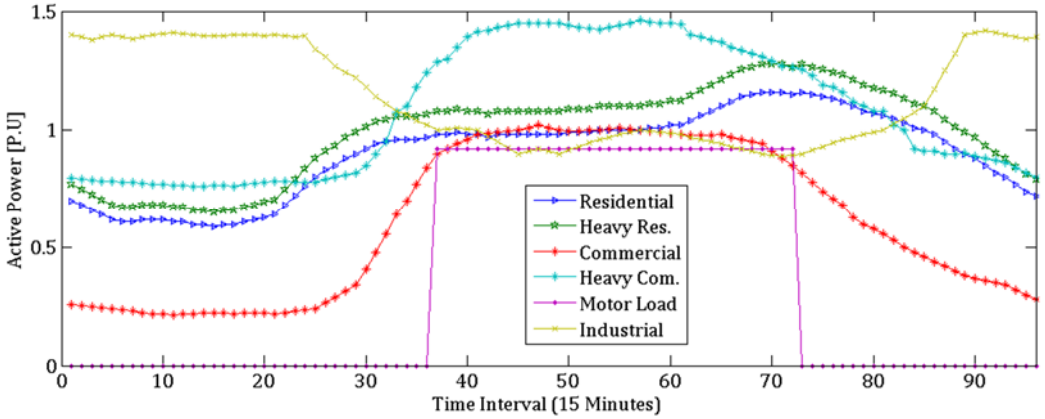

Figure 12.24. Different Daily Load Curves of Customers

Table 12.9. IEEE-123 node test Feeder averaged over day load data

Node No.	Load Type	P MW	Q MVAR	Node No.	Load Type	P MW	Q MVAR	Node No.	Load Type	P MW	Q MVAR
1	3	0.04	0.020	42	1	0.02	0.010	76	6	0.105	0.080
2	1	0.02	0.010	43	1	0.04	0.020	77	6	0.04	0.020
4	1	0.04	0.020	45	1	0.02	0.010	79	6	0.04	0.020
5	1	0.02	0.010	46	1	0.02	0.010	80	4	0.04	0.020
6	1	0.04	0.020	47	2	0.035	0.025	82	4	0.04	0.020
7	1	0.02	0.010	48	2	0.07	0.050	83	3	0.02	0.010
9	3	0.04	0.020	49	2	0.07	0.050	84	3	0.02	0.010
10	1	0.02	0.010	50	2	0.04	0.020	85	4	0.04	0.020
11	3	0.04	0.020	51	1	0.02	0.010	86	5	0.02	0.010
12	1	0.02	0.010	52	1	0.04	0.020	87	3	0.04	0.020
16	1	0.04	0.020	53	1	0.04	0.020	88	3	0.04	0.020
17	3	0.02	0.010	55	1	0.02	0.010	90	3	0.04	0.020
19	3	0.04	0.020	56	1	0.02	0.010	92	3	0.04	0.020
20	3	0.04	0.020	58	1	0.02	0.010	94	1	0.04	0.020
22	3	0.04	0.020	59	1	0.02	0.010	95	1	0.02	0.010
24	3	0.04	0.020	60	1	0.02	0.010	96	1	0.02	0.010
28	3	0.04	0.020	62	4	0.04	0.020	98	3	0.04	0.020
29	3	0.04	0.020	63	4	0.04	0.020	99	3	0.04	0.020
30	3	0.04	0.020	64	4	0.075	0.035	100	3	0.04	0.020

31	3	0.02	0.010	65	4	0.07	0.050	102	1	0.02	0.010
32	3	0.02	0.010	66	4	0.075	0.035	103	2	0.04	0.020
33	3	0.04	0.020	68	3	0.02	0.010	104	2	0.04	0.020
34	3	0.04	0.020	69	3	0.04	0.020	106	2	0.04	0.020
35	2	0.04	0.020	70	3	0.02	0.010	107	2	0.04	0.020
37	2	0.04	0.020	71	3	0.04	0.020	109	1	0.04	0.020
38	1	0.02	0.010	73	3	0.04	0.020	111	1	0.02	0.010
39	1	0.02	0.010	74	3	0.04	0.020	112	1	0.02	0.010
41	1	0.02	0.010	75	3	0.04	0.020	113	1	0.04	0.020
								114	1	0.02	0.010

12.4.2. Operating Scenarios

In this section, six different operating scenarios are studied as follows:

- Scenario 1: In this scenario, it is assumed that the proposed VVO engine operates in this grid but there is no EV in distribution network.
- Scenario II: This scenario investigates distribution network in the presence of EVs.
- Scenario III: In this scenario, a portion of EVs are considered as VAR injectors in the system.
- Scenario IV: This scenario investigates VVO engine results in the presence of EVs.
- Scenario V: In this scenario VVO performs in the presence of a portion of EVs as VAR support.
- Scenario VI: Last scenario, seeks a new VVO approach to find the optimum VAR injection amount and the optimal node of injection for EV charging stations capable of injecting VAR into the grid.

12.4.3. Scenario 1: VVO Performance without EV

As an initial condition, it is assumed that the network is operating using its initial settings without any VVO. The Initial setting of fixed CBs is shown in Table 12.10. In second mode, proposed VVO engine runs to optimize the network (still without any EV penetration) every 15-minutes for a complete day (96 time stages).

Table 12.10. Simulation and network general data

Fixed Capacitor Bank	Node	kVAR	Simulation Data		
CB01	83	200	Optimization Technique	Improved Genetic Algorithm	2mutation/ 2Crossover Steps
CB02	88	50	Power loss cost	C_l	0.06 ($/kWh)
CB03	90	50	Minimum Power Factor Limit	$PF_{min,i,t}$	0.9
CB04	92	50	Capacitor Bank operating cost	C_{CB}	2 ($/kVAR) [253]
OLTC/VR Mode	No. of Taps	Tap Position			
OLTC	17	0.9875	V2G with VAR injection operating cost	C_{Q-V2G}	0.8 ($/kVAR)
VR-1, VR-2, VR-3	5, 5, 5	1, 1, 1	Budget for system operation	$C_{Op-Budget}$	80000 ($)

The 15-minute interval is related to the setting of common smart meters that are able to capture data every 15 minutes. Hence, a 15-minute sliding window is defined for the VVO engine. Each sliding window includes three main steps: data capturing, optimization and control command dispatch. It has to be noted that previous comprehensive Volt-VAR solutions could not optimize network leveraging live (real-time or quasi real-time) smart meter data. Hence, from VVO point of view, it is quite possible to say that the proposed solution is quasi-real-time. Generally, the system difference at sliding window "*t+1*" changes smoothly from sliding window "*t*". Hence, the system is able to track system changes and make a better-than-before solution. It has to be stated that reducing sliding window size to 5 minutes might respond to system changes better that needs further investigations. An improved genetic algorithm (GA) with two-crossovers and two-mutation steps are used in order to achieve high level of precision. First, a random number between 0 and CB_{max} (maximum capacitor) is generated for each gene. Repeating this process, results in GA initial population. Second, two different crossover operators are employed in order to reproduce generation. Hence, two chromosomes considered as a parent and they are crossed over with a probability called PCHR-1. Then, chromosome rows are substituted with each other. In addition to data substitutions of

rows, gene's data are also selected randomly and displaced in second crossover step. Two mutation types of improved GA increase search space and prevent local optimum solutions of the system. A chromosome row is selected randomly in first mutation. Then, with a probability PMUT-1, random changes impose in several arrays of a chromosome by the second mutation.

Table 12.10 presents the initial settings of Volt-VAR control components and the optimization parameters. It should be mentioned that the algorithm design enables users to run VVO in quasi-real-time but at this stage of research it was performed offline to check the accuracy of the results and due to AMI data rate limitation that will become available to proposed optimization engine in upcoming studies. Table 12.11 compares the results of three initial network operating modes: First, there is no VVO in the system. Second, VVO performs with voltage control devices such as OLTC and VRs and third, VVO performs completely. The results show that the system can save about US$ 304 in a day by performing a proper VVO.

Table 12.11. VVO initial results (no VVO)

No.	Operating Scenario	Objective Function ($)	Active Power Loss (kW)
1	Initial (No-VVO)	9173.0	6370.1
2	VVO (Just OLTC/VR)	8963.5	6224.6
3	VVO (Complete)	8869.0	6159.0
Loss Reduction: 1-3		304	211

12.4.4. Scenario II: Network in Presence of EVs

In order to study the EV impact on distribution network, the assumption is made that different users own EVs with different consumption levels. For commercial and industrial loads, EV charging stations are considered as well. Hence, Figure 12.25 shows different EV load profiles (Residential, Workplace and Commercial) in both charging level-I and Level-II. Hence, the study considered EV charging Level I, Level II and the combination of them for EV stations in different locations (Residential (for residential/heavy residential loads), Workplace (for commercial loads), Commercial (for heavy commercial and industrial loads)). In addition, it assessed EV impacts on the system in two penetration levels (Normal and High) for different customers. For residential

customers, normal penetration level is equal to 2 EV per 10 houses and high penetration means 4 EV per 10 houses. Moreover, normal and high penetration levels for work, commercial and industrial locations are the existence of 2 and 4 charging stations at each location respectively. Figure 12.23 illustrates EV regions in case study.

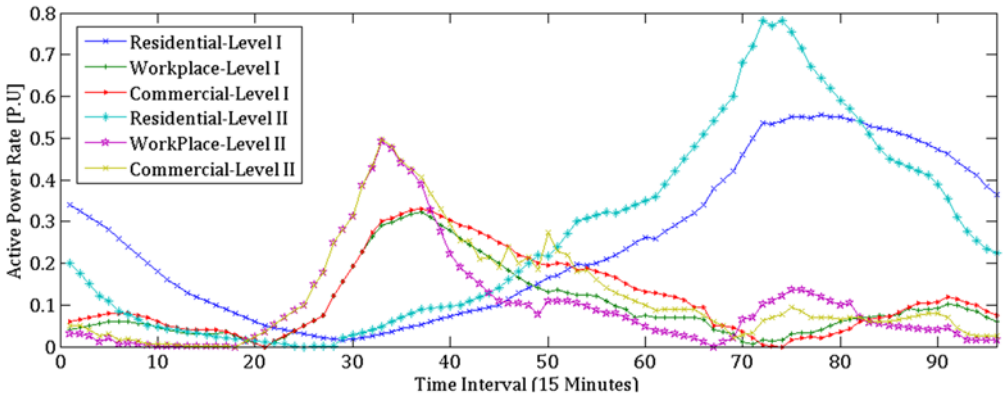

Figure 12.25. EV Load Curves for different consumers

Reference values for the P.U for Figure 12.24 and Figure 12.25 are calculated based on data received by smart meters in order to find load type Per-Unit values. For example, by multiplying active power of a node with a Per-Unit of its value in Figure 12.24, it is simply possible to find the smart meter active power amount. Here, distribution feeder in the presence of EVs with different charging levels and cases (level-I, level-II, 50% level-I and 50% level-II, 30% level-I and-70% level-II, 70% level-I and 30% level-II) is studied. Table 12.12 , shows the power loss cost amount obtained for scenario II. It has to be reminded that the grid has not been optimized by VVO yet.

12.4.5. Scenario III: Network in Presence of a portion of EVs as Reactive Power Injectors

Based on literatures [93]-[94], this study makes the following assumptions: EV charging station Level I, is capable of generating reactive power around 35 % of its active power [93] and the EV charging station Level II is able to inject VAR to the grid with a rate around 50% of its active power [94]. Moreover, this work studies EV effects when 20 percent of the EVs are able to inject VAR into the grid. The result of this scenario is given in Table 12.12. From Table 12.12, it is concluded that the system power loss costs reduced by reactive power generation of a part of EVs in different charging scenarios. The VAR

injection contribution of each EV is obtained from VVO power flow which determines system VAR needs. Hence, VVO finds VAR amount needed for each node of the system at each time stage and checks if an EV is able to inject required VAR (or a part of it) at that node in that moment or not . It is important to distinguish between placement and sizing problem (which is a planning problem) and real time operational constraints. This study tries to find the optimal VAR amount of each existed switchable CBs along distribution network feeder.

12.4.6. Scenario IV: VVO in Presence of EVs

In this scenario, VVO optimizes distribution feeder in the presence of EVs with different penetration (Normal, High), charging levels and sub-scenarios (level-I, level-II, 50% level-I and 50% level-II, 30% level-I and 70% level-II, 70% level-I and 30% level-II). The VVO minimizes the objective function and finds the optimal VAR level for switchable Capacitor Banks during each time stage. The result of this scenario is presented in Table 12.13. In order to compare total CB amount and the operating cost in different scenarios, VVO has regulated the OLTC and the VRs of the network in fixed rates shown in Table 12.10. It is foreseeable that the grid losses rise significantly because of the active power consumed by EVs that impose Ohmic loss to the grid.

Table 12.12. Scenario-II and Scenario-III comparison

EV Charging Levels (%)	Penetration Level	Scenario-2: V2G, No VAR injection ($)	Scenario-3: V2G with portion of VAR injection ($)	Difference for 96 time steps ($)
Level 1 -100%	High	9890.6	9861.3	29.3
	Low	9419.5	9404.9	14.6
Level 2 -100%	High	11953	11828	125
	Low	10385	10322	63
70-30	High	10480	10422	58
	Low	9701.9	9672.9	29
30-70	High	11305	11208	97
	Low	10088	10040	48
50-50	High	10887	10809	78
	Low	9893.6	9855.0	38.6

12.4.7. Scenario V: VVO in Presence of a portion of EVs as Reactive Power Supports

Similar to Scenario III, the case study consists of EVs (20 percent) with reactive power injection capability. Here, VVO tries to find the optimal configuration of CBs for distribution network in order to minimize the objective function which includes power loss costs and CB operating costs of the system. The result of this scenario is shown in Table 12.13 as well. Comparing Scenario IV and Scenario V results, one can conclude that in Scenario V, the VVO engine minimizes the objective function with less cost. It could also be derived that in some charging levels, the power loss cost increased (in Scenario V), while the total amount of the objective function was reduced. The reason lies in the fact that VAR sources of the network were increased by EVs so that the system reached a less objective function with less switchable CB amounts. As a result, although EVs increase distribution network Ohmic losses but, they might be employed as reactive power sources enabling network operators reduce system losses as well as expenses.

Table 12.13. Scenario-IV and Scenario-V comparison in presence of CBs found by VVO

EV Charging Levels (%)	Penetration Level	Scenario-IV: No VAR injection Active Power Loss (kW)	Scenario-V: With VAR injection Active Power Loss (kW)	Scenario-IV Objective Function ($)	Scenario-V: Objective Function ($)	Difference between objective functions for 96 time steps ($)
Level 1 - 100%	High	6772.5	6742	51152.4	49508.4	1644
	Low	6388.3	6492.6	44299.1	39849.3	4449.8
Level 2 - 100%	High	8120.7	8189.7	109194	103593	5601
	Low	7060.7	7035.3	81667	74531	7136
70-30	High	7153.7	7096	60785	54618	6167
	Low	6621.5	6640	54398.2	53861.6	536.6
30-70	High	7821.5	7763.8	78263	75580	2683
	Low	7003.1	6892.7	71884	69725.5	2158.5
50-50	High	7649.3	7412.5	65226	64605	621
	Low	6711.8	6753.8	67265	62725.4	4539.6

12.4.8. Scenario VI: VVO with New O.F for EVs

As concluded from Scenario V, reactive power injection by EVs could benefit distribution networks in terms of operating expenses. Hence, scenario VI seeks a new VVO approach to find the optimum VAR injection amount and to find the optimal node of injection for EV charging stations capable of injecting VAR into the grid as well. Thus, the VVO objective function is modified in order to consider the VAR injection operating cost of these EV charging stations. Here, the VVO is able to find the optimal VAR level of CBs and EVs with VAR injection capability by applying (5-31).

In summary, this scenario checks if VVO is able to find EV optimal VAR injection points (among available locations) and optimal values or not. The method of finding the optimal combination of the CB and EV charging station VAR locations are similar to the first Scenario. The EV optimal levels and locations are being found by GA in MATLAB environment. In this case study, the VAR injection amounts for EV charging stations are considered as 10 and 20 kVARs. According to [94] and [95], the reactive power injection service of V2Gs would be very cost-effective compared to other services such as coordinated charging, peak shaving and/or active regulations [95]. Therefore, this study assumes the VAR injection operating cost of EV charging station equal to 40% of CB operating cost. These amounts are given in Table 12.10. Table 12.14 compares Scenario V and Scenario VI results. Moreover, Table 12.15 compares total injected VAR amount into the system in Scenario V and Scenario VI. The results in Table 12.14 specify that the new VVO with new Objective Function led to a system with lower operating cost.

Table 12.14. Scenario-V and Scenario-VI comparison in presence of CBs found by VVO

EV Charging Levels (%)	Penetration Level	Scenario-V: Active Power Loss (kW)	Scenario-VI: New O.F. with VAR injection, Active Power Loss (kW)
Level 1 - 100%	High	6742	6601
	Low	6492.6	6356
Level 2 - 100%	High	8189.7	8174.5
	Low	7035.3	7111.6
70-30	High	7096	7203.3
	Low	6640	6582.6

30-70	High	7763.8	7727.1
	Low	6892.7	6815.3
50-50	High	7412.5	7303
	Low	6753.8	6698.95

Table 12.15. Scenario-V and Scenario-VI CBs and EV charging stations found by VVO

EV Charging Levels (%)	Penetration Level	Scenario-V Objective Function ($)	Scenario-VI: Objective Function ($)	Difference for 96 time steps ($)
Level 1 - 100%	High	49508.4	48317	1191.4
	Low	39849.3	39436.6	412.7
Level 2 - 100%	High	103593	86375	17218
	Low	74531	60093	14438
70-30	High	54618	53317	1301
	Low	53861.6	52694.9	1166.7
30-70	High	75580	68219	7361
	Low	69725.5	63830	5895.5
50-50	High	65005	62888	2117
	Low	62725.4	61318	1407.4

EV Charging Levels (%)	Penetration Level	Scenario-V: Total VAR amount (kVAR)	Scenario-VI: Total VAR amount: CB+EV (kVAR)
Level 1 - 100%	High	19900	20750
	Normal	15250	16450
Level 2 - 100%	High	45900	39750
	Normal	32200	26390
70-30	High	22200	23260
	Normal	22150	23000
30-70	High	32200	30850
	Normal	29900	29120
50-50	High	27150	28250
	Normal	26500	27850

EV Charging Levels (%)	Penetration Level	Scenario-VI Total Capacitor Bank (kVAR)	Scenario-VI: Total EV Charging Station VAR Injection (kVAR)
Level 1 - 100%	High	18510	2240
	Normal	14270	2180
	High	35670	4080

Level 2 - 100%	Normal	23950	2440
70-30	High	20280	2980
	Normal	20680	2320
30-70	High	27010	3840
	Normal	25600	3520
50-50	High	24810	3440
	Normal	24490	3360

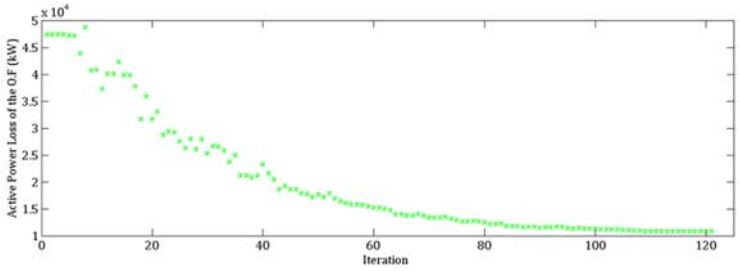

The result of Scenario VI shows that certain VAR amount is needed that the system could not supply in scenario V. Thus, by more reactive power injection into the grid in Scenario VI, the system leads to a less operating cost (objective function). In order to compare the discussed scenarios with each other, one of the EV charging/penetration cases (Charging scenario: Level-II, Penetration Level: Normal) is chosen and the results/figures related to this case are presented as follows:

The objective function active power loss convergence of VVO in Level II/Normal penetration case is shown in Figure 12.26. Figure 12.27 shows the Power Factor (PF) of all nodes in different time stages. As shown in Figure 12.27, all nodes in different time stages are more than minimum regulated Power Factor (PF_{min}) which is equal to 0.9. Moreover, it gives the weakest nodes of the system regarding PF (Node No: 47, 48, 49, 65 and 76). Comparing Power Factors in Figure 12.27, it is concluded that last scenario has reached to an acceptable PF range with less VAR injection amount as well. Figure 12.28 compares the apparent power loss spectrum in last two scenarios and Figure 12.29 demonstrates the apparent power loss of the system in sixth scenario as an example.

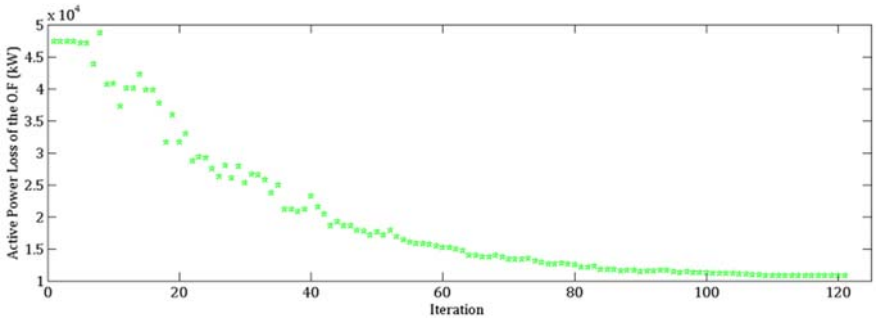

Figure 12.26. VVO Objective Function Loss Convergence in Level II/Normal Penetration Case

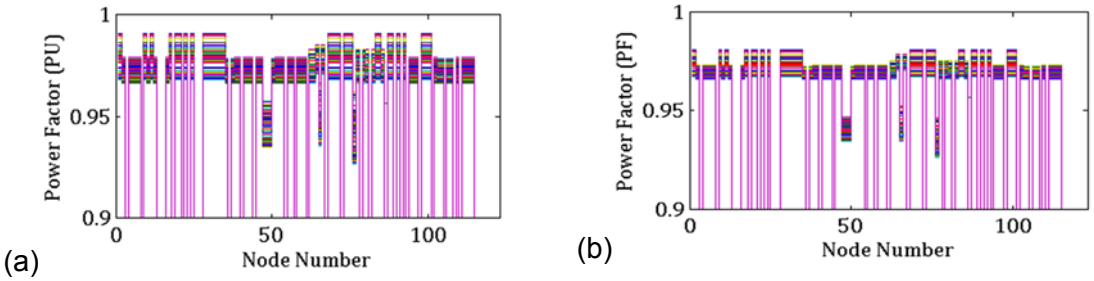

Figure 12.27. Power Factor of all nodes in different scenarios: (a) Scenario V and (b) Scenario VI for Level II/Normal Penetration Case.

The spectrums range from blue to red (Figure 12.28) presents the apparent power loss from the lowest to the highest value. Hence, it can be observed that the power loss of the system is in its highest rate (red region) at the end of the feeder and during peak time (Time stage-62 to 73). This study chose to simulate the apparent power loss rather than the active or reactive power losses for Figure 12.28 and Figure 12.29, because the apparent power loss includes both active and reactive power losses. Hence, it provides

more detail about loss minimization performed by the VVO engine compared with active power loss which does not include reactive power loss reduction.

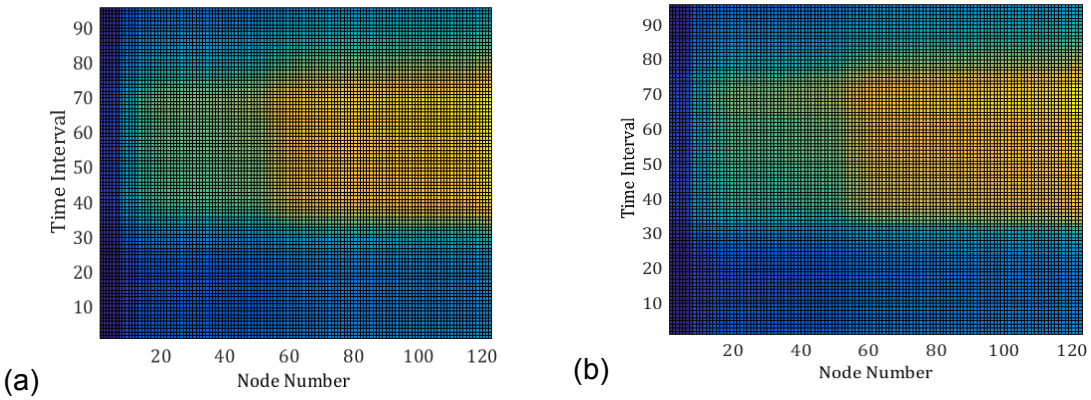

Figure 12.28. Apparent power loss histogram of all nodes at each time interval in different scenarios: (a) Scenario V and (b) Scenario VI for Level II/Normal Penetration Case.

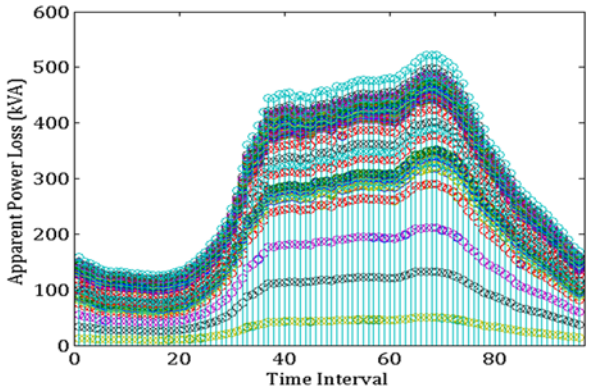

Figure 12.29. Apparent power loss of all nodes at each time interval in Scenario VI for Level II/Normal Penetration Case

Figure 12.30 represents the 3D plot of the voltage of all nodes of the system at each time stage for the last scenario and Figure 12.31 compares the voltage of the nodes of the system in discussed scenarios. It can be derived from Figure 12.31 that EVs increased the voltages of some nodes in scenario VI. Figure 12.32 shows the CB VAR amount for each node at each time stage in Scenario IV, V and VI found by VVO engine.

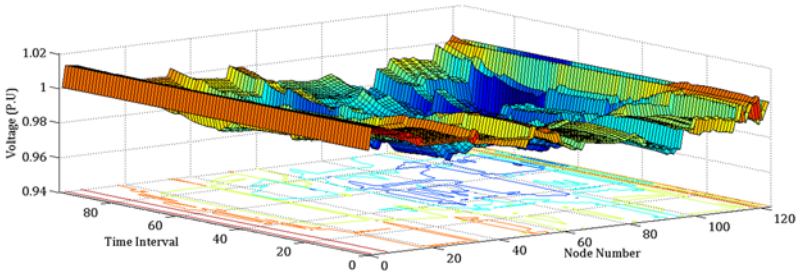

Figure 12.30. Voltage of all nodes at each time interval for Scenario VI (Level-II, Normal Penetration)

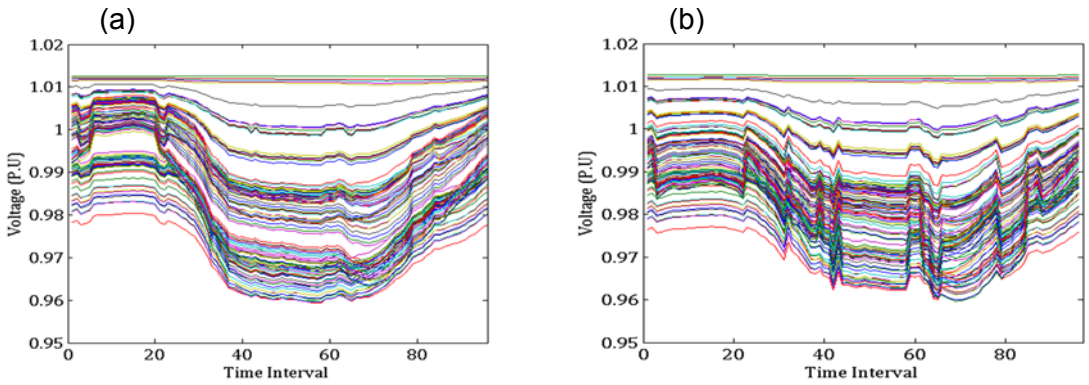

Figure 12.31. Voltage of all nodes during time interval in different scenarios: (a) Scenario V and (b) Scenario VI for Level II/Normal Penetration Case

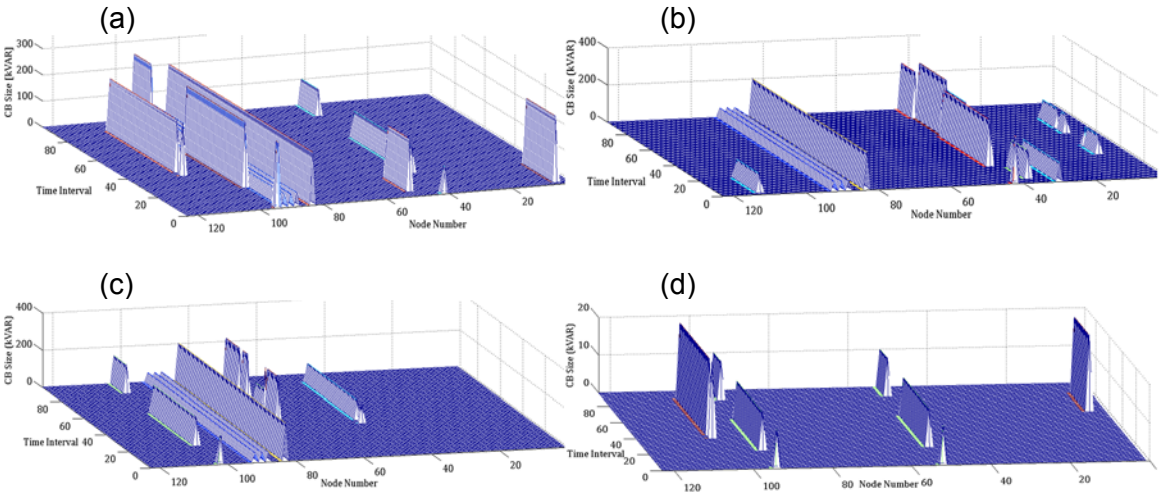

Figure 12.32. Switchable Capacitor Bank VAR injection amounts and points for all nodes in all time intervals in (a) Scenario IV, (b) Scenario V, (c) Scenario VI and VAR injection amount and location of EV charging stations in Scenario VI (d) for Level II/Normal Penetration Case.

As Figure 12.32 illustrated, Scenario IV applies more CBs available on the nodes of the system during a day compared with Scenario V and Scenario VI. Moreover, the

optimal locations of CB VAR injections have changes when VARs were injected by EVs. Finally, the last scenario (VI) allocates optimal CB (Figure 12.32 (c)) and EV charging stations VAR injection amounts and points (Figure 12.32 (d)).

12.4.9. Conclusions

This research studied the impact of EVs with different charging (I and II) and penetration levels (Normal and High) on smart grid adaptive VVO of distribution networks. The results proved the fact that it would be possible to supply a part of distribution network's required reactive power from EVs by changing the operating mode of AC/DC inverters without imposing any changes on the active power operating mode of the charger. This potentially brings upon a network with less reactive power compensation issue. Moreover, it could reduce the operational costs of switchable Capacitor Banks located within medium voltage substation and/or along distribution feeder. Hence, EVs capable of injecting VAR into the grid might change capacitor bank configuration of the network as well as the operating cost of the grid. Regardless of other economic factors such as investment costs and Internal Rate of Returns (IRR) that should be taken into account in future studies, EV reactive power injection would be an appealing approach especially in cases that EV charging stations are close to weak points of the network and/or the termination points which consume more reactive power. In the last scenario of this study, VVO benefited from reactive power generation of EV charging stations and gave the optimal VAR amounts of reactive power injection points of distribution network. Therefore, this study introduced a comprehensive VVO approach with the capability of employing EV charging stations as VAR injection sources to optimize distribution network loss and operating expenses at a same time. In order to test the accuracy of the proposed technique, a revised IEEE-123 node test feeder applied with different load types and consumption regions for EVs. Different charging scenarios and penetration levels assessed thoroughly in order to check the impact of V2Gs on the network and on the VVO. Finally, it is concluded that V2Gs in future distribution networks will impose new challenges and opportunities on the distribution network's short/long term planning that need to be taken into account in distribution network's dispatch-able energy and costs. The structure and design of proposed VVO in this study could be a great solution sample for distribution

network planners and/or operators to optimize their grids in accordance with new smart grid features by employing better-than-before efficient techniques.

12.5. Predictive Algorithm for Volt-VAR Optimization of Distribution Networks Using Neural Network

12.5.1. Case Study and Results

In this section, British Columbia Institute of Technology (BCIT) north campus distribution network applied as a case study. Figure 12.33 depicts the schema of BCIT campus grid. Table 12.16 presents the general data of the BCIT case study. This study uses Figure 3.10 of Chapter 3.5 as system topology. All theories presented in Chapter 9.1 are the basis of this study. This study uses (5-32) and (5-33) as objective function equations with constraints from (5-9) to (5-28).

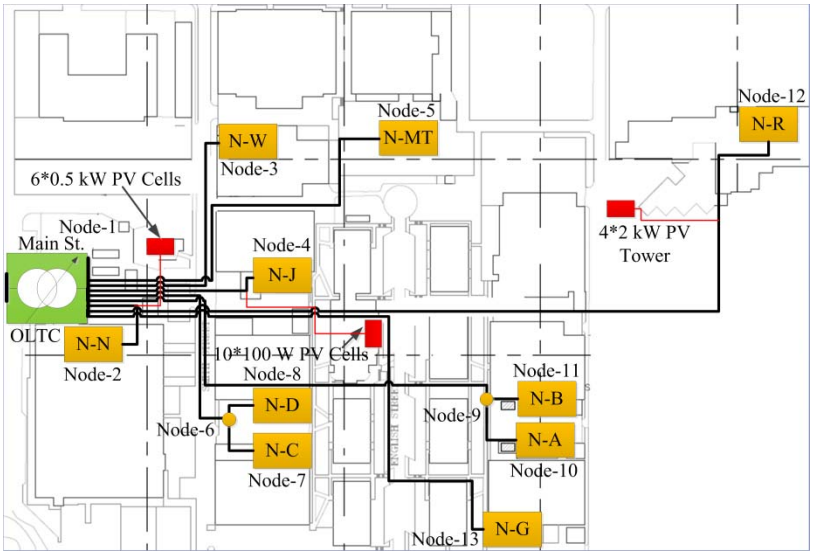

Figure 12.33. BCIT North Campus distribution network schema

It employs (5-42) and (5-43) for calculating the active and reactive power based on ZIP model of loads. As it is shown in Figure 12.33 and Table 12.16, the BCIT case study consists of 13 nodes. Each node has its own smart meter that is able to feed several neighbor buildings and measure active and reactive power at each time stage (15-minutes). The abovementioned nodes have switchable shunt capacitors with 10, 25 and 50 kW capacities.

Table 12.16. General Data of BCIT North Campus Case Study

Node No.	Average daily kW	Average daily kVAR	Smart Meter	Available CB (kVAR)
1	0	0	0	-
2	340.902	109.528	N-N	25,50
3	120.364	39.182	N-W	25,50
4	16.974	5.444	N-J	10
5	134.168	44.257	N-MT	10,25,50
6	0	0	0	25,50
7	58.05	19.041	N-C	10,25,50
8	50.497	16.011	N-D	10,25,50
9	0	0	0	0
10	65.468	21.474	N-A	25,50
11	29.482	9.671	N-B	10
12	91.141	29.56	N-R	10,25,50
13	36.473	11.859	N-G	10

Additionally, the network includes an OLTC located at the main substation that is able to regulate the voltage of the feeder from -5% to +5%. The OLTC consists of 17 tap steps (the middle tap is tap-0). The number of CB switching per day limit for each CB is equal to 10 and the number of the OLTC switching per day limit is assumed to be equal to 12. The temperature and dew point data of BCIT campus is collected from the Environment Canada. The coefficients of (2) and (3) are considered as $C_{loss} = 0.0928\ (\frac{\$}{kWh}), C_{CB} = 9\ (\$/(kVARyear))$ and $C_{CVR} = 0.06\ (\frac{\$}{kWh})$. Initially, the objective was to predict the load for November 1st, 2013. Hence, the Neural Network engine predicted the active/reactive power of each node at each time stage of November 1st 2013 based on gathered previous data. Table 12.17 gives a snapshot of Neural Network training inputs in a chosen node (node-2) in order to show a sample of data used by Neural Network training set. The initial settings for Neural Network engine are presented in Table 12.18. Hence, Neural Network engine predicted the active and reactive power of the November 1st, 2013 loads for every 15 minutes based on the settings depicted in Table 12.17, Table 12.18 and smart meter previous data mentioned in previous section, part-B.

Table 12.17. Snapshot of Neural Network Training Input for Node-2 (Each Column here, shows a row of NN training set)

Date/Time	31/10/2013 7:15	31/10/2013 7:30	31/10/2013 7:45	31/10/2013 8:00

Temperature (°C)	9	9	9	9.1
Dew Point (°C)	8.1	8.1	8.1	8.2
Time Stage Numerator	29	30	31	32
Day of week	4	4	4	4
Type of day	1	1	1	1
Previous week kW	361.15634	400.04278	411.66867	416.73031
Previous day kW	368.79626	403.91207	420.36389	416.54077
Previous day average kW	343.85237	343.85237	343.85237	343.85237

This study used MATLAB as simulation environment in order to design predictive VVO engine. The convergence rate of GA in the case study is considered to be equal to 0.9999. Then, the VVO engine used the predicted load of Neural Network engine to optimize the network for November 1st, 2013. The capacitor switching operation considered in three load levels: low level (less than 70 % of the average load), mid-level (70% to 110% of the aver. load) and peak level (more than 110% of the aver. load). The load model in CVR calculation was ZIP with the following values: $Z_p = 0.43, I_p = -0.06. P_p = 0.6, Z_q = 4.06, I_q = -6.65, P_q = 3.5$. After finding the optimal configuration of Volt/VAR control devices by the predictive VVO engine, the results of the optimization of a day-ahead algorithm was used on November 1, 2013 in order to test the performance of the predictive VVO. Table 12.19 compares the result of the study in five different scenarios:

- Scenario-I: No VVO in the system, predicting loads by Neural Network engine
- Scenario-II: Perform predictive VVO algorithm to optimize the system for targeted day
- Scenario-III: Implement predictive VVO algorithm results obtained by scenario-II in targeted day
- Scenario-IV: No VVO, consider network with real measured smart meter load data in targeted day
- Scenario-V: It is assumed that ideal VVO could be efficiently performed using real data of smart meters of targeted date in quasi real-time

Table 12.18. Neural Network Setting for BCIT North Campus

Node-No.	Number of Neurons	No. of training set rows	Train%-Validation%-Test %	Epoch
2	10	57888	80-15-5	121

3	10	57888	80-15-5	229
4	10	67008	80-15-5	339
5	10	70272	80-15-5	224
7	10	70272	80-15-5	167
8	12	67872	75-20-5	171
10	10	70272	80-15-5	173
11	10	70272	80-15-5	196
12	10	57888	80-15-5	139
13	12	67008	80-15-5	143

Table 12.19. Case Study Results for Different Scenarios

Scenario No.	Loss/operation costs ($)	CVR tap	Saved **kWh** by CVR	Saved active energy %	Objective Function Value ($)
1	C_l =462.4746	0	-	-	-
2	C_{lo} =434.4494	7	146.3175	3.8925	36.80425
3	C_{lo} =443.7502	7	147.3731	3.8926	36.87129
4	C_l =471.7791	0	-	-	-
5	C_{lo} =441.3558	7	147.3731	3.8926	39.26569

Figure 12.34 illustrates a comparison between predicted load of a sample node (node-2) and real data collected in targeted day. Furthermore, Table 12.20 gives the accuracy of each prediction by calculating Mean Absolute Percentage Error (MAPE) and the number of CB and OLTC switching for each node. In addition, the convergence of VVO engine to optimal solution is shown in Figure 12.35. It may possible to determine different components of ZIP load model via NN in order to see the impact of each component on VVO that might be considered in further studies. Figure 12.36 compares total active load curves of scenario-III and scenario-V for all nodes and Figure 12.37 depicts the voltage of all nodes at each time stage in Scenario-III. The capacitor bank switching operation of nodes in time stages that is found by predictive VVO is shown in Figure 12.38. The loss cost at each time stage resulted from scenario-III is given by Figure 12.39.

Table 12.20. Results of Prediction Accuracy and Number of CB Switching in predicted day (y_{pred}: Predicted Load, Y: Measured Load)

Node-No.	$MAPE\% = \frac{y - ypred}{y} \times 100$	No. of CB Switching in Scenario-III	No. of CB Switching in Scenario-V
1	-	-	-
2	2.3788	2	2
3	3.68	4	4
4	4.74	0	0
5	4.5187	2	2
6	-	-	0
7	4.6269	0	2
8	4.4278	4	0
9	-	-	0
10	4.12	10	10
11	4.62	0	0
12	3.68	4	2
13	4.4290	0	0

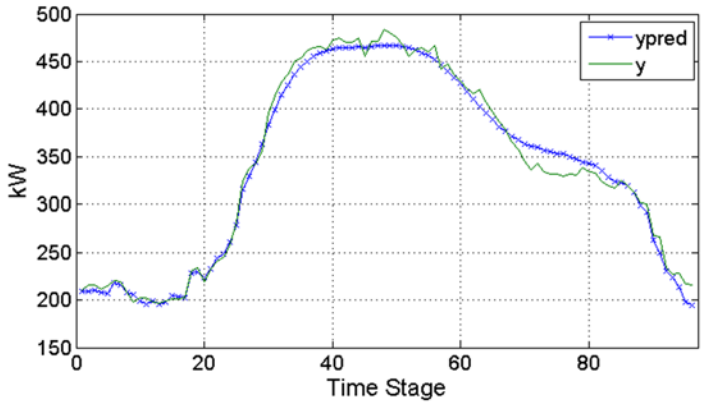

Figure 12.34. Predicted load (ypred) versus measured load (y) for node-2

12.5.2. Result Analysis

As observed from Figure 12.34 to Figure 12.39, the predictive VVO algorithm could predict the active and reactive loads of each node with an acceptable approximation (less than 5% error) and then, it proposed an efficient optimized configuration for Volt-VAR control devices of the grid.

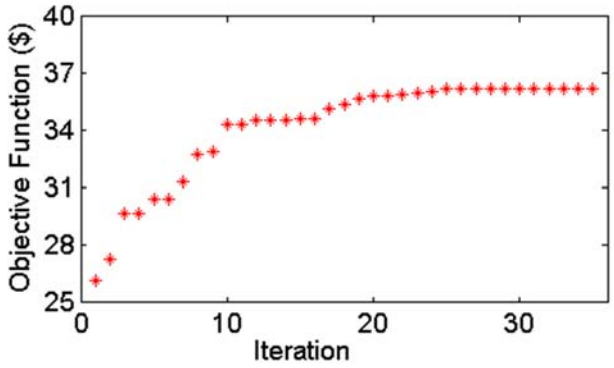

Figure 12.35. Objective Function value convergence in Scenario-III

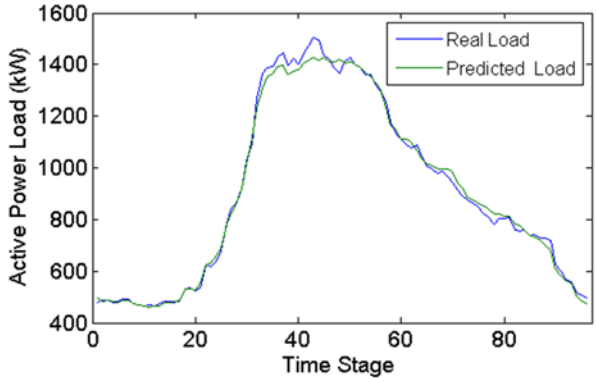

Figure 12.36. Total measured active power loads versus total predicted active power loads by predictive VVO

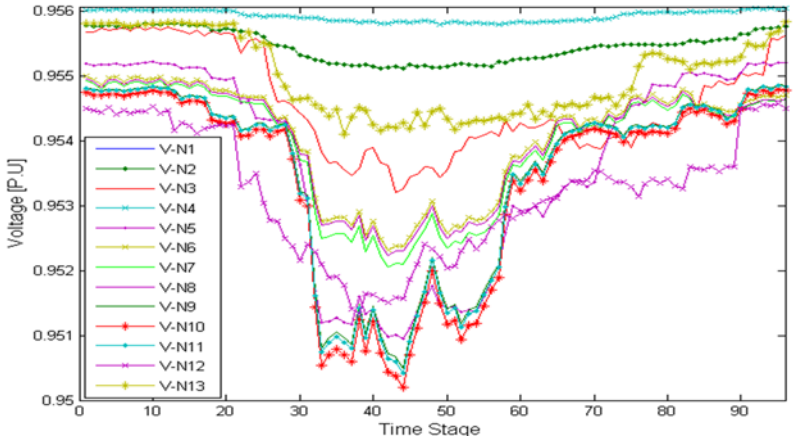

Figure 12.37. Scenario-III Node voltages at each time stage

As the BCIT campus distribution grid is very strong in terms of voltage profile, the predictive VVO could be able to set the OLTC tap in an adequate position (base voltage of the tap position: 114.75 V) for all time stages of predicted day.

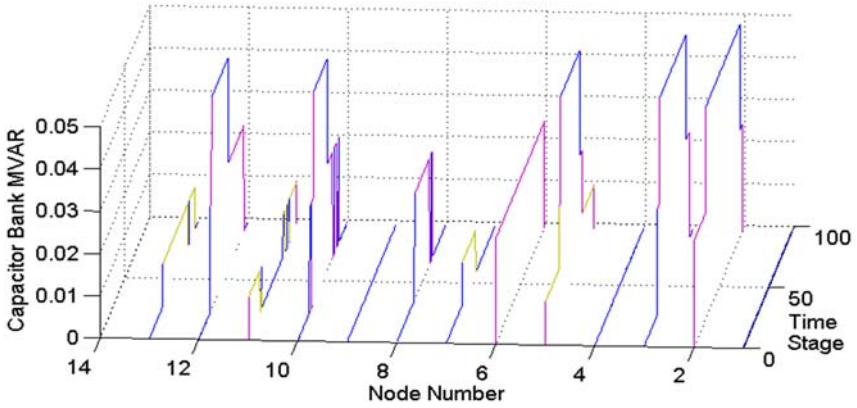

Figure 12.38. Capacitor Bank switching operations for all nodes at each time stage for Scenario-III

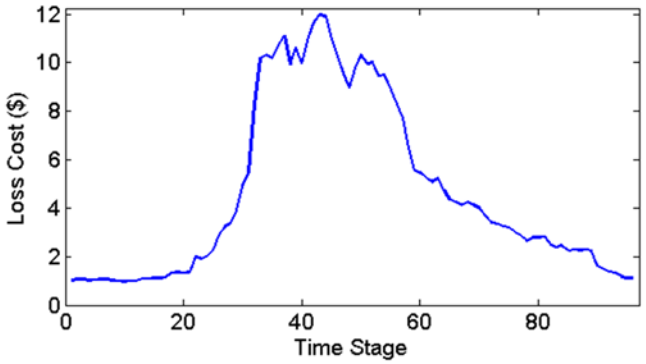

Figure 12.39. Loss Cost (C_{lo}) resulted from Scenario-III

On the other hand, comparing scenario-III with scenario-V leads to a conclusion that the benefit (objective function value) resulted from VVO in scenario-III (last column) is very close to the benefit resulted from VVO in scenario-V (last column). Moreover, the difference between the loss/operation costs in scenario-III is very close to scenario-V as well. Thus, the presented predictive VVO in this study optimized BCIT campus distribution network efficiently and the campus could save about $36.87 in targeted day using this technique. Furthermore, this approach solved the number of tap or CB switching limitation issue. Hence, this limitation could be simply given to the algorithm by network operators. It has to be stated that the accuracy of prediction highly depends on the amount and the types of available historical data. As in this case study, smart meter data was available since 2009-2010, the Neural Network prediction led to an acceptable error rate. Thus, more related and accessible historical data could train the Neural Network better. By development of smart meter installations in distribution networks, more real/semi-real time

data could be collected for different distribution network studies such as VVO in future. Thus, presented approach in this study could be a great candidate for Volt-VAR Optimization solution of future distribution networks. In addition, the concepts presented in this study could provide a basic framework for further studies regarding to design a novel real-time predictive algorithm able to optimize distribution network online for next real-time stages.

12.5.3. Conclusion

This study investigated a new predictive VVO algorithm for smart distribution networks. The algorithm predicted the active and reactive power loads of the next day based on downstream historical data received from local AMI and upstream global attributes received from DMS/SCADA. Then, it minimizes network loss cost, Capacitor Banks and CVR operating costs as well as maximizing saved energy through CVR method for the next day through an improved Genetic Algorithm.

The results of the study on BCIT campus distribution network showed that the proposed predictive algorithm is capable of predicting the active/reactive power loads of the system very close to real values through a comprehensive training set. Then, the predictive VVO found the optimal configuration of OLTC and CBs in the system for the next day. Comparing results of predictive VVO (Scenario-III) with the VVO that collected real data from the predicted day (Scenario-V) elucidated the fact that the predicted algorithm in this study could yield energy conservation and loss reduction to distribution networks very close to energy saving and loss reduction that can be obtained by real-time VVO. One of the main advantages of predictive VVO presented in this study is its ability to solve the issue regarding the limits that Capacitor banks and OLTCs/VRs have on their number of switching per day because of their lifetime. Most real/semi-real VVO strategies are still dealing with this issue. The reason lies in a fact that the limits on number of switching of CBs and/or OLTC/VR taps are defined by natural numbers in a day (not in real/semi-real time). Hence, presented approach in this study is able to get benefit from real-time data of previous days and tries to reach to a next day optimal configuration in a way that the number of CB or/and OLTC/VR tap switching is/are within desired range(s).

The existence of smart meter historical data could be one of the factors of success of the proposed approach in the studied network. Thus, by development and growth of smart meter installations in future distribution grids, the presented predictive approach in this study could be one of the great candidates for VVO scheme designs in future. Moreover, the concepts presented in this study could provide a basis for online predictive VVO designs that would be able to optimize the network for the next real-time stage through real data of previous time stage and other former data. In this design, the predictive VVO is able to correct and re-train itself based on received real-time data. The accuracy and the efficiency of this approach are going to be investigated by the authors of this study as their next VVO study.

12.6. A Novel Predictive Volt-VAR Optimization Engine for Smart Distribution Systems

12.6.1. Case Study and Results

As a case study for Chapter 9.2, British Columbia Institute of Technology (BCIT) north campus distribution network is applied in order to test the applicability and the accuracy of proposed predictive VVO. Figure 12.33 presents the single line diagram of BCIT campus grid. Table 12.21 presents the initial data of the BCIT distribution network. As shown in Figure 12.33 and Table 12.21, the BCIT distribution network has 13 different nodes. Each node has its own smart meter that is able to feed several buildings in campus and measure active and reactive power at each time stage (every 15-minute). Some nodes are equipped with switchable shunt capacitors with 10, 25 and 50 kVAR capacities. Moreover, the network includes an OLTC located at the main substation able to regulate the voltage of the feeder from -5% to +5%. The OLTC has 17 tap steps (the middle tap is tap-0). The number of CB switching per day limit for each CB is equal to 10 and the number of the OLTC switching per day limit is assumed to be equal to 12. The temperature and dew point data of BCIT campus is collected from the Environment Canada. The primary objective was to predict the load for November 1st, 2013. This study uses (9-2) to (9-9) for its Neural Network engine. Figure 3.11 of Chapter 3.5 presents system topology of this study. The objective function is (5-30), and the constraints are from (5-9) to (5-28).

Table 12.21. Data of BCIT North Campus Distribution Network

Node No.	Smart Meter	Average Daily kW	Average Daily kVAR	Available CB (kVAR)
1	-	-	-	-
2	N-N	340.902	109.528	25, 50
3	N-W	120.364	39.182	10, 25, 50
4	N-J	16.974	5.444	10
5	N-MT	134.168	44.257	10, 25, 50
6	-	-	-	25, 50
7	N-C	58.05	19.041	10, 25, 50
8	N-D	50.497	16.011	10, 25, 50
9	-	-	-	-
10	N-A	65.468	21.474	10, 25, 50
11	N-B	29.482	9.671	10
12	N-R	91.141	29.560	10, 25, 50
13	N-G	36.473	11.859	10

Hence, the prediction engine predicted the active/reactive power of each node at each time stage of November 1st 2013 (every 15 minutes: 96 time stages for a whole day) based on previous data gathered from historical data. Table 12.22 illustrates a snapshot of prediction engine training inputs for one of the nodes of system (node-2) to show a sample of data employed by Neural Network training algorithm. The initial settings and final error rates for prediction engine are given in Table 12.23.

Table 12.22. Prediction Engine Snapshot of Inputs for Node-2 (each column shows a row of Neural Network Training set)

Date	31/10/2013	31/10/2013	31/10/2013	31/10/2013
Time	10:00	10:15	10:30	10:45
Temperature (^{0}C)	9.4	9.6	9.6	9.6
Dew Point (^{0}C)	8.8	8.8	8.8	8.8
Time Stage Numerator	40	41	42	43
Day of week	4	4	4	4
Type of Day	1	1	1	1
Previous Week kW	471.3176	469.9430	465.3295	492.1121
Previous Day kW	476.3863	478.9818	479.4061	479.2406
Previous Day Average kW	343.8524	343.8524	343.8524	343.8524

Table 12.23. Prediction Engine Setting and final error rate for BCIT North Campus grid

Node No.	Number of Neurons	No. of Training Set Rows	Epoch	$MAPE = \frac{y - y_{pred}}{y} \times 100$ Offline Predictive VVO	MAPE Proposed Online Predictive VVO
2	10	57888	121	2.3788	1.97197
3	10	57888	229	3.6800	2.96101
4	10	67008	339	4.7400	2.73375
5	10	70272	224	4.5187	2.87417
7	10	70272	167	4.6269	2.65960
8	12	67872	171	4.4278	3.03760
10	10	70272	173	4.1200	2.72767
11	10	70272	196	4.6200	3.03670
12	10	57888	139	3.6800	3.05460
13	12	67008	143	4.4290	2.60904

Hence, the offline prediction engine predicted the loads for November 1st, 2013 for every 15 minutes based on the settings depicted in Table 12.22, Table 12.23 and smart meter previous data mentioned in previous section, part-B. This study used MATLAB environment in order to design predictive VVO engine. The optimization technique used for VVO engine is Genetic Algorithm with improved mutation and crossover steps. The convergence rate of GA in the case study is considered to be equal to 0.999. Then, based on the flowchart shown by Figure 9.2, the VVO engine primarily used the predicted load of Neural Network engine to optimize the network for targeted date offline. The capacitor switching operation considered in three load levels: low level (less than 70 % of the average load), mid-level (70% to 110% of the aver. load) and peak level (more than 110% of the average load). After finding the optimal configuration of Volt-VAR control devices by offline predictive VVO engine, the results of the optimization of a day-ahead algorithm was used on November 1, 2013 in order to test the performance of the predictive VVO. Table 12.24 compares the result of the study in following scenarios:

- Scenario-I: No VVO in the system (it is assumed that there is no Volt-VAR Optimization system exist in the grid)
- Scenario-II: Perform just offline (day-ahead) predictive VVO algorithm to optimize the system for targeted day. Here, only the offline parts of explained

flowchart (Figure 9.2) are working. The result of offline prediction will be implemented in targeted date without any changes.

- Scenario-III: Perform proposed predictive VVO algorithm to optimize system for targeted day: In this scenario, comprehensive proposed predictive engine shown in Figure 9.2 performs VVO in the system. In this proposed approach, the offline results have been updated with new collected data from smart meters.
- Scenario-IV: Ideal Case: it is assumed that ideal VVO could be efficiently performed using real data of smart meters of targeted date in real-time.

Table 12.24. BCIT North Campus Results in Different Scenarios

Scenario Number	Objective Function Value ($)	CVR Tap
Scenario-I: No VVO	474. 2441	0
Scenario-II: Offline VVO	440.9081	7
Scenario-III: Online Predictive VVO	438.9690	7
Scenario-IV: Ideal Case	438.9400	7

Figure 12.40 compares the results of load prediction for a sample node of the system (node-2). It compares three different scenarios: offline prediction (Scenario II), real measured (Scenario IV) and lives prediction (Scenario III).

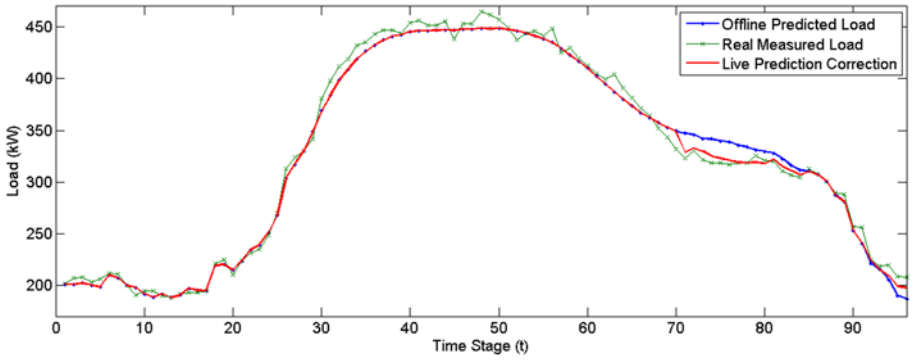

Figure 12.40. Offline Predicted load, real measured load and live predicted load for node-2

It is concluded that live prediction approach tried to fix offline prediction method and decreased prediction error. Moreover, it shows that the new updated prediction from Scenario III is more close to the real-time data collected from smart meters. Moreover, the convergence of VVO engine objective function is shown in Figure 12.41.

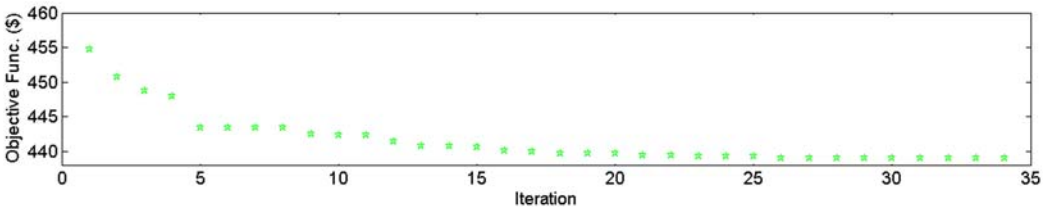

Figure 12.41. Objective Function value convergence in third scenario

Figure 12.42 compares total active power of Scenario II, Scenario-III and Scenario-IV for all nodes and Figure 12.43 gives the voltage of all nodes at each time stage in Scenario-III.

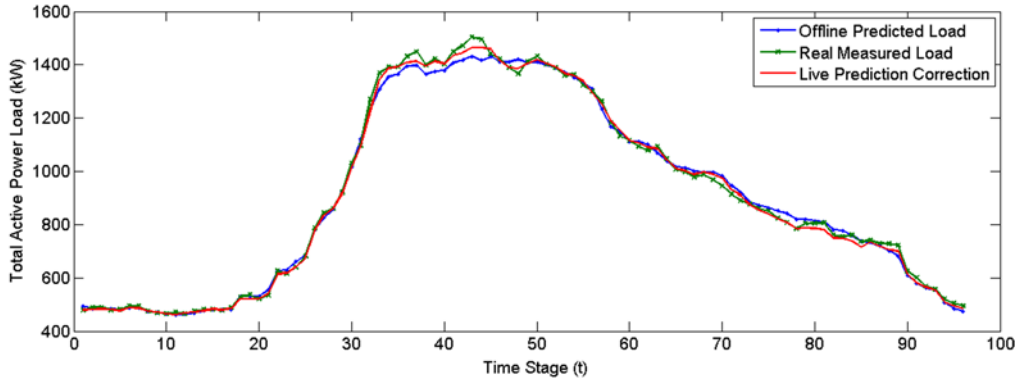

Figure 12.42. Total measured active power loads, total offline predicted active power loads and total live predicted active power load

As Figure 12.42 depicts, live prediction approach leads to less prediction error than offline prediction technique. Hence, this approach will bring more accuracy to the VVO Engine. Figure 12.43 shows that the CVR is also considered within VVO engine. Voltages of all nodes of the system are within lower limits of the ANSI band. The capacitor bank switching operation of nodes in time stages that is found by online predictive VVO is shown in Figure 12.44. This Figure shows the optimal amount and the optimal location of VAR injections found by VVO Engine that has to be injected by CBs in order to minimize distribution network loss. The loss cost at each time stage resulted from scenario-III is presented in Figure 12.45. This Figure compares the result of loss costs of the first and the third scenarios. As it is shown in Figure 12.45, and Table 12.24, the live predictive VVO engine served distribution network with more cost saving and loss reduction.

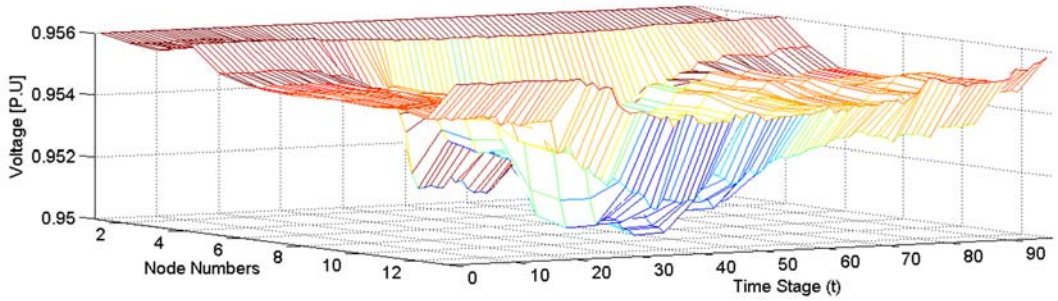

Figure 12.43. Node voltages for all nodes for all time stages in Scenario III by Live predictive VVO Engine

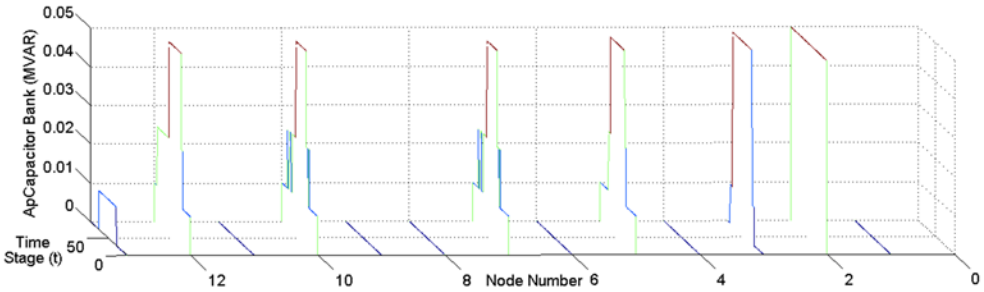

Figure 12.44. Capacitor Bank switching operations for all nodes for Scenario-III by Live Predictive VVO Engine

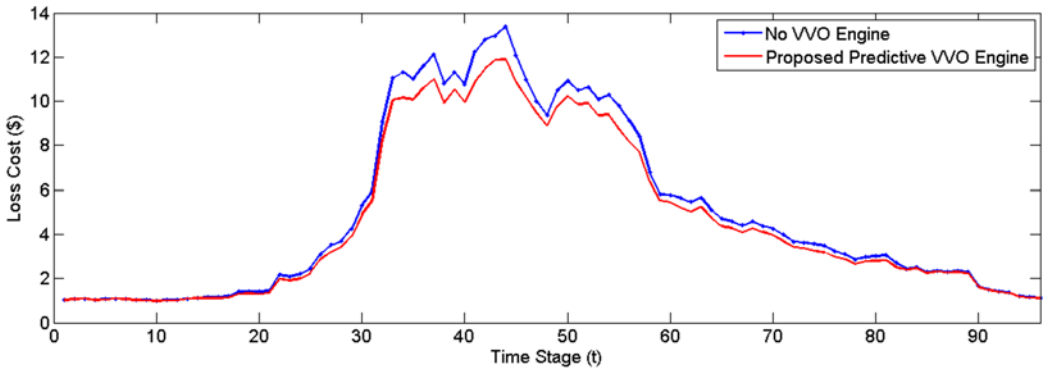

Figure 12.45. Comparison between Loss costs ($) resulted from Scenario-III (Live predictive VVO) and Loss costs resulted from Scenario-I (No VVO engine)

12.6.2. Result Analysis

As observed from Table 12.24, and from Figure 12.40 to Figure 12.45, the online predictive VVO algorithm was able to initially predict the active and reactive power loads of each node and then update the approach based on real-time measured data. Hence, it proposed an efficient optimized configuration for VVCC of distribution grid. As the BCIT

campus distribution grid is very strong in terms of voltage profile, the predictive VVO could be able to set the OLTC tap in an adequate position (base voltage of the tap position: 114.75 V) for all time stages. Moreover, comparing scenario-III with scenario-IV in Table 12.24 leads to a conclusion that the final results from VVO in scenario-III is very close to the results of an ideal case which is scenario-IV. Thus, the presented online predictive VVO in this study optimized BCIT campus distribution network efficiently and minimized distribution network loss and operating costs using this technique. Furthermore, this approach solved the number of tap or CB switching limitation issue by combining offline and online VVO engines that are working together.

It has to be noted that the accuracy of prediction techniques highly depends on the amount and the types of available historical data. As in this case study, smart meter data was available since 2009-2010, the prediction engine led to an acceptable approach. By development of smart meter installations in future smart distribution networks, more real time data could be collected for different distribution network studies such as VVO. Thus, presented approach in this study could be a great candidate for Volt-VAR Optimization solution of future distribution grids.

12.6.3. Conclusions

This study proposed a new real-time predictive VVO algorithm for smart distribution networks. The algorithm primarily predicted the active and reactive power loads of the next day based on downstream historical data received from local AMI and upstream global attributes received from DMS/SCADA. Then, it minimizes network loss cost and Capacitor Banks operating costs for the next day through an improved offline Genetic Algorithm. Then, it compared the result of predicted load with real-time data at each time stage. In cases that the error was not acceptable, new online VVO sliding window were activated in order to initially find the new optimal configuration of VVO assets based on VVO offline results and real-time data and then, update offline VVO results through an online prediction engine for time stages ahead. The results of the study on BCIT campus microgrid showed that the proposed predictive algorithm is capable of predicting the active/reactive power loads of the system very close to real values through a comprehensive training set and updating the prediction through sophisticated algorithm.

Then, the predictive VVO found the optimal configuration of CBs in the system at each time stage. Comparing the results of predictive VVO (Scenario-III) with an ideal case (Scenario-IV) elucidated the fact that proposed predicted algorithm in this study could yield to energy conservation and loss reduction of distribution networks very close to energy saving and loss reduction that can be obtained by real-time ideal VVO, even better than offline predictive VVO approach (Scenario II).

One of the main benefits of real-time predictive VVO presented in this study is its ability to solve the issue related to the limits placed on Capacitor banks and OLTCs/VRs to control the number of switching per day which adversely impacts their lifetime. Most real VVO strategies are still dealing with this issue. The reason lies in a fact that the limits on number of switching of CBs and/or OLTC/VR taps are defined by natural numbers in a day (not in real time). Hence, presented approach in this study is able to solve this issue in a way that the number of CB or/and OLTC/VR tap switching is/are within desired range(s). The existence of smart meter historical data could be one of the factors of success of the proposed approach. Hence, development and growth of smart meter installations in future distribution grids, could help proposed predictive approach to be more applicable and be as one of the great candidates for VVO scheme designs in near future.

12.7. A Novel Approach for Maintenance Scheduling of Volt-VAR Control Assets in Smart Distribution Networks

In this section, 33-node distribution network [254] is tested under different operating scenarios and/or conditions as a case study for Chapter 8 of this thesis. Moreover, the result of proposed AMI-based VVO with MSE is compared with other operating scenarios.

12.7.1. Case Study & Results

A distribution network with 33 nodes shown in Figure 12.46 is considered as test case. This network consists of a Medium Voltage (MV) substation with 132 kV/12.5 kV voltage levels. Medium voltage substation has an OLTC with 16 tap steps that can regulate

voltage level from +5 to -5 percent Per Units. There is a Voltage Regulator between node-13 and node-14 that is able to regulate voltage in 16 taps as well. Moreover, five different switchable shunt CBs are located respectively on node-7, node-14, node-25, node-30 and node-32. Each CB has 250 kVAR capacity and consists of five banks (each bank can inject 50 kVAR to the system). Here, (5-40), (5-47) to (5-51) uses for the objective function calculations of VVO problem and the constraints are (5-9) to (5-18) and (5-20) to (5-28).

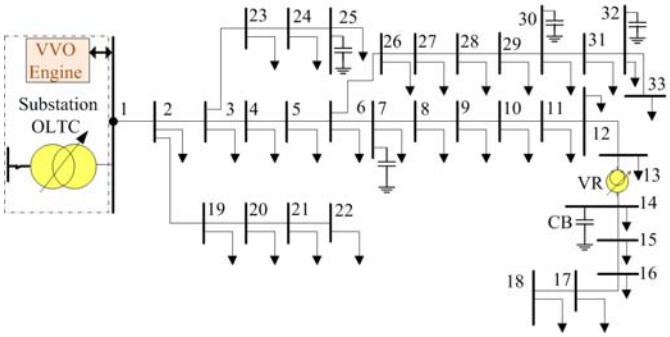

Figure 12.46. Single line diagram of 33-node distribution test feeder

Hence, Maintenance Scheduling Engine has to send seven different VVCCs (i.e. one OLTC, one VR and 5 CBs) to the maintenance according to (8-1) in different times of horizon year. For this reason, ERCOT historical load data [255] is used for load forecasting. The method employed for load forecasting in this study has been explained in section 12.5 of this chapter by the authors of this study. The only difference between the load forecasting of section 12.5 of this chapter and load forecasting of this study is that the load forecasting of MSE here is performed annually (not daily). MSE runs to provide the final maintenance strategy and/or solution for AMI-based VVO engine. The maintenance strategy results are expressed in Table 12.25. According to the results inTable 12.25, it is possible to assess the whole system in five different scenarios and/or maintenance times. In first scenario, it is assumed that the VVO problem is being solved without Maintenance Scheduling Engine. This scenario provides optimal operation of VVCCs without considering them going to maintenance. Thus, Maintenance Scheduling of VVCCs is still an issue in this scenario. In next step, MSE solves the maintenance scheduling problem and provide VVO with optimal periods that each of mentioned seven VVCCs should go to maintenance.

Table 12.25. Maintenance Scheduling Engine strategy results

Maintenance Order	Volt-VAR Control Component	Maintenance Date	Maintenance times stages	Maintenance Duration (hours)
1	VR	Wednesday 12/03/2014	4-39	9
2	CB-7, CB-14, CB-25	Monday 07/04/2014	1-24	6
3	OLTC	Monday 14/04/2014	1-48	12
4	CB-30, CB-32	Wednesday 14/05/2014	3-26	6

After solving maintenance scheduling problem by MSE, scenario-II and scenario-III investigate the impact of MSE on maintenance periods switchable shunt capacitors. Scenario-II looks at CB-7, CB-14 and CB-25. Scenario-III assesses CB-30 and CB-32. In scenario-IV, VR maintenance time is going to be shown and the last scenario tries to analyze OLTC Maintenance time through MSE main objective. Figure 12.47 illustrates 33-node distribution feeder losses for scenario-II (i.e. CB-7, CB-14 and CB-25 considered for maintenance) in three considered cases: (a) VVO without MSE, (b) VVO with MSE and (c) VVO interrupted by maintenance scheduling, i.e. VVO is totally separated from maintenance scheduling problem but MSE affect VVO performance. Table 12.26 represents the values of VVO and MSE objective functions in mentioned scenarios and cases. Hence, VVO has to be interrupted when a VVCC is under maintenance in third case. Table 12.27 gives the number of CBs, VR and OLTC switching during maintenance times in mentioned maintenance scenarios.

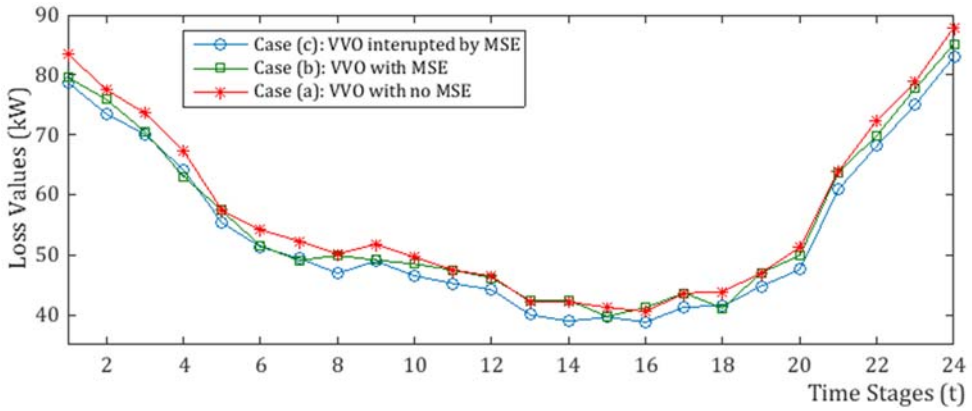

Figure 12.47. 33-node distribution feeder losses for scenario-II in three different operating cases

Table 12.26. VVO and Maintenance Scheduling Engine results in different operating scenarios

Volt-VAR Control Component	Operating Strategy	Objective Function ($)
CB-7, CB-14, CB-25	(a)	2092.181
	(b)	2105.770
	(c)	3858.448
CB-30, CB-32	(a)	2303.951
	(b)	2308.317
	(c)	4042.672
Voltage Regulator	(a)	3760.964
	(b)	3761.473
	(c)	6487.938
Tap Changer of Transformer	(a)	4045.555
	(b)	4100.573
	(c)	7823.130
Total Maintenance Results	(a)	12202.65
	(b)	12276.13
	(c)	22212.19

Moreover, Table 12.27 presents number of CBs, VR and OLTC Switching in different scenarios during maintenance times. In order to observe VR tap changes in fourth scenario and in order to see OLTC taps in fifth scenario, tap changes are investigated in abovementioned three cases shown respectively in Figure 12.48 and Figure 12.49.

Table 12.27. Number of CBs, VR/ OLTC Switching in different scenarios during maintenance times

Volt-VAR Control Component	Operating Strategy	Total Number of CB Switching	Total Number of VR Switching	Total Number of OLTC Switching
CB-7, CB-14, CB-25	VVOE without MSE	55	2	6
	VVOE With MSE	26	2	6
CB-30, CB-32	VVOE without MSE	39	5	8
	VVOE With MSE	29	5	8
Voltage Regulator	VVOE without MSE	52	3	7
	VVOE With MSE	47	0	4
Tap Changer of Transformer	VVOE without MSE	132	11	14
	VVOE With MSE	120	8	0

Figure 12.50 presents CB-7, CB-14 and CB-25 changes and Figure 12.51 gives bank changes of CB-30 and CB-32 in cases (a) and (b).

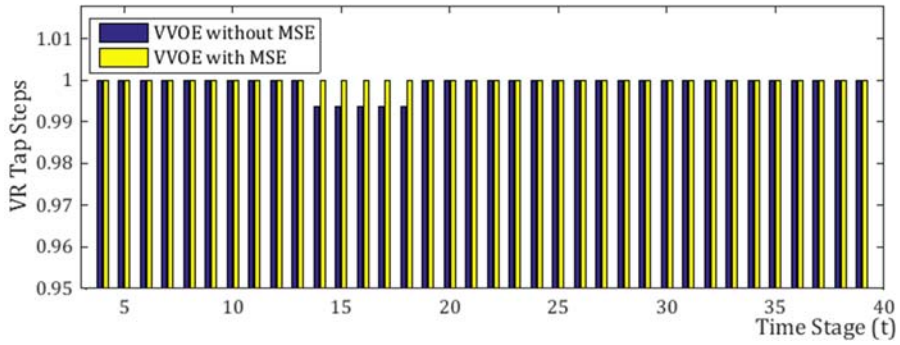

Figure 12.48. Voltage Regulator tap steps during maintenance time in two different cases

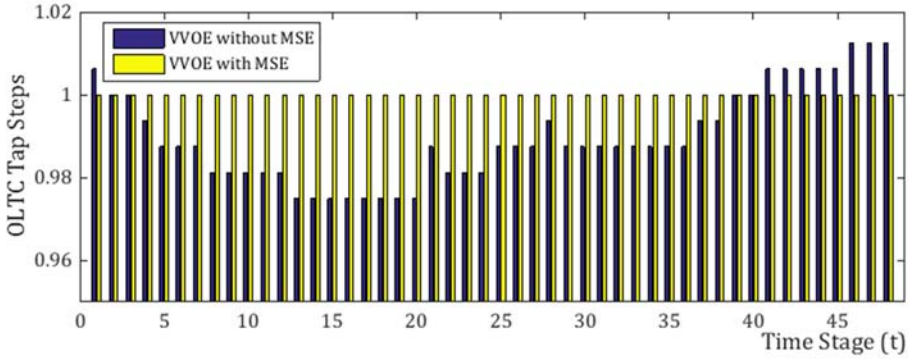

Figure 12.49. On-load tap changer steps during maintenance time in two different cases (VVO with/without MSE)

12.7.2. Result Analysis

The results of the study are shown in Figure 12.47 to Figure 12.51 and in Table 12.25 to Table 12.27. It is proved that the proposed solution for maintenance scheduling problem of VVCCs were able to solve both VVO and maintenance scheduling problems through a coordinated approach and had no negative impact on the performance of distribution network as well. Table 12.26 is given the fact that with fewest amount of lost benefit, it is possible to perform VVO without any interruption. The results showed that by utilizing MSE integrated with VVOE it is possible to save $9936.06 and prevent VVOE interruption (case (c)-case (b)). For different maintenance times, only $73.48 is needed for VVO with MSE strategy compared with pure VVO performance (case (2)-case (1)). In

other words, VVO with MSE approach results are very close to pure VVO as MSE found best maintenance time for horizon year.

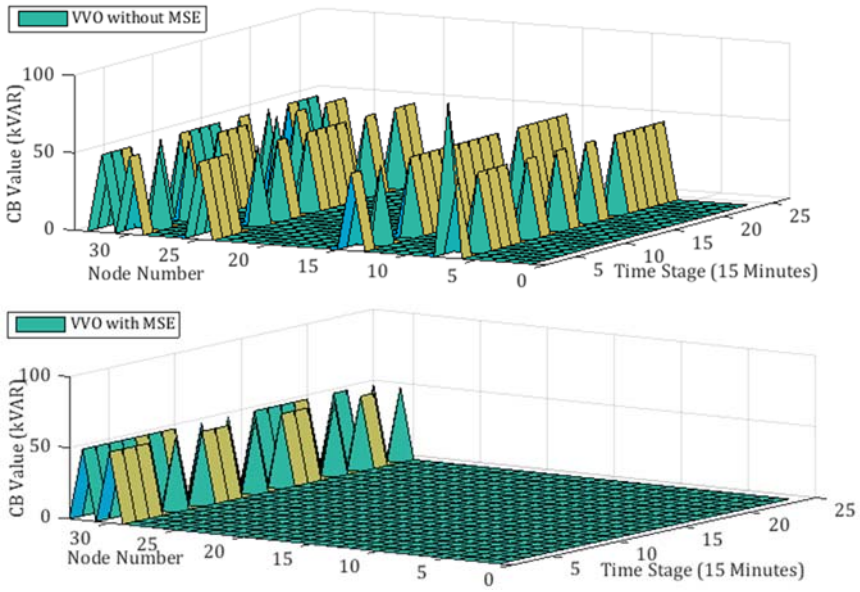

Figure 12.50. CB's amount and number of switching of Scenario-II in two operating cases (VVO with/without MSE)

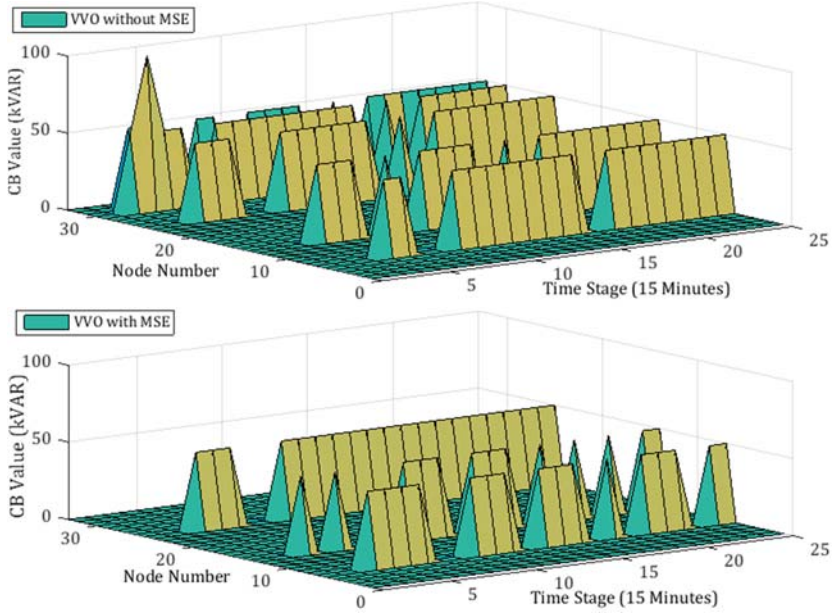

Figure 12.51. CB's amount and number of switching of Scenario-III in two operating cases (VVO with/without MSE)

Examining the initial results captured in Table 12.25, it can be concluded that MSE sent CBs to maintenance in periods of days that did not have high loads, i.e. fewest needs

for reactive power injection existed during those periods of days. Moreover, MSE did not send all CBs to maintenance in one day. This shows that there were periods of times in different days of the horizon year that could bring optimality. Additionally, Table 12.25, Figure 12.48 and Figure 12.49 are represented that the best days for OLTC/VR maintenances are days with less probable CVR operation (i.e. CVR value would be very few). These days need to have minimum tap switching numbers for VR and OLTC. Hence, it is necessary to predict the CVR values of the days of the horizon year through main MSE factors mentioned in Section 3 of this study. Table 12.27 proved the fact that VVO with MSE approach could minimize VVO objective function and respect VVCC optimal maintenance scheduling at a same time, with less number of bank and/or tap switching and very close to pure VVO scenario (i.e. when all VVCCs are available for VVO).

It is possible to observe in Figure 12.48 that MSE has found best date and time for VR to go to maintenance. This day of horizon year has lowest level of loads, and the maintenance time affected just 5 time stages (13 to 17). Regarding OLTC operation shown in Figure 12.49, it can be concluded that MSE put its lowest load profile of horizon year for OLTC maintenance. As OLTC maintenance time is very long (about 12 hours non-stop) compared with other existed VVCCs, and as OLTC is the most important voltage regulation asset of this feeder, it can be derived that OLTC maintenance affect VVO result more than other VVCCs. According to stated results, it can be concluded that the proposed approach of this study could solve maintenance scheduling of VVCCs in quasi real-time AMI-based VVOs effectively such that the performance and the efficiency of the VVO engine won't be affected. Moreover, it imposes minimum loss to distribution network operators and/or planners regarding unavailability of VVCCs when they are in maintenance.

12.7.3. Conclusion

This study proposed a novel approach for maintenance scheduling of Volt-VAR Control Components in quasi real-time AMI-based Volt-VAR Optimization of distribution networks by a coordinated command and control system between VVO Engine and MSE. As quasi real-time VVO solutions are going to be utilized more to minimize distribution network loss and increase energy conservation of termination points in near future,

applying a reliable Maintenance Scheduling Engine (explained in this study as MSE) in-line with recent smart grid VVO technologies (e.g. new AMI-based VVO solutions) as well as distribution network other requirements can help distribution network to be optimized more effectively. Hence, MSE of this study solved maintenance scheduling problem according to historical data such as previous year's loads, weighting factors, electricity price and/or value of loss minimization to find optimal maintenance periods for different types of Volt-VAR control assets within distribution network. In next step, VVO engine received MSE optimal results. Then, VVO engine regulated itself according to maintenance strategies sent by MSE. Thus, quasi real-time AMI-based VVO performed online without any interruption or interference caused by maintenance scheduling problem.

In order to verify the proposed approach’s efficiency and accuracy, 33-node distribution test feeder was applied and the results were investigated in five different scenarios and three different operating cases (VVO without MSE, VVO with MSE, VVO interrupted by maintenance scheduling problem). Result analysis shown that proposed MSE approach could find optimal maintenance periods within a horizon year in such a way that VVO engine would face with minimum losses during VVCC maintenance periods. Therefore, the best maintenance strategies according VVO engine and other main maintenance problem requirements could be found with proposed solution. As VVO objective function weighting factors have significant impact on maintenance scheduling problem, and as these weighting factors can also be affected by other maintenance factors such as value of loss minimization or the electricity price, optimal prediction of these factors in quasi real-time VVOs can be one of the further studies of future maintenance scheduling of VVCCs. In conclusion, this approach could be utilized as an "additive" part of existed AMI-based VVO solutions or as a part of future quasi real-time VVO techniques to lead future distribution networks to higher levels of optimality, accuracy and efficiency.

12.8. Smart Grid Adaptive Volt-VAR Optimization Engine utilizing Particle Swarm Optimization and Fuzzification

12.8.1. Case Study Simulation

In this section, 33-node distribution test feeder [254] is used for testing the correctness and the applicability of our proposed VVO engine. Figure 12.52 depicts single line diagram of the case study. The test feeder comprised of 33 nodes with 33 termination points (smart meters). The power was supplied from a HV/MV substation to a radial distribution network. Four different switchable shunt CBs located at node-1, node-7, node-23 and node-30 of the system. Capacitor banks range from 25 to 300 kVAR. Moreover, an OLTC located at HV/MV substation and a VR placed at node-13 both with 32 tap steps. Data of the case study active/reactive power loads at a specific time stage is shown in Table 12.28. This study primarily uses (5-29) as VVO objective function. It uses BFS for power flow ((5-53) to (5-56)). Moreover, the constraints used in this study are: (5-9) to (5-18), (5-20), (5-21), (5-23), (5-24), (5-26) and (5-27). When network operator intends to consider CVR and VR loss in VVO, (5-34) is used as the final VVO objective function. It is possible to give weighting factors to each VVO subparts. Each weighting factors can be found through Fuzzification technique explained in Chapter 10.4. An example of Fuzzification calculation can be found in (5-52).

PSO parameters such as the sum of acceleration constants is considered to be equal to four and the number of iteration steps is equal to 50. The VVO engine has been designed and programmed in MATLAB and distribution load flow performed by BFS with 100 sweeps. Maximum and minimum desired apparent power losses ($S_{LOSS,max}, S_{LOSS,min}$), considered 0.35 P.U and 0.1 P.U respectively by the operator. Furthermore, Maximum and minimum desired voltage deviations, ($V_{dev.min}, V_{dev.max}$) are equal to 10 and 0.1. For maximum and minimum CVR values, 0.01 and 0.001 are respectively determined and for VR loss, maximum and minimum settings are 0.05 and 0.005 P.U. For scenarios with weighting factors, loss cost are defined based on electricity price (0.12 $/kWh). Voltage deviation cost assumed to be eight times more than loss cost. Moreover, CVR and VR loss costs assumed to be ten times more than voltage deviation cost according to distribution network operator needs.

Table 12.28. 33-Node Distribution Feeder Load Data

Node No.	Active Power (kW)	Reactive Power (kVAR)	Node No.	Active Power (kW)	Reactive Power (kVAR)
1	100	60	17	60	20
2	100	60	18	90	40
3	90	40	19	90	40
4	120	80	20	90	40
5	60	30	21	90	40
6	60	20	22	90	40
7	200	100	23	90	50
8	200	100	24	420	200
9	60	20	25	420	200
10	60	20	26	60	25
11	45	30	27	60	25
12	60	35	28	60	20
13	60	35	29	120	70
14	120	80	30	200	100
15	60	10	31	150	70
16	60	20	32	210	100
			33	60	40

12.8.2. Operating Scenarios

In order to investigate the impacts of different VVO objective function sub-parts, six operating scenarios are presented in this sub-section:

- Scenario-1: VVO performs without weighting factor calculations and without CB operating cost minimization
- Scenario-2: VVO performs without weighting factor calculation but with CB operating cost minimization
- Scenario-3: VVO performs with weighting factor calculations through Fuzzification but without CB operating cost minimization
- Scenario-4: VVO performs with weighting factor calculations through Fuzzification and with CB operating cost minimization
- Scenario-5: CVR and VR loss minimization added to VVO. VVO performs without weighting factor calculations
- Scenario-6: CVR and VR loss minimization added to VVO. VVO performs with weighting factor calculations using Fuzzification.

12.8.3. Case Study Results

The result of the VVO engine presented in this study for all mentioned operating scenarios are given in Table 12.29. Furthermore, weighting factors obtained by Fuzzification for different scenarios are shown in Table 12.30. Distribution feeder node voltages for different operating scenarios (Scenario-2, 4, 5 and 6) are presented in Figure 12.53. Figure 12.54 represents the kVAR of shunt CBs and Figure 12.55 depicts LTC and VR tap positions in all operating scenarios under study found by VVO engine. Figure 12.56 illustrates apparent power loss of Scenario-6 compare with a blind system, i.e. without VVO. Figure 12.57 demonstrates VVO engine PSO convergence for Scenario-6 as well. This study uses PSO to check if stochastic optimization approaches such as PSO can help Volt-VAR Optimization to reach to more optimal solutions or not.

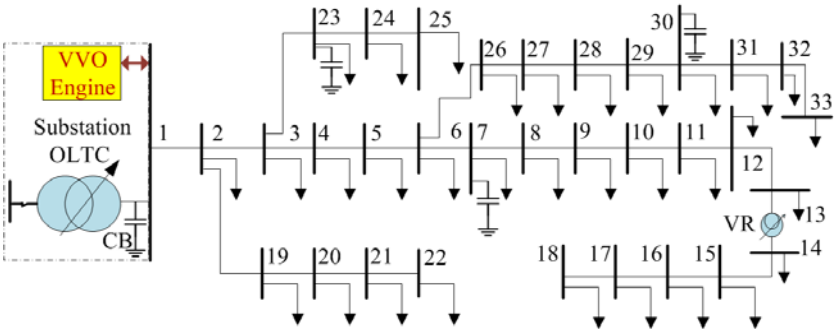

Figure 12.52. 33-node distribution feeder single line diagram

Table 12.29. Volt-VAR Optimization Results using PSO Algorithm

VVO Scenario	Apparent Power Loss (kVA)	Active Power Loss (kW)	Voltage Deviation ($\Delta \mathbf{V}$)	Objective Function ($)	Total Saving for a Complete Day ($)
No VVO	20.2265	15.6866	1.8474	-	-
Scenario-1	14.1939	13.2431	1.4476	853.4503	22.86182
Scenario-2	14.3683	13.4299	1.5165	927.9982	29.73072
Scenario-3	14.0207	13.0563	1.5146	211.5827	23.63392
Scenario-4	15.4120	14.2103	1.2797	158.6865	30.57404
Scenario-5	14.6154	13.6419	2.2060	66.7896	27.45708
Scenario-6	15.4341	14.2822	2.2004	106.7026	31.41320

Table 12.30. Weighting Factors from PSO in Different VVO Scenarios

Weighting Factor	Scenario-2	Scenario-4	Scenario-6
α	0.5366	0.5366	0.3493
β	1	1	0.2363
γ	-	0.1650	1
δ	-	-	1

12.8.4. Result Analysis

As seen in Table 12.29, VVO could optimize distribution networks effectively in all considered operating scenarios. Comparing Scenario-1 and Scenario-2, it can be concluded that by adding CB operating cost minimization sub-part in VVO objective function, VVO could produce new optimal results (which is less than previous optimal value) with less kVAR injected into the system to save CB operating cost.

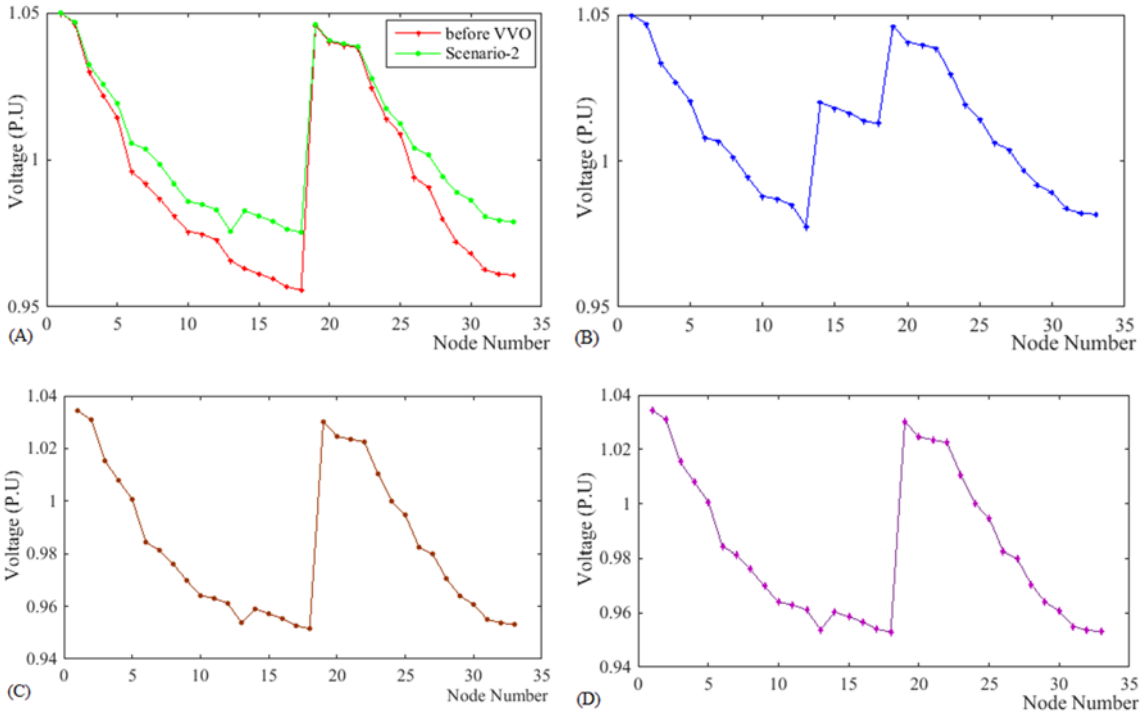

Figure 12.53. Node voltages of distribution feeder in different operating scenarios (A: Scenario-2, B: Scenario-4, C: Scenario-5 and D: Scenario-6)

Comparing Scenario-1 and Scenario-3, as well as comparing Scenario-2 and Scenario-4, shown inTable 12.29, Figure 12.53 to Figure 12.55, it can be shown that the operator could lead VVO algorithm to its desired operating needs through Fuzzification.

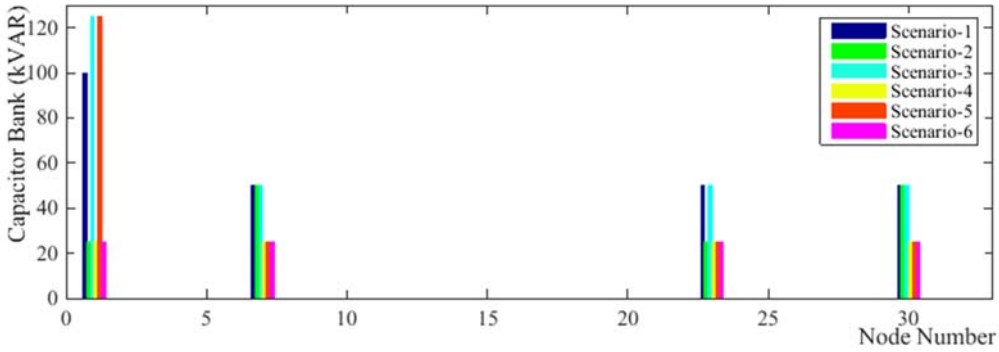

Figure 12.54. Values of shunt CBs in different operating scenarios achieved by proposed VVO engine

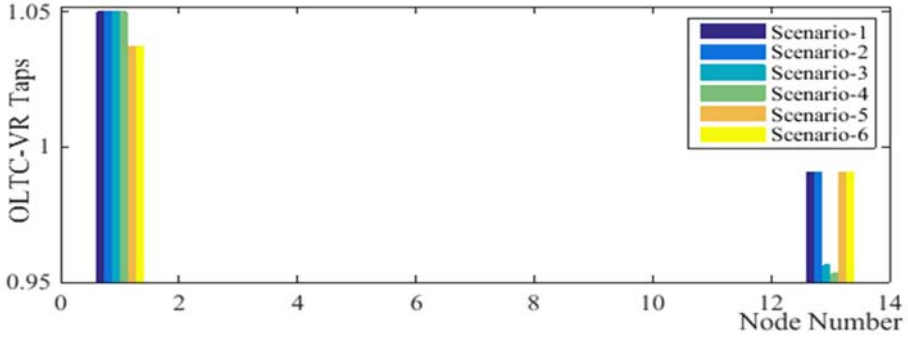

Figure 12.55. Tap position of LTC and VRs in different operating scenarios achieved by VVO engine

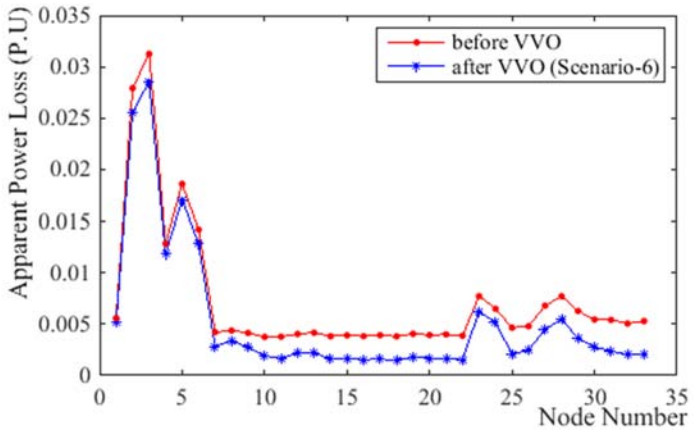

Figure 12.56. Apparent power loss in Scenario-6

For instance, weighting factors obtained by Fuzzification based on operating pre-set values in Scenario-4 (compared with Scenario-2) caused VR to be in lower tap to increase voltage as voltage deviation had more weight in Scenario-4.

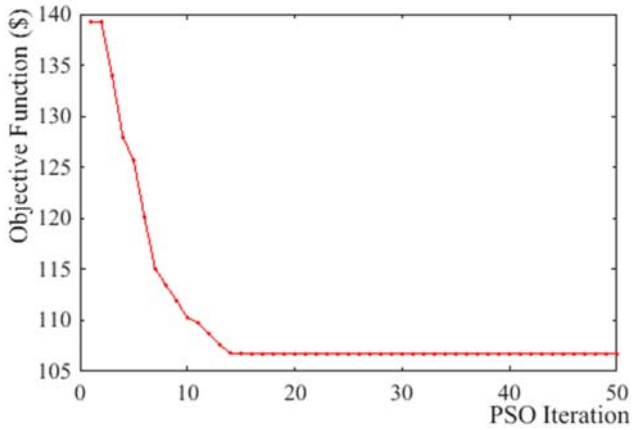

Figure 12.57. VVO engine PSO convergence in Scenario-6

In other words, voltage deviation in Scenario-4 was more important for the operator than voltage deviation in Scenario-2. By comparing Scenario-5 with Scenario-6, it is conceivable to conclude that VVO enabled CVR had pushed the last voltages of feeder nodes to lower limits of ANSI range, i.e. 0.95 P.U. On the other hand, the operator could push the VVO engine to a more applicable optimal solution in Scenario-6 due to feeder needs through defining pre-set values and by Fuzzification technique performed within the VVO engine. It has to be stated that as pre-set and cost values for Fuzzification are defined by the operator, different optimal configurations might be provided by the VVO engine according to the system levels of operation and requirement. Therefore, the proposed VVO engine optimized distribution feeder effectively in all herein discussed operating scenarios. Moreover, it defined fuzzy factors according to system operating condition and operator desirable values through Fuzzification technique and sent Volt-VAR control commands to VVCCs to update distribution feeder configuration with new optimal settings.

12.8.5. Conclusion

This study proposed a smart grid adaptive Volt-VAR Optimization engine using Particle Swarm Optimization algorithm. In order to determine weighting factor of each VVO objective function sub-parts, Fuzzification technique is used within the algorithm and six

different operating scenarios compared with each other in a sample 33-node distribution feeder to test the accuracy and the applicability of the proposed approach. Initial objective function, without CB operating cost minimization, was considered in the first operating scenario. Then, in the second operating scenario, CB operating cost minimization was added as a VVO objective function sub-part to the system that led to saving the operating cost of CBs through less CB kVAR injection. In the 3rd scenario, weighting factors was obtained by Fuzzification technique without considering the impact of CB operating cost minimization. Moreover, scenario-4 included this VVO objective function sub-part. CVR and VR loss minimization were added to the VVO objective function in the 5th operating scenario that made the optimization problem more complicated. Scenario-6 showed that by presenting pre-set values for Fuzzification technique, PSO would be able to appropriately optimize the distribution grid even in the presence of conflicting sub-parts in VVO objective.

Therefore, the results showed that by using the proposed VVO engine using PSO and Fuzzification, operators could lead distribution grids to higher level of optimization with regard to distribution network technical/economic needs. Employing Neural Network-Fuzzy as well as predictive-PSO approaches may assist VVO engine to be predictive and perform dynamically in each operating time stage. This could be one of the future works that might help in designing a more efficient smart grid based VVO engine for distribution networks. As a result, the approach presented in this study could be a great sample for smart grid adaptive VVO techniques which may emerge in the future that could facilitate the possibility of a well-matched optimization engine to be able to cover most future distribution network technical/economic operational needs.

12.9. Quasi Real-Time ZIP Load Modeling for Conservation Voltage Reduction of Smart Distribution Networks using Disaggregated AMI Data

This section investigates quasi real-time ZIP load models for CVR sub-part of new quasi real-time AMI-based VVO solution using historical disaggregated data.

12.9.1. ZIP Load Model for Conservation Voltage Reduction

As stated before, one of the most famed and most accurate techniques applied for load modeling in CVR studies is ZIP load model. As load model is not fully constant power, CVR can be performed to conserve energy at customer's premises. In order to determine the impact of each load model, it would be necessary to primarily study each of them:

- Constant Power (P): In constant-P loads demand would be constant regardless of voltage. Hence, if the load is fully constant power, by decreasing voltage network loss will increase. In this scenario, CVR will not lead to energy conservation but rather increases the power loss of the grid, and therefore has negative impact on VVO engine sub-parts. Some Examples of constant-P loads are incandescent light, resistive water heater, stovetop, oven, etc.
- Constant Impedance (Z): Here, the demand would be proportional to voltage squared. Thus, by maintaining voltage within lower limits of ANSI band, network loss would slightly be increased by CVR sub-part, although VVO engine would be able to mitigate the impact and conserve energy. Some important Constant-Z loads are electric motors, heat pumps, air conditioner, etc.
- Constant Current (I): Here, demand would be proportional to voltage. Therefore, by reducing voltage level, CVR sub-part could conserve energy. Losses could even be decreased slightly. There are few constant-I devices such as welding units, smelting, florescent, some power electronics, etc.

This study uses (5-40), (5-47) to (5-52) as its objective function equations. The constraints are as same as previous study. Different combination of the abovementioned loads can be observed in different times of a day in a residential building. It is possible to obtain active and reactive consumption of loads through equations of (5-42) and (5-43).

Moreover, changes in energy consumption (ΔE) as well as voltage reduction (ΔV) can be found by (5-44) and (5-45). By dividing (5-44) and (5-45) CVR Factor (CVR_f) is gained which presents the ratio of energy consumption and voltage reduction (5-46). Typically, CVR factor is between 0.5 and 1.5 [64]. Further studies such as EPRI in 2010 showed CVR Factor close to 0.8 [256]. Here, E_{base} and V_{base} are initial energy and voltage respectively. Then, E_{CVR} and V_{CVR} are system's energy and voltage after CVR. Due to the fact that the type, amount and duration of consumption vary throughout different times of a day, it is conceivable to define specific ZIP coefficients for each quasi real-time stage ($Z_{p-ele,i}$, $I_{p-ele,i}$, $P_{p-ele,i}$ for active power and $Z_{q-ele,i}$, $I_{q-ele,i}$, $P_{q-ele,i}$ for reactive power) that could be shown by (12-1) and (12-2).

$$P_t = \sum_{i=1}^{i=I} (P_{0-\,ele,i,t} \times (Z_{p-ele,i}(\frac{V}{V_0})^2 + I_{p-ele,i}(\frac{V}{V_0}) + P_{p-ele,i})) = \sum_{i=1}^{I} P_{ele,i} \qquad (12\text{-}1)$$

$$Q_t = \sum_{i=1}^{i=I} (Q_{0-\,ele,i,t} \times (Z_{q-ele,i}(\frac{V}{V_0})^2 + I_{q-ele,i}(\frac{V}{V_0}) + P_{q-ele,i})) = \sum_{i=1}^{I} Q_{ele,i} \qquad (12\text{-}2)$$

Here, $P_t$and $Q_t$are active and reactive power of each quasi real-time stage. Moreover, $P_{0-\,ele,i,t}$ and $Q_{0-\,ele,i,t}$are initial active and reactive powers of each element at time stage-*t* that can be obtained as follows:

$$P_{0-ele,i,t} = \frac{APCR_{ele}}{\sum APCR} \times P_{o,t} \qquad (12\text{-}3)$$

$$Q_{0-ele,i,t} = \frac{RPCR_{ele}}{\sum RPCR} \times Q_{o,t} \qquad (12\text{-}4)$$

Where, eledenotes element (i.e. appliance), $APCR$is Active Power Consumption Ratio and $RPCR$is Reactive Power Consumption Ratio. In order to reach an adequate approximation of ZIP coefficient for each quasi real-time stage, it would be necessary to define type of loads, amount and style of their consumptions in detail for each appliance in a typical North American residential house.

12.9.2. Load Disaggregation for Quasi Real-Time ZIP Coefficients

In order to find ZIP coefficients and model system loads accurately in quasi real-time, the following steps are respected in this study:

- Determining common home appliances for the study
- Determining type of appliances
- Approximate calculation of each appliance usage time and operating period
- Defining the impact factor of each appliance on VVO problem according to its energy consumption

Accordingly, Table 12.31 represents typical appliance type, items and impact factors exerted in this study. Impact factor percentage defines as the percentage of consumption of an appliance item in a day compared with another appliance in same appliance category. Knowing the impact factor could lead to a more accurate approximation of ZIP of each appliance category. Hence, it is a totally different concept compared with CVR Factor. The impact factor percentages of Table 12.31 have been determined according to the consumption amount of each item within its category for a typical North American residential house. These impact factors are obtained based on consumption amount and time of usage of each item. As can be illustrated from Table 12.31, most conventional appliances of a residential building are considered in this study. Assessing statistical and historical data [257]-[266], total active and reactive ZIP coefficients for each considered appliance shown in Table 12.31 are given in Table 12.32.

Table 12.31. Appliance classification for quasi real-time VVO study of this study

Appliance Name	Items Included:	Impact Factor (%)
Lighting	Incandescent Lights , LED Lamps, CFL Bulbs	45,10,45
Cooking Appliances	Oven and Microwave	80, 20
Home Entertainment	LCD TV, Laptop Charger, Game Console, PC	45,10,15,30
Air Conditioner	Window/Wall mounted Air Conditioner	100
Dish Washer	Conventional Standard Dish Washer	100
Dryer	Clothes Drier (35 loads per month)	100
Washing Machine	Top Load Washing Machine	100
Fridge	Standard Refrigerator	100
Freezer	Deep Chest Freezer	100
Water Heater	Mid-Efficiency	100
Other appliances	Vacuum, Fan, Coffee Maker	35.17, 6.7, 58.12

Now, using daily forecasted load profile and through statistical data [257]-[266], the time and duration of operation, as well as the active power consumption of each appliance is obtained. These are shown in Figure 12.58. Voltage dependency of several typical domestic loads has been given in [258]. Table-6 and Table-7 in [259] presented equipment contribution weight and active/ reactive ZIP model for different residential classes. ZIP model parameters of several tested appliances represented by [260]. To find ZIP load model entertainment section, this study extracted ZIP coefficients from [261]. To assess electricity home appliance consumption, [262] and [263] used in this study. Hourly load

profile of residential load in different operating conditions can be found in [262]. The percentage of usage of different types of loads within a day acquired from [265]. Load data analysis accomplished by [266] is the basis of the study in this study. Normalized hourly load profiles of different load types in a typical residential home used to categorize home appliances into different load types.

Table 12.32. ZIP Coefficients of different appliances in this study [257]-[266]

Item Number	Appliance Name	Z_p	I_p	P_p	Z_q	I_q	P_q
1	Lighting	0.634	-0.067	0.433	0.8125	-0.278	0.4655
2	Cooking Appliances	0.738	0.928	0.096	13.304	-22.192	10.488
3	Home Entertainment	-0.013	0.068	0.945	0.788	-0.6095	0.8215
4	Air Conditioner	1.17	-1.83	1.66	15.68	-27.15	12.47
5	Dish Washer	1	0	0	1	0	0
6	Dryer	1.02	0	-0.02	1.02	0	-0.02
7	Washing Machine	0.5	0	0.5	0.5	0	0.5
8	Fridge	5.03	-8.48	4.45	17.44	-28.62	12.18
9	Freezer	5.03	-8.48	4.45	17.44	-28.62	12.18
10	Water Heater	0.92	0.1	-0.02	0.15	0.86	-0.01
11	Other appliances	10.98	-16.86	8.88	35.03	-56.38	24.35

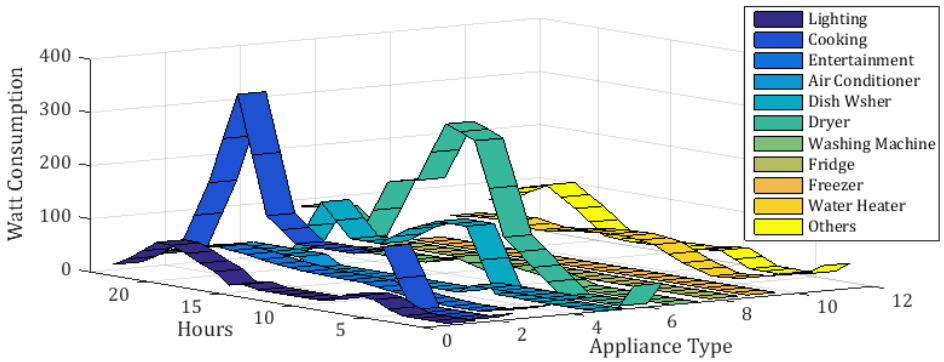

Figure 12.58. Active Power consumptions of different appliances every four quasi real-time stage.

Table 12.33. Consumption factors of different appliances every four quasi real-time stage

Time Stage	Item #1	Item #2	Item #3	Item #4	Item #5	Item #6	Item #7	Item #8	Item #9	Item #10	Item #11

1	0.0202	0.0542	0.101	0.1397	0.0059	0.21	0	0.0249	0.027	0.1828	0.2347
2	0.0361	0	0.1017	0.2493	0	0	0	0.0435	0.048	0.274	0.2476
3	0.0427	0	0.0624	0.295	0	0	0	0.0502	0.057	0.251	0.242
4	0.052	0	0.0109	0.3593	0	0	0	0.0596	0.069	0.2165	0.2327
5	0.1451	0	0.0051	0.3344	0	0	0	0.0526	0.066	0.166	0.231
6	0.2667	0	0.0045	0.295	0	0	0	0.0452	0.059	0.1255	0.2038
7	0.1426	0.2737	0.0106	0.1408	0.006	0.1123	0	0.0216	0.028	0.0998	0.1642
8	0.0909	0.391	0.0152	0.0419	0.0043	0.1605	0	0.0154	0.02	0.0998	0.1607
9	0.0313	0.275	0.0202	0.0327	0.1704	0.195	0.02	0.0124	0.016	0.1115	0.1154
10	0.0172	0.1974	0.023	0.0265	0.2698	0.2082	0.033	0.0105	0.013	0.1193	0.0822
11	0.0141	0.1615	0.0259	0.0216	0.2207	0.3314	0.034	0.0088	0.01	0.1049	0.0673
12	0.012	0.1376	0.0281	0.0184	0.1881	0.4157	0.035	0.0079	0.008	0.0941	0.0554
13	0.0122	0.1395	0.0291	0.0187	0.1716	0.4413	0.023	0.008	0.008	0.0938	0.0542
14	0.0124	0.142	0.0303	0.019	0.1552	0.4654	0.012	0.0084	0.008	0.0939	0.0532
15	0.023	0.1902	0.034	0.0204	0.1352	0.399	0.025	0.0092	0.009	0.0954	0.0592
16	0.0146	0.2511	0.039	0.0224	0.1144	0.3292	0.042	0.0103	0.01	0.0973	0.0697
17	0.0433	0.3658	0.0349	0.0178	0.0909	0.254	0.019	0.0084	0.008	0.0713	0.0868
18	0.0507	0.4476	0.0326	0.015	0.0765	0.2041	0.004	0.0072	0.007	0.0561	0.0994
19	0.074	0.3634	0.0412	0.039	0.1242	0.1416	0.004	0.0076	0.007	0.0663	0.1312
20	0.0993	0.271	0.0533	0.0436	0.1852	0.0695	0.005	0.0083	0.008	0.0819	0.175
21	0.1183	0.1987	0.0672	0.0511	0.1282	0.1269	0.005	0.0098	0.01	0.0924	0.1921
22	0.1039	0.1016	0.0917	0.0653	0.05	0.2142	0.007	0.0125	0.013	0.1158	0.2256
23	0.0688	0.0905	0.095	0.0776	0.0297	0.2477	0.004	0.0145	0.015	0.1293	0.2279
24	0.034	0.0731	0.098	0.094	0.004	0.2917	0	0.0172	0.018	0.1467	0.2233

This study used operating factors of [266] to find hourly consumption of each appliance separately. By dividing hourly consumption of each appliance from total hourly consumption of all appliances, hourly consumption factors of each appliance can be found using (12-3) and (12-4). Multiplying obtained time-stage consumption factors by ZIP coefficient of each appliance, ZIP of that time-stage can be found. Explained method can be written as (12-5). Therefore, Table 12.34 presents active and reactive power ZIP coefficients for each four quasi real-time stage (hourly).

$$ZIP_{P.q,t} = \sum_{ele=1} (Consumption\ Factor_{p,q,ele,t} \times ZIP_{p,q,ele,t}) \quad (12\text{-}5)$$

Table 12.34. Active and Reactive Power ZIP coefficients of different appliances every four quasi real-time stage

Time Stage	$Z_{p,t}$	$I_{p,t}$	$P_{p,t}$	$Z_{q,t}$	$I_{q,t}$	$P_{q,t}$
1	2.2769	-3.0293	1.7523	9.8687	-15.901	7.0322
2	2.5037	-3.5939	2.0902	11.140	-18.202	8.0622
3	2.5588	-3.7063	2.1475	11.842	-19.432	8.5902
4	2.6303	-3.8575	2.2271	12.784	-21.087	9.3029
5	2.5773	-3.7645	2.1872	11.730	-19.243	8.5129
6	2.4106	-3.458	2.0474	10.315	-16.785	7.4699
7	1.7718	-2.0780	1.3062	9.5685	-15.433	6.8643
8	1.6048	-1.6801	1.0753	9.1615	-14.639	6.4774
9	1.4938	-1.3738	0.8800	4.7573	-6.8040	3.0466
10	1.3810	-1.0929	0.7119	3.2346	-4.1066	1.8720
11	1.3187	-0.9319	0.6132	3.0661	-3.8282	1.7621
12	1.2629	-0.7942	0.5313	2.8909	-3.5360	1.6451
13	1.2586	-0.7789	0.5202	3.0815	-3.8478	1.7663
14	1.2556	-0.7669	0.5113	3.3269	-4.2501	1.9231
15	1.2363	-0.7929	0.5565	3.5111	-4.6547	2.1435
16	1.2384	-0.859	0.6206	3.825	-5.2854	2.4604
17	1.2245	-0.8876	0.6631	4.8384	-7.0429	3.2045
18	1.2212	-0.9116	0.6904	5.7595	-8.6376	3.8781
19	1.4346	-1.3446	0.9099	5.5351	-8.2132	3.6782
20	1.7040	-1.8727	1.1687	5.2584	-7.6875	3.4291
21	1.8453	-2.1541	1.3088	5.9172	-8.8800	3.9628
22	2.0919	-2.6368	1.5449	7.3052	-11.365	5.0597
23	2.1339	-2.7121	1.5782	8.0885	-12.744	5.6551
24	2.1633	-2.7618	1.5985	9.1788	-14.669	6.4900

This method is used to achieve ZIP coefficients for all 96 time stages in a day (i.e. for every 15 minutes). It has to be mentioned that the coefficients found here cannot fully show the exact load model in reality as many uncertainties, such as human factors or approximations such as the time and duration of usage, can affect load model coefficients. However, it is possible to state that quasi real-time load modeling could lead to more accurate VVO as its ZIP coefficients are changing in-line with VVO time stages compared to previous fixed load modeling where ZIP coefficients were considered constant throughout different operating time stages. The next section studies the performance of

modeled ZIPs for quasi real-time stages in an AMI-based VVO using 33-node distribution feeder.

12.9.3. Case Study and Result Analysis

A 33-node distribution feeder is employed to validate presented quasi real-time load model compared with conventional load models in this section. As seen in Figure 12.46, 33-node distribution network consists of one feeder with one OLTC with 16 tap steps on its medium voltage substation, a VR located between bus-13 and bus-14 and five 250 kVAR switchable shunt CBs located at bus-7, bus-14, bus-25, bus-30 and bus-32. Each CB has five 50 kVAR banks. As the aim of this study is to find quasi real-time ZIP models for a typical North American consumer, the case study is used typical residential houses for all consumers of 33-node distribution feeder.

Here, VVO engine optimizes distribution feeder through seven different Volt-VAR control components according to objectives and constraints. This grid is tested for a typical day in summer time in 96 quasi real-time stages (every 15 minutes). For each 15 minutes, AMI-based VVO optimizes distribution network by data captured from local AMI and load model presented in this study, and sends optimal control strategies to each Volt-VAR control component of the system. Figure 12.59 illustrates total loads of the case study in different quasi real-time stages of studied day. Table 12.35 compares the result of the objective function and energy conservation by CVR with two other conventional operating scenarios:

- Scenario-I: Offline VVO, when VVO is not performing in quasi real-time
- Scenario-II: VVO with constant ZIP coefficient, when only one ZIP set is used for all VVO time stages

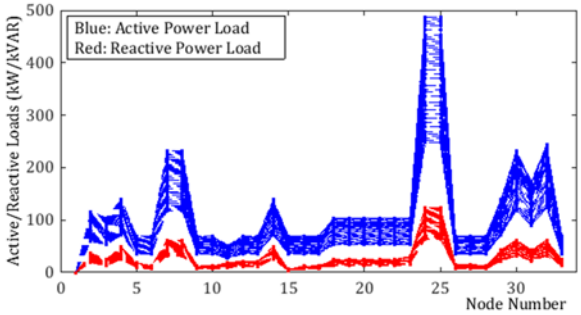

Figure 12.59. Active and reactive power load variations in different quasi real-time stages

Table 12.35. Initial results of VVO engine in comparison with Scenario-I and Scenario-II

VVO Engine Results	Scenario-I	Scenario-II	This Study
Objective Function ($)	29857.51	28727.23	28138.57
Time Stage Energy (kWh)	14995.22	14483.97	14227.94
Energy Conservation (%)	-	3.4095	5.1168
Power Loss (kW)	-	13103.15	12642.76
Voltage Reduction for Peak (Time stage-60 to time stage-85 in %)	-	1.3209	1.7363

Fuzzification technique is used in order to find accurate weighting factors ($\alpha, \beta, \gamma, \delta$ & ε) of each VVO objective sub-parts of this study. For instance, in order to find the weighting factor of VVO loss-sub-part:

$$C_{loss,b,t} = P_{loss,b,t} \times \pi_t \tag{12-6}$$

Here, $P_{loss,b,t}$ is loss of branch-b at time stage-t (kW) and $\pi_t$is the value of loss ($/kW) which gives $C_{loss,b,t}$ that is loss cost of branch-b at time stage-t ($). The Fuzzification loop within VVO algorithm for loss sub-part is as follows:

$$\begin{gathered} If\, C_{loss,b,t} \le C_{loss-min,b,t} \quad \alpha = 1 \\ Else\ if \quad C_{loss,b,t} > C_{loss-min,b,t} \;\&\&\; C_{loss,b,t} < C_{loss-max,b,t} \\ \alpha = \frac{\left|C_{loss,b,t} - C_{loss-min,b,t}\right|}{C_{loss-max,b,t} - C_{loss-min,b,t}} \\ else \quad \alpha = 0, \quad end \end{gathered} \tag{12-7}$$

This loop explains that weighting factor α will be equal to 0 when loss cost is more than maximum cost that grid operator intends to spend. This factor is equal to one when it is less than minim cost determined by grid operator and it is between 0 and 1 while loss cost is between minimum and maximum loss costs of the grid. Respectively, other weighting factors obtained for other sub-parts of VVO according to operating costs of VVCCs, and the value of saved energy. Figure 12.60 compares loss values and Figure

12.61 compares the value of consumed energy found by VVO engine of this study (with quasi real-time load model) with Scenario-I and Scenario-II.

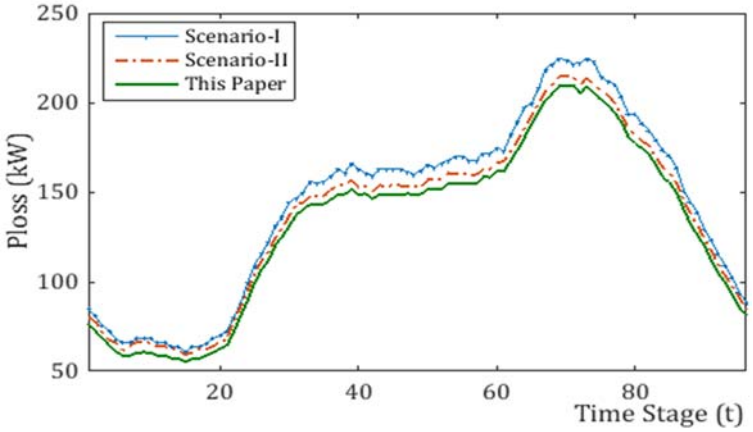

Figure 12.60. Active power loss values for different quasi real-time stages in different operating scenarios

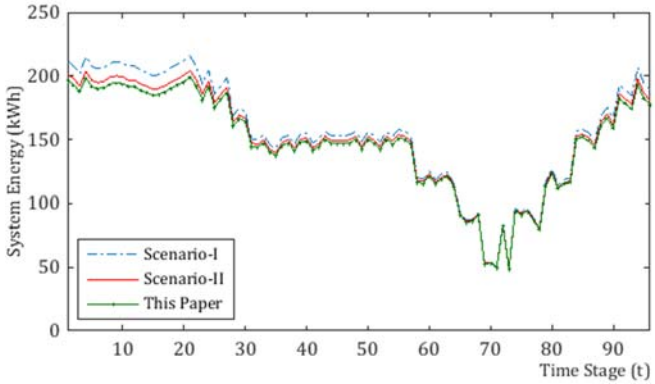

Figure 12.61. Energy consumption values for different quasi real-time stages in different operating scenarios

As seen from Table 12.35, Figure 12.60 and Figure 12.61, the CVR and the objective function results are very close to each other in this study and Scenario-II but as presented load modeling is more accurate, it finds better solutions and obtains deeper results for CVR. In other words, VVO engine performs better by quasi real-time models presented in this study rather than Scenario-II. It also led to better accuracy on computation of total conserved energy. It is possible to conclude that the approach presented in this study would give quasi real-time VVO engines opportunity to operate profoundly due to more detailed inputs that are given to the engine. The results of the objective function of the case study are shown in Figure 12.62. It can be observed that the objective function values were minimized at each and every quasi real-time stage.

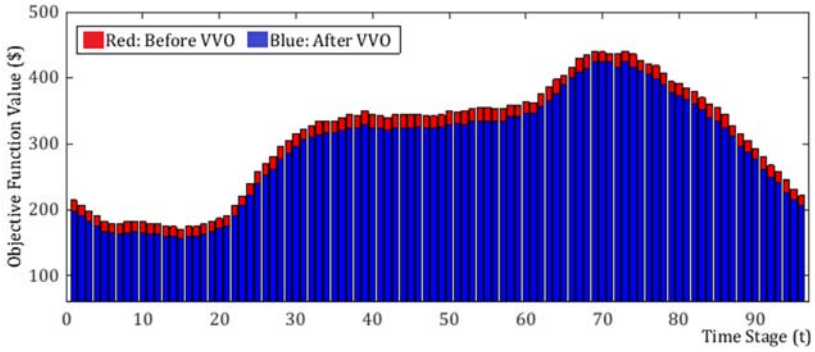

Figure 12.62. Objective function values resulted by quasi real-time VVO engine

Figure 12.63 represents Voltage Regulator performance and Figure 12.64 gives CB amount and operating strategies at each quasi real-time stage. From VR operation, it can be concluded that VR is participating in CVR only in peak times by increasing its taps. Hence, most of CVR action performed by OLTC at the beginning of the feeder. Figure 12.65 shows that the voltages of all nodes were being kept within the ANSI band.

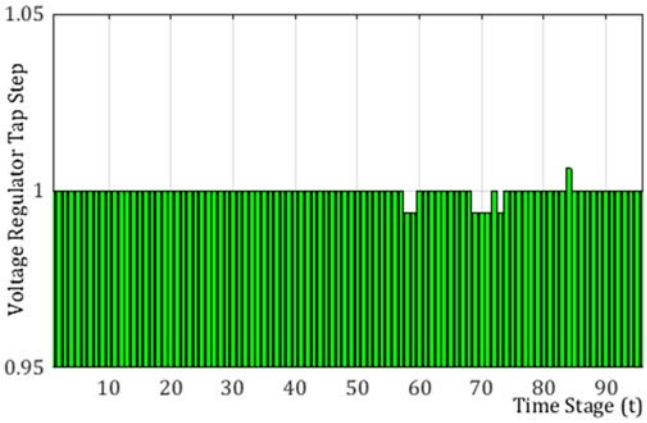

Figure 12.63. Voltage regulator tap step results in quasi real-time stages

Therefore, it is concluded that quasi real-time modeling of loads through ZIP coefficients improved new AMI-based VVO performance and increased the accuracy of energy conservation computations in CVR sub-part of VVO.

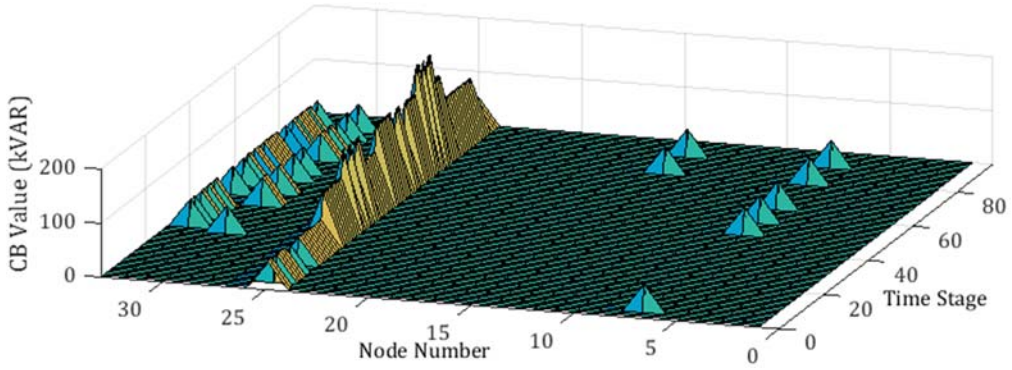

Figure 12.64. Capacitor bank values and switching operations resulted by quasi real-time VVO engine

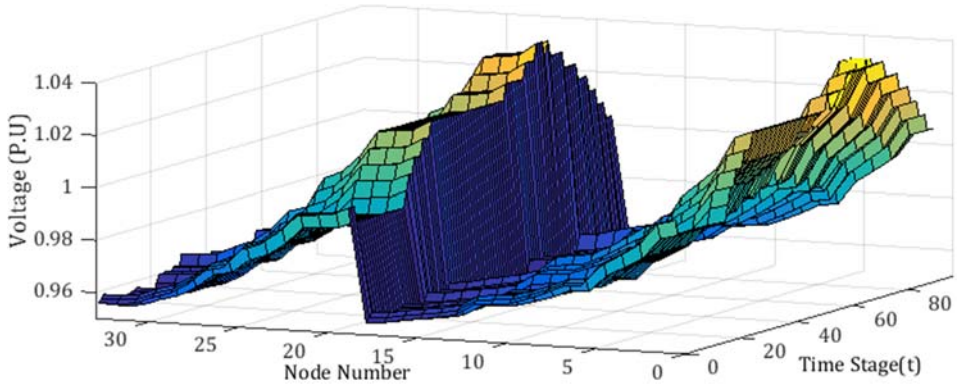

Figure 12.65. Voltages of all nodes of distribution system in different quasi real-time stages

12.9.4. Conclusions

This study presented quasi real-time ZIP load model using load disaggregation and statistical data for energy conservation through CVR. The study also showed the importance of Quasi real-time optimization techniques such as AMI-based VVO techniques, accurate quasi real-time load modeling throughout decomposing total residential consumption to its appliance consumptions, defining appliance types, operating duration and time of use. The main advantage of the approach presented in this study is its capability for improving VVO performance by using quasi real-time model of loads that are closer to reality compared with conventional load models. Hence, energy conservation is computed with more precision as well. For this reason, this study primarily introduced a new quasi real-time AMI-based VVO engine. Then, it explained load modeling concepts and ZIP coefficient calculation method for each quasi real-time stage.

Afterwards, the performance of the whole system was checked in 33-node distribution network as case study and the results were compared with conventional load modeling approach.

It has to be mentioned that several factors such as type of day, calendar, weather condition and seasonal factors could affect load types and the amount of consumptions. Hence, in order to find more precise coefficients, it is possible to follow the same steps explained in this study and find quasi rea-time ZIP load models for other types of days (e.g. off-day) and/or other seasons. This point could necessitate further studies related to new adaptive load models quasi real-time VVO or CVR solutions. Furthermore, other techniques such as sensor placement can increase the accuracy of quasi real-time load models despite the fact that this technique could be costly. Hence, it is possible to categorize statistical methods used in this study as the first steps for studying quasi real-time load modeling for novel CVR studies. New disaggregation methods could improve CVR (solely or as a part of VVO) performance unquestionably. In conclusion, quasi real-time AMI-based VVO could reach higher degrees of accuracy and efficiency through more precise quasi real-time load modeling such as quasi real-time ZIP load modeling presented in this study.

12.10. Real-Time Co-Simulated Platform for Novel Volt-VAR Optimization of Smart Distribution Network using AMI Data

12.10.1. Case Study & Result Analysis

In this section, 33 node distribution test feeder [254]-[267] shown in Figure 12.66 employed as distribution network model. Co-simulation platform used in this study presented in Chapter 11.1 of this thesis. Moreover, this study uses flowchart of Figure 11.2 for its VVO engine. This network was modeled in RSCAD with general data mentioned in Table 12.36. As it is shown in Table 12.36, studied network consists of 33 nodes with 32 loads. Active/reactive power loads of each node modeled in RSCAD was captured by VVO engine programmed in MATLAB environment. The network has an OLTC at its medium voltage substation and one VR at node-14. Both OLTC and VR are

able to adjust voltage level of their covered nodes from -5 percent to +5 percent. Moreover, both have 17 tap positions. Switchable shunt capacitor banks are located in five different locations of the feeder and can be switchable from 50 kVAR to 250 kVAR. With developed test setup, VVO engine operated in real-time co-simulated platform every 5 minutes for a complete day (288 time stages) according to VVO engine objectives (5-35) to (5-39) and constraints (5-9) to (5-18), (5-20), (5-21), (5-23), (5-24), (5-26) and (5-27).

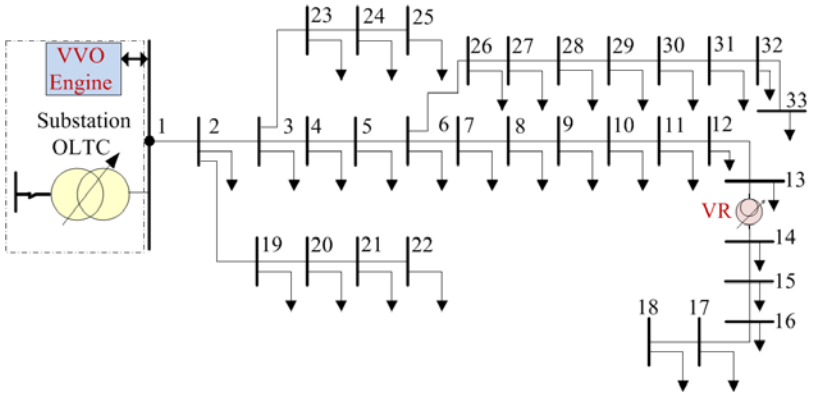

Figure 12.66. node distribution test feeder single line diagram

Flowchart shown in Chapter 11 is used for the optimization and the co-simulation platform uses RTDS for modeling the grid, RTDS GTNET for data aggregation and VVO engine designed in MATLAB. It uses DNP3 protocol to connect different parts of co-simulation together.

Table 12.36. General Data of 33-Node Test Feeder

Node No.	Location(s)	Range	Taps/Switches
OLTC	1	-5 to +5	16+1
VR	14	-5 to +5	16+1
CBs	7, 14, 25, 30, 32	50 to 250 kVAR	5 each
Costs	$/kW	$/Tap	$/kVAR-year
C_{loss}	0.09	-	-
C_{OLTC}	-	0.05	-
C_{VR}	-	0.05	-
C_{CB-j}	-	-	0.05
Optimization		Convergence	Initial Population
Improved-GA		0.999	551

Then, the VVO engine found optimal solutions of each time stage and sent control commands to VVO control components through OPC that connects MATLAB to RTDS by DNP3 communication protocol. Figure 12.67 shows the power consumption of all nodes of system during peak time.

Table 12.37. Initial Results of the case study

Scenario	Obj. Function Value ($)
before VVO	40710.02
After real-time VVO test	38170.16

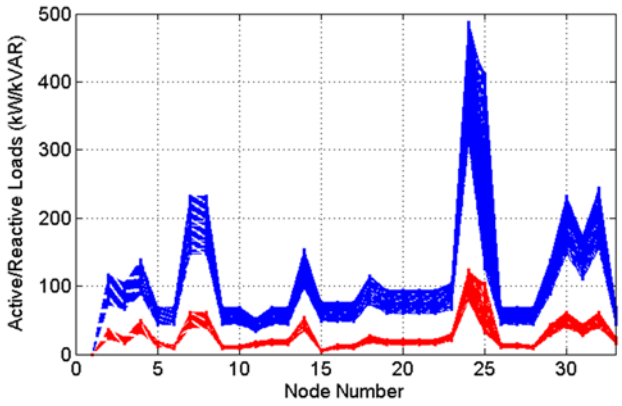

Figure 12.67. Active power consumption of all nodes of system from time stage 193 to time stage 288 (Blue: Active Power, Red: Reactive Power)

Figure 12.68 depicts VR tap positions during studied time stages. The final result of the study is presented in Table 12.37 and Figure 12.69.

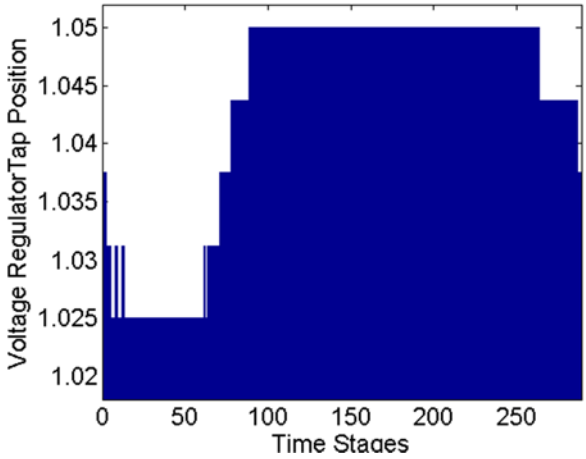

Figure 12.68. Tap positions of Voltage Regulator for 288 time stages

As proposed VVO was tested in quasi real-time, any voltage or tap real-time changes can be observed significantly through provided co-simulated environment. Figure 12.70 provides real-time voltage results of weak nodes of system (node-18 and node-33) for time stage-185 based on real-time samples.

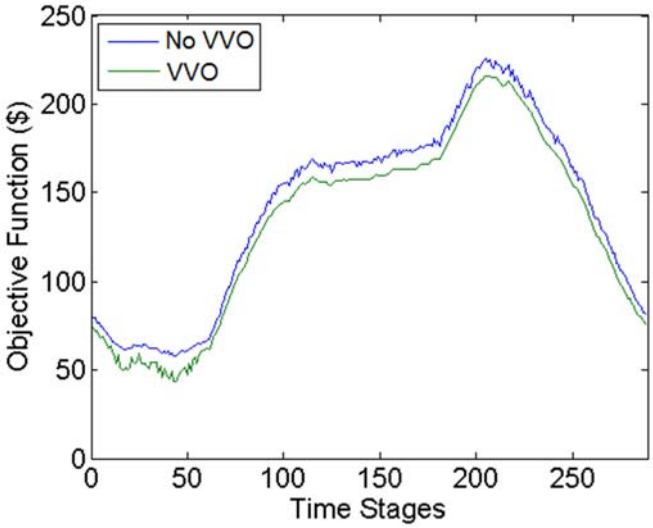

Figure 12.69. Objective function results for 288 time stages

Figure 12.71 presents Capacitor Bank switching results and finally, Figure 12.72 shows voltages of all nodes of system for all time stages during real-time co-simulation.

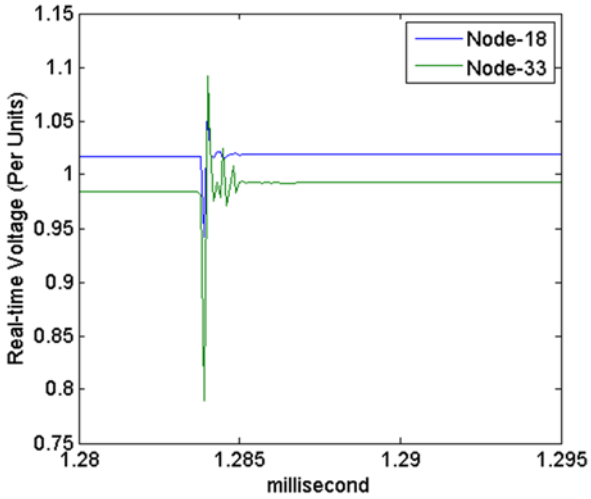

Figure 12.70. Real time voltages of the node-18 and node-33 for time stage-185

Table 12.38. Checklist of System Performance

Item	Passed (P)/Failed (F)	Item	Passed/Failed
Optimization Convergence	P	Real-time switching no impact on VVO	P
Load Flow Convergence	P	Real-time switching impose no harmful transients	P
Data Clarity	P	No Optimization failure	P
Same Results for both simulators	P	No real-time communication failure	P

Figure 12.72 proves the fact that VVO engine kept the voltages of all nodes of the system within ANSI standard (here: 18.1 kV-20.01 kV).

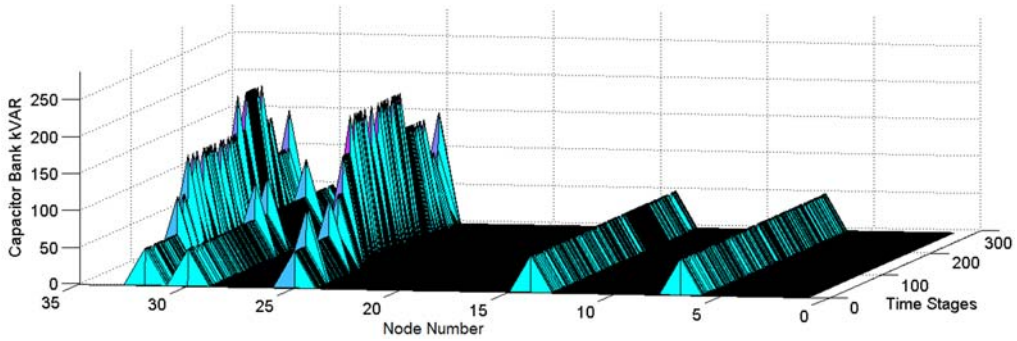

Figure 12.71. Capacitor bank switching operations for 288 time stages of the study

Moreover, it introduced a security margin (1.04375 Per Units) for OLTC and VR to avoid ANSI upper range (1.05 Per Units) violation. Table 12.38 gives a checklist regarding to the final optimization results.

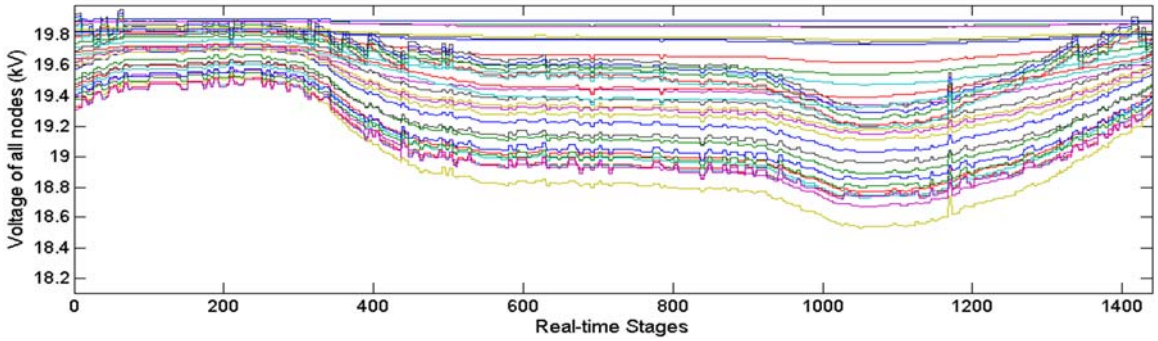

Figure 12.72. Voltage profile of all nodes of system during study time (288*5 time stages)

As a result, the performance and the applicability of proposed AMI-based VVO was tested through a co-simulated real-time environment with a reliable communication structure. Optimization engine performed well. OLTC and VR taps with CBs minimized distribution network loss precisely without any failure and/or error.

12.10.2. Conclusion

This study presented a real-time co-simulated environment for proposed AMI-based Volt-VAR Optimization engine that is able to minimize distribution network loss, Capacitor Bank, Tap Changer and Voltage Regulator operating costs as well as improve voltage profile of system nodes. The real-time co-simulation is performed by MATLAB OPC-Server and a Real-Time Digital Simulator (RTDS) and its modeling software RSCAD. DNP3 used as system communication protocol. VVO engine captured required AMI data every 5 minutes, minimized distribution network loss, improved voltage profile of system and sent control commands to VVO control components such as CBs, VR and OLTC modeled in RSCAD.

The result of study on 33 node distribution test feeder showed that proposed VVO engine is able to operate in real-time condition that is very close to reality without any failure. Hence, the applicability of the approach tested successfully. The algorithm did not face with any convergence issue, the algorithm BFS load flow performs well without any convergence problem. Furthermore, this approach shows that new smart grid-based VVO engines such as proposed one are able to lead distribution grids to higher levels of accuracy and efficiency through dynamic AMI data. As this study assumes no impact on the performance of the VVO engine as a result of constraints introduced by communication system, a related research to this study is to look into communication parameters and their impact on choices related to VVO engine optimization costs that are explained in section 12 of this Chapter.

12.11. Real-time Co-Simulated Platform for Energy Conservation of Smart Distribution Network using AMI-Based VVO Engine

12.11.1. Case Study and Results

In order to test the accuracy and the applicability of proposed VVO engine with CVR sub-part, 33 node distribution feeder [254]-[267] shown in Figure 12.46 is used. Table 12.36 shows general data of the case study. As shown in Table 12.36, the studied network consists of 33 nodes with 32 termination points, i.e. loads. Active/reactive power loads of each node modeled in RSCAD was collected by the VVO engine designed in MATLAB. The network has an LTC at its high to medium voltage substation and one VR at node-14. Both LTC and VR are able to adjust node voltage level of their coverage part from -5 percent to +5 percent through 17 taps.

Switchable shunt CBs are located in five different locations of the feeder and can be switched from 50 kVAR to 250 kVAR. VVO engine tested in explained quasi-real-time co-simulated platform every 15 minutes for a complete day (96 time stages). According to VVO engine objectives (5-40) and (5-41) that are obtained based on (5-36) to (5-39) and constraints (5-9) to (5-18), (5-20), (5-21), (5-23), (5-24), (5-26) and (5-27), VVO engine found optimal solutions of each quasi real-time stage and sent control commands to VVCCs through OPC that connects MATLAB to RTDS in DNP3 format. For CVR study, (5-42) to (5-46) equations are used.

The real-time co-simulation platform used in this study explained in Chapter 11.1 of this thesis. Figure 12.73 illustrates the active power consumptions of all nodes of the system collected by VVO engine from RTDS. The final result of the study is shown in Table 12.39 and Figure 12.74. As proposed VVO tested in quasi real-time, any voltage or tap real-time changes could also be observed clearly by provided co-simulated monitoring and control platform.

Table 12.39. Final Results of Case Study achieved by VVO engine in Co-simulated Platform

Scenario	Before Quasi Real-time VVO	After Quasi Real-time VVO
Objective Function ($)	29839.84	16415.56
Active Power Loss	13737.17	13103.15
$\Delta E\%$ obtained by CVR	-	3.044225
$\Delta V\%$ by CVR	-	3.36123
CVR Factor	-	0.8956
CB# 7, 14, 25, 30, 32 switching number	Fixed	43, 49, 39, 43, 44
LTC/VR Tap switching numbers	Fixed	17, 8

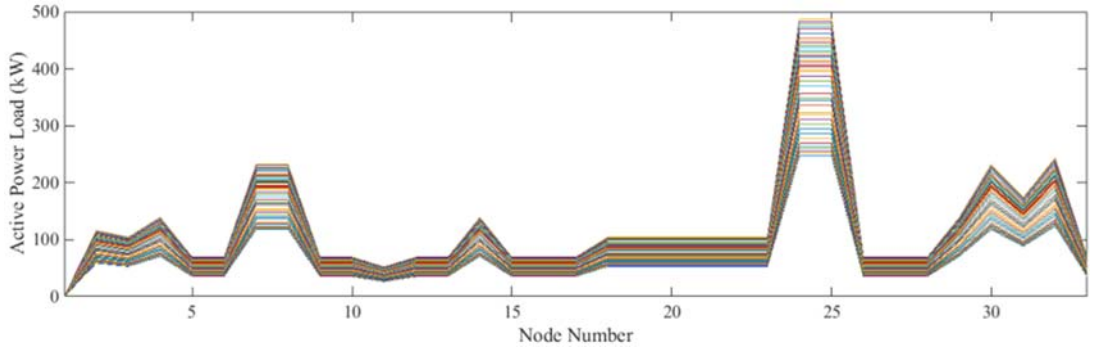

Figure 12.73. Active power consumption of all nodes of the system

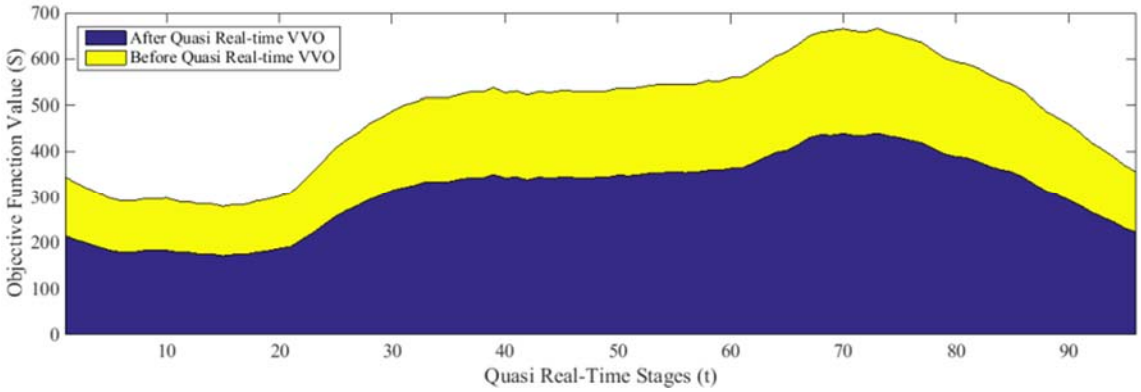

Figure 12.74. Objective function results for 96 operating time stages

Figure 12.75 presents LTC and VR tap positions found by the VVO engine for 96 operating time stages. Figure 12.76 represents quasi real-time voltage of node-18 at time

stage-60. Figure 12.77 shows the active power loss reduction of proposed VVO engine for different operating time stages and Figure 12.78 presents the percentage of saved consumed energy obtained by CVR sub-part of VVO engine objective function.

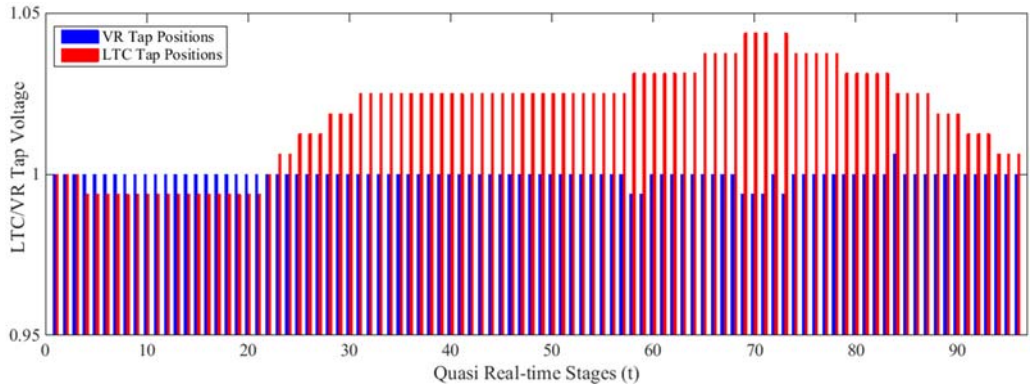

Figure 12.75. Tap positions of LTC and VR for 96 time stages

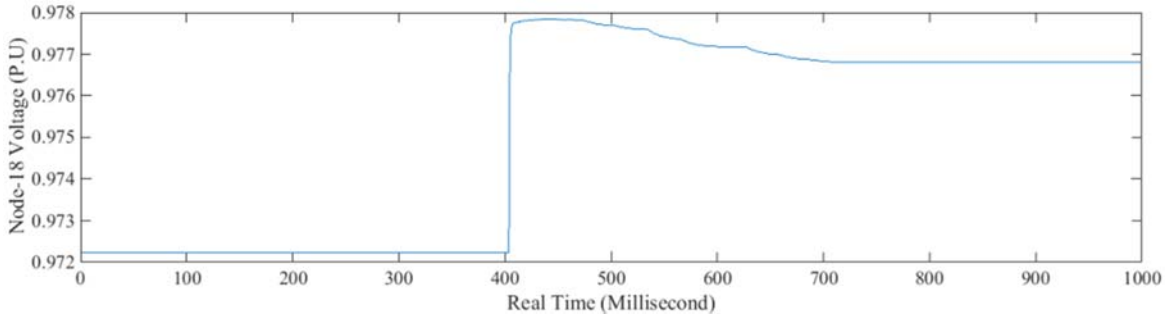

Figure 12.76. Real time voltages of the node-18 for time stage-60

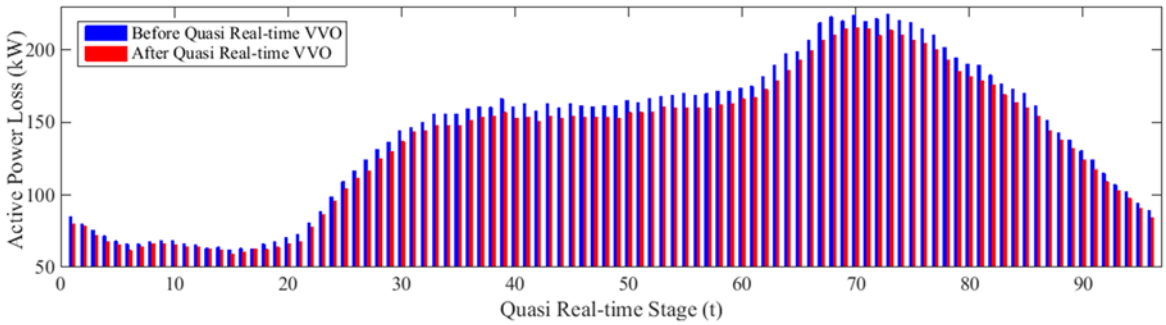

Figure 12.77. Active power loss results for 96 operating time stages

Figure 12.79 depicts CB switching results found by VVO engine for operating time stages and Figure 12.80 represents quasi real-time voltages of all nodes of the system during real-time co-simulation.

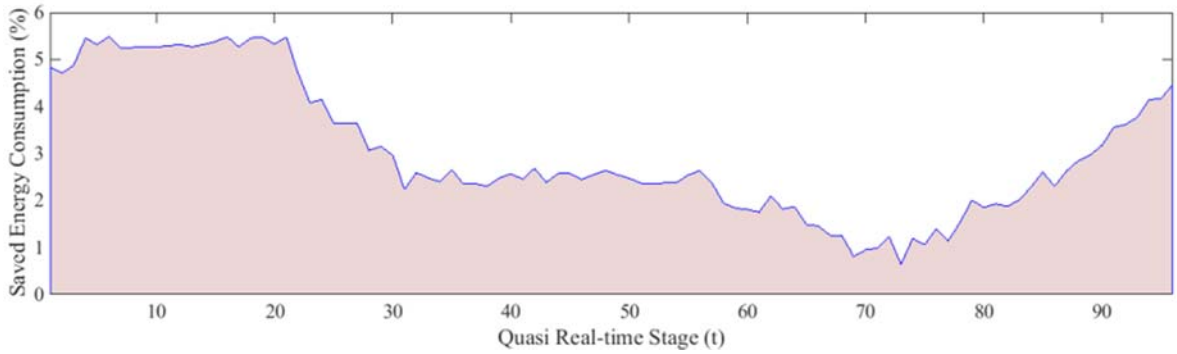

Figure 12.78. Energy consumption saved by CVR performance for 96 operating time stages

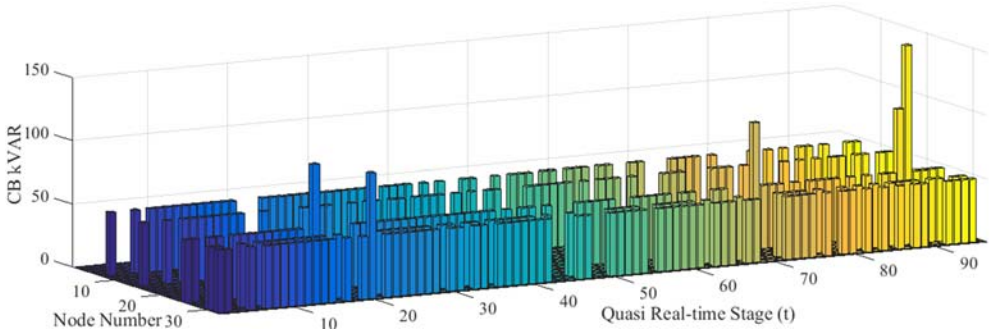

Figure 12.79. Capacitor bank optimal switching operations found by VVO for 96 operating time stages

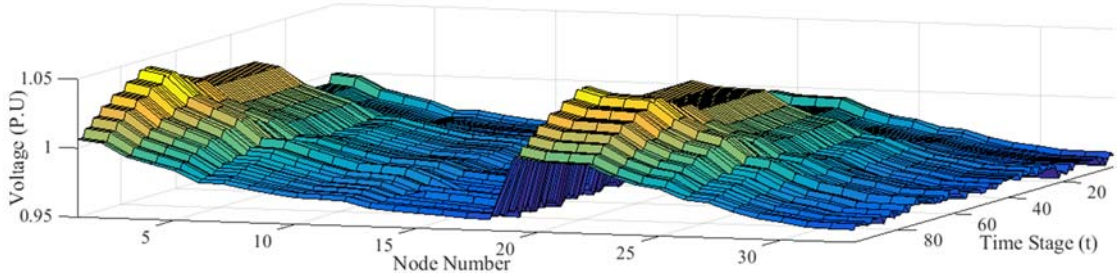

Figure 12.80. Voltage profile of all nodes of system during study time

12.11.2. Result Analysis

In conclusion, the performance and the applicability of proposed AMI-based VVO was tested in a co-simulated real-time platform with a reliable communication structure. Optimization engine performed well. LTC and VR taps with CB's VAR injections minimized the objective function precisely without any failure. Table 12.40, Figure 12.74 and Figure 12.77 show that proposed VVO engine minimized the objective function as well as active

power loss of the system at each quasi real-time stage. Moreover, it can be derived from the results that VVO engine CVR sub-part saved about 3.04 percent of consumed energy by reducing voltage about 3.36 percent. Figure 12.78 elucidates the fact that during peak, VVO engine CVR sub-part had less saved energy compared with other quasi real-time stages within studied day. Moreover, it can be concluded from Figure 12.75 that LTC raised the voltage of the feeder in peak time as node voltages of the feeder could not be kept within the ANSI range within peak time. In other words, in order to keep the voltages of end nodes of the system within ANSI band during peak, LTC raised the voltage level at the beginning of the feeder.

As seen in Figure 12.76, real-time voltage of node-18 of system monitored at quasi real-time stage-60. As VR tap raised in time stage-60, voltage of node-18 increased a bit. Figure 12.79 proves the fact that VAR injection during peak time helps system to reduce active and reactive power losses as most losses of a day occurs during peak. In addition, Figure 12.80 showed that VVO engine kept voltages of all nodes of the system within ANSI standard. Moreover, it defined security margins (1.04375, 0.95625 Per Units) for the LTC and VR to avoid ANSI upper-range and lower-range violations (1.05 and 0.95 Per Units). VVO engine's CVR component tried to lower voltage level of system nodes to save quasi real-time energy consumption. As a result, the proposed real-time co-simulated platform led the VVO engine to optimize the distribution feeder and brought distribution grid to higher level of efficiency, energy consumption saving and cost minimization.

12.11.3. Conclusions

This study presented a quasi-real-time solution for AMI-based VVO considering Conservation Voltage Reduction as a sub-part of VVO objective in a real-time co-simulated environment. VVO engine was able to capture quasi real-time AMI data from the field, i.e. RTDS, to optimize distribution network objective function. At each quasi real-time time stage, VVO engine minimized active power loss and the operating costs of VVCCs. Moreover, it performed CVR to conserve the energy consumption of loads. The VVO engine was set to optimize the grid every 15 minutes. Additionally, this study came up with a real-time co-simulation environment comprised of reliable communication platform, Real-Time Digital Simulator (RTDS) and VVO engine. The co-simulation

environment aimed for real-time monitoring and control as well as providing a test platform for proposed VVO engine. DNP3 used as communication protocol between VVO engine and VVCCs modeled in RTDS. In order to test correctness and the applicability of presented VVO, 33-node distribution network modeled in explained co-simulation environment. The results of the study proved well-performance of proposed AMI-based VVO. The results showed that the VVO engine enables system to achieve higher level of optimization and energy conservation. VVCC's quasi real-time control commands minimized the objective function without any failure at each quasi real-time stage. Moreover, it can be concluded from the results that CVR sub-part saved about 3.04 percent of consumed energy by reducing voltage about 3.36 percent. During peak, VVO engine CVR sub-part had less saved energy compared with other operating time stages. Real-time system values could be monitored through designed real-time co-simulation platform. VAR injection during peak helped system to reduce active and reactive power losses. VVO engine kept voltages of all nodes of the system within ANSI standard while VVO engine CVR sub-part attempted to lower voltage level of system nodes in order to save the energy consumption at each quasi real-time operating stage.

As a result, AMI-based VVO solutions such as the proposed VVO engine in this study, could lead distribution networks to gain higher levels of optimization, energy conservation and efficiency in the near future utilizing AMI data. Furthermore, real-time co-simulation platform presented in this study could provide VVO engine with a reliable real-time test environment. This could help electric power utilities to precisely test AMI-based VVO solution candidate performances before implementation.

12.12. Real-Time Communication Platform for Smart Grid Adaptive Volt-VAR Optimization of Distribution Networks

12.12.1. Case Study and Results Analysis

In this section, a 33-node distribution network [254]-[267] shown in previous sub-section 12.11 is emulated in RTDS, and presented smart grid-based VVO engine is considered to run in real-time receiving measurements every 15 minute and sending

control commands on the basis of optimization algorithm which takes decisions in accordance with the measurements received. Figure 11.3 and Figure 11.4 show co-simulation platform setup of this study. The aim of this study is to check the robustness of the co-simulation system explained in Chapter 11.2 and 11.3 through a communication emulator. Emulated distribution network consists of 32 loads, an OLTC at its medium voltage substation and one VR at node-14. Both OLTC and VR could adjust voltage level of nodes that are under their coverage from -5 percent to +5 percent. Additionally, both have 17 tap positions. Switchable shunt CBs are located in five different locations of the feeder and can be switched from 50 kVAR to 250 kVAR. At each quasi real-time stage, VVO engine receives measurements from AMI and optimize emulated network using previous study objective function and constraints. Then, it sends control signals to VVCCs via co-simulated platform. Here, the performance of presented VVO engine tested through four different communication network conditions emulated by WANem, introducing delays of 50ms, 100ms, 200ms and 1000ms with 10 % packet loss for each scenario. It was found that the VVO algorithm was robust in all conditions but with very high network delay (1000ms), the co-simulation platform hit its limit rendering the VVO algorithm from functioning properly. The network delay introduced causes delay in measurement acquisition as well as in sending control signal. The VVO engine is highly interactive as it waits for complete measurements before it takes a control action. Moreover, it waits for response of the system to imposed control signals in order to take further actions.

Thus, anything that causes a delay in measurement acquisition will cause a delay in control signal generation. The delay in measurement acquisition is not only because of the delay in the network but also because of the way communication protocol acts and how the measurements are read i.e. synchronously or asynchronously. As mentioned, this study used DNP3 protocol for measurement acquisition. The DNP3 protocol has a fragmentation function built within, where the measurements are fragmented into a maximum of 2048 bytes packets before it's given to the TCP layer. Moreover individual confirmations have to be sent by the master when each fragment is received from the outstation. Hence, receiving a set of measurements from a single device would mean that multiple request and confirmation commands have to be sent and received to acquire a complete set of measurement. This could make system highly susceptible to network delays. The abovementioned DNP3 protocol limitations can be found in [268]-[269].

Regarding to this fact, if an application is configured to read synchronously the server (OPC server in this study) that aggregates DNP3 measurements, then the application would not receive complete measurements till all the measurements are received by the server. As smart grid adaptive VVO engine requires all measurements to take corrective action, synchronous reading/writing function from the OPC MATLAB toolbox was used to read/write the measurements/control signals from/to OPC server. This introduced even more delay for the VVO algorithm to operate. Nevertheless with all delay conditions, the VVO algorithm was found to be robust and efficient. The Round Trip Time (RTD) and throughput of the Wireshark capture of DNP3 traffic in the network that introduces 100ms delay with a packet loss of 10% are shown in Figure 12.81 and Figure 12.82.

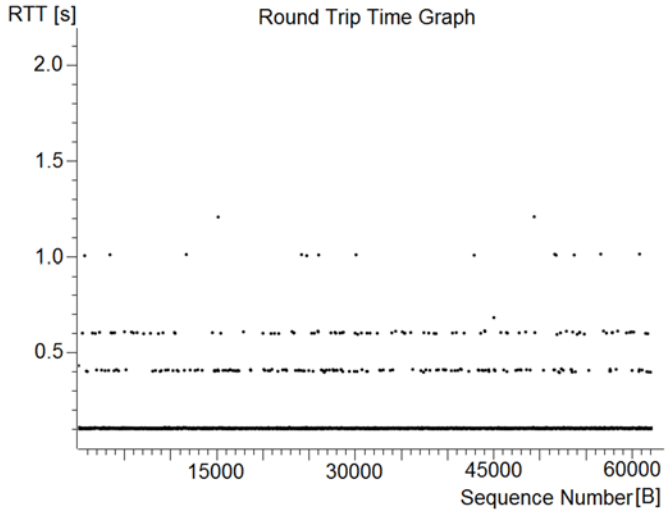

Figure 12.81. RTD of DNP3 measurements with network delay of 100ms and 10% packet loss

It can be seen from Figure 12.82 that when the VVO engine sends and receives DNP3 measurements to/from GTNET (IED/smart meter) periodic peaks in throughput is observed which is in-line with the algorithms when it receives/sends DNP3 messages (e.g. every 60 seconds).

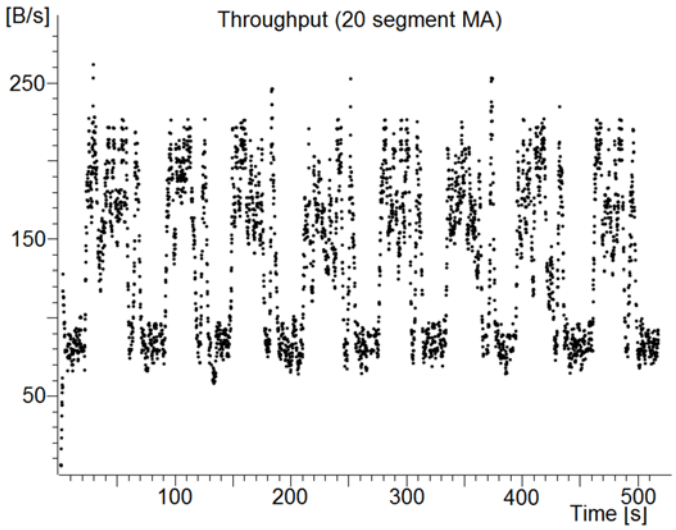

Figure 12.82. Throughput for DNP3 measurements with 100ms delay & 10% packet loss

Moreover, From the RTD graph, depicted in Figure 12.81, it can be concluded that 90% of the packets suffer a delay of 100ms which is introduced by network emulated by WANem and the rest of the 10% packets are actually re-transmitted packets corresponding to the ones being lost in the network as emulated by WANem. The re-transmission occurs only because DNP3 protocol is on top of the TCP protocol which ensures that the lost packets are re-transmitted irrespective of the delay that those packets would sustain. Re-transmitted packet is highlighted in black according to the Wireshark capture represented in Figure 12.83. The control center (137.226.160.108) polls for data from the outstation (137.226.160.83) and the outstation answers with a response. The control signals/commands (output of VVO engine) are then written by the control center, which acts as a master, and writes on the outstation which is described as a "Direct Operate".

In order to show the effect of delay, the throughput graph corresponding to the 1000ms network delay is given in Figure 12.84. It can be seen from Figure 12.84 that the VVO engine waits for the measurements to be received and then sends signals back to DNP3 outstation. Therefore, presented real-time co-simulation platform tested smart grid-based VVO engine performance in different communication operating scenarios. As a result, VVO engine was efficient and robust in most normal operating communication network scenarios. Due to DNP3 constraints explained in this section, the co-simulation

platform hits its limit rendering VVO engine from its proper functionality in very high network delays such as 1000ms (very high but rare communication network in reality).

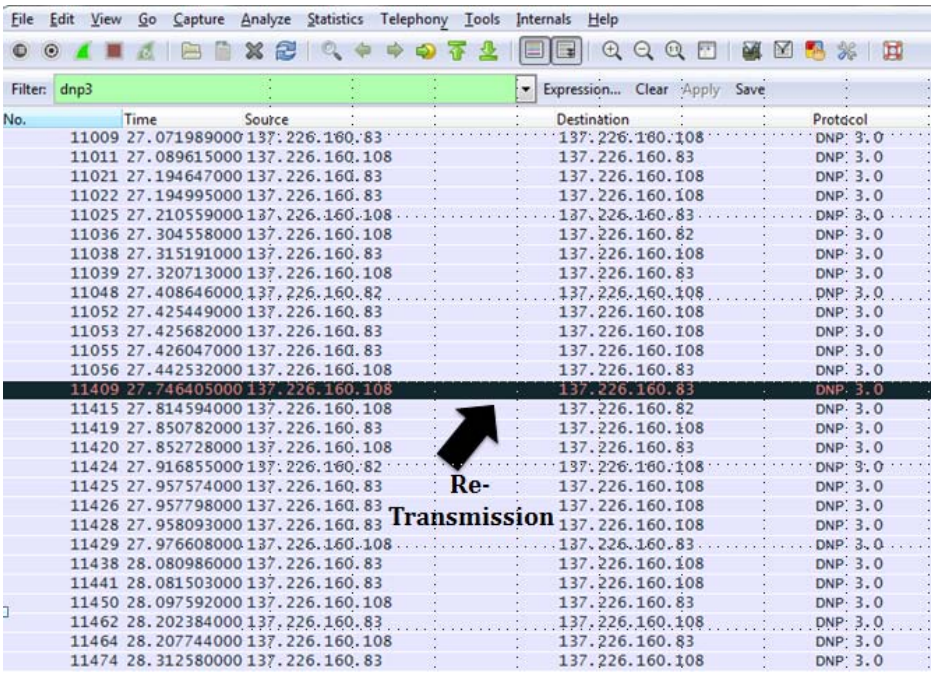

Figure 12.83. Wireshark capture of the DNP3 measurements

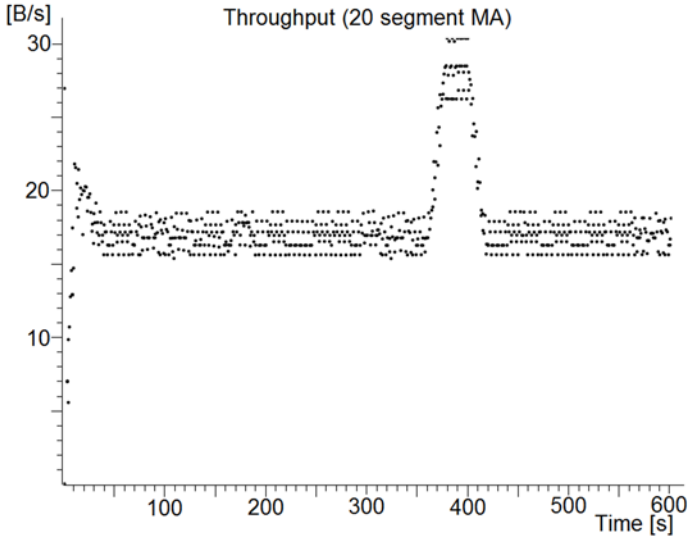

Figure 12.84. Throughput graph for 1000ms and 10% packet loss

In conclusion, using IEC 61850 MMS client server based measurement could solve this issue in networks with very high delays. Hence, IEC 61850 MMS and GOOSE could

be a great candidate for communication platform of real-time co-simulation of smart grid adaptive VVO.

12.12.2. Conclusions

This study investigated impacts of different communication network conditions on quasi real-time smart grid adaptive VVO using a real-time co-simulation platform. In this method, a co-simulated environment comprised of VVO engine in MATLAB, Volt-VAR control component's model in RTDS, data aggregator and communication platform with substation automation DNP3 protocol set to check the performance of VVO engine in the presence of different communication network conditions. This study primarily explained a quasi-real-time smart grid VVO engine. Then, it presented topology, features and aims of co-simulation as VVO engine test setup. In next step, VVO engine performance checked by communication parameters such as throughput and packet loss. The results obtained from 33-node distribution network study showed satisfactory performance of VVO in terms of data capturing, optimization and command sending, in the presence of normal communication network conditions (e.g. networks with 50, 100 and 200ms delays). Due to the inherent limitation of DNP3 protocol, VVO engine lost its robustness for communication with very high delay (1 second). According to the fact that real communication networks with very high delays such as presented network in this study are not common, it is possible to come to a certain conclusion that presented smart grid VVO engine is robust in presence of real communication networks.

In order to solve communication network protocol limitation, IEC 61850 MMS client server measurement could be an alternative candidate for smart grid adaptive VVO in presented co-simulated environment that is one of author's further studies. Moreover, in order to observe distribution network faults and/or reconfiguration, IEC 61850 GOOSE Messaging could be applied in the discussed co-simulation environment. In conclusion, this study showed that new quasi real-time smart grid based VVO engine that is tested under a real-time co-simulated environment in presence of different communication network conditions could model network operating condition in a satisfactory range closer to reality compared with conventional approaches. This could lead distribution networks to achieve higher level of accuracy, optimality and efficiency.

12.13. Real-Time Co-Simulation Monitoring and Control Platform for AMI-based Volt-VAR Optimization of Smart Distribution Networks

12.13.1. Case Study Simulation & Operating Scenarios

To test the correctness and the applicability of presented co-simulation platform (explained in Chapter 11.4) for the AMI-based VVO engine, 33-node distribution test feeder [254]-[267] is used in the presence of different load conditions. Figure 11.5 and Figure 11.6 show real-time co-simulation platform structure and monitoring platform used in this study. Figure 12.46 presents single line diagram and , shows general data of the case study. For the objective function, (5-35) and (5-47) to (5-50) are used. Moreover, for power flow, BFS technique with (5-53) to (5-56) is used. In order to find Fuzzification values, the concept of (5-52) algorithm is employed as well. Regarding system constraints, same constraints of previous study in sub-section 12.12 is used. The active/reactive consumptions of nodes are collected by the VVO engine. Here, the VVO engine tested in quasi-real-time, i.e. every 15 minutes for a complete day (96 time stages) and system performance monitored in real-time through RSCAD runtime. VVO found optimal solutions of each quasi real-time stage and sent control commands to VVCCs modeled in RSCAD through DNP3 protocol. Table 12.41, gives general VVO costs and Fuzzification values used in this study. To fully test the precision of AMI-based VVO in designed co-simulation platform, 12 different load conditions applied to the system. The aim is to ascertain the effective performance of VVO algorithm as well as the other parts of co-simulation platforms in different load conditions throughout an operating year. For this reason, ERCOT residential data [270] used to define 12 operating scenarios: Spring, summer, fall and winter load profiles. An off-day, the seasonal average and the peak-day of each season selected as three load profile samples. The load ratios of load conditions are shown in Figure 12.85. Load ratios are obtained by dividing loads at each quasi real-time stage by the average load of the system at that quasi real-time stage. The VVO engine results monitored via RSCAD runtime and the results, e.g. node voltages, branch currents, tap positions, CB's kVAR injections, stored in database for further studies. Hence, to check the precision of co-simulation platform, the platform was tested in 1152 operating quasi

real-time stages. To thoroughly assess co-simulation performance, five key operating factors were monitored and checked:

- Data collection from AMI: co-simulation platform monitored to receive correct data from AMI database.
- Algorithm-related factors: optimization convergence, BFS-load flow and Fuzzification have to work properly in different load conditions imposed to the system.
- Communication: signals from AMI to VVO engine and command signals from VVO to VVCCs in RSCAD monitored to be precise and without failure.

Synchronization: the time that load changes from one quasi real-time stage to another quasi real-time stage has to be the same in both RTDS and MATLAB environments. Control commands found by VVO engine in MATLAB have to be sent to the system in RTDS before next quasi real-time stage. Hence, time synchronization for data collection, data change and control command operation monitored in the case study. Switching: real-time operation of system monitored to check if there is any harmful transient caused by VVCC switching or not. The number of switching of each VVCC checked to avoid VVO inefficient operation.

12.13.2. Case Study Results

The objective function results and the values saved for each operating day is presented in Table 12.42. To compare the objective function values, the objective function of winter load profiles presented in Figure 12.86. Figure 12.87 gives the power loss reduction for winter as well. For each operating conditions, it is possible to monitor the voltage levels of all nodes of system to see if the ANSI range is respected or not through the monitoring platform. Figure 12.88 represents the voltage profile of system nodes in winter peak-day for all quasi real-time stages that was drawn from the VVO engine results. As mentioned before, it is possible to assess the VVO engine results such as voltages of system nodes shown in Figure 12.89 that were saved in database or monitor them in real-time by co-simulation monitoring platform. Figure 12.89 presents real-time monitoring examples for quasi real-time stage-95 at winter off-day load condition. The OLTC and VR tap positions can be monitored in real-time shown in Figure 12.89. Moreover, voltage of node-18 and CB positions observed by the monitoring platform in Figure 12.89.c, and

Figure 12.89.d. Figure 12.90 indicates CB's optimal kVAR of winter peak-day. Furthermore, VR voltage tap position results of winter, illustrated in Figure 12.91. Table 12.43 summarizes CB and VR tap switching numbers. The OLTC set by the VVO engine on tap-16 for all mentioned scenarios as it had to keep system node voltages within ANSI range through specifying upper and lower level margins, i.e. 0.95625 and 1.4375 per units, to avoid system fluctuation impacts on voltage quality.

Table 12.40. General Data of 33-Node Distribution Feeder

Node No.	Location(s)	Per Units / kVAR	Tap/kVAR
OLTC	1	-5% to +5% P.U	16+1
VR	14	-5% to +5% P.U	16+1
CBs	7, 14, 25, 30, 32	50 to 250 kVAR	5 each
Optimization		Improved GA	
Convergence Rate		0.999	

Table 12.41. VVO Coefficient-Factor Setups for the Case Study

Costs	$/kW	$/Tap	$/kVAR-year
π_t	0.12	-	-
$C_{w,t}$, $C_{r,t}$, $C_{c,t}$	-	0.09, 0.09	0.09
Fuzzification Values		$\boldsymbol{dmax}$	$\boldsymbol{dmin}$
f_{Loss}		60	20
f_{CB}, f_{OLTC}, f_{VR}		0.1, 0.1,0.1	0.095,0.95,0.95

12.13.3. Result Analysis

The precision, applicability and performance of the proposed VVO were tested in a real-time co-simulation environment in the presence of 12 different load conditions. From the monitored results shown in Table 12.42 and Figure 12.86, it can be concluded that the proposed VVO engine minimized the objective function at each quasi real-time stage. Monitoring OLTC, VR, CBs and voltage level of system nodes in all considered operating scenarios in Figure 12.88 and Figure 12.89 showed that the VVO engine kept all voltages within ANSI range completely. In low load conditions, e.g. off-days, VR tried to lower voltage as voltage can raise above the ANSI standard. Hence, VR changes are more than other scenarios as VR attempted to avoid over-voltage issues.

Table 12.42. AMI-Based Volt-VAR Optimization Engine Results

Objective Function ($)	Off-Day	Average	Peak Day
Spring	1460.301	1927.497	2852.86
Summer	1553.119	2598.059	2568.388
Fall	1737.101	1937.779	2797.116
Winter	1127.872	1877.186	2914.782
Saved by Obj. Function ($)	**Off-Day**	**Average**	**Peak Day**
Spring	376.3469	545.3844	604.5752
Summer	417.5315	432.0005	401.0212
Fall	476.1348	533.5346	519.4314
Winter	274.5305	513.7353	636.9723

Table 12.43. Number of Bank and/or Tap Switching of VVCCs

Total Injected kVAR, Average CB/VR Switch. No.	Off-Day	Average Day	Peak Day
Spring	30800, 35,18	39300, 37,16	48500, 36,10
Summer	33400, 35,12	44300, 38,9	44000, 40,19
Fall	35650, 41,15	37650, 34,10	47800, 41,14
Winter	26900, 46,32	37700, 31,11	49900, 38,11

In contrast, the VR optimal settings found by the VVO engine in peak scenarios, tried to put voltages on their maximum amounts as the system was facing voltage drop issues caused by high demand during the peak load condition. The VVO engine put fewer CBs with less amount of kVAR on low load scenarios, i.e. off-days, and injected more kVAR to the system in peak scenarios to compensate reactive power absorption and voltage drops. When two different CB combinations led to the same objective function values, the VVO engine selected the one with less VVCC operating costs. In other words, the VVO engine considered the values of VVCC switching properly. From Table 12.42, and the results shown in Figure 12.86 and Figure 12.87, it can be derived that the VVO engine's main focus was on loss minimization rather than VVCC operating costs according to initial settings of Fuzzification values. The minimum/maximum Fuzzification values have to be set by the system operator prior to the VVO engine's run time in accordance with system's operational needs. It would be possible to shift VVO engine focus on other VVO sub-parts rather than loss minimization by giving more weight to Fuzzification values of that VVO sub-part.

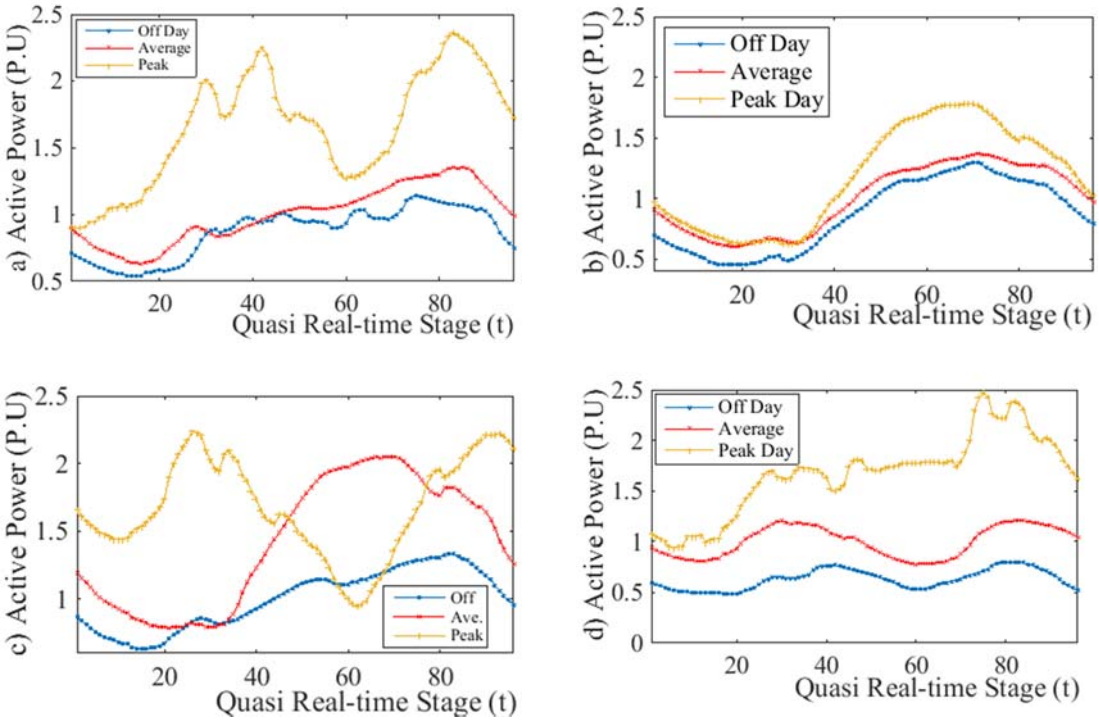

Figure 12.85. The active power consumption ratio of loads for different operating conditions (a: Spring, b: Summer, c: Fall and d: Winter)

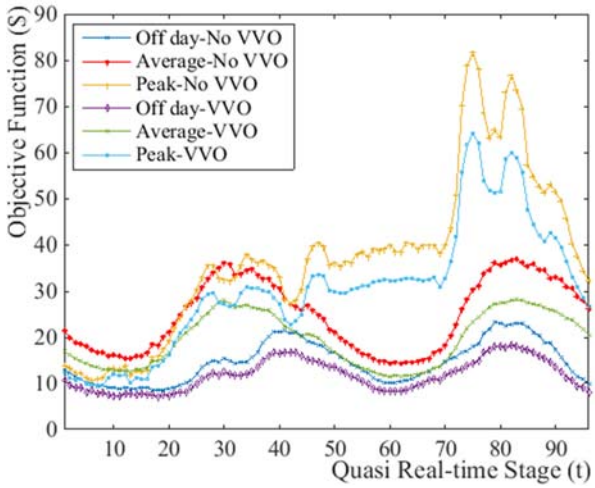

Figure 12.86. Objective function results by AMI-based VVO engine for winter

To check the performance of the co-simulation platform, different operational factors were monitored and tested in 1152 quasi real-time stages. The monitoring platform logged data from AMI for all operating time stages. Data received from AMI to the VVO engine without any fault.

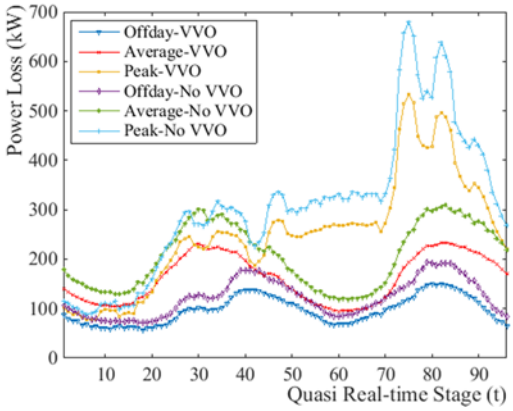

Figure 12.87. Loss results by AMI-based VVO engine for winter

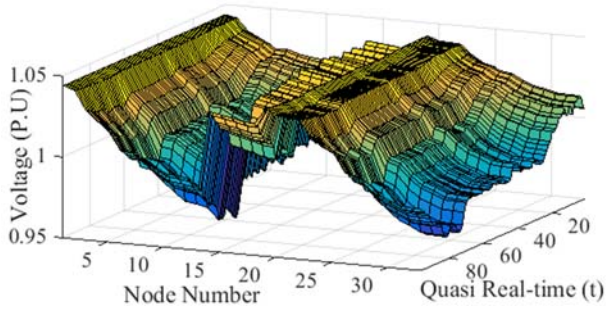

Figure 12.88. Voltage of all nodes in quasi real-time for winter peak-day

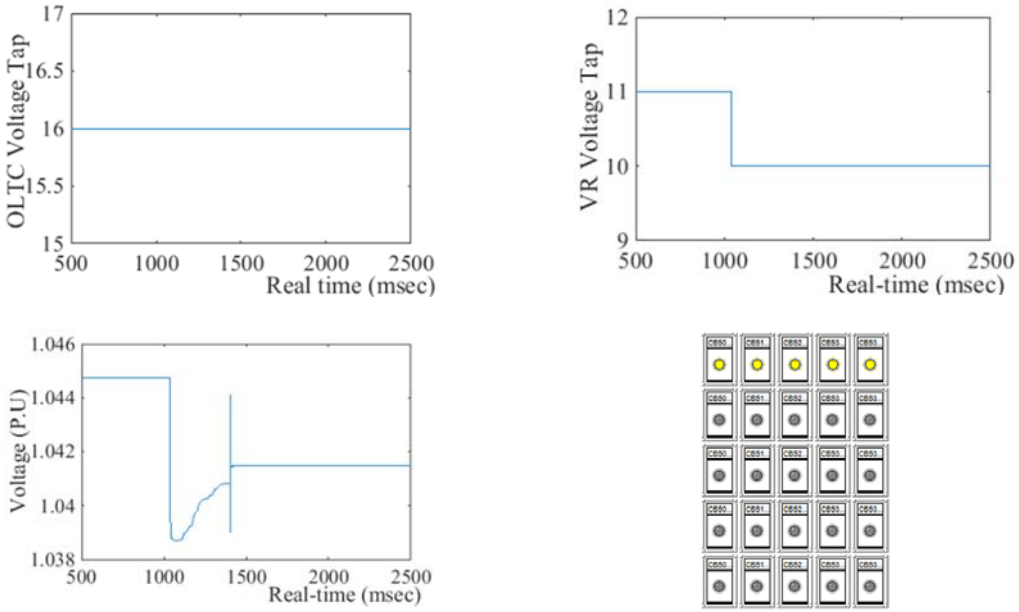

Figure 12.89. Online monitoring of OLTC, VR, node-18 and CBs in stage-95 at winter off-day

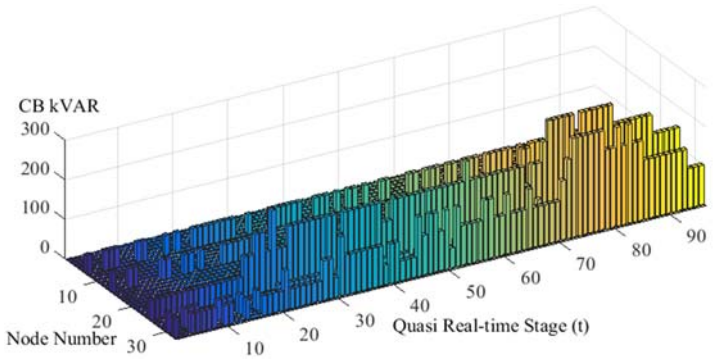

Figure 12.90. Optimal values of shunt CBs for winter peak-day

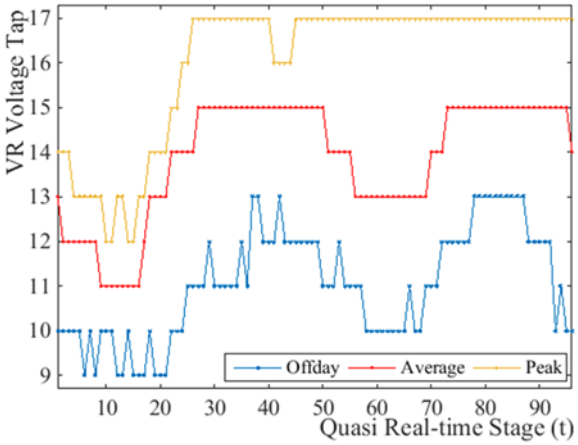

Figure 12.91. VR optimal voltage tap-positions of winter scenarios

Table 12.44. Final Monitoring Results of Co-Simulation System

Item	Passed/ Failed	Item	Passed/ Failed
VVO operation under load conditions	Passed	Data Collection from local AMI to VVO	Passed
Optimization Convergence	Passed	Control command from VVO to RSCAD	Passed
Load Flow/ Fuzzification	Passed	Real-time switching no. impact on VVO	Passed
Quasi real-time operation of VVO	Passed	Real-time switching transients	Passed
Data/Command Synchronization	Passed	No real-time communication failure	Passed
Same Results for both simulators	Passed	Overall Co-simulation Operation	Passed

Regarding the accurate operation of the VVO engine algorithm, the BFS converged and Fuzzification found optimal weights of each VVO sub-part in all 1152 operating times. It was realized that the algorithm performs fast during average load conditions as system is not facing with over or under-voltage issues. Moreover, in peak scenarios the VVO engine tried to avoid voltage drop by injecting more reactive power into the system. Hence, the selection set of CBs lessened compared with low load operating scenarios. Thus, the convergence speed decreases while similar objective function solutions increase. Moreover, the convergence rate has to be set rationally according to system performance in different load conditions as high convergence rate setting would decrease VVO speed and/or cause divergence. Signals from AMI to VVO engine and command signals from VVO engine to VVCCs in RSCAD were monitored during different operating scenarios. There were no communication failure events in co-simulation platform. This ensures reliability of communication platform comprising of two GTNET boards and OPC connecting with each other using DNP3 protocol. The time that load changes from one quasi real-time stage to another quasi real-time stage, were the same in both RTDS and MATLAB environments. In addition, it is proven that all control commands in MATLAB were sent to RTDS model before the starting time of next quasi real-time. Hence, time synchronization for data collection, data change and control command operation monitored and checked completely without facing any asynchronies. There were no harmful transients found in system switching scenarios to lower voltage quality. As a result, evaluating the performance and the applicability of AMI-based VVO engine with a real-time co-simulation monitoring and control platform with reliable communication led the system to optimize the distribution feeder with more accuracy and efficiency. Fuzzification technique could assist distribution network operator to give weights to VVO engine objective function sub-parts at each quasi real-time stage according to grid technical/economic needs. VVO engine performed well. OLTC and VR optimal taps as well as CB's optimal injected kVAR, minimized distribution network loss precisely without any failure and/or technical error within real-time co-simulation platform.

12.13.4. Conclusion

This study presented a real-time monitoring and control co-simulation environment for testing the precision and the performance of the proposed AMI-based Volt-VAR

Optimization engine using quasi real-time data. The real-time co-simulation platform monitored the AMI measurements, the VVO engine and VVCC control command accuracies using RTDS to model the distribution network with VVCC components, GTNET cards as measurement system and OPC server to connect the proposed AMI-based VVO engine designed in MATLAB into the rest of the system through DNP3 communication protocol. The monitoring platform monitored VVCC values/taps as well as other system parameters such as active/reactive power consumption of loads, voltage of system nodes and branch currents. To test the operation of the whole system, different operational factors were monitored in 1152 quasi real-time stages conforming to 3 different load conditions, i.e. off-day, average and peak-day, for four seasons of a year. The results proved correct performance of the proposed AMI-based VVO engine as well as the real-time co-simulation platform. The proposed VVO engine minimized the objective function of the system for each quasi real-time stage without any failure and/or divergence. Monitoring VVCCs and voltage level of all nodes of the system showed that the VVO engine enabled the system to keep all node voltages within ANSI standard range. Fuzzification values can initially be set to determine the flow of the AMI-based VVO engine in accordance with network operational and economic needs at each quasi real-time stage.

The co-simulation monitoring results showed that the system did not face any algorithm-related issues such as optimization, load flow and Fuzzification divergence and/or low speed. Moreover, it proved the fact that the required co-simulation operational factors such as data/command synchronizations between co-simulation parts, precise AMI data collection, reliable communication between co-simulation parts, and obtaining same results in MATLAB and RTDS were thoroughly respected in presented co-simulation platform. In conclusion, co-simulation environment presented in this study and the results obtained from that, can help operators and/or planners to evaluate and monitor the performance and the impact of new AMI-based VVO approaches on present and/or future distribution networks in a similar to reality environment before implementation. This could lead to more efficient, reliable and applicable VVO solutions for smart distribution networks in the near future.

12.14. Impact of Micro-CHP/PV Penetrations on Smart Grid Adaptive Volt-VAR Optimization of Distribution Networks using AMI data

12.14.1. Case Study Simulation

To test the accuracy and the applicability of the proposed smart grid-based VVO engine, 33-node distribution test feeder [254] is used in this section. Figure 12.92 and Figure 12.93 depict daily generation profiles of Micro-CHP units at node-33 of the case study and Table 12.36, presents general data of the case study.

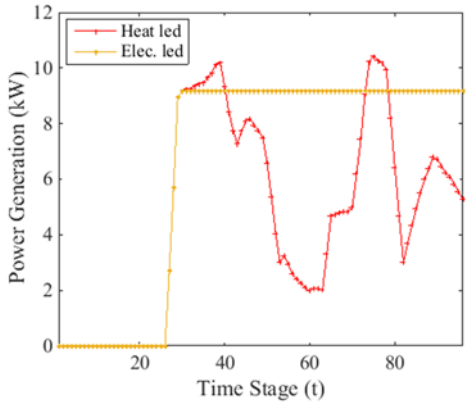

Figure 12.92. Daily generation profiles of Micro-CHP units at node-33 of the case study

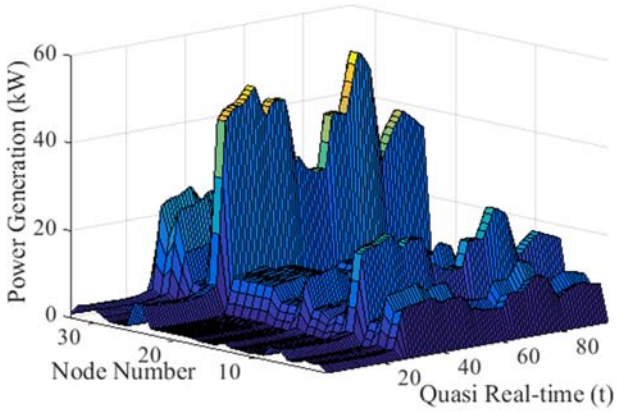

Figure 12.93. Active power generation profiles of micro-generation units in 33-node distribution feeder

This study is based on Chapter 6.2 of this thesis. As depicted in Table 12.36, studied network comprised of 33 nodes with 32 termination points, i.e. smart meters. The

active/reactive power consumption of nodes is collected by the VVO engine designed in MATLAB. The network includes an OLTC at its high to medium voltage substation and a VR at node-14. Both OLTC and VR are able to adjust voltage level of their coverage nodes from -5 percent to +5 percent through 17 taps. Switchable shunt CBs are located in five different locations of the feeder range from 50 to 250 kVAR. Here, VVO engine tested in quasi-real-time, i.e. every 15 minutes for a complete day (96 time stages). According to the VVO engine objectives (5-40), that can be calculated by using (5-41) to (5-56), and constraints (5-9) to (5-18), (5-20), (5-21), (5-23), (5-24), (5-26) and (5-27) VVO engine found optimal solutions of each quasi real-time stage and sent control commands to VVCCs. Table 12.45, gives VVO ZIP coefficients, different costs and Fuzzification values used in presented VVO engine during study. Moreover, Figure 12.94 shows the active power consumption of load for all quasi real-time stages collected from local AMI.

12.14.2. Operating Scenarios

To fully assess the impacts of different Micro-CHP/PV penetration levels on presented smart-grid based VVO objective function sub-parts, four operating scenarios studied:

- Scenario-1: VVO without Micro-CHP/PV penetration
- Scenario-2: VVO performs in normal penetration (NP) of Micro-CHP/PVs, i.e. 25 percent of nodes consist of Micro-CHP/PV units.
- Scenario-3: VVO performs in high penetration (HP) of Micro-CHP/PVs, i.e. 50 percent of nodes consist of Micro-CHP/PV units.
- Scenario-4: VVO performs in very high penetration (VHP) of Micro-CHP/PVs, i.e. 75 percent of nodes consist of Micro-CHP/PV units.

12.14.3. Case Study Results

The final result of the study is shown in Table 12.46. Figure 12.95 compares the objective function values for four different operating scenarios. Figure 12.96 gives the power loss reduction by the VVO engine. For each operating scenarios, it is possible to check the voltage levels of all nodes of system to be within ANSI range through monitoring platform. For instance, Figure 12.97 illustrates voltages of all nodes of the system in Scenario-4 at each quasi real-time stage.

Table 12.45. VVO Coefficient-Factor Setups for the Case Study

Load ZIP Coefficients	*Z*	*I*	*P*
Active	0.418	0.135	0.447
Reactive	0.515	0.023	0.462
Costs	\$/kW	\$/Tap	\$/kVAR-year
π_t,$C_{S.E,t}$	0.12	-	-
$C_{w,t}$, $C_{r,t}$	-	0.09	-
$C_{c,t}$	-	-	0.09
Fuzzification values	$\boldsymbol{dmax}$		$\boldsymbol{dmin}$
f_{Loss}	0.35 (P.U)		0.1 (P.U)
f_{CVR}	7 (%)		6 (%)
f_{CB}, f_{OLTC}, f_{VR}	0.1		0.09

Figure 12.96 gives the power loss reduction by the VVO engine. For each operating scenarios, it is possible to check the voltage levels of all nodes of system to be within ANSI range through monitoring platform. For instance, Figure 12.97 illustrates voltages of all nodes of the system in Scenario-4 at each quasi real-time stage. Figure 12.98 presents quasi real-time voltage of all nodes of the system found by the VVO engine in for all four operating scenarios. Figure 12.99 gives CB's optimal kVAR and Figure 12.100 depicts OLTC operations for all operating scenarios in quasi real-time as VVO control command examples. Table 12.47 summarizes the number of capacitor bank and/or tap switching of OLTC/VR for the studied day. Finally, Figure 12.101 represents the percentage of saved consumed energy obtained by CVR sub-part of VVO engine objective function in four explained scenarios for each quasi real-time stage.

Table 12.46. Volt-VAR Optimization Engine Results

Scenarios	Scenario-1	NP	HP	VHP
Objective Function (\$)	17967.93	16525.74	15103.54	13654.36
Power Loss (kW)	15679.72	13477.8	11558.48	9886.308
$\Delta E\%$ by CVR	4.342111	4.773744	5.194733	5.581884
$\Delta V\%$ by CVR	4.775398	5.228552	5.67508	6.087458
CVR Factor	0.907936	0.912401	0.914834	0.916583

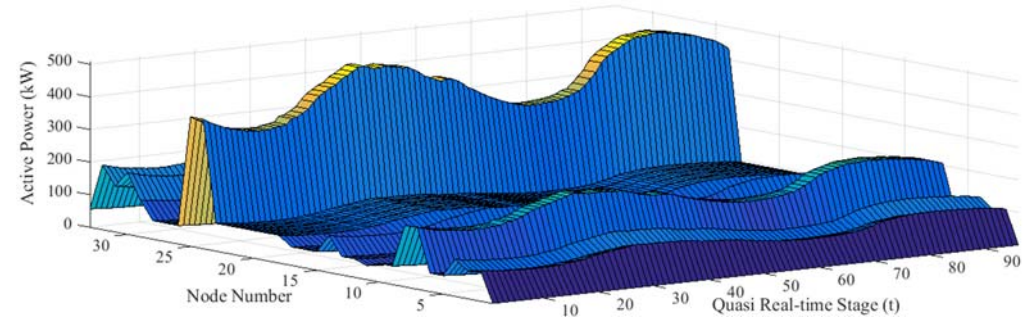

Figure 12.94. The active power consumptions of loads for all quasi real-time stages

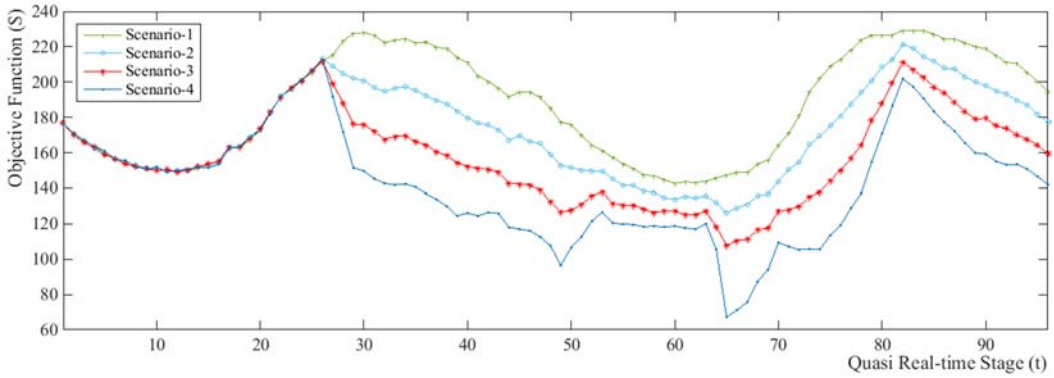

Figure 12.95. Objective function results by the smart grid-based VVO for different operating scenarios

Table 12.47. Number of Bank and/or Tap Switching of VVCCs

Scenarios	Scenario-1	NP	HP	VHP
CB-7	54	50	51	37
CB-14	56	52	51	41
CB-25	44	53	39	39
CB-30	51	52	47	45
CB-32	52	54	48	41
Total No. Switching	261	257	236	203
Total kVAR	15500	15150	14200	13150
OLTC-1	21	22	26	33
VR 13-14	6	8	2	10

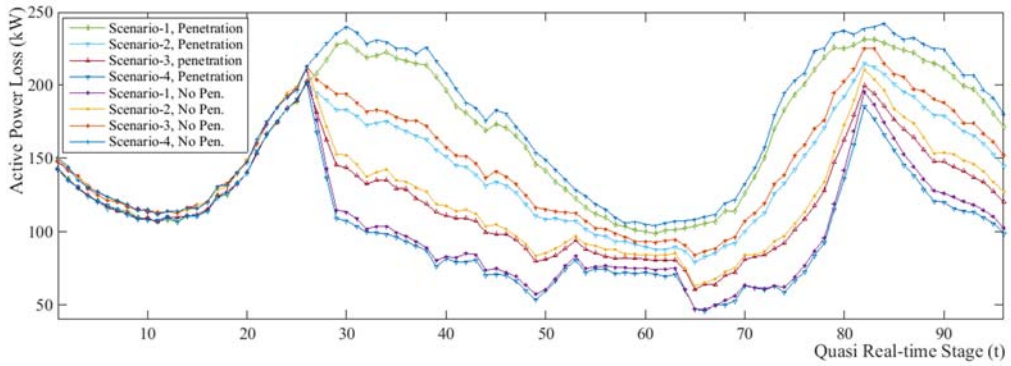

Figure 12.96. Active power loss results by the smart grid-based VVO for different operating scenarios

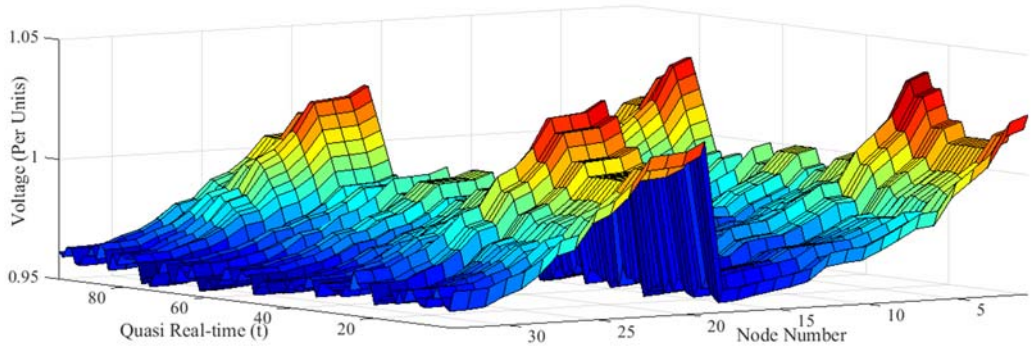

Figure 12.97. Voltage of all nodes of the system in Scenario-4

12.14.4. Result Analysis

The correctness and the applicability of a smart-grid based VVO were tested in four different operating scenarios in the aforementioned case study. From Table 12.46 and Figure 12.95, it can be seen that the proposed VVO engine accurately minimized the objective function as well as the active power loss of the system at each quasi real-time stage. Comparison of Scenario-1 with Scenario-4 shows that the smart grid-based VVO engine could minimize the objective function as well as power loss better in the last scenario. The reason lies in the fact that by increasing penetration of Micro-CHP/PV, system generation will increase as well. This can decrease power loss of the system. Moreover, Figure 12.96 shows that the VVO engine slightly decreased power loss at each scenario compared with the case that the system has the same generation without VVO optimization.

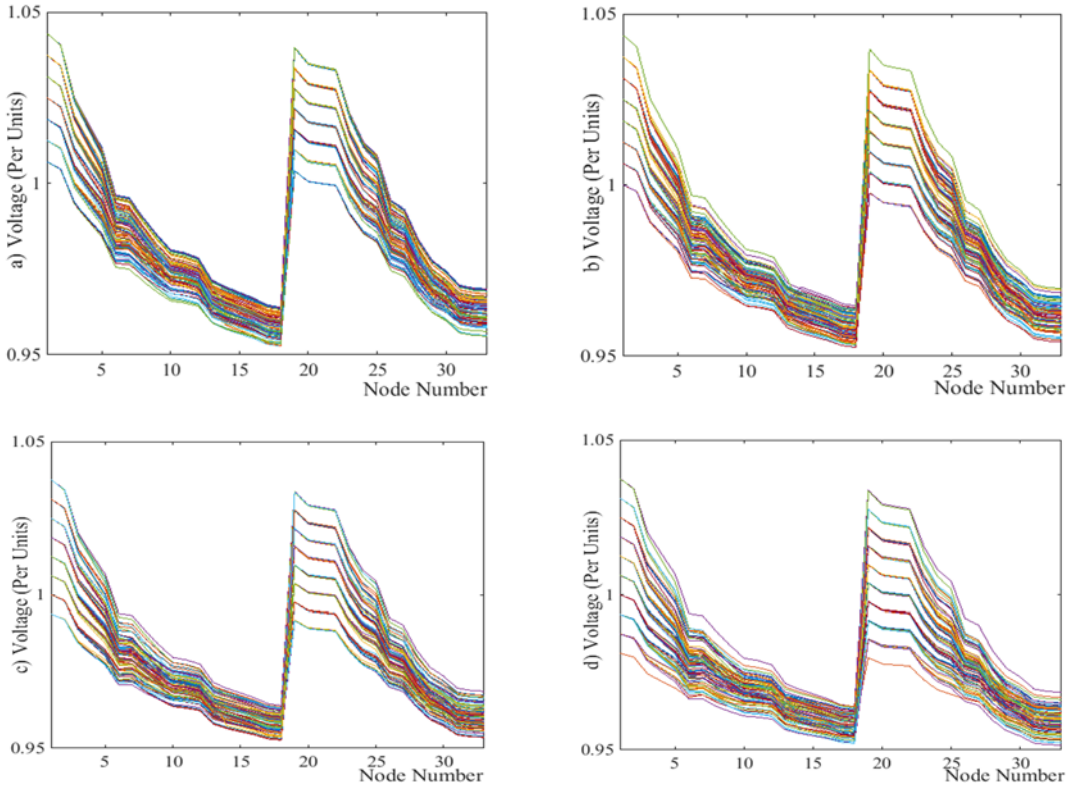

Figure 12.98. Quasi real-time voltage profile results for different operating scenarios (a: Scenario-1, b: Scenario-2, c: Scenario-3 and d: Scenario-4)

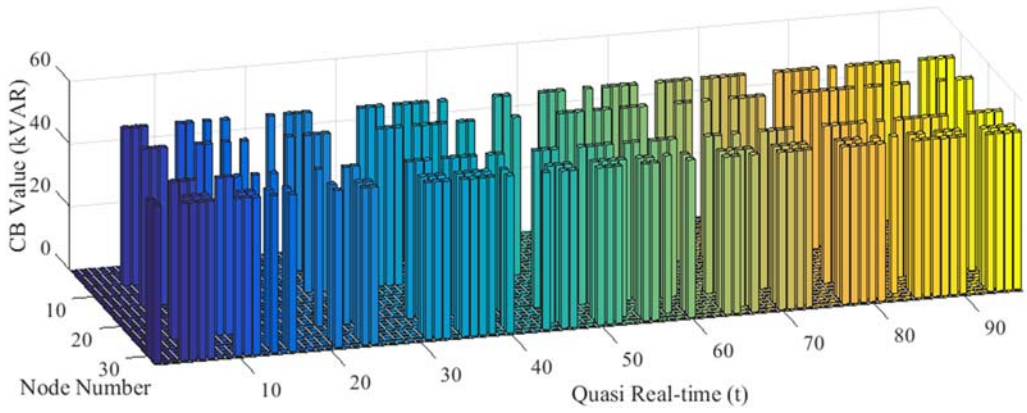

Figure 12.99. Optimal Values of shunt CB in Scenario-4 achieved by AMI-based VVO engine

Monitoring voltage level of all nodes of the system in all considered operating scenarios in Figure 12.97 and Figure 12.98 showed that the VVO engine kept all voltages within ANSI range and performed CVR to conserve the energy consumption. Figure 12.98 explains that by increasing Micro-CHP/PV penetration, the generation is increased the

VVO engine could better lower the voltage to conserve energy in last scenario rather than other scenarios.

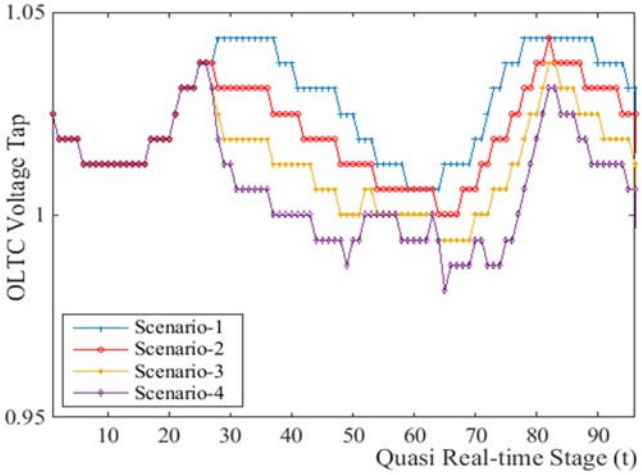

Figure 12.100. OLTC optimal tap positions for different operating scenarios

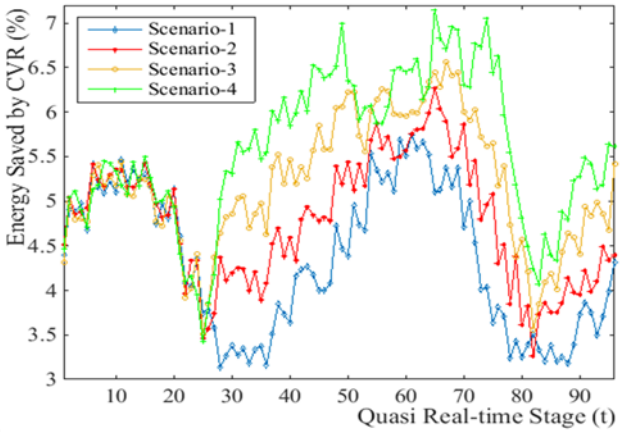

.

Figure 12.101. Saved energy resulted by CVR in different operating scenarios

Figure 12.99 illustrated that the operating cost minimization sub-part of VVO engine led the system to adopt less kVAR in most quasi real-time stages (e.g. 50 kVAR). Moreover, as seen in Table 12.47, by increasing penetration level of Micro-CHP/PVs, VVO can minimize distribution network loss with less total kVAR injection and fewer CB number of switching. Figure 12.100 gave the fact that the OLTC located in node-1 of the case study had more impact on VVO as it covers more nodes of the system. By more penetration of Micro-CHP/PV units, OLTC reduced the voltage of the system better with more number of tap operation.

Regarding the impact of Micro-CHP/PV on CVR sub-part of VVO, it is possible to conclude from Table 12.46 and Figure 12.101 that increasing Micro-CHP/PV penetration level could lead to more effective CVR. There are two main reasons for this. First, by increasing Micro-CHP/PV penetration level, system generation will increase as well. Thus, it would be easier for VVO engine to lower voltage levels of nodes to perform CVR. In other words, by increasing generation of the system due to Micro-CHP/PV penetration, voltage reduction of CVR will be increased. This fact is shown in Table 12.46. Second, CVR led to more energy consumption saving by increasing Micro-CHP/EV penetration as characteristics of load remained the same in all scenarios. Table 12.45 showed the ZIP coefficients of system loads. Some smart grid components such as EV could change the characteristics of loads which can cause changes in ZIP coefficient values and mix. The results showed that if the load characteristics are not fully constant power, it is possible to expect that increasing Micro-CHP/PV penetration would save more energy. As both energy consumption and voltage reduction improved by increasing Micro-CHP/EV penetration, CVR factor of feeder shown in Table 12.46 can be slightly improved as well. It can be realized from Table 12.45 that Fuzzification and cost values defined in this study led VVO engine to focus more on CVR sub-part rather than loss reduction sub-part. It is conceivable to achieve more loss reduction by giving more weight to VVO loss minimization sub-part rather than CVR sub-part. This could lead VVO engine to focus more on loss minimization by injecting more kVAR to the system while performing less CVR.

As a result, the study of the impact of Micro-CHP/PV penetration led smart grid-based VVO engine to optimize distribution feeder with more accuracy. Fuzzification technique could assist distribution network operator to give weights to VVO engine objective function sub-parts at each quasi real-time stage according to grid technical/economic needs.

12.14.5. Conclusion

This study presented a smart-grid adaptive VVO engine capable of minimizing grid loss, Volt-VAR control assets and CVR costs using local AMI data. Moreover, in order to assess the performance of the VVO engine in the presence of different Micro-CHP/PV

penetration levels, i.e. normal, high, and very high, 33-node distribution feeder is used. The test results showed considerable variations in the performance of the proposed smart grid VVO as a result of Micro-CHP/PV penetration level. The study shows that increasing Micro-CHP/PV penetration enabled the VVO engine to minimize the objective function better. It minimized the active power loss cost slightly better as well. VVO injected less reactive power to the system with fewer number of CB switching as grid generation elevated by increasing Micro-CHP/PV penetration level. Moreover, CVR effectiveness improved by increasing Micro-CHP/PV penetration due to the enhancement of local active power generation of the system. Hence, OLTC could reduce system voltage level more by increasing Micro-CHP/PV penetration. In summary, an effective weighting strategy for smart grid-based VVO sub-systems based on micro-generation penetration levels would be critically important for voltage and reactive power optimization of future distribution networks. Fuzzification technique used in this study, led to better performance of smart grid-based VVO in the presence of different Micro-CHP/PV penetration levels. The results showed that Fuzzification values of the VVO engine that is set by the network operator can define VVO key strategy and flow at each quasi real-time operating stage. Considering the impact of Micro-CHP/PV penetration on smart grid-based VVO could help distribution network planners and/or operators to adopt effective technologies according to their impacts on distribution grid.

Moreover, studying the impact of Micro-CHP/PV penetration could result in more accurate VVO solutions as conventional VVO approaches do not take Micro-CHP/PV impact on CVR energy conservation into account in their calculations. Applying predictive algorithms to find weighting factors for each quasi real-time stage for VVO engine sub-parts can be a novel future study that might help VVO to perform more efficient in the presence of different micro-generation penetration and load conditions. In conclusion, the result of this study can help new smart grid-based VVO solutions with CVR sub-part using AMI data to be more efficient and accurate in the presence of different micro-generation penetrations.

12.15. Community Energy Storage (CES) VVO Study

This section investigates VVO performance in the presence of a Community Energy Storage (CES) system. As mentioned in Chapter 6.3, CES is typically used for different distribution grid operating purposes. One of the main tasks of CES is peak shaving. In peak shaving, CES tries to generate active power during peak time to lower the peak demand of the system. This can decrease system loss, conserve energy and help the main grid generation to supply energy to customers easier. Here in this study, the objective function and constraints are as same as Micro-CHP/PV study explained in previous section of this chapter.

12.15.1. Case Study Simulation

In order to investigate the performance of proposed VVO engine in the presence of CES, 33-node distribution feeder [254] is employed. Other case study features such as 33-node topology, VVCC location and VVCC features are as same as section 12.14. In this study, it is assumed that a 50 kW, 100 kWh CES unit is located at node-30 of the system. In other words, this CES is able to supply 50 kW of the active power in about 2 hours. As one of the main tasks of CES is peak shaving, this study assumes that CES discharges at peak quasi real-time stages for two hours (8 quasi real-time stages). CES charges in lightest load conditions of quasi real-time stages of a day. In other times of a day, CES operates in standby mode without any impact on VVO as well as the grid. Figure 12.102 shows the charging/discharging scenario of CES in studied day with 96 quasi real-time stages. It is assumed that CBs are located at node-7, 14, 25, 30 and 32 in system without CES and node-7, 14, 25 and 32 in system with CES at node-30. Table 12.48 gives the general data and Table 12.49 presents main settings of the VVO study. The objective function and constraints used in this study is as same as section 12-14 except Micro-CHP/PV constraints.

12.15.2. CES Discharging Results & Result Analysis

In this sub-section, two different scenarios are compared with each other in order to check the performance and the VVO:

- Scenario-I: VVO performs without CES unit
- Scenario-II: VVO performs in the presence of CES unit for peak shaving

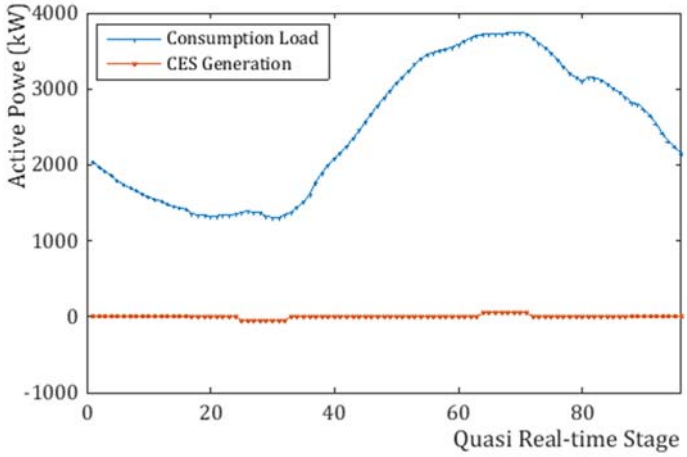

Figure 12.102. Charging/discharging of CES and case study consumption load

Table 12.48. General Data of 33-Node Distribution Feeder

Node No.	Location(s)	Voltage/kVAR	Tap/kVAR Range	Tap/ Switches
OLTC	1	-5% to +5%	16+1	LTC
VR	14	-5% to +5%	16+1	VR
CBs	7, 14, 25, 30, 32	25 to 250 kVAR	5 each	CBs
Optimization			Improved GA	
Initial Population, Conv. Rate			551, 0.999	

Table 12.49. VVO Main settings of the Case Study

Load ZIP Coefficients	*Z*	*I*	*P*
Active	0.418	0.135	0.447
Reactive	0.515	0.023	0.462
Costs	$/kW	$/Tap	$/kVAR-year
π_t	0.05	-	-
$C_{S.E,t}$	0.05	-	-
$C_{w,t}$, $C_{r,t}$	-	0.09	-
$C_{c,t}$	-	-	0.09
Fuzzification values	$\boldsymbol{dmax}$		$\boldsymbol{dmin}$
f_{Loss}, f_{CVR}	0.35 (P.U), 7 (%)		0.1 (P.U), 6 (%)
f_{OLTC}, f_{VR}, f_{CB}	0.1		0.09

As explained before in Chapter 6.3, the best operating mode of CES inverter for peak shaving is when it fully generates the active power. Hence, this study assumes rated active power generation for CES during eight quasi real-time peak stages (from time stage-64 to time stagel-72). Table 12.50 compares the results of scenario-I and scenario-II. Figure 12.103 shows the peak shaving of load by CES.

Table 12.50. Volt-VAR Optimization Engine Results

Scenarios	Scenario-I	Scenario-II
Total Objective Function ($)for peak time stages	217.0249	211.6855
Total Power Loss (kW) for peak time stages	1262.686	1216.145
Final CVR factor for peak time stages	0.8837	0.8909

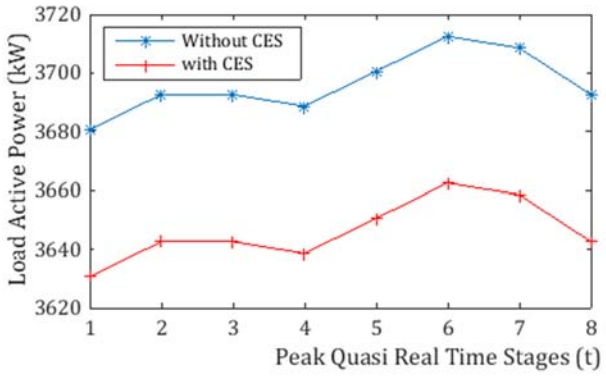

Figure 12.103. Load active power during peak quasi real-time stages

Assuming same generation from the high voltage source, Figure 12.104 and Figure 12.105 compare the active power loss and the objective function values of scenario-I with scenario-II respectively. From Table 12.50, Figure 12.104 and Figure 12.105, it can be concluded that the CES could decrease distribution network loss and VVO objective function better than scenario-I that consist of switchable CB instead of CES on node-30. Moreover, from CVR point of view, the VVO could conserve more energy in the presence of CES unit as it generates active power to the system. Figure 12.106 shows OLTC and VR taps in both scenarios. This figure shows that there is no change in OLTC and VR tap positions in scenario-I and scenario-II. Figure 12.107 represents sizes and locations of CBs in two different scenarios and Figure 12.108 shows the voltage profile of system nodes during peak in two scenarios studied in this section.

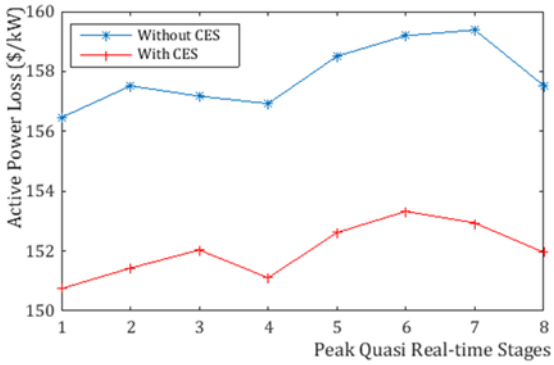

Figure 12.104. Active power loss during peak quasi real-time stages

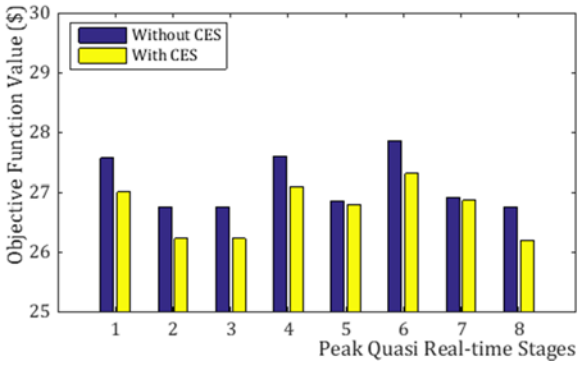

Figure 12.105. Objective function values for peak quasi real-time stages

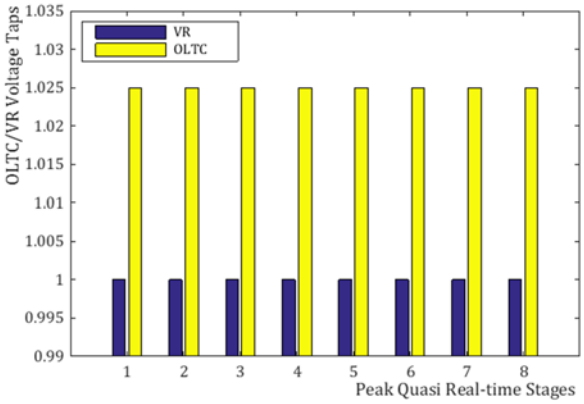

Figure 12.106. OLTC and VR tap positions in both scenarios during peak quasi real-time stages

Figure 12.107 shows that as in first scenario, VVO put CB on node-30, the value of other CBs in other locations are different compared with scenario-II. Moreover, Figure 12.108 gives the fact that voltage profile of the system improved by employing CES in the system in scenario-II during peak quasi real-time intervals. In brief, the CES performed its peak shaving task while it improved voltage profile of the system, increased CVR energy

consumption and reduced power loss significantly by supplying 50 kW active power locally.

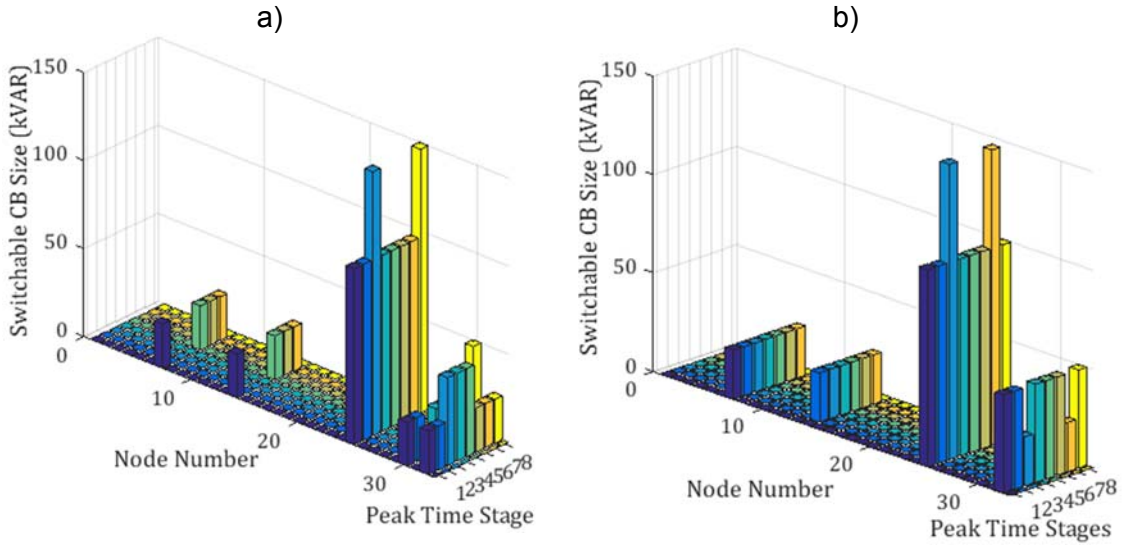

Figure 12.107. Switchable shunt CB Sizes and locations in a) Scenario-I and b) Scenario-II

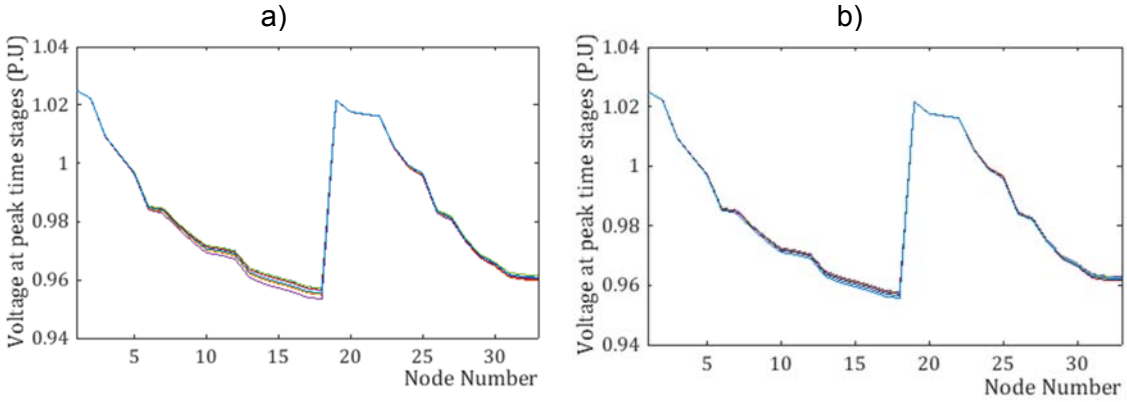

Figure 12.108. Voltage profile of the system in a) Scenario-I and b) Scenario-II (CES Discharging)

Thus, from VVO point of view, CES performs better than CBs. However, a comparison between the installation and the operation costs of CES and CBs has to be taken into account by network planners in generation expansion plans of distribution networks.

12.15.3. CES Charging Results & Result Analysis

Typically, CES has to be charged during light load conditions. As explained in Chapter 6.3, the charging time has to be less than two times of discharge time. As such, this study assumed two-hours of charging time at light load conditions (from quasi real-time 25 to quasi real-time-33). Here, two scenarios are compared with each other:

- Scenario-I: VVO performs without CES
- Scenario-II: VVO perform with CES in charging mode

In second scenario, CES receives the active power from the grid to be charged. Table 12.51 shows the results of CES discharging compared with the first scenario.

Table 12.51. Volt-VAR Optimization Engine Results in CES charging mode

Scenarios	Scenario-I	Scenario-II
Total Objective Function ($)for peak time stages	27.9941	28.3067
Total Power Loss (kW) for peak time stages	207.3906	212.0636
Final CVR factor for peak time stages	0.9035	0.9028

Assuming no change in high voltage source generation, Figure 12.109 and Figure 12.110 compare the active power loss and the objective function values during light load condition respectively.

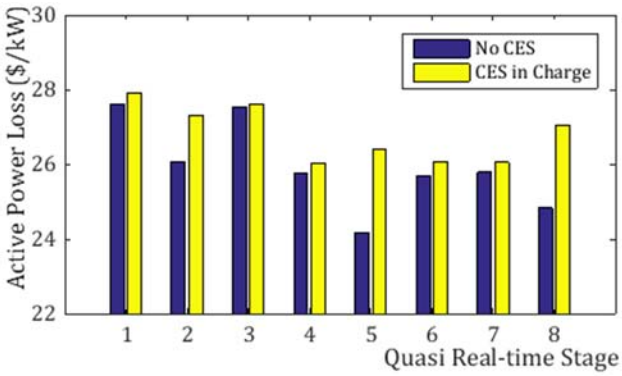

Figure 12.109. Power loss values for light load quasi real-time stages

This comparison shows that the active power loss as well as the objective function value increased slightly during charge times but as the VVO objective function value is not very much, this slight raise in objective function value is negligible. Figure 12.111 gives

the OLTC and VR tap positions in both scenarios. The OLTC and VR tap positions were same in both scenarios.

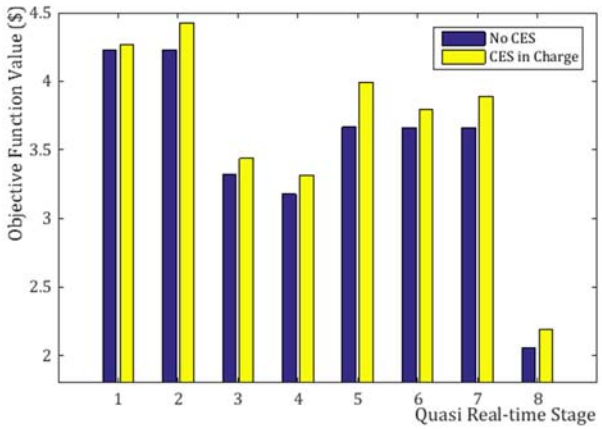

Figure 12.110. Objective function values for light load quasi real-time stages

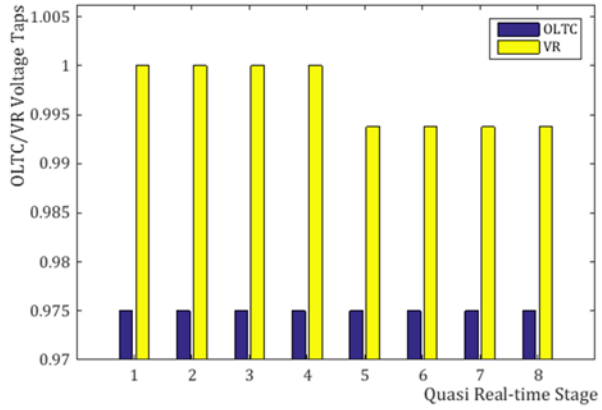

Figure 12.111. OLTC and VR tap positions in both scenarios during light load time stages

Finally, Figure 12.112 represents the voltage profile of the system in both scenarios. It shows that the voltage profile of the system decreased a bit by CES charging. From CVR point of view, the saved energy consumption reduces by CES charging but as the whole saved energy during light load conditions is not much system can accept CES charging with no problem. As stated in Chapter 6.3, one may argue that charging CES can be performed in longer period in order to lower the negative impact of charging on VVO objectives by receiving fewer amount of active power from the grid and by injecting reactive power into the system through CES 4-quadrant inverter at a same time. This may improve system performance a bit but as system objective function value is very small

during light load condition, and as CES operating costs and battery lifetime is also important for the network operators, this argument may not be justifiable.

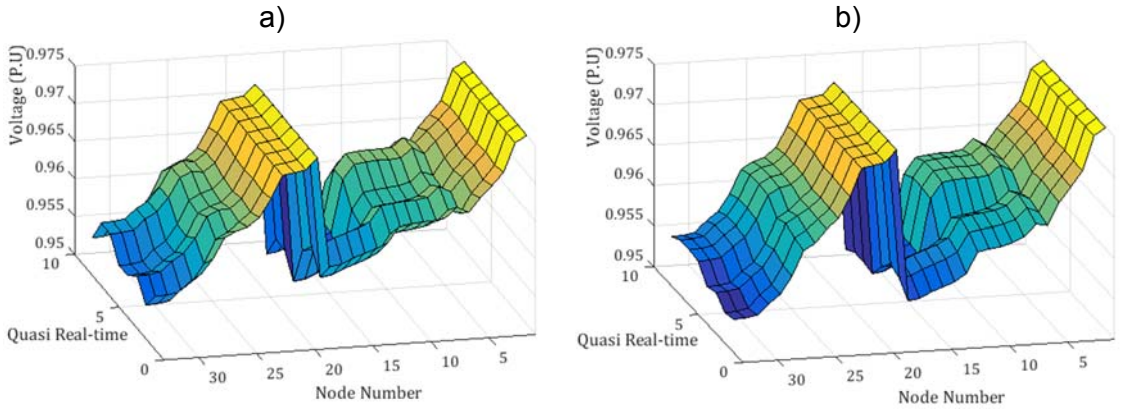

Figure 12.112. Voltage profile of the system in a) Scenario-I and b) Scenario-II (CES Charging)

12.15.4. Conclusion

This study investigates VVO performance in the presence of a 50 kW/100 kWh Community Energy Storage system. The results showed significant improvement on VVO performance while CES discharging in peak quasi real-time stages. Thus, utilizing CES as one of the crucial components of smart microgrids could help microgrids on different operating aspects such as VVO as well as EV, PV and DER integrations to the grid. Moreover, CES systems are beneficial for both utilities and costumers by improving system reliability, stability and economic operation.

The peak shaving and some other tasks of CES systems such as voltage regulation, reactive power support are in-line with VVO objectives. Hence, new solution proposed for VVO can be considered as a part of CES control in future. Furthermore, as recent CES unit communication are using DNP3 or IEC 61850 [271], it is possible for proposed VVO to be integrated to CES units using these communication protocols. It has to be mentioned that the VVO engine that intends to operate with CES has to work properly with BMS as well as other energy management systems provided for CES. A CES energy management system sample presents in [272]. Other CES tasks such as performing in island mode for outage management has to be defined for the VVO in future to avoid any task confliction between CES and VVO. In addition, CES integrated with renewable

resources such as PV has different operating features and/ modes that has to be taken into account while using CES as a Volt-VAR Optimization component. A sample of the operating modes of Toronto Hydro CES integrated with local PV has been studied in [273]. CES installations lead system to use less CBs in future. Moreover, employing CES in more than one discharging/charging cycle in a day may increase the efficiency of VVO by decreasing the power loss, saving more energy and decreasing VVCC number of switching. However, using CES in more charging/discharging cycles may increase CES operational costs that have to be taken into account in future. Moreover, some studies have recently investigated the impact of CES on distribution network planning. For instance, [274] assessed the impact of CES on capacitor placement planning problem. Further studies regarding the interaction between CES systems and short-term planning of distribution grids considering new smart grid-based VVO solutions could be beneficial in terms of distribution network reliability, quality and efficiency.

12.16. Impact of EV Penetration on Volt-VAR Optimization of Distribution Networks using Real-Time Co-Simulation Monitoring Platform

12.16.1. Case Study Simulation

To test the correctness and the applicability of presented AMI-based VVO engine in the presence of EV penetrations, 33-node distribution test feeder [254], [267] is used. Figure 12.113 depicts single line diagram and Table 12.52, represents general data of the case study. Studied network comprised of 33 nodes with 32 termination points, i.e. smart meters modeled in RSCAD in RTDS. The active/reactive power consumptions of nodes that are collected by the VVO engine, which is designed in MATLAB. Here, VVO engine tested in explained quasi-real-time co-simulation platform, i.e. every 15 minutes for a complete day (96 time stages). According to the VVO engine objectives (5-40) that is obtained by using (5-42) to (5-51) without Fuzzification factors and same constraints of Micro-CHP/PV study shown in section 12.14 of this chapter, as well as (5-57) and (5-58), VVO engine found optimal solutions of each quasi real-time stage and sent control commands to VVCCs via OPC server that connects MATLAB to RTDS via DNP3 in real-time. Real-time co-simulation platform explained in Chapter 11.1 is used in this study.

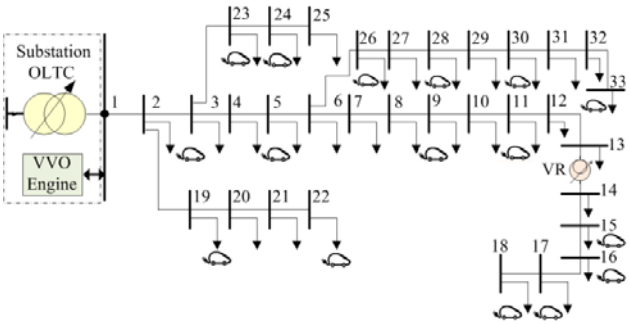

Figure 12.113. 33-node distribution feeder single line diagram

Table 12.52. General Data of 33-Node Distribution Feeder

Node No.	Location(s)	Tap/Reactive Power	Tap/kVAR Range
OLTC, VR	1, 14	-5 to +5	16+1
CBs	7, 14, 25, 30, 32	50 to 250 kVAR	5 each
Costs	$/kW	$/Tap	$/kVAR-year
C_{loss}	0.09	-	-
C_{OLTC},C_{VR},$C_{CB,c}$	-	0.05, 0.05	0.05
Optimization		Improved GA	
Convergence Rate		0.999	

12.16.2. Operating Scenarios

To fully assess the impacts of different EV penetration levels on presented AMI-based VVO objective function sub-parts, four operating scenarios studied: Scenario-1: VVO performs without EV penetration, Scenario-2: VVO performs in low penetration of EVs, i.e. 25 percent of nodes consist of EVs, Scenario-3: VVO performs in normal penetration of EVs, i.e.50 percent of nodes consist of EVs and Scenario-4: VVO performs in high penetration of EVs, i.e. 75 percent of nodes consist of EVs. For modeling EVs in charging mode, accurate modeling such as ZIP model has to be utilized. ZIP coefficient values of residential loads have been obtained in [259]. For EVs, [257] has evaluated ZIP coefficients for four different types of EVs, i.e. a Nissan LEAF, a Tesla Roadster, a Tesla Model S, and a Chevy Volt shown in Table-1 to Table-4 of [257]. Each EV type consists of different ZIP coefficient values as it has its own load characteristics. To consider the effects of EV different types, it is assumed that all EV types has equal share of distribution along feeder. In other words, each four EV model has 25% of EV market and customer's

usage. Moreover, the active power consumed by each residential house assumed to be around 4 kW. By dividing consumption of each node to this value, the number of residential houses at each node was found. Moreover, by normalizing EV ZIP values, and adding EV consumption share to the loads, new ZIP values for each operating scenarios were obtained shown in Table 12.53. Figure 12.114 shows the active/reactive power consumptions of all nodes of the system collected by the VVO engine from RTDS.

Table 12.53. Active/Reactive ZIP Coefficients in different EV Scenarios

ZIP Coefficients	*Z*	*I*	*P*
Active, No EV	0.418	0.135	0.447
Reactive, No EV	0.515	0.023	0.462
Active, EV-Normal Penetration	0.413	0.138	0.449
Reactive, EV-Normal Penetration	0.512	0.026	0.462
Active, EV-High Penetration	0.408	0.140	0.452
Reactive, EV-High Penetration	0.510	0.028	0.462
Active, EV-Very H Penetration	0.402	0.143	0.455
Reactive, EV-Very Penetration	0.507	0.031	0.462

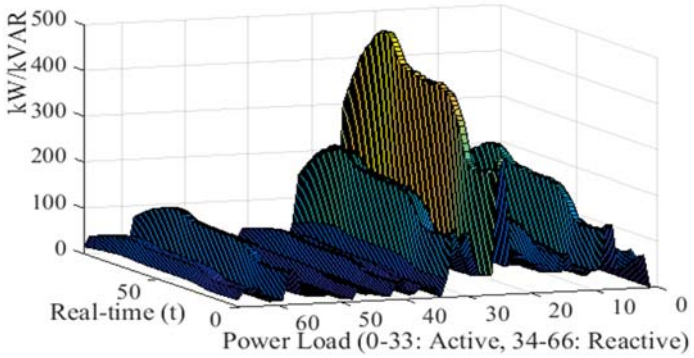

Figure 12.114. The active/reactive power consumptions of nodes in first operating scenario (VVO with no EV penetration)

12.16.3. Case Study Results

The final result of the study is shown in Table 12.54. Figure 12.115 compares the objective function values for four different operating scenarios. Figure 12.116 gives the power loss reduction by the VVO engine. For each operating scenario, it is possible to check the voltage levels of all nodes of system to be within ANSI range through monitoring platform.

Table 12.54. Volt-VAR Optimization Engine Results

Scenario	No EV	EV-LP	EV-NP	EV-HP
Saved from Objective Function ($)	13424.28	13917	14148.97	15154.75
Saved Active Power Loss (kW)	634.0259	651.5614	663.1591	677.0941
$\Delta E\%$ by CVR	3.044225	2.954183	2.887564	2.802961
$\Delta V\%$ by CVR	3.36123	3.338001	3.217036	3.151273
CVR Factor	0.90568	0.88501	0.89758	0.88947

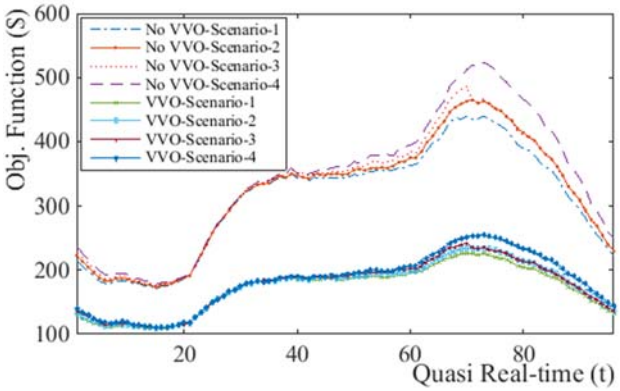

Figure 12.115. Objective function results by the AMI-based VVO for different operating scenarios

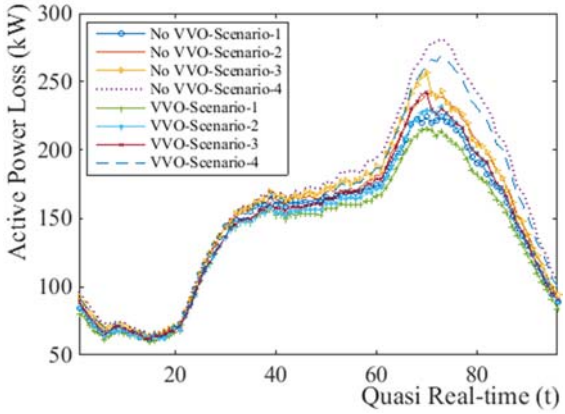

Figure 12.116. Active power loss results by VVO for different operating scenarios

For instance, Figure 12.117 illustrates voltages of all nodes of the system in Scenario-3 at each quasi real-time stage. As presented VVO tested in quasi real-time, any

voltage or tap real-time changes could also be observed by designed co-simulation monitoring and control platform. Figure 12.118 presents real-time voltage of node-18 of the system found by the VVO engine in quasi real-time stage-78.

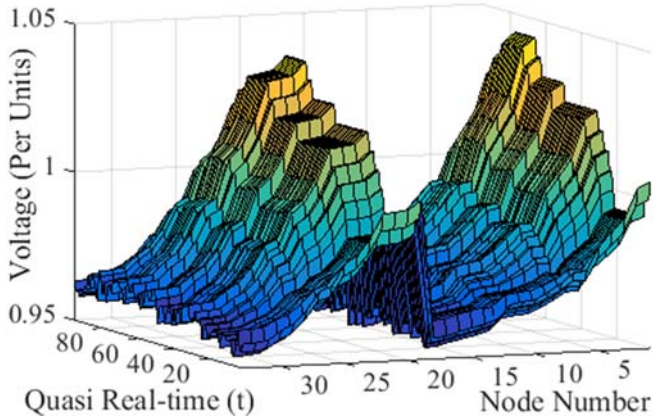

Figure 12.117. Voltage of all nodes of the system in Scenario-3

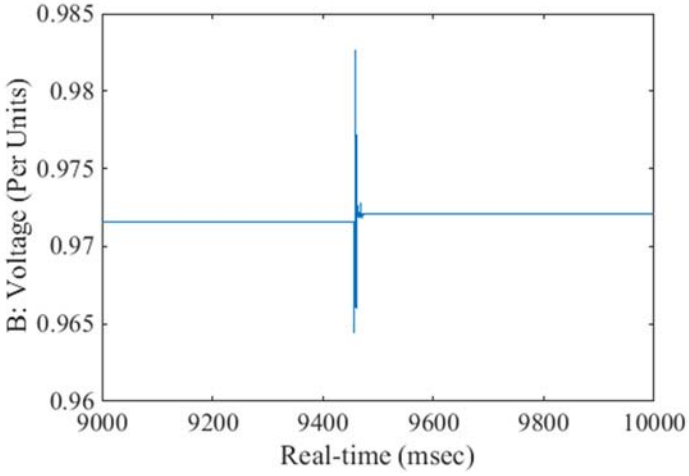

Figure 12.118. Real-time monitoring voltage results of Node-18 for time stage-78

Figure 12.119 gives CB's optimal kVAR and Figure 12.120 depicts OLTC and VR operations for all quasi real-time stages in operating Scenario-3 as VVO control command examples. Table 12.55 summarizes the number of capacitor bank and/or tap switching of OLTC/VR for the studied day.

Table 12.55. Number of Bank and/or Tap Switching of VVCCs

Scenarios	NO-EV	EV-LP	EV-NP	EV-HP
CB-7	43	47	41	41
CB-14	49	48	37	41
CB-25	39	40	38	31
CB-30	43	40	39	33
CB-32	44	46	33	27
Total kVAR	15850	15050	16400	18350
OLTC-1	17	15	16	19
VR-14	8	4	6	6

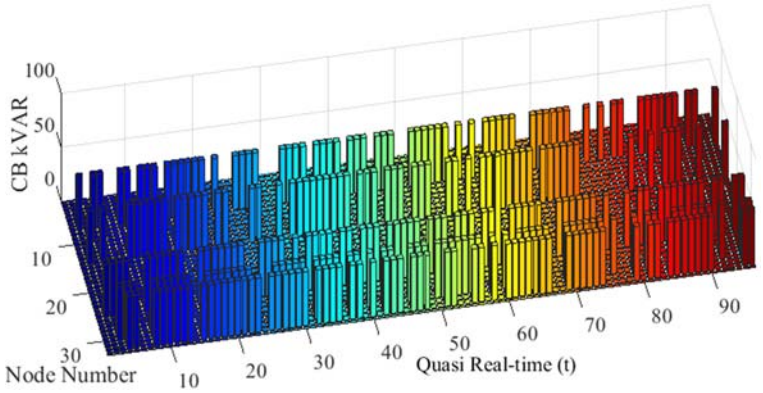

Figure 12.119. Optimal Values of shunt CBs in different operating scenarios achieved by AMI-based VVO engine

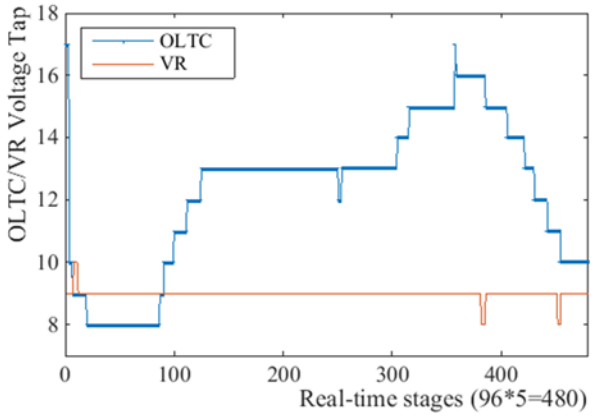

Figure 12.120. OLTC/VR optimal tap positions for operating scenario-3

Finally, Figure 12.121 presents the percentage of saved consumed energy obtained by CVR sub-part of VVO engine objective function in four explained scenarios during peak time stages.

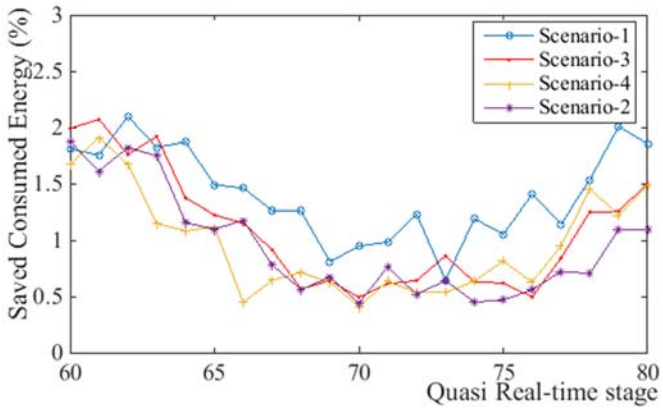

Figure 12.121. Saved energy in four operating scenarios during peak time stages

12.16.4. Result Analysis

The performance and the applicability of an AMI-based VVO were tested in a co-simulated real-time platform in four different operating scenarios as case study. From Table 12.54, Figure 12.115 and Figure 12.116, it can be concluded that the proposed VVO engine minimized the objective function, as well as the active power loss of the system at each quasi real-time stage precisely. Comparing Scenario-1 to Scenario-4 shows that the AMI-based VVO engine could minimize the objective function as well as power loss better in the 1st scenario. The reason lies in the fact that system's total load increases by adding EV penetration levels to the grid but, as shown in Table 12.54, saved values, i.e. the difference between a system without VVO and a system with VVO, raised by increasing EV penetration level. Table 12.55 gives the reason for this phenomenon. As the AMI-based VVO engine injected more kVAR to the system, total saved power losses as well as total saved objective function values raised by increasing EV penetration level.

Regarding the impact on EV on CVR sub-part of VVO, it is possible to conclude from [257], [259], Table 12.53, Table 12.5 and Figure 12.121 that increasing EV penetration level could lead to less effective CVR. There are two main reasons for this conclusion. First, by increasing EV penetration level, system load will be increased as well. Hence, in order to keep voltage within lower limits of ANSI range and to avoid any low-voltage issue, the AMI-based VVO engine tries to lower voltage level less while EV penetration is increased. In other words, by increasing loads of the system due to EV

penetration, voltage reduction of CVR will be decreased. Second, the type and the mix of EVs have significant impact on CVR. As Table-I to Table-IV of [257] show, different EV types have different ZIP models. Some have power constant characteristics such as Type-1 and Type-4 in [257], some have current constant characteristics (such as Type-2 in [257]) and some have a mix characteristic such as Type-3 [257]. As explained in previous sub-sections, this study assumed all EV types have same share in the distribution feeder. Thus, Table 12.53 ZIP coefficients were gained according to this rational assumption. As seen in Table 12.53, increasing EV penetration, decreased impedance constant coefficients that have most impact on CVR energy saving improvement. As a result and as shown in Table 12.54, by increasing EV penetration, CVR led to less saved energy consumption as well as less voltage reduction. That is the reason why CVR factors in Scenario-2 to Scenario-4 are less than Scenario-1 in Table 12.54. In brief, this study showed that EV types and mix that are being used within distribution networks have considerable impact on CVR performance. Monitoring voltage level of all nodes of the system in all considered operating scenarios showed that the VVO engine kept all voltages within ANSI range and performed CVR to conserve the energy consumption. Figure 12.118 presented the real-time monitoring of the system while AMI data was captured in quasi real-time. Figure 12.119 illustrated that the operating cost minimization sub-part of VVO engine led system to adopt less kVAR in most quasi real-time stages (e.g. 50 kVAR). Figure 12.120 gave the fact that the OLTC located in node-1 of the case study had more impact on VVO as it covers more nodes of the system. Operating cost minimization of both OLTC and VR within VVO objective function led system to have few tap switching numbers within studied operating steps, i.e. 96 time stages. This fact is shown in Table 12.55 as well.

As a result, the proposed real-time co-simulation platform led the AMI-based VVO engine to optimize distribution feeder with more precision. Moreover, different EV penetration levels affected AMI-based VVO performance in different manners. Increasing EV penetration level increased total saving of the system. It increased kVAR injection but decreased CVR performance as VVO could not reduce voltage (due to system ANSI constraint) and energy conservation (due to EV type and mix that raised constant power coefficient of total load).

12.16.5. Conclusion

This study presented an AMI-based VVO engine capable of minimizing grid loss, Volt-VAR control assets and CVR costs at each quasi real time stage. Moreover, it introduced a real-time co-simulation platform comprised of the VVO engine, grid model and monitoring platform using DNP3 protocol, in order to assess the performance of presented VVO in presence of different EV penetration levels, i.e. low, normal and high. As a case study, 33-node distribution feeder is modeled. The test results showed considerable changes in AMI-based VVO performance by increasing EV penetration level. The results of this study proved that the EV's type, mix and their usage rate have significant impacts on quasi real-time VVO operation. Each EV type has its own ZIP characteristics that can affect CVR in different fashion. EV penetration with high constant-power charging characteristics led VVO engine to perform less CVR, i.e. energy conservation, but higher loss reduction as shown in this study. In contrast, penetration of EVs with high constant-impedance and/or constant-current charging characteristics could increase CVR energy conservation with less VVO engine focus on loss reduction.

Considering the impact of EV penetration on AMI-based VVO could help distribution network planners to adopt effective technologies according to their impacts on distribution grid. Moreover, studying the impact of EV penetration could result in more precise AMI-based VVO approach as conventional VVO approaches do not take EV impact on CVR energy conservation into account in their calculations. In conclusion, the result of this study can help new AMI-based VVO solutions with CVR sub-part to be more precise in presence of different EV penetrations. Moreover, the real-time co-simulation platform presented in this study can be a great sample for testing real-time operation of AMI-based VVO before implementation.

12.17. Real Time Co-Simulation Platform for Smart Grid Volt-VAR Optimization using IEC 61850

12.17.1. Case Study Simulation

In order to check the performance and the applicability of the VVO engine, 33-node distribution test feeder [254], [267] is used in this section. Figure 12.122 illustrates single line diagram of 33-node distribution feeder and Table 12.40, presents general data of the case study. As shown in Table 12.40, this feeder comprises 33 nodes with 32 termination points, i.e. measuring points, modeled in RTDS. The active/reactive power consumption and/or generation of nodes are collected by measurement aggregators for VVO engine designed in MATLAB. Here, the performance of the VVO engine tested in quasi-real-time co-simulation platform, shown in Figure 11.10 and Figure 11.11 explained in Chapter 11.5 and 11.6, every 15 minutes for a complete day (96 time stages).

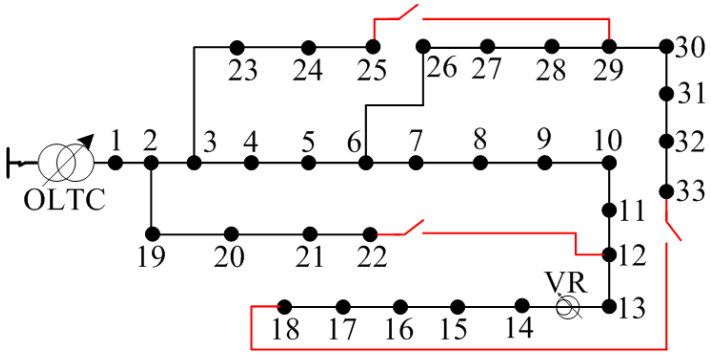

Figure 12.122. 33-node distribution feeder single line diagram

The measurements were acquired and the control signals sent to VVCC via DNP3 protocol. Any status changes due to automatic re-configuration of the grids were reported to the engine using the IEC 61850 MMS protocol. Finally the fault detection and automatic service restoration was done using the IEC 61850 GOOSE services. According to the VVO engine objectives (5-40) to (5-56) and constraints (5-9) to (5-18), (5-20), (5-21), (5-23), (5-24), (5-26), and (5-27), the VVO engine found optimal settings of VVCCs at each real-time stage and sent control commands to them via OPC server.

12.17.2. Operating Scenarios

To fully investigate the performance and the accuracy of the VVO engine, two operating scenarios were considered for the studied day. In the first scenario, the VVO performs in normal operating condition. As the VVO engine is designed to perform reliably in all different operating scenarios, it should accurately react to any changes in system configuration due to abnormal conditions such as faults. Hence, the second operating scenario investigates the VVO engine performance during a fault condition. As seen in Figure 12.122, three normally open branches (node-25 to node-29, node-22 to node-12, and node-33 to node-18) specified for fault conditions to feed the system nodes from other paths. As mentioned before, this study assumes that IEC 61850 compatible normally closed breakers on the system nodes, enable the system to isolate the fault from other parts of the feeder in real-time. In the second scenario, the performance of the VVO engine was tested under a line-to-ground fault condition. Different initial setting factors for the VVO engine are given in Table 12.56. Figure 12.123 depicts active power load of system nodes in different quasi real-time operating stages.

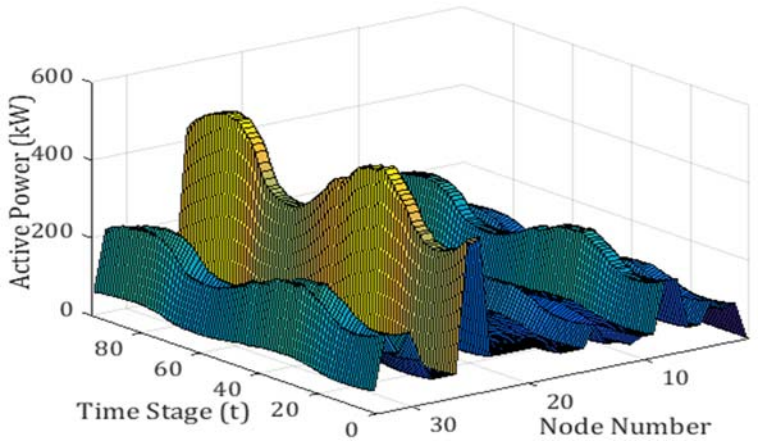

Figure 12.123. The active power of nodes in different quasi real-time stages

12.17.3. Case Study Results

It is assumed that a line-to-ground fault occurs at node-15, starting from quasi real-time stage-60 to quasi real-time stage-76 in the second operating scenario. Hence, node-15 has to be isolated from other parts of the grid. When the fault occurs, the IED that covers node-15 and emulated in RTDS detects an over current and initiates a trip signal

to appropriate circuit breakers that are located on both sides of node-15. As node-15 is isolated from the system, the GTNET board generates a GOOSE message, notifying this change in the status of breakers (node-14 and node-15 breaker).

Table 12.56. VVO Coefficient-Factor Setups for the Case Study

Load ZIP Coefficients	*Z*	*I*	*P*
Active, Reactive	0.418, 0.515	0.135, 0.023	0.447, 0.462
Costs	$/kW	$/Tap, $/kVAR-year	
π_t *and* $C_{S.E,t}$	0.1	-	-
$C_{w,t}$, $C_{r,t}$ *and* $C_{c,t}$	-	0.09, 0.09	0.09
Fuzzification values	$\boldsymbol{dmax}$		$\boldsymbol{dmin}$
f_{Loss}, f_{CVR}	0.45 P.U, 6.5(%)		0.25 P.U, 6 (%)
f_{CB}, f_{OLTC}, f_{VR}	100, 0.1, 0.1		22.5, 0.09, 0.09

Upon reception of these GOOSE messages, appropriate SIED, that is breaker of node-33 in this case, acts and closes branch 33 to 18 to feed the rest of feeder nodes, i.e. node-18, node-17 and node-16 from another path. Thus, the system reconfigures itself according to the fault till the fault clears. This reconfiguration is made available on the NI-cRIO IED that supports MMS server via the analogue output boards of the RTDS in real-time. This IED informs VVO of the system reconfiguration, thereby enabling VVO to find an optimal solution for the system according to the grid configuration in different operating conditions, e.g. normal and fault conditions. When the fault cleared at time stage-77, the same process repeats itself, and the VVO settings is turned back to the initial configuration. Figure 12.124 shows system monitoring platform for the fault scenario. The push button shown in Figure 12.124 generates line-to-ground fault in real-time. The final result of the study is shown in Table 12.57. Figure 12.125 compares the objective function values for different operating cases. Figure 12.126 presents OLTC voltage tap operation during the 96 operating time stages. Figure 12.127 represents the consumption energy saved by the VVO engine's CVR function at each quasi real-time stage in different operating scenarios. For all scenarios, it is possible to monitor voltage levels of all nodes of the system to be within ANSI range through co-simulation monitoring platform.

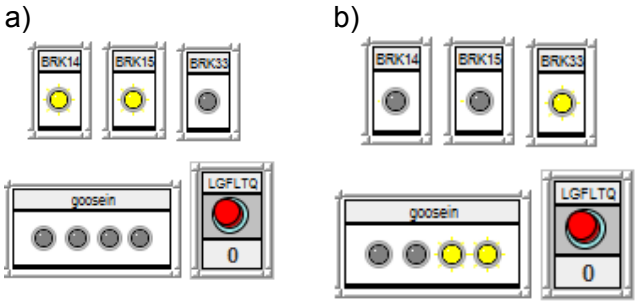

Figure 12.124. Monitoring platform in different operating scenario (a: no fault, b: fault on node-15)

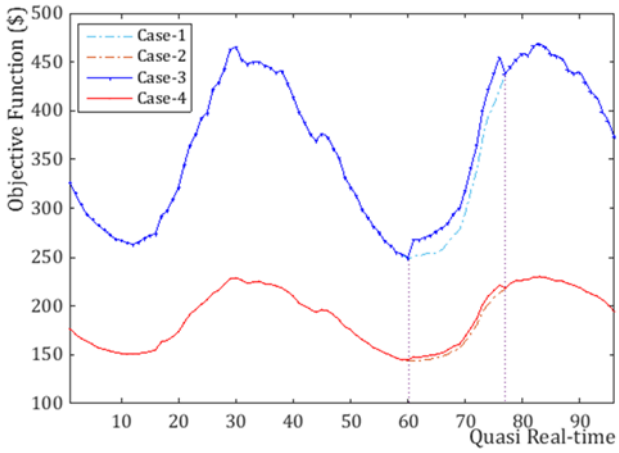

Figure 12.125. Objective function results (case-1: no VVO, no reconfiguration, 2: VVO, no reconfiguration, 3: no VVO with reconfiguration and 4: VVO with reconfiguration.

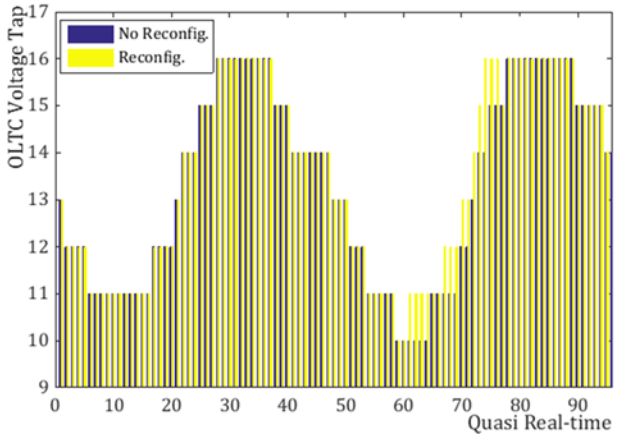

Figure 12.126. OLTC optimal tap positions found by smart grid-based VVO engine

For instance, Figure 12.128 illustrates voltages of all nodes of the system in two different scenarios during quasi real-time stag-60 to quasi real-time stage-76. Figure

12.129 presents the real-time measurements for OLTC and VR tap changes as well as node-18 and node-33 voltage changes in quasi real-time stage-75, obtained by the monitoring platform.

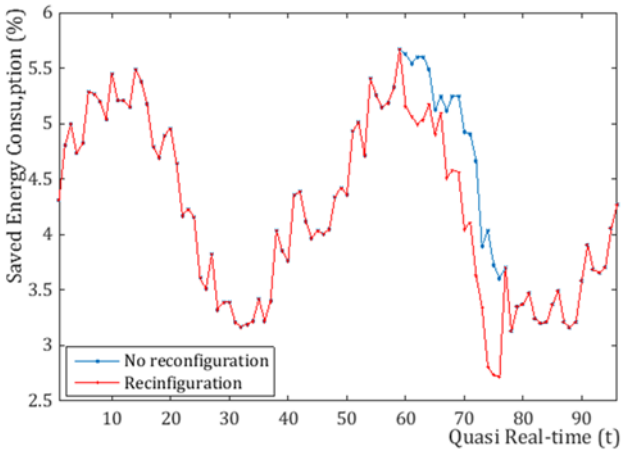

Figure 12.127. Saved energy by CVR subpart in different operating scenarios

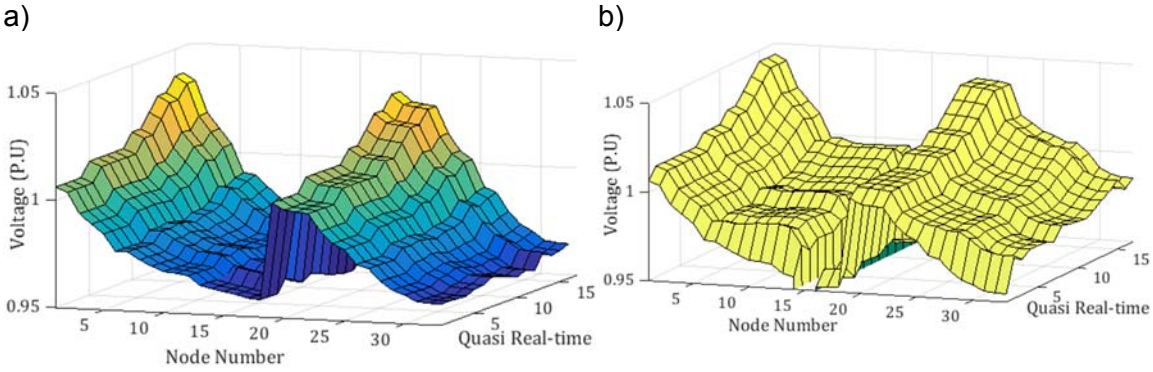

Figure 12.128. Voltage of all nodes of the system from quasi real-time stage-60 to 76 (a: normal condition, b: fault on node-15(system reconfiguration))

Finally, Figure 12.130 gives CB's optimal kVAR for a complete day for the second scenario. Table 12.58 summarizes the number of capacitor bank and tap switching of OLTC/VR for the day analyzed here.

12.17.4. Result Analysis

The performance of VVO engine was tested by presented real-time co-simulation platform.

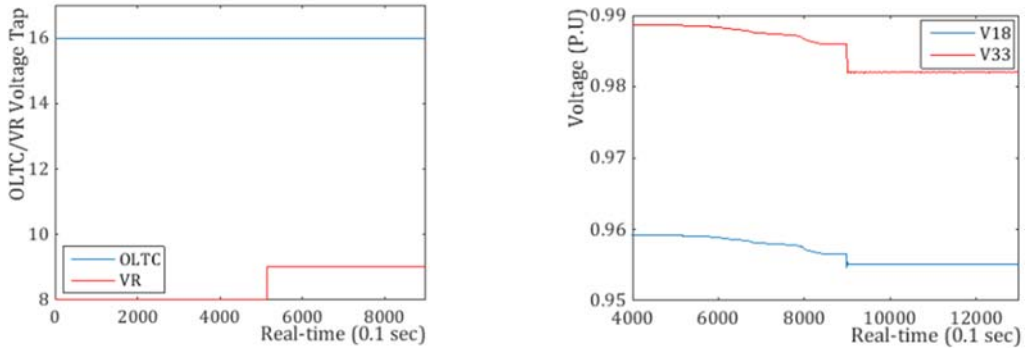

Figure 12.129. Real-time monitoring of OLTC/VR tap-positions and node-18, node-33 voltages during fault condition (quasi real-time stage-75)

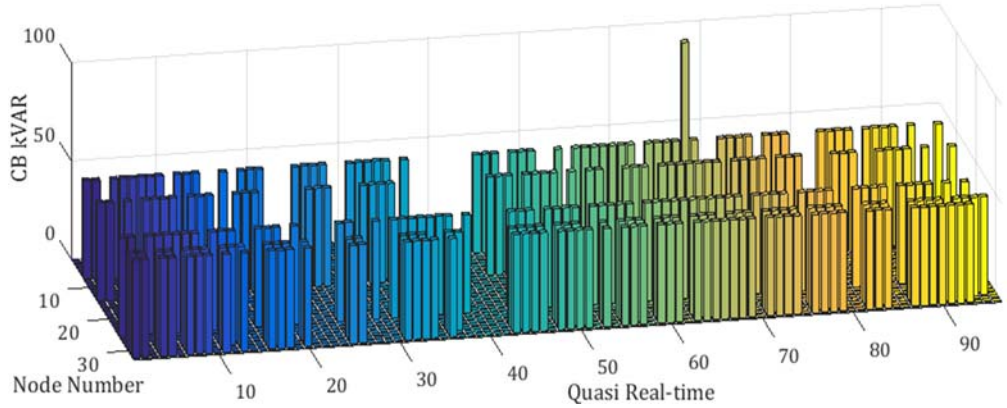

Figure 12.130. Optimal Values of shunt CBs found by smart grid-based VVO engine in second scenario

Table 12.57. Volt-VAR Optimization Engine Results

Scenario	Scenario-1	Scenario-2
Saved Objective Value ($)	16256.68	16170.84
Reduced Power Loss (kW)	756.83	712.51
$\Delta E\%$ by CVR	4.332459	4.216384
$\Delta V\%$ by CVR	4.767447	4.634376
CVR Factor	0.907455	0.908525

Table 12.58. Number of Bank and/or Tap Switching of VVCCs

Scenarios	VVO-No Reconfiguration	VVO-Reconfiguration
CB-7, 14, 25	38, 37, 38	39, 37, 38
CB-30, 32	42, 39	41, 39
Total kVAR	15150	15300
OLTC-1, VR-14	21, 6	23, 6

The real-time performance of the VVO engine was checked online via the monitoring platform. Figure 12.124 depicts a part of the monitoring platform illustrating the breaker and GOOSE status during normal and fault conditions. The breaker configuration changes were also checked in MATLAB to ascertain that the VVO engine operates with new system configuration. From Fig. 10 and Table 12.57, it can be seen that the system minimizes the objective function less effectively during the fault, as the system was reconfigured and as one node was isolated from the system. Moreover, Figure 12.126 shows that the OLTC voltage tap changes were in-line with the system reconfiguration during the fault. Figure 12.127 and Table 12.57 show that the CVR sub-system performs well in both fault and normal scenarios. The results show that although the energy consumption saved by VVO engine was reduced during the fault, the percentage of the voltage reduction decreased too. As such, the CVR factor remains very close to the normal operating scenario. The results of Table 12.58 and Figure 12.130 prove that the VVO engine injects more reactive power into the system during the fault because of system's configuration needs. Moreover, Figure 12.128 shows that the system node voltages adjust accurately during the fault time stages. Real-time measurements were observed through the monitoring platform for quasi real-time stages. Figure 12.129 proves that the VVO engine performs well in real-time. It should be noted that the time of receiving breaker status notification by the VVO is critical. According to this study, the VVO engine can be in three different modes while receiving the reconfiguration notification by IEC 61850 MMS. First, VVO has received the AMI data but it has not yet started its optimization run yet. Second, VVO is in the middle of its optimization calculations and third, the VVO has completed its task for that time stage and is waiting for the next quasi real-time stage data. In the first and third cases, VVO checked the status of breakers before it began its optimization. Thus, there was not any problem on the performance of VVO in these cases. In the second case, VVO finds an acceptable system solution with the previous settings. It checks the breaker status and realizes that it has to re-compute its solution with updated grid configuration. As AMI data is made available to the VVO every 15 minutes, there was enough time for the VVO engine to find the optimal settings with the new configuration in most cases. Otherwise, VVO would request new AMI data after receiving new configuration of the system to set new real-time frames before sending any control command to VVCCs. Thus, IEC 61850 enabled the VVO engine to receive accurate network configuration updates.

12.17.5. Conclusion

This study proposes a smart grid-based VVO engine capable of minimizing loss, Volt-VAR control assets and CVR costs using AMI data. It presents a real-time co-simulation platform comprising of the VVO engine, grid model in RTDS and runtime monitoring platform using IEC 61850 MMS and GOOSE messaging. In order to test the performance of the proposed VVO, the system was studied in the presence of normal as well as fault operational conditions. The VVO engine could receive the AMI data through measurement aggregator and OPC server. Moreover, control commands sent to real-time VVCCs in grid model in RTDS through DNP3 protocol. The VVO engine could undergo testing with 96 quasi real-time stages of a full day.

A line-to-ground fault imposed into the system to check the impact of network reconfiguration on the VVO engine performance. IEC 61850 GOOSE could generate, isolate fault and closed the circuit from another path to feed the remaining isolated but not faulty nodes. At a same time, the VVO engine could receive breaker status updates via IEC 61850 MMS and could find new optimal settings of VVCCs according to the new configuration and topology of the system. The results of the case study, i.e. 33-node distribution feeder, show accurate performance of the VVO engine in the operating scenarios considered here. Furthermore, this study demonstrates how new VVO solutions benefit from reliable and applicable communication protocols such as IEC 61850. VVO performed reliably without any failure in different operating conditions such as normal or faulty conditions. Hence, the realistic method this study presented for the deployment of AMI-based VVO engines working with IEC 61850 MMS and GOOSE can benefit future grids in terms of loss minimization, energy conservation and reliable operation. In conclusion, the result of this study can help distribution network companies and/or operators to achieve higher levels of optimization and control over their assets by investigating new smart grid-based VVO solutions with CVR function such as the proposed approach of this study in a closer-to-reality co-simulation environment presented in this study

Chapter 13.

Analysis Abstract

This chapter gives a brief report on the aims, key results and result analyses of studies discussed in Chapter 12 of this thesis.

Study of section 12.1 investigated the basic approach for proposing a near real-time adaptive VVO and its topology by using AMI data as well as Multi-Agent System concept. The objective function of this study was minimizing the apparent power loss of the system. Three types of residential loads considered in the case study. In first steps the effects of each VVCC in VVO studied separately and in last step, implementation of a near real-time VVO engine with 15-minute time intervals discussed. The study results showed optimal configuration of VVCCs to minimize the apparent power loss of the system. The result of this study was the basis of other studies of this thesis.

Study of section 12.2 tried to minimize the energy loss cost as VVO objective. Moreover, it defined three levels of optimization for proposed VVO (substation only, substation and along feeder(s), all feeder(s) by using DGs). The BCIT case study with five different load types studied and in last part, the effect of using FESS on proposed VVO assessed. The results of this study showed significant cost saving by applying proposed VVO solution and even more saving by using FESS in the system.

Study of section 12.3 assessed the impact of V2Gs on proposed VVO engine. The initial objective of the engine was minimizing the apparent power loss. In second step, CB operating cost minimization added to the VVO objective function. Six different load regions defined for IEEE 37-node distribution network case study. Each load region comprised of different load type and characteristics. Two penetration levels of EV, i.e. normal and high, studied in the presence of VVO. Next, the study assumed that 10% of EVs would be able to support reactive power. The initial results showed considerable amount of loss reduction, especially during peak, using VVO engine. The result analysis proved the fact that daily operation cost of CBs can be reduced by utilizing V2G dispatch-able sources as VAR supporters.

Study of section 12.4 competed the previous study. The main VVO objective of this study was minimizing the active power loss cost as well as the operating cost of CBs considering grid and EV technical constraints. In order to study EV penetration impact on proposed VVO better, a larger case study (IEEE 123-Node distribution grid) used with six different load regions as case study. Six different scenarios investigated in this study: system without EV penetration, system with EV penetration, system with a portion of EVs as VAR supporters, system with VVO and EV penetration, system with VVO and a portion of EVs as VAR supports, and VVO with new objective function to consider V2G reactive power cost in the objective of the VVO engine to find optimal locations of EV charging stations from VVO point of view. The result of this study explained that using a portion of V2Gs as VAR supporters could bring upon a grid with fewer reactive power compensation need and with less CB size and switching number. Moreover, the VVO benefits resulted by V2G VAR supporters could be considered in sizing and placement of EV charging station planning problems.

Section 12.5 presented a study on a day-ahead VVO algorithm using artificial neural network. The VVO objective was maximizing the benefit of loss cost minimization, CB operating cost minimization and CVR benefit maximization. ZIP load model used for the CVR study. Neural Network engine predicted the next day quasi real-time interval loads based on its inputs. The results of this study compared with the ideal case where it was assumed that all loads of the next day quasi real-time intervals are known. The VVO engine results found in this study were very close to the ideal case. This study was the basis of the next study on proposing a live predictive engine for VVO.

Study of section 12.6 proposed a predictive VVO approach using VVO engine, neural network engine and CVR engine working together. It proposed and explained sliding window concept for the VVO to operate in real-time. The objective of the VVO engine was minimizing active power loss and CB operating costs. This approach solved VVCC number of switching per day issue as well. Moreover, the result analysis showed closes objective function minimization to the ideal case.

Study of section 12.7 investigated a new approach for solving maintenance scheduling problem of AMI-based VVO by introducing a Maintenance Scheduling Engine

(MSE) concept. The objective of the VVO engine was active power loss, VVCC operating and CVR costs minimization. Moreover, the objective of MSE was to maximize VVO benefit and to minimize VVCC maintenance fixed and variable costs. The results and result analysis showed that proposed approach could solve maintenance scheduling of VVCC issue without any interruption on the operation of VVO using communication between VVO engine and MSE. This solution considered as an additive part of proposed VVO.

In the study of section 12.8 the PSO algorithm and Fuzzification technique used for solving VVO problem. Here in this study, the objective was minimizing the apparent power loss, voltage deviation and voltage deviation from CVR target. The engine used Fuzzification factors to properly weight each VVO subpart the results of this study showed proper operation of the PSO algorithm. Moreover, it showed that how giving weighting factors to each VVO subpart could lead system to a better optimization results that are in compliance with system and operator needs more.

Study 12.9 focused on finding a more accurate load modeling for AMI-based VVO. The objective of the VVO engine was minimizing of loss, VVCC operational and CVR costs. This study stated the fact that at each quasi real-time interval, the ZIP factor of loads can be different as different types of appliances are used in different times of a day. Hence, it provided a quasi-real-time ZIP models from disaggregated statistical data. The result of this study improved proposed AMI-based VVO performance by using quasi real-time ZIP load coefficients. Moreover, it increased the accuracy level of saved energy consumption calculation in CVR part of the VVO objective function.

Study 12.10 proposed basic design of real-time co-simulation platform for proposed VVO engine using RTDS simulator and DNP3 protocol. The main objective of this study was to minimize the active power loss cost as well as VVCC operational costs. This study performed for 288 time intervals of a day (5-minutes time intervals) to check the precision and the applicability of proposed VVO engine. The results of this study depicted proper performance of the engine during all quasi real-time intervals without any failure.

Study of section 12.11 improved previous study by adding CVR analysis into the system. Hence, the CVR minimization added to the objective function of proposed VVO to conserve the energy consumption. The results of this study showed about 3 percent of energy saving by lowering 3.36 percent of the voltage level.

In next study (section 12.12), communication parameter impact on proposed VVO and real-time co-simulation platform assessed with the same objective function of section 12.10 study. WanemPC software used to emulate different communication conditions such as delays and packet loss and to impose them into the system. The result of testing co-simulation platform showed well operation of the whole system in normal delay conditions. However, due to the inherent limitation of DNP3 protocol, VVO engine lost its robustness in high delay conditions such as 1 second.

Further investigations regarding the performance evaluation of proposed VVO engine with real-time co-simulation test platform continued. Study of section 12.13 fully evaluated VVO performance for 12 different load profiles. The accuracy of proposed VVO engine checked for each season of a year under average load, off-day load and peak load conditions. As such, the VVO engine tested 1152 times using different quasi real-time intervals in a year. The VVO objective minimized the active power, VVCC operational and CVR costs. Fuzzification technique is used to find the accurate weights of each VVO objective function subparts. In addition, comprehensive monitoring platform presented in this study by using RTDS run-time platform. The results showed well-performance of the VVO engine in different load conditions that a system may face with. The result of this study could assist distribution network planners to achieve higher levels of accuracy and efficiency in their system using proposed VVO solution.

Study of section 12-14 assessed the impact of Micro-CHP/PV penetrations on proposed VVO engine. Three penetration levels (low, normal, and high) considered in the system case study. The VVO engine aimed to minimize active power loss as well as VVCC operational and CVR costs. The results of this study showed that increasing penetration of Micro-CHP/PVs enable VVO to minimize its objective function better. VVO could inject less reactive power with fewer number of CB switching per day. In addition, CVR effects

improved by increasing Micro-CHP/PV unit's penetration. Fuzzification technique led to better VVO performance in the presence of this type of DER.

Study of section 12.15 investigated the impact of CES on smart grid-based VVO proposed in this thesis. It used a 50 kW/100 kWh CES unit that was discharging during peak to evaluate the efficiency of the VVO. The VVO objective function was as same as previous section. The results of this study showed significant improvement on objective function minimization of the VVO, peak demand reduction and peak loss reduction by using CES during peak quasi real-time intervals. CES charging period had very small negative impact on the objective function of proposed VVO. As CES units are used for different operational purposes in the grid, optimal using of their four-quadrant inverter for VVO aims needs more investigation in future.

Study of section 12.16 evaluated the impact of EV penetration on smart grid-based VVO of this thesis using real-time con-simulation platform. This study applied the same VVO objective function of previous study. Three levels of EV penetration considered for the case study. Moreover, this study modeled EVs as ZIP loads in order to reach to a more accurate model of EVs. Three different ZIP coefficients for EV defined in literatures of this study. This study employed these coefficients to check the impact of EV penetrations on proposed AMI-based VVO in presented real-time co-simulation platform using DNP3 protocol. The result analysis of this study proved that EV type, mix and usage rate have considerable impact on AMI-based VVO solution. Each EV type could increase or decrease the result values of each VVO subparts in different fashion. Furthermore, the results of this study could help increasing AMI-based VVO solution accuracy by proper modeling of dispatch-able sources such as EVs.

The last study of Chapter 12 presented a real-time co-simulation platform for proposed smart grid adaptive VVO engine by using IEC 61850 MMS and GOOSE. This study explained a comprehensive real-time co-simulation test platform for the VVO engine to operate with IEC 61850 standard commands and/or messages such as MMS and GOOSE. It checked the impact of fault condition and network reconfiguration condition on the performance of the VVO engine. For this reason, IEC 61850 GOOSE generated when a line-to-ground fault occurred in the system. At a same time, IEC 61850 were sent

network configuration changes to the VVO engine. The results of this study showed accurate and efficient performance of proposed VVO in normal and fault with reconfiguration conditions. Furthermore, it showed how proposed VVO engine can operate with and get benefit from advanced IEC 61850 MMS and GOOSE messaging communication standard.

Chapter 14.

Smart Grid Adaptive VVO Roles in Distribution Network Planning Studies

14.1. Preface

Distribution network planning is one of the fundamental parts of distribution networks studies. Basically, distribution network planning aims to improve distribution network reliability, stability, power quality and efficiency in short-term, mid-term and long-term horizons based on distribution system technical and economic needs. Generally, short-term planning studies distribution network for a short-term horizon, e.g. upcoming year or two years. The mid-term planning typically deals with distribution network issues for upcoming years and long-term planning studies distribution network for “upcoming decade(s)” time frame. Here, the main focus is on short and mid-term planning of distribution networks, i.e. near horizon time frames. Each distribution network planning has to follow four consecutive steps to be completed: The first step is grid topology investigation. This step gives distribution network planners an overview of present distribution network topology, infrastructure and asset features and needs. Moreover, as topology is the basis of the operation mode of grid assets, understating grid topology could assist distribution network planners to capture general approximation regarding the operation of the assets.

The second step is to understand grid issues. Each distribution network grapples with its own issues. Weak-points, aged assets and blind parts of distribution grids has to be found in this step, based on historical data, reports and grid topology. In third step, distribution network planner has to find a proper solution for each grid issue according to system technical needs by considering economical factors. The planners can welcome new ideas and novel approaches in order to find the best possible solutions for their grid issues. In last step, the planners need to perform risk assessment on solution candidates.

Typically, the main goals of distribution network short and mid-term planning is to maintain, upgrade and expand distribution networks to improve system level of operation,

reliability, security, stability, quality of service, power quality and efficiency with keeping asset's lifetimes, less carbon footprints and less expenses. Although governmental policies and budget are the key factors of distribution network planning, customer needs can also be taken into account by the network planners. Moreover, distribution network planning problem has to respect Distribution System Operator (DSO) and environmental needs. Environmental factors can be a part of governmental policies as well. Measurements, monitoring, control and optimization of distribution network components such as loads and generation units are the main tools of planners to find short and/or mid-term solutions of distribution networks. In other words, it is possible to consider distribution network planning problem, and optimization problem based on system data according to system economical and technical needs. The result of this optimization problem can be in wide range of field actions. Preventive action, corrective action, change in the configuration, change in the operational mode, change in maintenance, installation (assets and systems), renovation and modernisation are some of the actions resulted by the short term planning optimization problem.

Solving planning optimization problems are crucial for the grid. For instance, system oversizing could increase unnecessary costs of the system. Under-sizing could bring lots of issues such as system overloading and asset failures into the system which leads to rise in system costs. Hence, it is important for network planners to have adequate estimation of network component present features, situations and locations in first step. System configuration, sources of energy supply, load profile and types, asset's location, size and type, measurement tools and/or systems, monitoring and control systems, optimization and management systems, and standards/protocols for communication structure present overall condition of distribution network. Some of the main tasks of distribution network planning are sizing (dimensioning), allocating and type (technology) selection of system assets such as DGs, fixed and switchable shunt CBs, and etc. For each allocation and sizing problem, several costs have to be taken into account:

- Capital Costs (includes Installation Cost): Typically, is a fixed cost that has to be paid for purchasing the assets and or technology.
- Operation & Maintenance (O&M) Costs: O&M costs are generally include variable costs of system that are based on system operation and fixed costs that are apart from system operation changes.

Moreover, reliability indices, network policies and/or strategies that have to be followed by the optimization problem can be included in the optimization problem as objectives, constraints, or incentives/penalties. Other factors that can be considered in planning problem are: time and period of use, internal rate of return of using technology, net benefit gained by using technology, required space, and etc.

Regarding the MV grids, it is possible to classify MV network planning problems into two parts. The first part is HV/MV substation. Substation upgrades, monitoring, control and protection are the main problems. Transformers, measurement devices, IEDs, switchgears as well as automation system are technologies that have to be updated in order to increase system level of observability, reliability and efficiency. The second types of problems are related to distribution feeder components. Cables, Dispersed Generation, loads, VVCCs, smart meters, fuses are some of the main feeder assets that are considered in distribution network planning problems. Moreover, DMS, AMI and demand response are some of the infrastructural systems that their features and needs can be studied in planning problems. For the energy management planning, the effects of system transparency, efficiency (loss minimization, benefit with less expenses), load/generation monitoring, market observation (electricity price) and operational management (generation/load and purchase forecasts, optimization) has to be taken into account. Finally, each approved planning problem (that is based on system policies and data) has to be implemented in specified time period. Moreover, a checking period has to be defined to evaluate the impact of implemented technology in the system through adequate measurement, monitoring and control data. Necessary reviews and/or modifications can be suggested for the planning problem based on explained assessment. Therefore, distribution network planners have to track the performance of each previous planning project in order to propose corrective and/or upgrading plans for specified planning horizons.

14.2. Smart Grid role in Distribution Network Planning

The expansion of smart grids in distribution system can be seen as a result of system needs to be more reliable and efficient. Demand slight growth in most countries worldwide, global warming, as well as growth in customer’s expectation on receiving

reliable energy with high quality of service can be some of the main reasons of interests of utilities and planners to smart grid technology development plans. Smart grid could be a complete solution package for utilities and planners to respond to this demand and enhance grid efficiency, reliability and quality. Smart grids provide IT, communication and power-based intelligence layers over distribution network assets to enhance system level of observability, availability and efficiency. Hence, distribution network planners are seen smart grids as a solution to their planning problems. As such, smart grid expansion, has recently become a part of distribution network planning problems. The smart grid expansion can be in asset expansion such as DGs, CES, EVs, DERs or in system expansion such as EMS, AMI, DMS, monitoring and control.

Both smart grid expansion plans can be implemented in both substation and distribution feeder level. It has to be mentioned that most of smart grid plans have been formed as governmental policies which typically provide incentives for using renewable clean energies instead of using fossil-type generation. As cost-benefit analysis is an inseparable part of planning problems, these incentive policies could ease smart grid planning establishments in distribution networks. Basically, overall system operation (grid, monitoring, control and management systems) specifies system expansion specifications. Penetration of renewables, energy storage systems, backup generations, DGs, EV charging stations, locating monitoring and control are some of the factors that can change distribution network modes of operation as well as system expansion plans. In brief, the expansion of smart grids can be seen as one of the most important tasks of distribution network planning. Thus, planners prefer smart grid-based solutions for distribution networks as these types of solutions are in compliance with smart grid expansion and other planning strategies and policies more than other solutions.

14.3. Smart Grid Adaptive VVO Interactions with Distribution Network Planning Studies

It is possible to investigate the impacts of proposed smart grid-based VVO engine in this thesis in different ways. First, the costs-benefits of this approach have to be compared with conventional approaches or approaches with centralized control. In brief, proposed VVO benefits can be summarized as:

1. Power loss minimization at each quasi real-time interval
2. Energy Conservation using CVR
3. Minimization of switchable CB, OLTC, VR operating costs
4. Less AMI data capturing costs compared with centralized VVO approaches
5. Provide better solution for VVCC Maintenance scheduling problem
6. More reliable solution compared with centralized approach
7. Topology in-line with smart grid control and expansion

On the contrary, the main costs of utilizing this approach include but not limited to:

1. Installation costs (cabling, PC, AMI, communication and setting measurement aggregator costs)
2. Operation & Maintenance costs (VVCC operational costs, crew costs)

The first three benefits, increases system level of efficiency and power quality more than conventional techniques. Regarding operation and maintenance costs, proposed VVO offers new maintenance strategy that solves maintenance scheduling of VVCC problem with no extra cost. This approach provides system with less AMI data transfer cost compared with centralized approach. Moreover, it is compatible with smart grid expansion planning. Therefore, proposed VVO engine can be an attractive solution candidate for VVO from distribution network planner's point of view. The value of this approach became clearer when planners intend to use this approach in a system with decentralized control.

14.3.1. Smart Grid-based VVO from Distribution Network Planning Point of View

From distribution network planning point of view, proposed VVO engine could be suitable for distribution network topologies with decentralized control such as microgrids. It increases system efficiency, reliability and quality and solves couple of distribution network issues such as maintenance scheduling and number of switching per day issue of VVCCs. This proposed solution seems to be cost effective as it has better O&M costs-benefit result, less AMI costs and less communication setting work. Moreover, It is mostly in-line with smart grid expansion and other network planning policies. Regarding risk assessment of this approach, a pilot project need to be implemented. Without a pilot

project, it is hard to fully check the risk of utilizing this solution. Furthermore, the VVO engine proposed in this thesis has to be prepared as a real product in first step. This thesis tried to evaluate risk assessment though using real-time co-simulation platform. The results proved well-performance of the VVO engine in the presence of different load/ network conditions in close-to-reality co-simulation platform. The results of the study on proposed VVO engine that is reliably working with AMI data, as well as DNP3 and IEC 61850 communication protocols can be considered as initial authentication of proposed solution. Further investigations need to be done regarding cost-benefit and risk assessment of proposed VVO as future studies. As stated, making proposed VVO as a product and performing a pilot project could help cost-benefit and risk assessment studies on giving more accurate estimation of solution success.

In order to perform comprehensive risk assessment of any VVO, seven steps has to be followed. The first step is identifying and classifying VVO. In this step, different parts of VVO and its system level of performance has to be primarily identified and then classified. For proposed VVO solution this classification can be summarized as Volt-VAR control assets, optimization & control, monitoring, topology, system level of performance and communication. The second step is identifying technology risk control. Here, the technology of proposed VVO is based on AMI data and other smart grid components. Hence, the risk of each sub-technologies has to be defined. The third step is implementation of control. As mentioned in previous paragraph, pilot project would be necessary for risk assessment to establish a base line for the evaluation of risk this solution may cause. The fourth step is comparing claims with the evidences gathered from implementation. Here in this applicable, the claims can be optimization algorithm failure, communication failure or VVO negative impact on DG performance. These claims are checked in proposed VVO using real-time co-simulation platform. The fifth step verifies and measures the risk level of the system in the presence of applied VVO. The sixth step identifies gaps and the last step proposes risk corrective plan.

In brief, this thesis tried to specify proposed VVO benefits compared with other conventional approaches. Moreover, it checked the performance and reliability of proposed VVO by using a real-time co-simulation platform with advanced communication protocols such as DNP3 and IEC 61850. To perform comprehensive risk assessment and

cost benefit for distribution network plan, proposed VVO engine can be tested in a pilot project as a real product.

14.3.2. Smart Grid-based VVO Impacts on Distribution Network Planning Problems

In order to study the impacts of proposed VVO solution on distribution network planning problem, it is possible to classify grid components into four different groups.

The first group is generating units. DGs, Cogeneration units, DERs, renewable resources such as PVs and storage system such as CES are some of the local generating units discussed in different studies of this thesis. One group of distribution network planning problems are finding optimal location, size and technology of these generating units in the system. The results of different studies in this thesis showed the fact that utilizing these units could increase system efficiency, reduce loss and increase energy conservation. Moreover, this thesis showed that it is possible to use smart inverters for DGs as well as 4-quadrant inverters of CES for reactive power support purposes. This could lead system to a higher level of loss reduction and energy conservation. Moreover, it could save VVCC lifetime by decreasing switching number of each of them. These benefits can be considered in distribution network planning objective function as new values. Considering these new benefits that can be obtained for each quasi real-time interval, could lead distribution network planning to more cost-effective solutions. Even these factors may affect optimal location and sizing of these dispersed generations. In brief, from VVO point of view, dispersed generation could significantly benefit VVO efficiency. Contrariwise, from distribution network planning point of view, dispersed generation expansion, allocation and sizing are some of the optimization problems that has to answer to system different technical and economic needs. Considering the value of savings resulted by proposed VVO in the objective function of the planning problem could lead to a better optimal solution.

The second group are loads and dispatch-able resources such as V2Gs. Different load types considered in different studies of this thesis such as residential, commercial and industrial loads. Moreover, this thesis provide a better approach for load model based on quasi real-time ZIP load modeling to precisely calculate VVO benefits and to model

loads and dispatch-able resources such as EVs with more precision. These studied could definitely help distribution network planning problems on their sizing, allocation and technology selection problems that are depending on load type, mix and level such as fixed/switchable capacitor placement. Moreover, this thesis showed that in near future it is possible to receive reactive power supports from V2Gs and EV charging stations. Considering the value of loss reduction via these sources within planning objective function may help planning problems to reach to a better optimal solution. For instance, in order to solve EV charging station allocation and size, it is now conceivable to consider EV charging station benefit on loss reduction through reactive power support in planning problem. One of the thesis studies showed that EV optimal location changed and reduced the usage of switchable CBs in the system. In brief, considering AMI-based VVO benefits in planning problem seems to be a more accurate method as it shows the real values of each component of the system as well as their interactions with each other.

The third group of grid components are Volt-VAR Control Components (VVCCs). One of the main tasks of distribution network planning is to find the optimal size, location and type of fixed and switchable CBs, as well location and type of OLTCs and VRs in the system. As explained, the size and location of CBs can be changed in planning problem by changing load centers due to utilizing dispersed generation (group-one) and dispatch-able resources (group-two) and penetration of these two groups. For instance, using of components in these two groups, that are able to support reactive power compensation, could lead to a system with less need to CB. Hence, CB size and placement planning problem has direct relation with penetration of generation, load and dispatch-able resource penetrations and operational conditions. These may impose some changes into VVCC systems such as CB relocation, CB upgrade or change. Another important impact of VVO on VVCCs is related to the CVR part. As CVR tries to lower voltage level of termination points into lower limits of ANSI band to conserve energy, it can have considerable impact on the location of VRs or even CBs. Typically, VRs are located in places where the voltage regulation is needed. These VRs are mostly placed close to system nodes which they have under-voltage issues in general or during peak. In recent years, penetrations of dispersed generation according to smart grid expansion plans have led voltages of these nodes to higher values than expected. This fact was one of the key motivations of utilities to re-think about lowering voltage levels of termination points to conserve energy that

nowadays called CVR. Therefore, CVR has never been a part of VR allocation planning problem objective function. Considering CVR benefits (that can be obtained through using VRs) in VR planning problems could change the optimal locations of VRs. In brief, proposed VVO studies could help VVCC planning problems to be more accurate.

The last group is the intelligence layers that different components such as monitoring, control and optimization tools can provide. First, it has to be reminded that proposed VVO uses AMI data to perform at each quasi real-time interval. Hence, it brings visibility from substation into the edge of the feeder. Quasi real-time optimization could be an applicable solution which is in compliance with control and monitoring systems. Predictive VVO proposed in this thesis and the AMI data could provide a great substation to feeder database that can be used for different planning purposes. Moreover, proposed VVO as one of the tasks of DMS can be integrated with other systems using recent communication protocols/standard such as DNP3 and IEC 61850. Moreover, the last study of Chapter.12 showed that proposed VVO would be able to perform in different system operational and configuration modes. In planning problem of these intelligence layer tools, AMI-based VVO benefits can be considered as well.

In conclusion, proposed VVO engine in this thesis could help different distribution network planning as well as smart grid expansion problems in terms of accuracy and efficiency.

Chapter 15.

Conclusions and Future Works

This chapter primarily presents principal conclusions of this dissertation and then, it explains recommendations and probable future works.

15.1. Conclusions

This thesis proposed a smart grid adaptive Volt-VAR Optimization approach for smart distribution networks using smart grid technologies such as AMI, dispersed generations and dispatch-able sources. Using quasi real-time data from AMI provided an unprecedented opportunity for distribution system to be optimized more effectively. The main topology as well as command and control strategy of proposed VVO primarily introduced. In first steps of design, three levels of performance considered for the VVO engine; VVO could confine its operation to distribution substation, VVO could perform within substation and along distribution feeder(s) and VVO could benefit from other available Volt-VAR control sources such as DGs, V2Gs and CES of the system. Several VVO studies were completed to investigate the impacts of V2Gs and CES on proposed VVO engine. The results of these studies showed the fact that utilizing these sources as active power and VAR supporters can enhance the efficiency of proposed VVO. Moreover, their impacts on VVO optimal results and on related distribution network planning problems are considerable that could hardly be ignored in recent VVO studies. Comprehensive objective function presented for the VVO engine which is comprised of Conservation Voltage Reduction as significant VVO subpart. Considering CVR as a part of VVO led proposed VVO to conserve energy besides completing other VVO objectives. In order to perform the optimization closer to real-time, predictive techniques proposed in this thesis. First, a day-ahead predictive algorithm presented that could predict the quasi real-time loads of the next day to act online. Then, a novel predictive engine proposed based on online sliding window concept to present a more dynamic and applicable engine for VVO. Predictive solutions provided in this thesis could solve VVCC allowable switching number of per day issue. In order to solve maintenance scheduling problem of VVCCs in

an AMI-based VVO approach, a Maintenance Scheduling Engine (MSE) proposed in this thesis. MSE is able to operate with the VVO engine taking both VVO and maintenance scheduling objective/constraints into account. The results of maintenance scheduling study showed that this approach could solve maintenance scheduling of VVCC issue without interference with the grid and/or VVO engine tasks. In order to complete VVO objective function structure and to design a VVO approach in-line with system and/or operator needs, weighting factors defined for each VVO engine objective function subpart. Fuzzification technique employed to find accurate weighting factors of each subpart based on distribution grid operational/economic requirements. Quasi real-time ZIP load modeling proposed in this thesis in order to be more precise on calculating the saved energy using CVR.

In order to test the performance and the applicability of proposed VVO, a real-time co-simulation platform set up using RTDS, GTNET measurement aggregator, OPC-toolbox and DNP3 communication protocol. Thus, both theoretical and experimental studies were performed to validate proposed VVO results from different system operational aspects. This real-time co-simulation platform helped checking the performance of the VVO in different distribution network operational conditions. Checking the performance and the efficiency of proposed VVO for 5-minute quasi real-time interval operation, checking the VVO performance in different communication conditions, and testing proposed VVO in 12 different load profiles of a year, i.e.1152 quasi real-time intervals, were some of the studies of this thesis that used mentioned real-time co-simulation platform as a test-bench. The results of these studies proved well-performance of proposed VVO in different normal operating conditions of distribution networks. The impacts of Micro-CHP/PV and EV penetrations on proposed VVO verified using mentioned real-time co-simulation platform. The results of Micro-CHP/PV study demonstrated improvement in VVO efficiency by increasing penetration of such DERs in the system. Moreover, the results of EV penetration study showed that the type, mix and usage rate have substantial impacts on VVO efficiency that need to be taken into account in smart grid-based VVO studies. At last but not least, a real-time co-simulation platform provided for testing the precision, efficiency and applicability of proposed VVO in the presence of a fault condition that could change distribution network configuration. IEC 61850 communication standard, used in co-simulation platform design to assist VVO

understanding grid configuration changes in order to perform reliably without any interruption and/or failure. The results of this study proved robust performance of proposed VVO using IEC 61850 MMS and GOOSE messaging.

In conclusion, the quasi real-time smart grid adaptive VVO engine proposed in this dissertation could lead smart distribution networks to achieve higher levels of accuracy, efficiency and reliability. As control topology of proposed VVO solution in this thesis is in consonance with distributed command and control topology of smart grids, proposed VVO solution provides a robust-but-flexible approach for VVO to be updated according to distribution network technical/economic future needs. Therefore, distribution networks smartening up plans could also be mitigated using proposed VVO solution of this thesis.

15.2. Recommendations for Future Works

According to comprehensive theoretical and experimental analysis executed in this thesis, in order to propose an efficient and applicable smart grid adaptive VVO solution, it is possible to recommend several future works that could benefit smart distribution grids in terms of accuracy, efficiency, and reliability. Regarding the study on investigating the impact of dispatch-able sources such as EVs, as reactive power support sources, on smart grid adaptive VVO, economic factors such as investment costs and Internal Rate of Return (IRR) can be taken into account in distribution network planning study in order to evaluate the cost-effectiveness of using V2Gs as reactive power supporting sources. Regarding the optimization technique, approximation-based techniques such as Meta modeling could be great candidates for having a faster prediction engine optimization for presented online sliding window. Regarding maintenance scheduling of VVCCs, As VVO objective function weighting factors have significant impact on the maintenance scheduling problem, and as these factors can be affected by other maintenance factors such as value of loss minimization, the electricity price, or market clearing price, optimal prediction of these factors in quasi real-time VVOs can be one of the studies for future maintenance scheduling of VVCCs.

Regarding CVR studies, economic factors such as VVO AMI costs, VVO engine cost, existing VVCC operating/switching costs, required VVCC costs, VVCC switching

value cost, communication facility costs, revenue earned by loss reduction, revenue earned through energy consumption saving and the value of demand reduction have to be taken into account in CVR planning cost-benefit analysis. As lost-revenue value is still a major concern of some electric power utilities, further study on comprehensive cost-benefit analysis of quasi real-time CVR could assist utilities on their CVR plan choices. Regarding quasi real-time ZIP modeling for CVR, It has to be stated that significant factors such as day type, calendar, weather, seasonal variations, environmental conditions and geographical factors could affect load types and consumptions. Hence, it is possible to track the same steps explained in this thesis to find more accurate quasi real-time ZIP coefficients for other types of days as well as other seasons. This could necessitate further studies related to new adaptive load models of quasi real-time CVRs. Other techniques such as sensor placement that may increase the accuracy of quasi real-time load models could also be studied as future work despite the fact that these techniques could be costly. New disaggregation methods could also improve CVR (solely or as a part of VVO) performance. As such future works can be focused on more efficient disaggregation methods in order to find more accurate quasi real-time ZIP coefficients of loads.

In order to solve DNP3 communication network protocol limitation in very high delay conditions, IEC 61850 MMS client server measurement could be an alternative candidate for smart grid adaptive VVO in presented co-simulated environment of this thesis. Applying predictive algorithms to find weighting factors for each quasi real-time stage for VVO engine sub-parts can be a novel future study that may help VVO to perform more efficient in the presence of different micro-generation penetration, dispatch -able resource penetration and loads. Regarding community energy storage systems, further studies need to be investigated on designing a management tool to coordinate different but related CES tasks with proposed VVO engine objective in future.

Another important future study can be on updating proposed VVO engine to efficiently work in electricity markets with different pricing strategies. For this reason, the VVO engine possessor has to primarily defined. The VVO engine has to build a direct link to Distribution System Operator (DSO) to initially capture the needs of the market as well as the grid and then, help DSO on its operation and maintenance tasks. Hence, the role of smart grid based VVO solution could be an interesting topic of a future study.

As explained in Chapter 13, comprehensive cost-benefit analysis of proposed VVO necessitates realization of VVO as a product. Hence, studies on making proposed VVO as a product could be another future study. Proposed VVO could have a user friendly interface that could enable its users to benefit from different options such as accessibility to library of distribution grid models and various components. Moreover, they may intend to design their own grid in VVO platform or select VVO objective function due to their grid needs from VVO objective function library. These noteworthy options as well as attaching proposed VVO engine to real distribution network components e.g. VVCCs and control systems, e.g. DMS/SCADA, through advanced communication protocols could be a valuable practical future work. Complete cost-benefit analysis can be executed in future through finding the key expenses of VVO implementation besides evaluating VVO short-term/long-term benefits for distribution grids.

Last but not least, smart grid adaptive VVO roles in distribution network short-term, mid-term and long-term planning problems can be further investigated. As stated in Chapter 13, various distribution network planning problems are in direct relation with VVO problem. The performances of planning studies such as VVCC, DG, DER, EV charging station sizing, placement and type selections can be improved by taking proposed smart grid adaptive VVO considerations into account in the objective of their optimization problems. Changes in the results of these planning studies have significant impact on distribution network as well as smart grid expansion plans.

References

[1] Electrical Power Systems and Equipment-Voltage Ratings, ANSI Standard C 84.1, 1995.

[2] CAN3-C235-83-Preferred voltage levels for AC systems, 0 to 50 000 V, Canadian Standard Association (CSA), 1983, reaffirmed, 2010.

[3] H. Farhangi, "The Path of Smart Grid," *IEEE Power & Energy Magazine*, vol. 8, no. pp. 18-28, Jan. 2010.

[4] H. Farhangi, "A road map to integration," *IEEE Power Energy Magazine*, vol. 12, no. 3, pp. 52-66, May/Jun. 2014.

[5] J. D. McDonald, "Integrating DA with AMI May Be Rude Awakening For Some Utilities," *Renew Grid*, 20 Feb. 2013.

[6] D. Divan, R. Moghe, and A. Prasai, "Power Electronics at the Grid Edge, the Key to Unlocking Value from the Smart Grid," *IEEE Power Electronics Magazine*, pp. 16-21, 18 Dec. 2014.

[7] B. Uluski, "Volt/VAR Control and Optimization Concepts and Issues," Electric Power Research Institute (EPRI), 2011, [Online] Available: http://cialab.ee.washington.edu/nwess/2012/talks/uluski.pdf

[8] H. Farhangi, "Paradigm Shift in Transitioning from a Centralized Grid to a Decentralized Grid," *IEEE Canadian Review*, Smart Grid Part-1, pp. 18-20, Spring 2014.

[9] L. F. Blume, "Characteristics of Load Ratio Control Circuits for Changing Transformer Ratio Under Load," *Transaction of the American Institute of Electrical Engineers*, vol. 51, no. 4, pp. 952-956, Dec. 1932.

[10] S. Narita, and M. S. A. A. Hammam, "A Computational Algorithm for Real-time Control of System Voltage and Reactive Power, Part I Problem Formulation," *IEEE Transactions on Power Apparatus and Systems*, Vol. 90, pp. 2495-2501, Nov. 1971.

[11] S. Narita, and M. S. A. A. Hammam, "A Computational Algorithm for Real-time Control of System Voltage and Reactive Power, Part II Algorithm if optimization," *IEEE Transactions on Power Apparatus and Systems*, Vol. 90, pp. 2502-2508, Nov. 1971.

[12] A. Kishore, and E. F. Hill, “Static Optimization of Reactive Power Sources by Use of Sensitivity Parameters,” *IEEE Transactions on Power Apparatus and Systems*, Vol. 90, pp. 116-1173, May 1971.

[13] A. Kuppurajulu, and K. Raman Nayar, “Optimisation of Capacitor Installations in Distribution Systems,” *IEE-IERE Proceedings*, India, vol. 10, issue. 6, pp. 186-199, Nov.-Dec. 1972.

[14] R. Billinton, and S. S. Sachdeva, “Real and Reactive Power Optimization by Suboptimum Techniques,” *IEEE Transactions on Power Apparatus and Systems*, vol. 92, no. 3, pp. 950-956, 1973.

[15] R. R. Shoults, and M. S. Chen, “Reactive Power Control by Least Square Minimization,” *IEEE Transactions on Power Apparatus and Systems*, vol. 95, no. 1, pp. 325-334, Jan-Feb1976.

[16] S. Rama Iyer, K. Ramachandran, and S. Hariharan, “New Technique for Optimal Reactive-power Allocation for Loss Minimisation in Power Systems,” *IEE Generation, Transmission and Distribution*, vol. 130, issue 4, 178-182, 1988.

[17] J. S. Thorp M. Ilic-Spong and M. Varghese, “Optimal Secondary Voltage-VAr Control Using Pilot Point Information Structure,” in *Proc. 23rd Conference on Decision and Control*, Las Vegas, NV, Dec. 1984.

[18] J. J. Grainger, and S. Civanlar, “Volt/VAr Control on Distribution Systems with Lateral Branches Using Switched Capacitors and Voltage Regulators, Part I: The Overall Problem,” *IEEE Transactions on Power Apparatus and Systems*, vol. PAS-104, no. 11, pp. 3278-3283, Nov. 1985.

[19] J. J. Grainger, and S. Civanlar, “Volt/VAr Control on Distribution Systems with Lateral Branches Using Switched Capacitors and Voltage Regulators, Part II: The Solution Method,” *IEEE Transactions on Power Apparatus and Systems*, vol. PAS-104, no. 11, pp. 3284-3290, Nov. 1985.

[20] I. Roytelman, and S. M. Shahidehpour, “Practical Aspects of Distribution Automation in Normal and Emergency Conditions,” *IEEE Transactions on Power Delivery*, vol. 8, no. 4, pp. 2002-2008, Oct. 1993.

[21] I. Roytelman, B. K. Wee, and R. L. Lugtu, “Volt/VAr Control Algorithm for Modern Distribution Management System,” *IEEE Transactions on Power Systems*, vol. 10, no. 3, pp. 1454-1460, Aug. 1995.

[22] S. Auchariyamet and S. Sirisumrannukul, “Volt/VAr Control in Distribution Systems by Fuzzy Multiobjective and Particle Swarm,” in *Proc. 6th International conference on Electrical Engineering/ Electronics, Computer, Telecom. and Info. Tech., ECTI-CON*, Pattaya, Thailand, May 2009.

[23] A. Rahideh, M. Gitizadeh and A. Rahideh, “Fuzzy Logic in real time voltage/reactive power control in FARS regional electric network,” *Electric Power System Research*, no. 76, pp. 996-1002, Feb. 2006.

[24] B. Alencar de Souza and A. M. F de Almeida, “Multiobjective Optimization and Fuzzy Logic Applied to Planning of the Volt/VAr Problem in Distribution Systems,” *IEEE Transactions on Power Systems*, vol. 11, pp. 1274–1281, Aug. 2010.

[25] A. T. Saric and A. M. Stankovic, “A Robust Algorithm for Volt/VAr Control” in *Proc. Power System Conference and Exposition, PSCE09, IEEE PES*, Seattle, WA, 2009.

[26] G. A. Bakare, G. Krost, K. Venayagamoorthy and U. O. Aliyu, “Comparative Application of Differential Evolution and Particle Swarm Techniques to Reactive Power and Voltage Control,” in *Proc. International Conference on IA Applications to Power Systems*, Niigata, Japan, Nov. 2007.

[27] D. H. Spatti, I. N da Silva, W. F. Usida and R. A. Flauzino, “Real-Time Voltage Regulation in Power Distribution System Using Fuzzy Control,” *IEEE Transactions on Power Delivery*, vol. 25, pp. 1112–1123, Apr. 2010.

[28] R. Singh, F. Tuffner, J. Fuller and K. Schneider, “ Effects of Distributed Energy Resources on Conservation Voltage Reduction (CVR)” in *Proc. IEEE Power and Energy Society General Meeting,* San Diego, CA, USA, Jul. 2011.

[29] S. Auchariyamet and S. Sirisumrannukul, “Optimal Daily Coordination of Volt/VAr Control Devices in Distribution Systems with Distributed Generators,” in *Proc. 45th International Universities Power Engineering Conference (UPEC)*, Cardiff, Wales, Sep. 2010.

[30] W. Huang, G. X. Xia, N. Kobayashi and X. Xu, “Distributed Generation on Distribution System Voltage Regulation: An Optimization-based Approach,” in *Proc. IEEE Power and Energy Society General Meeting*, Minneapolis, MN, USA, Jul. 2010.

[31] E. Jauch, “Volt/VAr Management? An Essential “SMART” Function,” in *Proc. IEEE PES Power System Conference and Exposition, PSCE09*, Seattle, WA, Mar. 2009.

[32] N. Markushevich, “The Benefits and Challenges of the Integrated Volt/VAr Optimization in the Smart Grid Environment,” in *Proc. IEEE Power and Energy Society General Meeting,* San Diego, CA, USA, Jul. 2011.

[33] R. W. Uluski, “VVC in Smart Grid Era,” in *Proc. IEEE Power and Energy Society General Meeting*, Minneapolis, MN, USA, Jul. 2010.

[34] E. T. Jauch, “Possible Effects of Smart Grid Functions on LTC Transformers” *IEEE Transactions on Industry Applications*, vol. 47, pp 1013–1021, Apr. 2011.

[35] V. Dabic, S. Cheong J. Peralta, and D. Acebedo, “BC Hydro's Experience on Voltage VAR Optimization in Distribution System,” in *Proc. IEEE PES Transmission and Distribution Conference and Exposition*, New Orleans, LA, USA, Apr. 2010.

[36] H. Fakham, F. Colas and X. Guillaud, “Real-time Simulation of Multi-Agent System for Decentralized Voltage Regulation in Distribution Network,” in *Proc. IEEE Power and Energy Society General Meeting*, San Diego, CA, USA, Jul. 2011.

[37] A. Ajaja, “Reinventing Electric Distribution,” *IEEE Potentials*, vol. 29, pp. 29-31, Jan.-Feb. 2010.

[38] Electric Power Research Institute (EPRI), “EPRI Smart Grid Demonstration Update,” (An EPRI Progress Report, March 30, 2011).

[39] G. Stanciulescu, H. Farhangi, A. Palizban, and N. Stanchev, “Communication Technologies for BCIT Smart Microgrid,” in *Proc. IEEE PES Innovative Smart Grid Technologies (ISGT)*, Washington DC, Jan. 2012.

[40] H. Farhangi, “Campus Based Smart Microgrid at British Columbia Institute of Technology in Vancouver, Canada,” *Presented at Cigré 2011 Bologna Symposium*, Italy, Sept. 2011.

[41] A. Palizban, and H. Farhangi, “Low Voltage Distribution Substation Integration in Smart Microgrid,” in *Proc. IEEE 8th International Conference on Power Electronics*, Jeju Island, South Korea, Jun. 2011.

[42] H. Farhangi, “Intelligent Microgrid Research at BCIT,” in *Proc. IEEE Electric Power Conference, EPEC’08*, Vancouver, Canada, Oct. 2008.

[43] S. Lefebvre, G. Gaba, A. O. Ba, D. Asber, A. Richard, C. Perreault, and D. Chattrand, “Measuring the Efficiency of Voltage Reduction at Hydro-Quebec Distribution,” *in Proc. IEEE Power and Energy Society General Meeting, 21st Century*, Pittsburg, PA, USA, Jul. 2008.

[44] A. Ajaja, “Volt and VAr Control for Energy Efficiency at Hydro-Quebec Distribution,” *Metering International, SmART Energy*, Issue 3, 2011.

[45] H. Fakham, A. Ahmidi, F. Colas, and X. Guillaud, “Multi-Agent System for Distributed Voltage Regulation of Wind Generators Connected to Distribution Network,” in *Proc. IEEE PES Innovative Smart Grid Technologies Conference Europe (ISGT Europe)*, Gothenburg, Sweden, Oct. 2010.

[46] T. L. Wilson, “Measurement and Verification of Distribution Voltage Optimization Results for IEEE Power & Energy Society” in *Proc. IEEE Power and Energy Society General Meeting, Minneapolis*, MN, USA, Jul. 2010.

[47] H. Diaz, I. Harnisch, R. Sanhueza, and R. Olivares, “Feeder Reconfiguration and Capacitor Placement in Distribution Systems: An Approach for Simultaneous Solution Using a Genetic Algorithm,” *I. R. C. Ingenierfa journal*, vol. 18, no. 1, pp. 144-153, Apr. 2010.

[48] G. Svenda, V. Strezoski, Z. Simendic, and V. Mijatovic, “Real time Voltage Control Integrated in DMS,” in *Proc. 20th International Conference on Electricity Distribution, CIRED*, Prague, Jun. 2009.

[49] A. Mohd, “Supervisory Control and Energy Management of an Inverter-based Modular Smart Grid,” in *Proc. IEEE PES Power Systems Conference and Exposition*, Seattle, WA, USA,15-18 March 2009.

[50] A. Vaccaro, G. Velotto, and A. F. Zobaa, “A Decentralized and Cooperative Architecture for Optimal Voltage Regulation in Smart Grids,” *IEEE Transactions on Industrial Electronics*, vol. 58, no. 10, pp. 4593-4602, Oct. 2011.

[51] H. Johal, Wei Ren, Yan Pan, and M. Krok, “An integrated approach for controlling and optimizing the operation of a power distribution system,” in *Proc. IEEE PES Innovative Smart Grid Technologies Conference Europe (ISGT Europe)*, Gothenburg, Sweden, Oct. 2010.

[52] M. J. Krok, and S. Genc, “A Coordinated Optimization Approach to Volt/VAr Control for Large Power Distribution Networks,” in *Proc. American Control Conference on O'Farrell Street*, San Francisco, CA, USA, June 29 -July 2011.

[53] Department of Energy, Energy Efficiency in Distribution Systems, Impact Analysis Approach, 30 November, 2012, [Online]. Available: https://www.smartgrid.gov/recovery_act/program_impacts/energy_efficiency_improvements_distribution_systems.html

[54] M. Prevallet, and T. Johnson, Regional Director-Energy Automation Solutions, Integrated Volt/VAR Control, COOPER Power System, [Online]. Available: http://assets.fiercemarkets.net/public/smartgridnews/Optimizing_Voltage.pdf

[55] Volt-VAr management solutions for smart grid distribution automation applications, Volt-VAr management solutions, ABB Company, [Online]. Available: https://library.e.abb.com/public/d9e73a8d3d91161bc1257b6a006cc340/VVMS%20brochure_final_v4.pdf

[56] M. Shahidehpour, and Y. Wang, Hierarchical and Distributed Control of Voltage/VAR, Published: DOI: 10.1002/0471462926.ch9, John Wiley & Sons, Feb. 2005.

[57] S. Borlase, Smart Grids: Infrastructure, Technology, and Solutions, CRC Press, ISBN-10: 1439829055.1st edition, Oct. 24 2012.

[58] DTE Energy, Volt-VAR Optimization, May 21, 2014, [Online]. Available: http://naruc.org/International/Documents/DTE%20Energy_May%2021_Wednesday__2_15PM_eng.pdf

[59] D. Divan, Grid Edge Control, IEEE T&D Meeting, April 2014, [Online]. Available: http://www.ieee-pes.org/presentations/td2014/td2014p-000693.pdf

[60] EVVOLUTION: Decentralized VVO Unlocks CVR Savings, GRIDCO Systems, 2015.

[61] R. F. Preiss, and V. J. Warnock, "Impact of Voltage Reduction on Energy and Demand," *IEEE Transactions on Power Apparatus and Systems*, vol. 97, no. 5, pp. 1665-1671, Sep. 1978.

[62] R. F. Preiss, V. J. Warnock, "Impact of Voltage Reduction on Energy and Demand: Phase II," *IEEE Transactions on Power Systems*, vol.1, no. 2, pp. 92-95, May 1986.

[63] D. M. Lauria, "Conservation Voltage Reduction (CVR) at Northeast Utilities," *IEEE Transactions on Power Delivery*, vol. 2, no. 4, pp. 1186-1191, Oct. 1987.

[64] B. W. Kennedy, and R. H. Fletcher, "Conservation Voltage Reduction (CVR) at SNOHOMISH County PUD," *IEEE Transactions on Power Systems*, vol. 6, no. 3, pp. 986-998, Aug. 1991.

[65] D. Kirshner, "Implementation of Conservation Voltage Reduction at Commonwealth Edison," *IEEE Transactions on Power Systems*, vol. 5, no. 4, pp. 1178-1182, Nov. 1990.

[66] N. S. Markushevich, I. C. Herejk, and R. E. Nielsen, "Functional Requirements and Cost-benefit Study for Distribution Automation at B.C. Hydro," *IEEE Transactions on Power Systems*, vol. 9, no. 2, pp. 772- 781, May 1994,.

[67] T. L. Wilson, "Energy Conservation with Voltage Reduction-Fact or Fantasy", in *Proc. IEEE Rural Electric Power Conference*, Colorado Springs, Co, May 2002.

[68] R. H. Fletcher, and A. Saeed, "Integrating Engineering and Economic Analysis for Conservation Voltage Reduction," in *Proc. IEEE Power and Energy Society General Meeting*, pp. 725-730, Chicago, IL, USA, Jul. 2002.

[69] Global Energy Partners LLC, Utility Distribution System Efficiency (DEI), Northwest Energy Efficiency Alliance Report #08-192, Portland, Oregon, USA, Jun. 27, 2008.

[70] L. Schwartz, Is It Smart If It Is Not Clean? Strategies for Utility Distribution Systems, Part One, RAP, Montpelier, Vermont, USA, May 2010.

[71] K. P. Schneider, F. K. Tuffner, J. C. Fuller, and R. Singh, Evaluation of Conservation Voltage Reduction (CVR) on a National Level, Pacific Northwest National Laboratory, United States Department of Energy, DE-AC05-76RL01830, Jul. 2010.

[72] M. Wakefield, EPRI Smart Grid Demonstration Initiative & Early Results, EPRI Clean Energy-Session 7, GreenGov Symposium, Washington DC, USA, Nov. 2011.

[73] Electric Authority, Te Mana Hiko, [Online]. Available: https://www.ea.govt.nz/

[74] S. Rahimi, M. Marinelli, and F. Silvestro, "Evaluation of Requirements for Volt/Var Control and Optimization Function in Distribution Management Systems," in *Proc. 2nd IEEE ENERGYCON Conference and Exhibition, Future Energy Grids and Systems Symposium*, Florence, Italy, Sep. 2012.

[75] Z. Shen, and M. E. Baran, "Gradient based Centralized optimal Volt/Var Control Strategy for Smart Distribution System," in *Proc. IEEE PES Innovative Smart Grid Technologies (ISGT)*, Washington DC, USA, Feb. 2013.

[76] M. Diaz-Aguilo, J. Sandraz, R. Macwan, F. de Leon, D. Czarkowski, C. Comack, and D. Wang, "Field-Validated Load Model for the Analysis of CVR in Distribution Secondary Networks: Energy Conservation," *IEEE Transactions on Power Delivery*, vol. 28, no. 4, Oct. 2013.

[77] J. Solanki, N. Venkatesan, and S. Khushalani, "Coordination of Demand Response and Volt/Var Control Algorithm using Multi Agent System," in *Proc. 2012 IEEE PES Transmission and Distribution Conference and Exposition*, Orlando, USA, May 2012.

[78] B. Shah, A. Bose, and A. Srivastava, "Load Modeling and Voltage Optimization using Smart Meter Infrastructure," in *Proc. IEEE PES Innovative Smart Grid Technologies (ISGT)*, Washington DC, USA, Feb. 2013.

[79] IEEE Std. 2030, IEEE Guide for Smart Grid Interoperability of Energy Technology and Information Technology Operation with the Electric Power System (EPS), End-Use Applications, and Loads, Sep. 2011.

[80] Z. Xiao, T. Li, M. Huang, J. Shi, J. Yang, J. Yu, and W. Wu, "Hierarchical MAS based Control Strategy for Microgrid," *Energies Journal*, vol. 3, no.9, pp. 1622-1638, Sep. 2010.

[81] K. P. Schneider, and T. F. Weaver, "A method for evaluating Volt-VAR Optimization field demonstrations," *IEEE Transactions on Smart Grid*, vol. 5, no. 4, pp. 1696-1703, Jul. 2014.

[82] R. Uluski, “Using standards to integrate distributed energy resources with distribution management systems,” in *Proc. 22nd International Conference on Electricity Distribution (CIRED)*, Stockholm, Sweden, Jun. 2013.

[83] R. C. Green, L. Wang, and M. Alam, “The Impact of Plug-in Hybrid Electric Vehicles on Distribution Networks: a Review and Outlook,” in *Proc. IEEE Power and Energy Society General Meeting*, Minneapolis, USA, Jul. 2010.

[84] S. S. Raghavan, and A. Khaligh, “Impact of Plug-in Hybrid Electric Vehicle Charging on a Distribution Network in a Smart Grid Environment,” in *Proc. IEEE PES on Innovative Smart Grid Technology (ISGT)*, Washington DC, Jan. 2012.

[85] C. Weiller, “Plug-in Hybrid Electric Vehicle Impacts on Hourly Electricity Demand in the United States,” *Energy Policy Journal*, vol. 39, pp. 3766-3778, 2011.

[86] Z. Darabi, and M. Ferdowsi, “Plug-in Hybrid Electric Vehicles: Charging Load Profile Extraction Based on Transportation Data,” in *Proc. IEEE Power and Energy Society General Meeting*, Detroit, Michigan, Jul. 2011.

[87] S. Shao, T. Zhang, M. Ipattanasomporn, and S. Rahman, “Impact of TOU Rates on Distribution Load Shapes in a Smart Grid with PHEV Penetration,” in *Proc. IEEE PES Transmission and Distribution Conference and Exposition,* New Orleans, LA, USA, Apr. 2010.

[88] K. Clement, H. Haesen, and J. Driesen, “Coordinated Charging of Multiple Plug-In Hybrid Electric Vehicles in Residential Distribution Grids,” in *Proc. IEEE PES Power Systems Conference and Exposition*, Seattle, USA, Mar. 2009.

[89] S. Acha, T. C. Green, and N. Shah, “Effects of Optimised Plug-in Hybrid Vehicle Charging Strategies on Electric Distribution Network Losses,” in *Proc. IEEE PES Transmission and Distribution Conference and Exposition*, New Orleans, LA, USA, Apr. 2010.

[90] S. Gao, K. T. Chau, C. C. Chan, and D. Wu, “Loss Analysis of Vehicle-to-Grid Operation,” in *Proc. IEEE Vehicle ad Power Propulsion Conference (VPPC)*, Lille, France, Sep. 2010.

[91] M. C. Kisacikoglu, B. Ozpineci, and L. M. Tolbert, “Effects of V2G Reactive Power Compensation on the Component Selection in an EV or PHEV Bidirectional Charger,” in *Proc. IEEE Energy Conversion Congress and Exposition (ECCE)*, pp.870-876, Atlanta, Georgia, USA, Sep. 2010.

[92] M. C. Kisacikoglu, B. Ozpineci, and L. M. Tolbert, “Reactive Power Operation Analysis of a Single-Phase EV/PHEV Bidirectional Battery Charger,” in *Proc. 2011 8th International Conference on Power Electronics (ECCE)*, pp. 585-592, Jeju, Korea, May/Jun. 2011.

[93] M. C. Kisacikoglu, B. Ozpineci, and L. M. Tolbert, “Examination of a PHEV Bidirectional Charger System for V2G Reactive Power Compensation,” in *Proc. 26th Annual IEEE Applied Power Electronics Conf. and Exposition (APEC)*, Fort Worth, USA, Mar. 2011.

[94] M. A. Fasugba, and P. T. Krein, “Gaining Vehicle-to-Grid Benefits with Unidirectional Electric and Plug-in Hybrid Vehicle Chargers,” in *Proc. IEEE Vehicle Power and Propulsion Conference*, Chicago, USA, Sep. 2011.

[95] M. Ehsani, M., Falahi, and S. Lotfifard, “Vehicle to Grid Services: Potential and Applications,” *Energies Journal*, vol. 5, pp. 4076-4090, 2012.

[96] M. C. Kisacikoglu, B. Ozpineci, and L. M. Tolbert, “EV/PHEV bidirectional charger assessment for V2G reactive power operation,” *IEEE Transactions on Power Electronics*, vol. 28, no. 12, pp. 5717-5727, Dec. 2013.

[97] W. Yang, Z. Zhang, J. Wang, and Y. Gao, “Simulation of Electric Vehicle charging station and harmonic treatment,” in *Proc. 2012 International Conference on Systems and Informatics (ICSAI2012)*, pp. 609-613, Yantai, China, May 2012.

[98] S. Zhang, X. Ai, W. Liang, and R. Dong, “The influence of the electric vehicle charging on the distribution network and the solution,” in *Proc. IEEE Asia Pacific Conf. and Exposition on Transportation Electrification*, Beijing, China, Aug. 31/Sept. 3, 2014.

[99] A. Bosovic, M. Music, and S. Sodovic, “Analysis of the impacts of plug-in electric vehicle charging on the part of a real medium voltage distribution network,” in *Proc. IEEE PES Innovative Smart Grid Technologies (ISGT)*, Istanbul, Turkey, Oct. 2014.

[100] A. Kriukov, and M. Gavrilas, “Smart energy management in distribution networks with increasing number of electric vehicles,” in *Proc. International Conference and Exposition Electrical and Power Engineering*, Lasi, Romania, Oct. 2014.

[101] R. C. Leou, C. L. Su, and C. N. Lu, “Stochastic analyses of electric vehicle charging on distribution network,” *IEEE Transactions on Power Systems*, vol. 29, no. 3, pp. 1055–1063, May 2014.

[102] J. D. Hoog, T. Alpcan, M. Brazil, D. A. Thomas, and I. Mareels, “Optimal charging of electric vehicles taking distribution network constraints into account,” *IEEE Transactions on Power Systems*, vol. 30, no. 1, pp. 365–375, Jan. 2015.

[103] S. Feuerhahn, R. Hollinger, C. Do, B. Wille-Haussmann, and C. Wittwer, “Modeling a vendor independent IEC 61850 profile for energy management of Micro-CHP units,” In *Proc. IEEE PES Innovative Smart Grid and Technologies*, Berlin, Germany, Oct. 2012.

[104] M. Houwing, R. R. Negenborn, and B. D. Schutter, “Demand response with Micro-CHP systems,” *Proceedings of the IEEE*, vol. 99, no.1, pp. 200-213, Jan. 2011.

[105] M. Tasdighi, H. Ghasemi, and A. Rahimi-Kian, “Residential microgrid scheduling based on smart meters data and temperature dependent thermal load modeling,” *IEEE Transactions on Smart Grid*, vol. 5, no.1, pp. 349-357, Jan. 2014.

[106] H. Aki, “The penetration of micro CHP in residential dwellings in Japan,” In *Proc. IEEE Power and Energy Society General Meeting*, Tampa, FL, USA, Jun. 2007.

[107] F. Mahdloo, M. Manbachi, M. S. Ghazizadeh, and R. Vasigh, “New efficient approach for optimal sizing and placement of micro combined heat and power systems on low voltage grids,” In *Proc. CIGRE Canada Conference*, Toronto, ON, Canada, Sept. 2012.

[108] D. Kamperis, G. M. A. Vanalme, and W. L. Kling, “The ability of a Dutch LV network to incorporate high penetration level of μ-CHPs considering network topology and units control strategy, ” In *Proc. IEEE PES Innovative Smart Grid and Technologies*, Manchester, UK, Dec. 2011.

[109] S. Alyami, Y. Wang, C. Wang, J. Zhao, and B. Zhao, “Adaptive real power capping method for fair overvoltage regulation of distribution networks with high penetration of PV system,” *IEEE Transactions on Smart Grid*, vol. 5, no.6, pp. 2729-2738, Nov. 2014.

[110] X. Liu, A. Aichhorn, L. Liu, and H. Li, “Coordinated control of distributed energy storage system with tap changer transformer for voltage rise mitigation under high photovoltaic penetration,” *IEEE Transactions on Smart Grid*, vol. 3, no.2, pp. 897-906, Jun. 2012.

[111] M. N. Kabir, Y. Mishra, G. Ledwich, Z. Y. Dong, and K. P. Wong, “Coordinated control of grid-connected photovoltaic reactive power and battery energy storage systems to improve the voltage profile of a residential distribution feeder,” *IEEE Transactions on Industrial Informatics*, vol. 10, no.2, pp. 967-977, May 2014.

[112] M. J. E. Alam, K. M. Muttaqi, and D. Sutanto, “Mitigation of rooftop solar PV impacts and evening peak support by managing available capacity of distributed energy storage systems,” *IEEE Transactions on Power Systems*, vol. 28, no.4, pp. 3874-3884, Nov. 2013.

[113] M. J. E. Alam, K. M. Muttaqi, and D. Sutanto, “An approach for online assessment of rooftop solar PV impacts on low-voltage distribution networks,” *IEEE Transactions on Sustainable Energy*, vol. 5, no.2, pp. 663-672, Apr. 2014.

[114] M. J. E. Alam, K. M. Muttaqi, and D. Sutanto, “A SAX-based advanced computational tool for assessment of clustered rooftop solar PV impacts on LV and MV networks in smart grid,” *IEEE Transactions on Smart Grid*, vol. 4, no.1, pp. 577-585, Mar. 2013.

[115] R. Tonkoski, D. Turcotte, and T. H. M. El-Fouly, “Impact of high PV penetration on voltage profiles in residential neighborhoods,” *IEEE Transactions on Sustainable Energy*, vol. 3, no.3, pp. 518-527, Jul. 2012.

[116] D. Infield, and F. Li, “Integrating micro-generation into distribution systems - a review of recent research, ” In *Proc. IEEE Power and Energy Society General Meeting*, Pittsburg, PA, Jul. 2008.

[117] B. Asare-Bediako, W. L. Kling, and P. F. Ribeiro, “Integrated agent-based home energy management system for smart grid applications, ” In *Proc. IEEE PES Innovative Smart Grid Technologies Europe*, Copenhagen, Denmark, Oct. 2013.

[118] M. Thomson, and D. G. Infield, “Network power-flow analysis for a high penetration of distributed generation,” *IEEE Transactions on Power Systems*, vol. 22, no.3, pp. 1157-1162, Aug. 2007.

[119] A. P. Feltrin, D. A. Quinjano and J. R. S. Mantovani, “Volt-VAR Multiobjective Optimization to Peak-Load Relief and Energy Efficiency in Distribution Networks,” *Published online in IEEE Transactions on Power Delivery*, Jul. 2014.

[120] A. Borghetti, F. Napolitano, and C. A. Nucci, “Volt/Var Optimization of Unbalanced Distribution Feeders via Mixed Integer Linear Programming,” In *Proc. Power Systems Computation Conference (PSCC)*, Wroclaw, Aug. 2014.

[121] H. Ahmadi, J. R. Marti, and H. W. Dommel, “A Framework for Volt-VAR Optimization in Distribution Systems,” *Published online in IEEE Transactions Smart Grids*, Dec. 2014.

[122] S. Genc, and M. Baggu, “Look Ahead Volt/VAR Control: A Comparison of Integrated and Coordinated Methods,” In *Proc. IEEE PES T&D Conference and Exhibition*, Chicago, IL, Apr. 2014.

[123] S. Rahimi, K. Zhu, S. Massucco , F. Silvestro, and D. Steen, “Using the Advanced DMS Functions to Handle the Impact of Plug-In Electric Vehicles on Distribution Networks,” in *Proc. IEEE International Electric Vehicle Conference (IEVC)*, Florence, Italy, Dec. 2014.

[124] K. Daroj, “The Revision of Volt/Var Planning and Management in a Distribution System Connected with Distributed Generators,” in *Proc. 2013 International Conference on Electrical Machines and Systems*, Busan, Korea, Oct. 2013.

[125] W. Shang, S. Zheng, L. Li, and M. Redfern, “A new volt/VAR Control for Distributed Generation,” in *Proc. 48th International Universities Power Engineering Conference (UPEC)*, Dublin, Ireland, Sep. 2013.

[126] F. Zavoda, C. Perreault, and A. Lemire, “The Impact of a Volt &VAr Control System (VVC) on PQ and Customer’s Equipment”, in *Proc. IEEE PES Transmission and Distribution Conference and Exposition*, New Orleans, L.A, U.S.A, Apr. 2010.

[127] H. Delmas, Volt VAR Control Implementation at Hydro Quebec, [Online]. Available:http://grouper.ieee.org/groups/td/dist/da/VVC%20implementation%20at%20Hydro%20Quebec.pdf

[128] Smart Metering & Infrastructure Program Business Case, [Online]. Available: https://www.bchydro.com/content/dam/BCHydro/customer-portal/documents/projects/smart-metering/smi-program-business-case.pdf

[129] A. Bettencourt, and J. Malenfant, Hydro One Approach to Smart Grid A Presentation to the OEB’s Smart Grid Advisory Committee, October 22, 2013.

[130] Distributed Dynamic Voltage/VAR Control and Monitoring of Distribution Feeders, Varentec Project, Hydro One Networks Inc.; London Hydro Inc.; Entegrus Inc.; Enwin Utilities Ltd., [Online]. Available:http://www.energy.gov.on.ca/en/smart-grid-fund/smart-grid-fund-projects/varentec/

[131] N. A. Niazi, A. Sheikholeslami, and A. R. K. Varaki, “Global Generation Maintenance Scheduling with Network Constraints, Spinning Reserve, Fuel, and Energy Purchase from Outside,” in *Proc. IEEE Electrical Power and Energy Conference*, London, ON, Canada, pp. 330-336, Oct. 2012.

[132] M. Manbachi, A. H. Parsaeifard, and M. R. Haghifam, “A New Solution for Maintenance Scheduling using Maintenance Market Simulation based on Game Theory,” in *Proc. IEEE Electrical Power and Energy Conferenc*e, Montreal, QC, Canada, Oct. 2009.

[133] M. Manbachi, F. Mahdloo, M. R. Haghifam, A. Ataei, and C. K. A. Yoo, “New Solution for Maintenance Scheduling of Power Systems, using a Genetic Algorithm and Monte-Carlo Simulation,” *Eksploatacja I Niezawodnosc - Maintenance and Reliability*, vol. 4, no. 48, pp. 82-90, 2010.

[134] D. Metz, M. Conlon, and D. F. Mengapche, “Advantages of a Dynamic Smart Grid Training Tool for DSO Control Center Staff,” in *Proc. IEEE Power Engineering Conference*, Dublin, Ireland, Sep. 2013.

[135] M. Manbachi, A. H. Parsaeifard, and M. R. Haghifam, “A New Solution for Maintenance Scheduling of Distributed Generations based on Monte Carlo Simulation and Game Theory,” in *Proc. International Conference on Renewable Energies & Power Quality*, Granada, Spain, Mar. 2010.

[136] S. Hong, H. Li, and F. Wang, “Maintenance Scheduling of Distribution System with Optimal Economy and Reliability,” *Engineering Journal*, vol.5, pp. 14-18, Jun. 2013.

[137] E. Abbasi, M. Fotuhi-Firuzabad, and A. Abiri-Jahromi, “Risk Based Maintenance Optimization of Overhead Distribution Networks Utilizing Priority Based Dynamic Programming,” in *Proc. IEEE Power and Society General Meeting*, Calgary, AB, Canada, Jul. 2009.

[138] A. Moradkhani, M. R. Haghifam, and S. M. Abedi, “Risk based Maintenance Scheduling in the Presence of Reward Penalty Scheme,” *Electric Power System Research*, vol. 121, pp.126-133, Apr. 2015.

[139] A. D. Janjic, and D. S. Popovic, “Selective Maintenance Schedule of Distribution Networks Based on Risk Management Approach,” *IEEE Transactions on Power Systems*, vol. 22, no. 2, pp. 597-604, May 2007.

[140] S. R. McCormick, K. Hur, S. Santoso, A. Maitra, and A. Sundaram, “Capacitor Bank Predictive Maintenance and Problem Identification using Conventional Power Quality Monitoring Systems,” in *Proc. IEEE Power and Society General Meeting*, Denver, CO, USA, Jun. 2004.

[141] D. W. Holladay, B. D. Dallman, and C. H. Grigg, “Reliability Centered Maintenance Study on Voltage Regulators,” in *Proc. IEEE Transmission and Distribution Conference*, Albuquerque, MN, Oct. 2006 .

[142] M. Mahmoudi, A. Elbarkany, and A. El Khalifi, “Towards a Strategy of Optimization the Maintenance Activities of the MV/LV PDS Transformers,” in *Proc. 5th IESM Conference*, Rabat, Oct. 2013.

[143] USAID, Best Practices in Distribution Systems Operation and Maintenance (O&M), Drum Training Program, Ministry of Power, USA, 2006.

[144] Substation, Automation and Maintenance, Alexander Publishers, Newport Beach. CA, USA, 2010.

[145] M. A. Fotouhi Ghazvini, H. Morais, and Z. Vale, “Multi-Criteria Short-term Maintenance Outage Scheduling in Smart Distribution Systems,” in *Proc. CIRED Worshop*, Lisbon, Portugal, May 2012.

[146] Y. Reddy Jahanmogan, Y. V. Pavan Kumar, and K. Padma Raju, “Distributed ANNs in a Layered Architecture for Energy Management and Maintenance Scheduling of Renewable Energy HPS Microgrids,” in *Proc. IEEE Advances in Power Conversion and Energy Technologies*, Mylavaram, India, Aug. 2012.

[147] H. Simonis. (2010, August 2) Electrical Distribution Network Maintenance and Reconfiguration. [Online]. Available: https://hsimonis.wordpress.com

[148] M. Biserica, Y. Besanger, R. Caire, O. Chilard, and P. Deschamps, “Neural Networks to Improve Distribution State Estimation-Volt Var Control Performances,” *IEEE Transactions on Smart Grid*, vol. 3, no. 3, pp. 1137-1144, May 2012.

[149] P. I. Hwang, M. G. Jeong, and S. I. Moon, “Volt/VAR Optimization of the Korean Smart Distribution Management System,” in *Proc. 22nd International Conference on Electricity Distribution (CIRED)*, Stockholm, Sweden, June 2013.

[150] U.S Department of Energy, Electricity Delivery and Energy Reliability, American Recovery and Reinvestment Act of 2009, Application of Automated Controls for Voltage and Reactive Power Management, Initial Results, Smart Grid Investment Grant Program, Dec. 2012.

[151] F. L. Quilumba, W. J. Lee, H. Huang, D. Y. Wang, and R. L. Szabados, “Using Smart Meter Data to Improve the Accuracy of Intraday Load Forecasting Considering Customer Behavior Similarities,” *IEEE Transactions on Smart Grid*, vol. 6, no. 2, pp. 911-918, Mar. 2015.

[152] M. Alizadeh, An. Scaglione and Z. Wang, “On the impact of Smart Grid metering infrastructure on load forecasting,” in *Proc. Forty-Eighth Annual Allerton Conference*, Allerton House, UIUC, Illinois, USA, Sept. 29/Oct. 1, 2010

[153] S. C. Huang, C. N. Lu, and Y. L. Lo, “Evaluation of AMI and SCADA Data Synergy for Distribution Feeder Modeling,” *IEEE Transactions on Smart Grid*, vol. 6, no. 4, pp. 1639-1647, Jul. 2015.

[154] L. Hernandez, C. Baladr´on, J. M. Aguiar, B. Carro, A. J. Sanchez-Esguevillas, J. Lloret, and J. Massana, “A Survey on Electric Power Demand Forecasting: Future Trends in Smart Grids, Microgrids and Smart Buildings,” *IEEE Communications Surveys & Tutorials*, vol. 16, no. 3, pp. 1460-1494, Third-Quarter 2014.

[155] X. We “Chaotic artificial Neural Network in reactive Power optimization of distribution network” in *Proc. China International Conference on Electricity Distribution (CICED2010)*, Nanjing, China, Sep. 2010.

[156] I. Dzafic, H. T. Neisius, and D. Ablakovic, “Multi Process Real-Time Network Applications in Distribution Management System,” In *Proc. IPEC Conference*, Singapore, Oct. 2010.

[157] A. Zakarizadeh, H. Modaghegh, and S. Jadid, “Real-Time Volt/VAR Control using Advance Metering Infrastructure System in FAHAM Project,” In *Proc. 22nd International Conference on Electricity Distribution (CIRED)*, Stockholm, Sweden, Jun. 2013.

[158] M. Thesing, “Integrating Electric Meter Data with Distribution Automation Applications,” In *Proc. IEEE PES T&D Conference and Exhibition*, Orlando, FL, May 2012.

[159] T. Helmer, Volt/VAR Control Options and How to Leverage AMI Data, Published in the issue of PowerGrid International, BLACK & VEATCH, August 2012.

[160] NEMA, Volt/VAR Optimization Improves Grid Efficiency, [Online]. Available https://www.nema.org/Policy/Energy/Smartgrid/Documents/VoltVAR-Optimazation-Improves%20Grid-Efficiency.pdf

[161] J. St. John , How Smart Meters Are Helping Utilities With Voltage Management, Greentech media, Jan. 13, 2014, [Online]. Available: http://www.greentechmedia.com/articles/read/smart-grid-snapshot-ami-enabled-voltage-control-on-the-rise

[162] R. Bottura, F. Napolitano, and C. A. Nucci, "ICT-Power Co-Simulation Platform for the Analysis of Communication-based Volt/Var Optimization in Distribution Feeders," in *Proc. IEEE PES Innovative Smart Grid Technologies Conference, (ISGT 2014)*, Washington DC, Feb. 2014.

[163] K. P. Schneider, and T. F. Weaver, "Volt-VAR Optimization on American Electric Power Feeders in Northeast Columbus," in *Proc. IEEE PES Transmission and Distribution Conference and Exposition*, Orlando, FL, May. 2012.

[164] R. R. Dothinka, A. Agalgaonkar, and K. Muttaqi, "On-line Voltage Control in Distribution Systems with Multiple Voltage Regulating Devices," in *Proc. 2014 IEEE PES General Meeting*, National Harbor, MD, USA, Jul. 2014.

[165] H. Ahmadi, and J. R. Marti, "Load Decomposition at Smart Meters Level Using Eigenloads Approach", *IEEE Transactions on Power Systems*, vol. 30, no. 6, pp. 3425-3436, Nov. 2015.

[166] N. Markushevich, and L. Wenpeng, "Achieving greater VVO benefits through AMI implementation," in *Proc. IEEE Power and Energy Society General Meeting*, San Diego, CA, USA, Jul. 2011.

[167] S. T. Mak, "Dynamic modeling of the distribution feeder using Smart Meters data to support feeder VOLT-VAR control," in *Proc. IEEE PES Transmission and Distribution Conf. and Exposition*, Orlando, FL, USA, May 2012.

[168] J. C. Fuller, S. Ciraci, J. A. Daily, A. R. Fisher, and M. Hauer, "Communication simulations for power system applications," in *Proc. Workshop of Modeling and Simulation of Cyber-Physical Energy Systems (MSCPES)*, Berkeley, CA, USA, May 2013.

[169] V. Kounev, D. Tipper, M. Levesque, B. M. Grainger, T. McDermott, and G. F. Reed, “A Microgrid co-simulation framework,” in *Proc. Workshop of Modeling and Simulation of Cyber-Physical Energy Systems (MSCPES)*, Seattle, WA, USA, Apr. 2015.

[170] C. Zhao, D. Liu, H. Zhu, Y. Wang, and Y. Chen, “Co-simulation research and application for active distribution network based on Ptolemy II and Simulink,” in *Proc. China Int. Conf. Electricity Distribution (CICED)*, Shenzhen, China, Sep. 2014.

[171] W. Guo, J. Lin, W. Song, and X. Chen, “A simulation platform of active distribution network based on co-simulation of GridLAB-D and Matlab,” in *Proc. Int. Conf. Power System Technology (POWERCON)*, Chengdu, China, Oct. 2014.

[172] P A. Pegoraro, F. Pilo, G. Pisano, S. Ruggeri, and S. Sulis, “Co-simulation of distribution active management and distribution state estimation to reduce harmful effects of inaccuracies,” in *Proc. IEEE Power Tech (POWERTECH)*, Grenoble, France, Jun. 2013.

[173] J. Hsu, J. Lin, T. Y. Chen, and W. D. Guo, “Power distribution network co-simulation for cost-effective system design,” in *Proc. IEEE Electrical Design of Advanced Packaging & Systems (EDAPS)*, Shatin, Hong-Kong, Dec. 2009.

[174] V. Zamani, and M. Baran, “Feeder monitoring for Volt/VAR control in distribution systems,” in *Proc. IEEE PES General Meeting Conf. and Exposition*, National-Harbor, MD, USA, Jul. 2014.

[175] X. Wang, P. Zhang, Z. Wang, V. Dinavahi, G. Chang, J. A. Martinez, A. Davoudi, A. Mehrizi-Sani, and S. Abhyankar, “Interfacing issues in Multiagent simulation for smart grid applications,” *IEEE Transactions on Power Delivery*, vol. 28, no. 3, pp. 1918-1927, Jul. 2013.

[176] M. Ibrahim, and M. M. A. Salama, “Using distributed intelligence and wireless communication to control and coordinate multiple capacitor banks,” in *Proc. IEEE PES T&D Conf. and Exposition*, Chicago, IL, USA, Apr. 2014.

[177] M. Ibrahim, and M. M. A. Salama, “Smart distribution system volt/VAR control using distributed intelligence and wireless communication,” *IET Generation, Transmission and Distribution*, vol. 9, no. 4, pp. 307-318, Mar. 2015.

[178] D. Montenegro, and G. A. Ramos, “Real time observability analysis for distribution networks,” in *Proc. IEEE Power Tech (POWERTECH)*, Grenoble, France, Jun. 2013.

[179] D. A. Atanackovic, and V. Dabic, “Deployment of real-time state estimator and load flow in BC Hydro DMS - challenges and opportunities,” in *Proc. IEEE Power and Energy Society General Meeting (PES)*, Vancouver, BC, Canada, Jul. 2013.

[180] S. C. Muller, H. Georg, C. Rehtanz, and C. Wietfeld, “Hybrid simulation of power systems and ICT for real-time application,” in *Proc. 3rd IEEE PES Innovative Smart Grid Technologies Europe (ISGT Europe)*, Berlin, Germany, Oct. 2012.

[181] Communication networks and systems for power utility automation-Part 7-420: Basic communication structure-Distributed energy resources logical nodes, IEC 61850-7-420-2009 standard, Oct. 2009.

[182] T. S. Ustun, A. Hadbah, and A. Kalam, “Interoperability and interchangeability considerations in Microgrids employing IEC61850 standard,” in *Proc. IEEE Int. Conf. Smart Energy Grid Engineering (SEGE)*, Oshawa, ON, Canada, Aug. 2013.

[183] F. Coffele, C. Booth, and A. Dyśko, “An adaptive overcurrent protection scheme for distribution networks,” *IEEE Transactions on Power Delivery*, vol. 30, no. 2, pp. 561-568, Apr. 2015.

[184] F. Clavel, E. Savary, P. Angays, and A. Vieux-Melchior, “A network simulator for IEC61850 architecture,” in *Proc. PCIC Europe Conference*, Istanbul, Turkey, May 2013.

[185] S. Kwon, C. Chu, J. Cho, S. Yoon, “Development of IEC 61850 based feeder IEDs for self-healing operation in distribution network,” in *Proc. CIRED Workshop*, Lisbon, Portugal, May 2012.

[186] Z. Zhu, B. Xu, G. Han, and M. Gao, “Study on the feeder topology modeling and IED configured methods for IEC61850,” in *Proc. China International Conference on Electricity Distribution*, Shenzhen, China, Sept. 2014.

[187] M. Eriksson, M. Armendariz, O. O. Vasilenko, A. Saleem, and L. Nordström, “Multiagent-based distribution automation solution for self-healing grids,” *IEEE Transactions on Industrial Electronics*, vol. 62, no. 4, pp. 2620-2628, Apr. 2015.

[188] M. Mao, F. Mei, P. Jin, and L. Chang, “Application of IEC61850 in energy management system for microgrids,” in *Proc. IEEE 5th Int. Power Electronics for Distributed Generation Systems (PEDG)*, Galway, Ireland, Jun. 2014.

[189] J. Wang, Z. Bu, X. Zhai, and Z. Li “A low-voltage microgrid control method based on standardized information model,” in *Proc. IEEE Workshop on Electronics, Computer and Applications*, Ottawa, ON, Canada, May 2014.

[190] J. Mocˇnik, and A. Žemva, “Controlling voltage profile in smart grids with remotely controlled switches,” *IET Generation, Transmission and Distribution*, vol. 8, no. 8, pp. 1499-1508, Aug. 2014.

[191] M. Nasri, H. Farhangi, A. Palizban, and M. Moallem, “Application of Intelligent Agents in Smart Grids for Volt/VAR Optimization and Conservation Voltage Reduction,” in *Proc. IEEE Canada Electrical Power and Energy Conference*, London, Ontario, Oct. 2012

[192] M. Nasri, H. L. Ginn, and M. Moallem, “Application of intelligent agent systems for real-time coordination of power converters (RCPC) in microgrids,” *IEEE Energy Conversion Congress and Exposition (ECCE) Conference*, Pittsburgh, PA, USA, PP. 3942 – 3949, Sep. 2014.

[193] B. Shahbi, Application of Narrow Band Power Line Communication in Volt/VAR Optimization, Master Engineering Thesis, School of Engineering Science, Faculty of Applied Sciences, Simon Fraser University, Mar. 2014.

[194] I. Ramalla, and N. Namburi, “Analytical Review of Loss Reduction Techniques in Indian Power Distribution Sector-Techno Managerial Approach,” *International Journal of Research in Engineering and Technology*, vol. 3, special issue. 12, pp. 30-34, Jun. 2014.

[195] Incentive Mechanisms for Managing Transmission and Distribution Losses, Regulated Industries Commission, T&TEC, Consultation Document, May 2005.

[196] T. Gonen, Electric Power Distribution System Engineering, Second Edition, CRC Press, Taylor & Francis Group, Dec. 14, 2007.

[197] On-Load Tap-Changer OILTAP MS, Operating Instructions BA 65/04, Page-6, [Online]. Available: http://www.reinhausen.com/en/desktopdefault.aspx/tabid-52/2069_read-5211/

[198] D. Dohnal, On-Load Tap-Changers for Power Transformers, PB 25 2/06 EN - F0126405-09/13-dp-Maschinenfabrik Reinhausen GmbH, 2013.

[199] A. J. Pansini, Guide to Electrical Power Distribution Systems, 6th Edition, CRC Press, Jun. 2005.

[200] Voltage Regulator, Robust, Maintenance Free Solutions, GE Digital Energy, GEA-12803A (E) English 150630, 2015. [Online]. Available: https://www.gedigitalenergy.com/products/brochures/HVMV/VoltageRegulator_GEA12803A.pdf1.

[201] QPole, Pole Mounted Capacitor System, ABB Company, 2010, [Online]. Available:https://library.e.abb.com/public/a8c42d637aa10aa2c12577ee0055faad/ABB_DPDQPole_Qpole_revB_EN.pdf

[202] R. G. Andrei, “A Novel Fuseless Capacitor Bank Design Using Conventional Single Bushing Capacitors,” *IEEE Transactions on Power Delivery*, vol. 14, no. 3, pp. 1124-1133, 1999.

[203] R. Se´vigny, S. Me´nard, C. Rajotte, and M. McVey, “Capacitor Measurement in the Substation Environment: A New Approach,” in *Proc. IEEE 9th International Conference on Transmission and Distribution*, pp. 299–305, Montreal, QC, Canada, 2000.

[204] ANSI/IEEE Standard 18, IEEE Standard for Shunt Capacitors, 1992.

[205] Capacitor Technologies, Victoria, Australia, [Online]. Available: www.captech.com.au

[206] Ramasamy Natarajan, Power System Capacitors, CRC Press, Taylor & Francis Group, 2005.

[207] CQ900-Capacitor Controller, ABB Company, 2012, [Online]. Available: http://www.abb.ca/product/db0003db004279/9b04ded0266732fac1257af700221a88.aspx

[208] S&C IntelliCap 2000, Automatic Capacitor Controls, Descriptive Bulletin 1024-30 September 3, 2013, USA, [Online]. Available: http://www.sandc.com/products/automation-control/automatic-capacitor controls.asp

[209] Capacitor bank protection and control REV615, Dedicated capacitor bank protection and control in utility and industrial power distribution systems, ABB Company, Online]. Available: http://new.abb.com/medium-voltage/distribution-automation/numerical-relays/capacitor-and-filter-bank/capacitor-bank-protection-and-control-rev615

[210] Multilin C70, Capacitor Bank Protection & Control System, GE Digital Energy, [Online]. Available: https://www.gedigitalenergy.com/multilin/catalog/c70.htm

[211] IEEE 802-2014, Revision to IEEE std. 802-2001 IEEE Standard for Local and Metropolitan Area Networks: Overview and Architecture Sponsored by the LAN/MAN Standards Committee, 12 June 2014 IEEE-SA Standards Board. [Online]. Available: https://standards.ieee.org/getieee802/download/802-2014.pdf

[212] M. C. Kisacikoglu, B. Ozpineci, L. M. Tolbert, and F. Wang, “Single-phase inverter design for V2G reactive power compensation,” in *Proc. 26th Annual IEEE Applied Power Electronics Conference and Exposition (APEC)*, Fort Worth, TX, USA, Mar. 2011.

[213] L. J. Borle, Zero Average Current Error Control Methods for Bidirectional AC-DC Converters, PhD thesis, Curtin University of Technology, Perth, Australia, 1999.

[214] Functional Specifications for Community Energy Storage (CES) Unit, Revision 2.2, American Electric Power (AEP), 12 Sep. 2009.

[215] H. Asgeirsson, DTE Energy: Energy Storage Demonstration Projects, IEEE PES General Meeting - Energy Storage Super Session, 2011.

[216] SAE J1772, SAE Charging Configurations and Ratings Terminology, SAE International, Hybrid Committee, Version. 031611, 2011.

[217] P. Fairley, "An Easy Smart-Grid Upgrade Saves Power," *IEEE Spectrum Magazine*, vol. 47, no. 10, pp. 13-14, Oct. 2010.

[218] B. Uluski, "Smart Distribution Application and Their Integration in A Smart Grid Environment," *Presented at: IEEE Power and Energy Society General Meeting*, Detroit, Michigan, USA, Jul. 2011.

[219] W. Su, and J. Wang, "Energy Management Systems in Microgrid Operations," *The Electricity Journal*, vol. 25, no. 8, pp. 45-60, Oct. 2012.

[220] A. Kam, A. Barnes, and V. Martinelli, "Optimal Placement of an Inline Voltage Regulator on a Secondary Distribution System," in *Proc. CIRED Workshop*, Paper: 0096, Rome, Italy, Jun. 2014.

[221] "Centralized or Distributed? It's Not Necessarily Either/Or," *The Electricity Journal*, vol. 28, no. 3, pp. 1, 6-7, Apr. 2015.

[222] M. A. Peskin, P. W. Powell, and E. J. Hall, "Conservation Voltage Reduction with Feedback from Advanced Metering Infrastructure," in *Proc. IEEE PES T&D Conference and Exposition*, Orlando, FL, USA, May 2012.

[223] C. Hertzog, The Evolution of "Just-in-Time" for Utilities, Aug 25, 2014, Smart Grid Library, [Online]. Available: http://www.smartgridlibrary.com/tag/negawatts/

[224] IEEE 1547-2003, Clause 4.1.1, Standard for Interconnecting Distributed Sources with Electric Power Systems, [Online]. Available: https://standards.ieee.org/findstds/standard/1547-2003.html

[225] IEC 61850, Power Utility Automation, Relevant Application: EMS, DMS, DA, SA, DER, AMI, Storage, EV, [Online]. Available: http://www.iec.ch/smartgrid/standards/

[226] J. Benders, "Partitioning procedures for solving mixed variables programming problems," *Numerische Mathematics*, vol. 4, pp. 238-252, 1962.

[227] A. M. Geoffrion, "Generalized benders decomposition", *Journal of Optimization Theory and Applications*, vol. 10, no. 4, pp. 237–260, Oct. 1972.

[228] M. Shahidehpour, and Y. Fu, “Benders decomposition applying Benders decomposition to power systems,” *IEEE Power & Energy Magazine*, vol. 3, no. 2, pp. 20-21, Mar./Apr. 2005.

[229] M. Shahidehpour, and Y. Fu, Benders Decomposition in Restructured Power Systems, Electric Power and Power Electronics Center, Illinois Institute of Technology.

[230] Y. Li, J. D. Mc Calley, A General Benders Decomposition Structure for Power System Decision Problems, Department of Electrical and Computer Engineering Iowa State University, IEEE 978-1-4244-2030, 2008.

[231] R. M. Freund, Benders’ Decomposition Methods for Structured Optimization, including Stochastic Optimization, Massachusetts Institute of Technology, April 29, 2004.

[232] A. J. Conejo, E Castillo, R. Minguez and R. Garcia-Bertrand, Decomposition Techniques in Mathematical Programming, ISBN-10 3-540-27685-8 Springer Berlin Heidelberg New York, 2006.

[233] M.S. Bazaraa, J. J. Jarvis, and H. D. Sherali, Linear Programming and Network Flows, Chapter 7, Wiley, 1990.

[234] M. J. Bagajevicz, and V. Manousiouthakis, “On the Generalized Benders Decomposition,” *Computers them. Engineering Journal*, vol. 15, no. I0, pp. 691-700, 1991.

[235] G. Cote, and M Laughton, “Decomposition techniques in power system planning: the Benders partitioning method,” *International Journal of Electrical Power Energy Systems*, vol. 1, no. 1, Pages: 57-64, 1979.

[236] L. F. B. Baptistella, “Decomposition approach to problem of unit commitment schedule for hydrothermal systems” *Control Theory and Applications, IEE Proceedings*, vol. 127, no. 6 , Nov. 1980.

[237] A. Monticelli, and R. Romero, “A hierarchical decomposition approach for transmission network expansion planning,” *IEEE Transactions on Power Systems*, vol. 9, no. 1, pp. 373-380, Feb. 1994.

[238] A. J. Conejo, and N. Alguacil, “Multiperiod optimal power flow using Benders decomposition”, *IEEE Transactions on Power Systems*, vol. 15, no. 1, pp. 196-201, Feb. 2000.

[239] M. Shahidehpour, Y. Fu, Z. Li, “Security-Constrained Unit Commitment with AC Constraints,” *IEEE Transactions on Power Systems*, vol. 20, no. 3, pp. 1538-1550, Aug. 2005.

[240] V. Miranda, J. V. Ranito, L. V. Proenca, “Genetic algorithm in optimal multistage distribution network planning” *IEEE Transactions on Power System*, vol. 9, no. 4, pp.1891-1898, 1996.

[241] RTDS Manual, Real Time Digital Simulations for the Power Industry, RTDS Technologies, Mar. 2012.

[242] IEEE Power & Energy Society, 1646-2004- IEEE Standard Communication Delivery Time Performance Requirements for Electric Power Substation Automation, 2005.

[243] TATA Consultancy Services, "WANem 2.0 Wide Area Network Emulator," TATA Consultancy Services, 2008.

[244] Communication networks and systems for power utility automation -Part 7-1: Basic communication structure - Principles and models, IEC 61850-7-1-2011 standard, Apr. 2012.

[245] Communication networks and systems for power utility automation -Part 7-2: Basic information and communication structure- Abstract communication service interface (ACSI), IEC 61850-7-2-2010 standard, Apr. 2011.

[246] Communication networks and systems in substations – Part 8-1: Specific Communication Service Mapping (SCSM) – Mappings to MMS, IEC 61850-8-1-2011 standard, Feb. 2012.

[247] Communication networks and systems in substations – Part 9-1: Specific Communication Service Mapping (SCSM) – Sampled values, IEC 61850-9-1-2003 standard, Feb. 2004

[248] Communication networks and systems in substations – Part 5: Communication requirements for functions and device models – Sampled values, IEC 61850-5-2013 standard, Jun. 2014

[249] Communication networks and systems in substations – Part 6: Configuration description language for communication in electrical substations related to IEDs, IEC 61850-6-2010 standard, Jun. 2010

[250] Distribution System Analysis Subcommittee, IEEE 34 Node Test Feeder, [Online]: http://www.ewh.ieee.org/soc/pes/dsacom/testfeeders/index.html

[251] IEEE 37-Bus Feeder, IEEE PES Distribution System Analysis Subcommittee's Distribution Test Feeder Working Group, [Online]. Available: http://ewh.ieee.org/soc/pes/dsacom/testfeeders/index.html

[252] Distribution System Analysis Subcommittee, IEEE 123 Node Test Feeder, Jul. 2015, [Online]. Available: http://ewh.ieee.org/soc/pes/dsacom/testfeeders/

[253] S. Paul, and W. Jewell, “Optimal Capacitor Placement and Sizes for Power Loss Reduction using Combined Power Loss Index-Loss Sensitivity Factor and Genetic Algorithm,” in *Proc. IEEE Power and Energy Society General Meeting*, San Diego, CA, Jul. 2012.

[254] M. E. Baran, and F. F. Wu, “Network Reconfiguration in Distribution Systems for Loss Reduction and Load Balancing,” *IEEE Transactions on Power Delivery*, vol. 4, no. 3, pp. 1401-1407, Apr. 1989.

[255] Load Profiling Guide. 2013-2014 Data, ERCOT Electricity Market. [Online]. Available:http://www.ercot.com/mktrules/guides/loadprofiling/index.html

[256] A. Awad, Smart Grid Applications, Informatik 7 Rechnernetze und Kommunikationssysteme, October 2014, Page 21. [Online]. Available: http://www7.cs.fau.de/de/wpcontent/uploads/sites/2/2014/08/lect4_smartgridapplications.pdf

[257] E. Sortomme, A. I. Negash, S. S. Venkata, and D. S. Kirschen, “Voltage Dependent Load Models of Charging Electric Vehicles,” *in Proc. IEEE Power and Energy Society General Meeting*, Vancouver, BC, Canada, Jul. 2013.

[258] C. Higgins, B. Patel, S. Ingram, S. Brooke, G. Bryson, and D. Randles, “The Application of Conservation Voltage Reduction (CVR) to Distribution Networks with High Uptake of Heat Pumps and Electric,” in *Proc. CIRED Workshop*, Rome, Italy, Jun. 2014.

[259] A. Bokhari, A. A, R. Dogan, M. Diaz-Aguiló, F. León, D. Czarkowski, Z. Zabar, L. Birenbaum, A. Noel, and R. E. Uosef, “Experimental Determination of the ZIP Coefficients for Modern Residential, Commercial, and Industrial Loads,” *IEEE Transactions on Power Delivery*, vol. 29, no. 3, pp. 1372-1381, Jun. 2014.

[260] N. Lu, Y. Xie, Z. Huang, F. Puyleart, and S. Yang, “Load Component Database of Household Appliances and Small Office Equipment,” in *Proc. IEEE Power and Energy Society General Meeting - Conversion and Delivery of Electrical Energy in the 21st Century*, Pittsburgh, PA, 20-24 Jul. 2008.

[261] L. F. Quilumba Wei-Jen Lee, H. Huang, D. Y. Wang and R. L. Szabados, “Load Model Development for Next Generation Appliances,” in *Proc. IEEE Industry Applications Society Annual Meeting (IAS)*, Orlando, FL, 9-13 Oct. 2011.

[262] Electric Home Appliance Consumption & Cost, Roseville Electric 2013. [Online]. Available:https://www.roseville.ca.us/civicax/filebank/blobdload.aspx?blobid=7086

[263] Home energy consumption list A list of electric household appliances, and their operating cost, Atco Energy Sense, [Online]. Available: http://www.atcoenergysense.com/Documents/Home-Energy-Consumption-List-webversionFINAL.pdf

[264] Hourly Load Profiles, Xcel Energy, Appendix D, . [Online]. Available: http://www.xcelenergy.com/staticfiles/xe/Corporate/Corporate%20PDFs/AppendixD-Hourly_Load_Profiles.pdf

[265] U.S. Department of Energy, 2010 Building Energy Data Book, March 2011, [Online]. Available: http://buildingsdatabook.eren.doe.gov/

[266] Office of Energy Efficiency and Renewable Energy, Building America Analysis – Existing Homes, [Online]: http://energy.gov/eere/buildings/downloads/building-america-analysis-existing-homes

[267] T. M. Khalil, A. V. Gorpinich, "Reconfiguration for Loss Reduction of Distribution System using Selective Particle Swarm Optimization," *International Journal of Multidisciplinary Sciences and Engineering*, vol. 3, no. 6, pp. 16-21, Jun. 2012.

[268] X. Lu, Z. Lu, W. Wang, and J. Ma, "On Network Performance Evaluation toward the Smart Grid: A Case Study of DNP3 over TCP/IP," In *Proc. IEEE Global Telecommunications Conference*, Houston, TX, Dec. 2011.

[269] A. Ortega, C. M. Schweitzer, and A. Akira Shinoda, "Performance Analysis of Smart Grid Communication Protocol DNP3 over TCP/IP in a Heterogeneous Traffic Environment," In *Proc. IEEE Colombian Conference on Communications and Computing (COLOCOM)*, Medellin, May 2013.

[270] ERCOT Load Profiles (2013-2014), [Online]. Available: http://www.ercot.com/mktinfo/loadprofile/alp/

[271] Community Energy Storage, How eCamion created an Urban First, *Batteries International*, Issue 90, Special Print, Winter 2013-2014.

[272] K. M. M. Huq, M. E. Baran, S. Lukic, and O. E. Nare, "An Energy Management System for a Community Energy Storage System," in *Proc. IEEE Energy Conversion Conference (ECCE)*, Raleigh, NC, USA, pp. 2759-2763, Sep. 2012.

[273] A. Bukhari, Community Energy Storage, Grid Solutions, Asset Management, Toronto Hydro, August 20, 2013. [Online]. Available: http://www.ontarioenergyboard.ca/oeb/_Documents/EB-2013-0294/SGAC_Toronto%20Hydro%20CES%20Presentation.pdf

[274] D. Q. Hung, and N. Mithulananthan, "Community Energy Storage and Capacitor Allocation in Distribution Systems," in *Proc. 21th Australasian Universities Power Engineering Conference*, Brisbane, QLD, Australia, Sep. 2011.

Appendix A.

Formula Realizations

Based on Power Triangle (Figure A. 1) which shows the characteristics of a power system, it is possible to derive relations between active, reactive and apparent power of a system as follows:

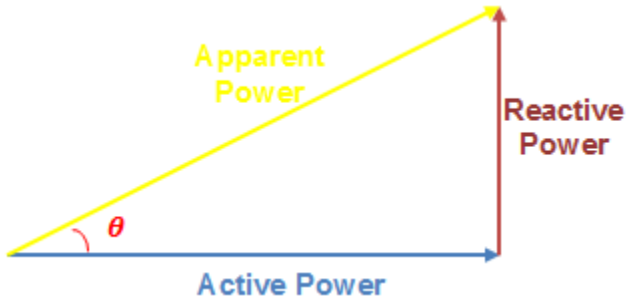

Figure A. 1. Power Triangle Concept

$$kVA = \sqrt{kW^2 + kVAr^2}, \quad S = \sqrt{P^2 + Q^2} \tag{A-1}$$

In order to reduce system total loss, it is possible to write the objective as minimizing total apparent power loss of network as follows:

$$min\{S_{f,t}^{i}\} = min\{({P_{loss,total}}^2 + {Q_{loss,total}}^2)^{0.5}\} \tag{A-2}$$

The above equation consists of total active and total reactive power losses. Each can be obtained based on loss calculation of all feeders and/or lines at every time stages:

$$P_{loss,total} = \sum_{t=1}^{T}\sum_{f=1}^{F} P_{loss,f,t} \tag{A-3}$$

$$Q_{loss,total} = \sum_{t=1}^{T}\sum_{f=1}^{F} Q_{loss,f,t} \tag{A-4}$$

As stated before, it is possible to consider other objective functions based on economic factors. For instance, a proper objective could be minimization of network energy loss cost:

$$Total\ Apparent\ Energy\ Loss\ Cost = (\$/kVAh) \times kVA \times h \tag{A-5}$$

$$\min S_{Loss} = \min(C_{loss} \times S \times h_t) = \min(C_{loss}(\sqrt{P_{loss,total}^2 + Q_{loss,total}^2})h_t) \quad \text{(A-6)}$$

The active and the reactive power loss determination method can be obtained based on main power system and Kirchhoff's laws. General model of a distribution line between bus-i and bus-j is shown in Figure A. 2:

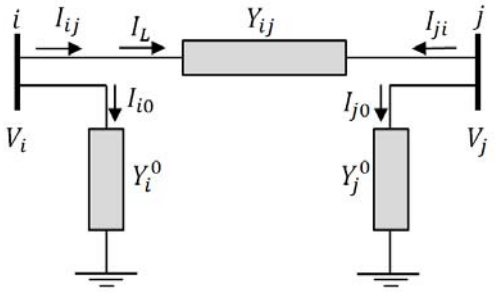

Figure A. 2. Typical line model of distribution networks

Now it is possible to write voltage and current relations based on system series and shunt admittances:

$$I_{ij} = I_l + I_{i0} = Y_{ij}(V_i - V_j) + Y_i^0 V_i \quad \text{(A-7)}$$

$$I_{ji} = -I_l + I_{j0} = Y_{ij}(V_j - V_i) + Y_j^0 V_j \quad \text{(A-8)}$$

$$I_{ij}^* = V_i(Y_{ij} + Y_i^0)^* - Y_{ij}^* V_j^* \quad \text{(A-9)}$$

The apparent power loss of the system can be obtained by:

$$S_{ij} = V_i I_{ij}^* = V_i^2(Y_{ij} + Y_i^0)^* - V_i Y_{ij}^* V_j^* \quad \text{(A-10)}$$

$$S_{ji} = V_j I_{ji}^* = V_j^2(Y_{ij} + Y_j^0)^* - V_j Y_{ij}^* V_i^* \quad \text{(A-11)}$$

$$S_{Loss} = S_{ij} + S_{ji} = V_i^2(Y_{ij} + Y_i^0)^* - V_i Y_{ij}^* V_j^* + V_j^2(Y_{ij} + Y_j^0)^* - V_j Y_{ij}^* V_i^* \quad \text{(A-12)}$$

Then, we define:

$$Y_{ij} \triangleq G_{ij} + jB_{ij} \rightarrow Y_{ij}^* = G_{ij} - jB_{ij} \quad \text{(A-13)}$$

$$Y_i^0 \triangleq G_i^0 + jB_i^0, Y_j^0 \triangleq G_j^0 + jB_j^0 \tag{A-14}$$

Thus,

$$\begin{aligned} S_{Loss} &= S_{ij} + S_{ji} \\ &= \left(G_{ij} - jB_{ij}\right)V_i^2 + (G_i^0 - jB_i^0)V_i^2 - V_i\left(G_{ij} - jB_{ij}\right)V_j^* \\ &+ \left(G_{ij} - jB_{ij}\right)V_j^2 + (G_j^0 - jB_j^0)V_j^2 - V_j\left(G_{ij} - jB_{ij}\right)V_i^* \end{aligned} \tag{A-15}$$

According to complex representation:

$$S_{Loss} = P_{Loss} + jQ_{Loss} \tag{A-16}$$

Thus,

$$P_{Loss} = G_{ij}(V_i^2 - V_iV_j^* + V_j^2 - V_jV_i^*) + \ G_i^0V_i^2 + G_j^0V_j^2 \tag{A-17}$$

$$Q_{Loss} = -B_{ij}(V_i^2 - V_iV_j^* + V_j^2 - V_jV_i^*) - \ B_i^0V_i^2 - B_j^0V_j^2 \tag{A-18}$$

It is possible to mathematically show that:

$$V_iV_j^* + V_jV_i^* = 2|V_i|\left|V_j\right|\cos\theta_{ij} \tag{A-19}$$

Finally,

$$P_{Loss} = G_{ij}(V_i^2 + V_j^2 - 2|V_i|\left|V_j\right|\cos\theta_{ij}) + \ G_i^0V_i^2 + G_j^0V_j^2 \tag{A-20}$$

$$Q_{Loss} = -B_{ij}(V_i^2 + V_j^2 - 2|V_i|\left|V_j\right|\cos\theta_{ij}) - \ B_i^0V_i^2 - B_j^0V_j^2 \tag{A-21}$$

Now, for transformer tap changer, it is possible to employ Unified Branch Model of distribution system (Figure A. 3).
Based on Figure A. 3, current equations can be written based on KCL law as follows:

$$I_{ij} = \alpha_{ij}{}^*I_{pq} = \alpha_{ij}{}^*\left[\left(V_p - V_q\right)Y_{ij} + V_pY_i^0\right] = \alpha_{ij}{}^*\left[\left(\alpha_{ij}V_i - \alpha_{ji}V_j\right)Y_{ij} + \alpha_{ij}V_iY_i^0\right] \tag{A-22}$$

$$I_{ji} = \alpha_{ji}{}^*I_{qp} = \alpha_{ji}{}^*\left[\left(V_q - V_p\right)Y_{ij} + V_qY_j^0\right] = \alpha_{ji}{}^*\left[\left(\alpha_{ji}V_j - \alpha_{ij}V_i\right)Y_{ij} + \alpha_{ji}V_jY_j^0\right] \tag{A-23}$$

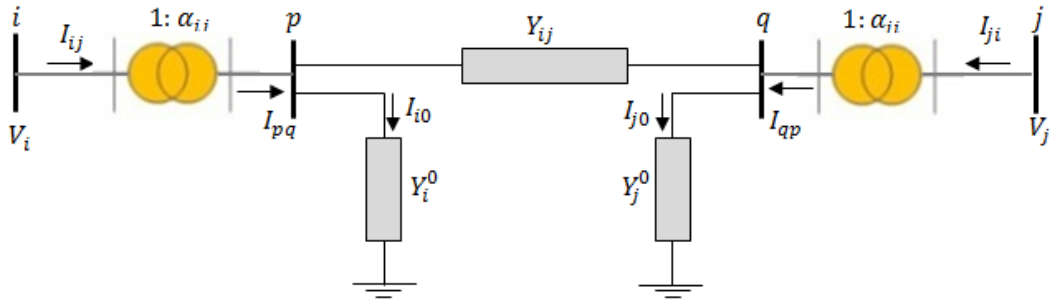

Figure A. 3. Transformer turn ratio between two nodes of a system

$$I_{ij} = (\alpha_{ij}^2 V_i - \alpha_{ij}{}^* \alpha_{ji} V_j)\, Y_{ij} + (\alpha_{ij}^2 V_i) Y_i^0 \tag{A-24}$$

$$I_{ji} = (\alpha_{ji}^2 V_j - \alpha_{ji}{}^* \alpha_{ij} V_i)\, Y_{ij} + (\alpha_{ji}^2 V_j) Y_j^0 \tag{A-25}$$

$$S_{ij} = V_i I_{ij}^* = \alpha_{ij}^2 V_i^2 \left(Y_{ij} + Y_i^0\right)^* - \alpha_{ij}{}^* \alpha_{ji} V_i Y_{ij}^* V_j^* \tag{A-26}$$

$$S_{ji} = V_j I_{ji}^* = \alpha_{ji}^2 V_j^2 \left(Y_{ij} + Y_j^0\right)^* - \alpha_{ji}{}^* \alpha_{ij} V_j Y_{ij}^* V_i^* \tag{A-27}$$

$$\begin{aligned} S_{Loss} &= S_{ij} + S_{ji} \\ &= \alpha_{ij}^2 V_i^2 \left(Y_{ij} + Y_i^0\right)^* - \alpha_{ij}{}^* \alpha_{ji} V_i Y_{ij}^* V_j^* + \alpha_{ji}^2 V_j^2 \left(Y_{ij} + Y_j^0\right)^* \\ &\quad - \alpha_{ji}{}^* \alpha_{ij} V_j Y_{ij}^* V_i^* \end{aligned} \tag{A-28}$$

We know that,

$$Y_{ij} \triangleq G_{ij} + jB_{ij} \rightarrow Y_{ij}^* = G_{ij} - jB_{ij} \tag{A-29}$$

$$Y_i^0 \triangleq G_i^0 + jB_i^0, Y_j^0 \triangleq G_j^0 + jB_j^0 \tag{A-30}$$

$$for\ LTC\ voltage\ control: \alpha_{ij}{}^* = \alpha_{ij}, \alpha_{ji}^* = \alpha_{ji} \tag{A-31}$$

Finally, total active and reactive power loss of the system can be obtained when following notations were also considered:

$$G_{ij} = G_f,\ G_i^0 = G_{ij}^0,\ B_{ij} = B_f,\ B_i^0 = B_{ij}^0,\ G_j^0 = G_{ji}^0,\ B_j^0 = B_{ji}^0 \tag{A-32}$$

$$\sum_{f=1}^{F} P_{loss,f,t} = \sum_{f=1}^{F} \begin{Bmatrix} G_{f,t}\begin{bmatrix}(\alpha_{ij,t}V_{i,t})^2 + (\alpha_{ji,t}V_{j,t})^2 - \\ 2\alpha_{ij,t}V_{i,t}\alpha_{ji,t}V_{j,t}\cos\theta_{ij,t}\end{bmatrix} \\ +G_{ij,t}^0(\alpha_{ij,t}V_{i,t})^2 + G_{ji,t}^0(\alpha_{ji,t}V_{j,t})^2 \end{Bmatrix} \tag{A-33}$$

$$\sum_{f=1}^{F} Q_{loss,f,t} = \sum_{f=1}^{F} \begin{Bmatrix} -B_{f,t}\begin{bmatrix}(\alpha_{ij,t}V_{i,t})^2 + (\alpha_{ji,t}V_{j,t})^2 - \\ 2\alpha_{ij,t}V_{i,t}\alpha_{ji,t}V_{j,t}\cos\theta_{ij,t}\end{bmatrix} \\ -B_{ij,t}^0(\alpha_{ij,t}V_{i,t})^2 - B_{ji,t}^0(\alpha_{ji,t}V_{j,t})^2 \end{Bmatrix} \tag{A-34}$$

$$Y_{f,t} = G_{f,t} + jB_{f,t} \tag{A-35}$$

For transformer tap changer we know that,

$$I_{ij} = (\alpha_{ij}^2 V_i - \alpha_{ij}{}^*\alpha_{ji}V_j)\ Y_{ij} + (\alpha_{ij}^2 V_i)Y_i^0 \tag{A-36}$$

$$I_{ji} = (\alpha_{ji}^2 V_j - \alpha_{ji}{}^*\alpha_{ij}V_i)\ Y_{ij} + (\alpha_{ji}^2 V_j)Y_j^0 \tag{A-37}$$

$$Y_{BUS} = \begin{bmatrix} \alpha_{ij}^2(Y_{ij} + Y_i^0) & -\alpha_{ij}{}^*\alpha_{ji}Y_{ij} \\ -\alpha_{ji}{}^*\alpha_{ij}Y_{ij} & \alpha_{ji}^2(Y_{ij} + Y_j^0) \end{bmatrix} \tag{A-38}$$

The admittance matrix basically shows that:

$$If\ \ i \neq j \rightarrow g_{ij,t} + jb_{ij,t} = -\alpha_{ij}{}^*\alpha_{ji} \times Y_{ij} = -\alpha_{ij}\alpha_{ji} \times Y_{ij} \tag{A-39}$$

$$If\ \ i = j \rightarrow g_{ij,t} + jb_{ij,t} = \alpha_{ij}^2 \times (Y_{ij} + Y_{ij}^0) \tag{A-40}$$

If we write above formulation on all $i = j$ branches at each time stage, then the following equation is obtained:

$$g_{ij,t} + jb_{ij,t} = \begin{cases} \sum_{j \in J} \alpha_{ij,t}^2 \left(Y_{ij,t} + Y_{ij,t}^0\right) & i = j \\ -\alpha_{ij,t}\alpha_{ji,t}Y_{ij,t} & i \neq j \end{cases} \tag{A-41}$$

Based on ASNI Standard (C84.1-1995) voltage at each bus should be between following range:

$$V_{i,t}^{min} \leq V_{i,t} \leq V_{i,t}^{max} \xrightarrow{ANSI\ (C\ 84.1)} 0.95\ P.U \leq V_{ir,t} \leq 1.05\ P.U \quad \text{(A-42)}$$

It is known that each generating unit cannot generate power more or less than its capability. This fact can be obtained from “Capability Curve” of a generator which shows active and reactive power operating ranges. For instance a typical capability curve is presented in link below (Figure A. 4). Hence, the following constraints should be considered for each generating unit of the system. It should be mentioned that the minimum and maximum active or reactive power of generating units are known parameters inside optimization problem.

$$P_{i,t}^{min} \leq P_{i,t} \leq P_{i,t}^{max} \quad \text{(A-43)}$$

$$Q_{i,t}^{min} \leq Q_{i,t} \leq Q_{i,t}^{max} \quad \text{(A-44)}$$

$$P_{DGi,t}^{min} \leq P_{DGi,t} \leq P_{DGi,t}^{max} \quad \text{(A-45)}$$

$$Q_{DGi,t}^{min} \leq Q_{DGi,t} \leq Q_{DGi,t}^{max} \quad \text{(A-46)}$$

For active and reactive power balance constraints, it is possible to derive their equations via power flow relations as follows:

$$S_i = V_i I_i^* \quad \text{(A-47)}$$

$$I_i = \sum_{j=1}^{J} Y_{ij} V_j \rightarrow S_i = V_i (\sum_{j=1}^{J} Y_{ij} V_j)^* = V_i \sum_{j=1}^{J} {Y_{ij}}^* {V_j}^* \quad \text{(A-48)}$$

$$V_i = |V_i| \angle \theta_i\ ,\ \ Y_{ij} \triangleq G_{ij} + jB_{ij} \rightarrow Y_{ij}^* = G_{ij} - jB_{ij} \quad \text{(A-49)}$$

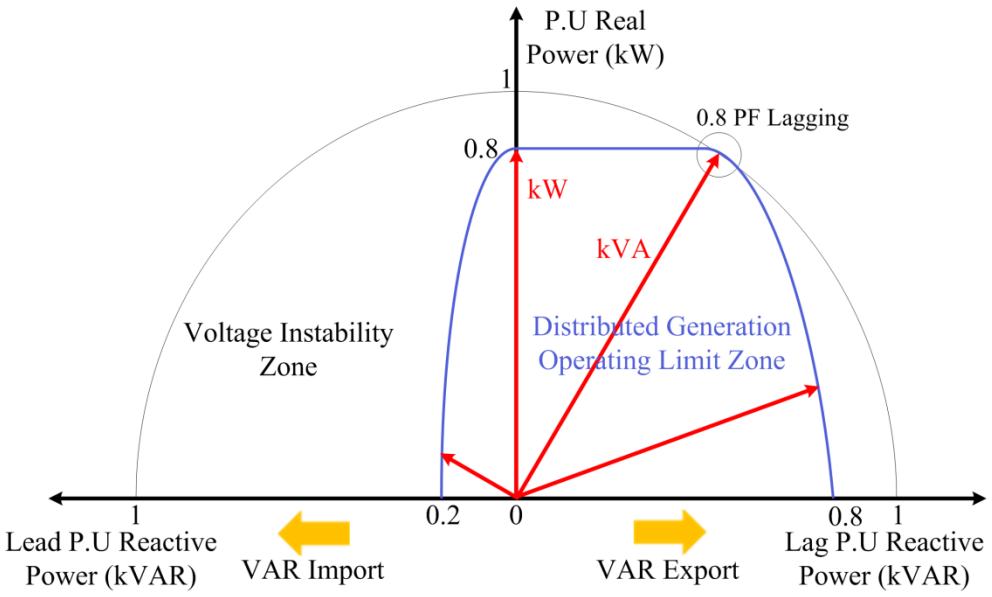

Figure A. 4. Common capability curve of a generator

$$\Rightarrow S_i = (|V_i|\angle\theta_i)\ \sum_{j=1}^{J}(G_{ij} - jB_{ij})(|V_j|\angle - \theta_j) = \sum_{j=1}^{J}(|V_i|\angle\theta_i)(|V_j|\angle - \theta_j)(\ G_{ij} - jB_{ij}) = \sum_{j=1}^{J}(|V_i||V_j|\ \angle(\theta_i - \theta_j))(\ G_{ij} - jB_{ij}) \quad \text{(A-50)}$$

From Euler relation, a phasor can be expressed as:

$$V_i = |V_i|\angle\theta_i = |V_i|(cos\ \theta_i + j\ sin\ \theta_i) \quad \text{(A-51)}$$

Thus,

$$S_i = \sum_{j=1}^{J}|V_i||V_j|(\ cos(\theta_i - \theta_j) + j\ sin(\theta_i - \theta_j))(\ G_{ij} - jB_{ij}) \quad \text{(A-52)}$$

It is also known that,

$$S_i = P_i + jQ_i \quad , (\theta_i - \theta_j) = \theta_{ij}, j \in J = (i + \sigma_i) \quad \text{(A-53)}$$

Hence, the final active and reactive power equations can be obtained:

$$P_i = \sum_{j=1}^{J}|V_i||V_j|[G_{ij}\ cos\ \theta_{ij} + B_{ij} sin\ \theta_{ij}] \quad \text{(A-54)}$$

$$Q_i = \sum_{j=1}^{J} |V_i||V_j|\left[G_{ij} sin\,\theta_{ij} - B_{ij}\, cos\,\theta_{ij}\right] \quad \text{(A-55)}$$

Therefore, for all system nodes at each time stage-*t*:

$$P_{i,t} = P_{Gi,t} - P_{Li,t} = \sum_{j}^{J} V_{i,t}V_{j,t}(g_{ij,t}\cos\theta_{ij,t} + b_{ij,t}\sin\theta_{ij,t}) \quad \text{(A-56)}$$

$$Q_{i,t} = Q_{Gi,t} - Q_{Li,t} = \sum_{j}^{J} V_{i,t}V_{j,t}(g_{ij,t}\sin\theta_{ij,t} - b_{ij,t}\cos\theta_{ij,t}) \quad \text{(A-57)}$$

For power factor constraint, it is possible to derive power factor from "Power Triangle" (Figure A. 1) as well:

$$\cos\theta = \frac{Active\ Power\ (kW)}{Apparent\ Power\ (kVA)} = \frac{P}{S} = Power\ Factor = PF \quad \text{(A-58)}$$

According to system power flow, each node of the system has specific power factor. It is possible to define a desired range (minimum/maximum) for specific buses of network in order to track their efficiency with desired range:

$$PF_{i,t}^{min} \leq \left|PF_{i,t}\right| \leq PF_{i,t}^{max} \quad \text{(A-59)}$$

Each feeder branch (distribution line) has a maximum thermal (power) loading limits that should be considered. A line cannot transmit power more than its maximum thermal loading because of its physical limitation.

$$S_{f,t} \leq S_{f,t}^{max} \quad \text{(A-60)}$$

In order to calculate transformer tap-changer and voltage regulator constraints, it is possible to use following relation:

$$\gamma_{tr,t} = 1 + tap_{tr,t}\frac{\Delta V_{tr,t}}{100} = \text{Turn ratio of OLTC} \quad \text{(A-61)}$$

$$\gamma_{vr,t} = 1 + tap_{vr,t}\frac{\Delta V_{vr,t}}{100} = \text{Turn ratio of VR} \quad \text{(A-62)}$$

Where,

$$tap_{tr,t} \in \left\{-tap_{tr,t}{}^{max}, \dots, -1, 0, 1, \dots, tap_{tr,t}{}^{max}\right\} \quad \text{(A-63)}$$

$$tap_{vr,t} \in \left\{-tap_{vr,t}{}^{max}, \dots, -1, 0, 1, \dots, tap_{vr,t}{}^{max}\right\} \quad \text{(A-64)}$$

For instance, if we have a VR with 17 taps (one tap is 0), $\Delta V_{vr,t} = \%0.625$:

$16\ \text{Tap steps from } 0.95 \text{ to } 1.05 \rightarrow \frac{0.1}{16} = 0.00625 \text{ or } = \%0.625$

Then, as an example, for a full turn ratio:

$\gamma_{vr,t} = 1 + 8(0.00625) = 1.05$

Moreover, maximum number of OLTC and/or VR switching can be considered through below formulations. These maximum values are known in optimization problem.

$$\sum_{t=1}^{T} N_{tr,t} \leq N_{max\ tr,t} \quad \text{(A-65)}$$

$$\sum_{t=1}^{T} N_{vr,t}^{i} \leq N_{max\ vr,t}^{i} \quad \text{(A-66)}$$

For capacitor bank constraint, it is possible to consider each CB with $\beta_{c,t}^{max}$ banks such that each bank has $\Delta q_{c,t}^{i}$ kVAr capacity:

$$Q_{c,t}^{i} = \beta_{c,t}^{i} \Delta q_{c,t}^{i}, \quad \beta_{c,t}^{i} = \left\{0,1,2, \dots, \beta_{c,t}^{max}\right\} \quad \text{(A-67)}$$

The following constraint added in order to meet the reactive power demand such that the total reactive power provided by capacitor banks does not exceed the required reactive power of the system.

$$\sum_{i=1}^{I} Q_{c,t}^{i} \leq \sum_{i=1}^{I} Q_{L,t}^{i} \quad \text{(A-68)}$$

Appendix B.

Benders Decomposition: Simple Mathematical Example

In order to understand benders decomposition technique better, a simple example is explained here. The objective function of the first example is:

$$Min\ (x + y) \tag{B-1}$$

$$s.t. \qquad 3x + y \geq 4 \tag{B-2}$$

$$x \geq 0,\ y \in \{-8, -7, \dots, 7, 8\} \tag{B-3}$$

$$c^T = [1],\ d^T = [1],\ E = [2],\ F = [1],\ h = [3] \tag{B-4}$$

Here is benders decomposition solution for the abovementioned problem:
*Iteration-1
Master Problem-1

$$Min\ \ Z_{lower} \tag{B-5}$$

$$s.t. \qquad Z_{lower} \geq y \quad y \in \{-8, -7, \dots, 7, 8\} \tag{B-6}$$

$$\rightarrow \quad Z_{lower} = -8 \quad when\ \hat{y} = -8 \tag{B-7}$$

Slave Problem-1

$$Min\ x \tag{B-8}$$

$$s.t. \qquad 3x \geq 4 - \hat{y}, \quad x \geq 0 \tag{B-9}$$

or Slave Probem-2

$$Max(4 - \hat{y})u \tag{B-10}$$

$$3u \leq 1, \quad u \geq 0 \tag{B-11}$$

$$\hat{y} = -8 \rightarrow \quad Max\ 12u \tag{B-12}$$

$$3u \leq 1, \quad u \geq 0 \tag{B-13}$$

$$\rightarrow u = \frac{1}{3} \rightarrow Z_{upper} = \hat{y} + \left(12 \times \frac{1}{3}\right) = -4 \tag{B-14}$$

$$\left|Z_{upper} - Z_{lower}\right| > \varepsilon \tag{B-15}$$

*Iteration-2
Master Problem-2
Benders Cut:

$$Z_{lower} = y + (4 - y) \times \frac{1}{3} \tag{B-16}$$

$$Min \ \ Z_{lower} \tag{B-17}$$

$$s.t. \ \ Z_{lower} \geq y + \left(4 - (-8)\right)\frac{1}{3} \rightarrow \ \ Z_{lower} \geq -4 \ \ for\ \hat{y} = -8 \tag{B-18}$$

Slave Problem-1 or Slave Problem-2:

$$Max(4 - \hat{y})u \qquad \hat{y} = -8 \rightarrow Max\ 12u \tag{B-19}$$

$$3u \leq 1, \quad u \geq 0 \tag{B-20}$$

$$u = \frac{1}{3} \rightarrow Z_{upper} = -8 + 4 = -4 \tag{B-21}$$

$$Z_{upper} = Z_{lower} = -4 \tag{B-22}$$

Therefore,

$$\left|Z_{upper} - Z_{lower}\right| < \varepsilon \rightarrow \text{Converged} \tag{B-23}$$

Appendix C.

Review of Backward Forward Sweep Technique

Generally speaking, Backward Forward Sweep (BFS) power flow is one of the most applicable power flow techniques is radial distribution networks. As in distribution networks, the ratio of resistance and inductance is not less than 1 ($\frac{R}{X} \lessapprox 1$), Newton-Raphson technique convergence decreases in distribution networks. Thus, BFS technique could be a better approach than other conventional power flow techniques. The figures and formulations of this appendix derived from the following references: (a) R. D. Zimmerman, Comprehensive Distribution Power Flow: Modeling, Formulation, Solution Algorithms and Analysis, Cornell University, Jan. 1995. (b) A. Alsaadi, B. Gholami, An Effective Approach for Distribution System Power Flow Solution, World Academy of Science, Engineering and Technology Vol:3 2009-01-23.

BFS technique can be summarizes through the following steps:

1. K=0 (K: iteration)
2. Initial guess for node voltages
3. K= K+1
4. By knowing load models and node voltages, we calculate node currents
5. By knowing node currents, we calculate branch currents (backward)
6. By knowing source voltage and branch currents, we calculate node voltages (forward)
7. Check the convergence rate satisfied or not. If yes, done. If no, back to step-3. (Convergence tolerance: when the difference of node voltage in two iteration is less than epsilon)

In order to assess the formulations of BFS technique, Figure C. 1 depicts a three-phase four-wired system. It is possible to write self and mutual impedances of this system as follows:

$$[Z_{abcn}] = \begin{bmatrix} Z_a & Z_{ab} & Z_{ac} & Z_{an} \\ Z_{ba} & Z_b & Z_{bc} & Z_{bn} \\ Z_{ca} & Z_{cb} & Z_c & Z_{cn} \\ Z_{na} & Z_{nb} & Z_{nc} & Z_n \end{bmatrix} \quad \text{(C-1)}$$

For a balanced system, It is possible to assume the voltage of neutral wire equal to zero. Then, it is possible to use the following impedance matrix instead of the above impedance matrix:

$$[Z_{abc}] = \begin{bmatrix} Z_{an} & Z_{abn} & Z_{acn} \\ Z_{ban} & Z_{bn} & Z_{bcn} \\ Z_{can} & Z_{cbn} & Z_{cn} \end{bmatrix} \tag{C-2}$$

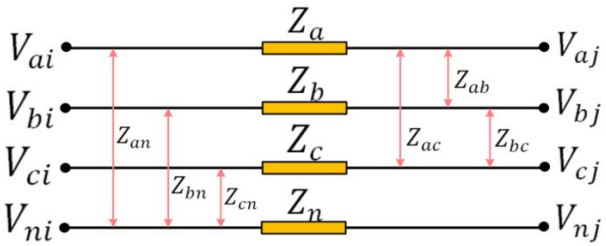

Figure C. 1. Three-phase four-wired system

In order to obtain the relations between node voltages and branch currents, the following equation can be written:

$$\begin{bmatrix} V_{aj} \\ V_{bj} \\ V_{cj} \end{bmatrix} = \begin{bmatrix} V_{ai} \\ V_{bi} \\ V_{ci} \end{bmatrix} - \begin{bmatrix} Z_{an} & Z_{abn} & Z_{acn} \\ Z_{ban} & Z_{bn} & Z_{bcn} \\ Z_{can} & Z_{cbn} & Z_{cn} \end{bmatrix} \begin{bmatrix} I_a \\ I_b \\ I_c \end{bmatrix} \tag{C-3}$$

In distribution network, models can be based on injected current equations. As such, it is possible to calculate the apparent power of node-n of the system as follows:

$$S_n = (P_n + jQ_n) \qquad n = 1, 2, \dots, N \tag{C-4}$$

In order to calculate the injected current to node-*n* at iteration-*k*, the following formulation can be used:

$$I_n^k = I_{n(V_n^k)}^{real} + jI_{n(V_n^k)}^{imag} = \left(\frac{P_n + jQ_n}{V_n^k}\right)^* \tag{C-5}$$

Here, V_n^k is the voltage of node-*n* at iteration-*k*. Figure C. 2 presents a typical branch model in radial distribution networks. According to Figure C. 2, active and reactive powers of node-*n* can be simply found:

$$P_n = P_{DG-n} - P_{L-n}\,, \quad Q_n = Q_{DG-n} - Q_{L-n} + Q_{CB-n} \tag{C-6}$$

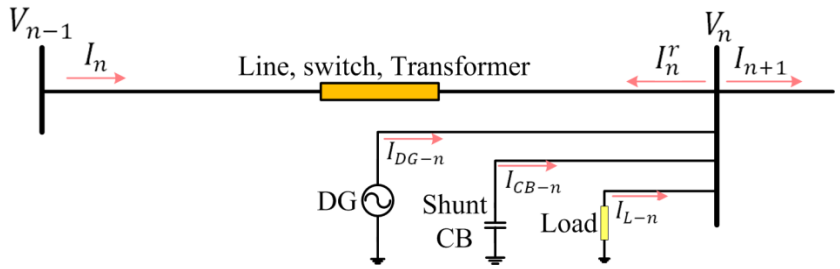

Figure C. 2. Typical branch model of in radial distribution system

Typically, distribution networks loads are modeled as constant-power, constant-current and constant-impedance. If the load model is constant-power or impedance-power, by changing the voltages of loads, the currents of them are changed as well. Hence, the load current can be found by load voltage. When:

$$S_{L-n} = \begin{bmatrix} S_{L-n}^a \\ S_{L-n}^b \\ S_{L-n}^c \end{bmatrix} \quad \& \; V_n = \begin{bmatrix} V_n^a \\ V_n^b \\ V_n^c \end{bmatrix} \tag{C-7}$$

For constant-power, constant-current and constant-impedance loads with Wye grounded connection, the currents of node-*n* can be found respectively by:

$$Constant - P \;\&\; I\; Wye: I_{L-n} = (\frac{S_{L-n}}{V_n})^* \tag{C-8}$$

$$Constant - Z\; Wye: I_{L-n} = (\frac{S_{L-n}^*}{|V_n|^2}) \times V_n \tag{C-9}$$

For constant-power, constant-current and constant-impedance loads with ungrounded delta connection, the currents of node-*n* can be found respectively by:

$$Constant - P\; delta: I_{L-n} = (\gamma^T \times (\frac{S_{L-n}}{V_n}))^* \tag{C-10}$$

$$Constant - I\; delta: I_{L-n} = \gamma^T \times I_{L-n} \tag{C-11}$$

Where,

$$\gamma = \begin{bmatrix} 1 & -1 & 0 \\ 0 & 1 & -1 \\ -1 & 0 & 1 \end{bmatrix} \tag{C-12}$$

$$Constant - Z\ delta: I_{L-n} = (Y_{L-n}) \times V_n \tag{C-13}$$

$$Y_{L-n} = \begin{bmatrix} y_{L-n}^{ca} + y_{L-n}^{ab} & -y_{L-n}^{ab} & -y_{L-n}^{ca} \\ -y_{L-n}^{ab} & y_{L-n}^{ab} + y_{L-n}^{bc} & -y_{L-n}^{bc} \\ -y_{L-n}^{ca} & -y_{L-n}^{bc} & y_{L-n}^{bc} + y_{L-n}^{ca} \end{bmatrix} \tag{C-14}$$

For a ZIP load model, it is possible to use the following equations in order to find the active and relative power of loads:

$$P_n = P_{0_n}(Z_p(\frac{V_n}{V_{0_n}})^2 + I_p(\frac{V_n}{V_{0_n}}) + P_p) \tag{C-15}$$

$$Q_n = Q_{0_n}(Z_q(\frac{V_n}{V_{0_n}})^2 + I_q(\frac{V_n}{V_{0_n}}) + P_q) \tag{C-16}$$

For shunt CB model, it is possible to find node current though the following equations:

When we have: $V_n = \begin{bmatrix} V_n^a \\ V_n^b \\ V_n^c \end{bmatrix}$ and $y_{CB-n} = j(\frac{Q_{CB-n}}{|V_n|^2})$

$$I_{CB-n} = -Y_{CB-n} \times V_n \tag{C-17}$$

$$For\ Wye\ Grounded: \quad Y_{CB-n} = \begin{bmatrix} y_{CB-n}^a & 0 & 0 \\ 0 & y_{CB-n}^b & 0 \\ 0 & 0 & y_{CB-n}^c \end{bmatrix} \tag{C-18}$$

$$For\ delta\ Ungrounded: \quad Y_{CB-n} = \begin{bmatrix} y_{CB-n}^{ca} + y_{CB-n}^{ab} & y_{CB-n}^{ca} \\ -y_{CB-n}^{ab} & y_{CB-n}^{bc} \end{bmatrix} \tag{C-19}$$

Moreover, for DG units, the following equations can be used for node current calculation:

When we have: $V_n = \begin{bmatrix} V_n^a \\ V_n^b \\ V_n^c \end{bmatrix}$

$$For\ Wye\ Grounded: \quad I_{DG-n} = (\frac{S_{DG-n}}{V_n})^* \tag{C-20}$$

When we have: $V_n = \begin{bmatrix} V_n^{ab} \\ V_n^{bc} \end{bmatrix}$

$$For\ delta\ Ungrounded: \quad I_{DG-n} = \begin{bmatrix} \frac{-S_{DG-n}^{ca}}{V_{DG-n}^{ab} + V_{DG-n}^{bc}} - \frac{S_{DG-n}^{ab}}{V_{DG-n}^{ab}} \\ \frac{S_{DG-n}^{ab}}{V_{DG-n}^{ab}} - \frac{S_{DG-n}^{bc}}{V_{DG-n}^{bc}} \end{bmatrix} \tag{C-21}$$

For distribution line model with series impedance and shunt capacitances (Figure C. 3), the following formulations can be utilized for backward and forward voltage and current calculations:

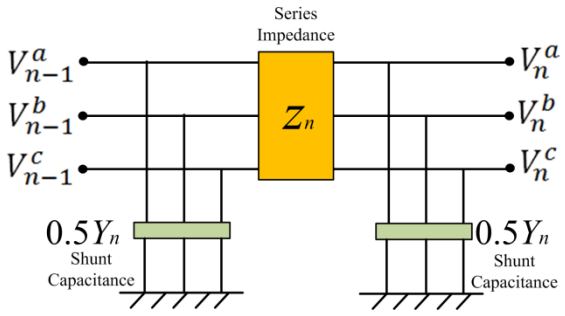

Figure C. 3. Distributed line model

For backward:

$$V_{n-1} = V_n + Z_n(\frac{1}{2}Y_nV_n - I_n^r) \tag{C-22}$$

$$I_n = \frac{1}{2}Y_n(V_n + V_{n-1}) - I_n^r \tag{C-23}$$

For forward:

$$V_n = V_{n-1} + Z_n(\frac{1}{2}Y_nV_{n-1} - I_n) \tag{C-24}$$

$$I_n^r = \frac{1}{2}Y_n(V_n + V_{n-1}) - I_n \tag{C-25}$$

In order to find phase and line current calculations, the following equations can be used:

$$\begin{bmatrix} I_n^a \\ I_n^b \\ I_n^c \end{bmatrix} = Z_{n-phase} \begin{bmatrix} V_n^a \\ V_n^b \\ V_n^c \end{bmatrix} - \begin{bmatrix} V_{n-1}^a \\ V_{n-1}^b \\ V_{n-1}^c \end{bmatrix} \quad \text{(C-26)}$$

$$\begin{bmatrix} I_n^a \\ I_n^b \end{bmatrix} = Z_{n-line} \begin{bmatrix} V_n^{ab} \\ V_n^{bc} \end{bmatrix} - \begin{bmatrix} V_{n-1}^{ab} \\ V_{n-1}^{bc} \end{bmatrix} \quad \text{(C-27)}$$

$$Z_{n-line} = \begin{bmatrix} 1 & -1 & 0 \\ 0 & 1 & -1 \end{bmatrix} \frac{1}{3} Z_{n-phase} \begin{bmatrix} 1 & 0 \\ 0 & 1 \\ -1 & -1 \end{bmatrix} \quad \text{(C-28)}$$

If a breaker and/or switch exist between lines, the following equations calculate voltages and currents on node-*n* in backward and forward steps:
For backward:

$$V_{n-1} = V_n,\ I_n = -I_n^r \quad \text{(C-29)}$$

For forward:

$$V_n = V_{n-1},\ I_n^r = -I_n \quad \text{(C-30)}$$

If there is a transformer or VR within the line, the following equations calculate the voltage and current of node-*n*:
For backward:

$$V_{n-1} = (Z_n^{SP}) \times (I_n^r - Y_n^{SS} V_n) \quad \text{(C-31)}$$

$$I_n = Y_n^{PP} V_{n-1} + Y_n^{PS} V_n \quad \text{(C-32)}$$

For forward:

$$V_n = (Z_n^{PS}) \times (I_n - Y_n^{PP} V_{n-1}) \quad \text{(C-33)}$$

$$I_n^r = Y_n^{SP} V_{n-1} + Y_n^{SS} V_n \quad \text{(C-34)}$$

As it is known, each transformer can have specific winding. Here as an example. The admittance matrices of a grounded Wye-Wye connection are presented:

$$Y_{trans-n} = \begin{bmatrix} Y_n^{PP} & Y_n^{PS} \\ Y_n^{SP} & Y_n^{SS} \end{bmatrix} = \begin{bmatrix} \frac{y_n}{\alpha_n^2} \times I & -\frac{y_n}{\alpha_n \beta_n} \times I \\ -\frac{y_n}{\alpha_n \beta_n} \times I & \frac{y_n}{\beta_n^2} \times I \end{bmatrix} \quad \text{(C-35)}$$

$$I = \begin{bmatrix} 1 & 0 & 0 \\ 0 & 1 & 0 \\ 0 & 0 & 1 \end{bmatrix} \quad \text{(C-36)}$$

Here, $\alpha_n$denotes transformer primary tap and $\beta_n$denotes transformer secondary tap.
As explained, BFS considers node voltages equal to source voltage in order to calculate current of each node of the system in first step. Then, it calculated branch currents based on Kirchoff's Current Law (KCL). It is possible to represent injected currents into branches through a matrix called BIBC (Bus Injection to Branch Current) which has only 0 and 1 elements. Hence, the BIBC matrix would be a m*(n-1) matrix with m-branches and n-nodes. Matrix [I] denotes node current matrix.

$$[B] = [BIBC][I] \quad \text{(C-37)}$$

Here, matrix [B] presents how feeder branches are connected to each other. Hence, it is possible to calculate branch currents in backward mode. Next, BFS has to calculate node voltages based on branch currents branch impedances. It is possible to write node voltages as a function of branch currents, branch impedances and voltage of the source. Hence, BCBV (Branch Current to Bus Voltage) matrix can be obtained.

$$[V_n] = [V_1] - [BCBV][B] \quad \text{(C-38)}$$

the BCBV matrix would be a (n-1)*m matrix with m-branches and n-nodes. Thus, the voltages of all nodes of the system obtain in forward mode. By putting [B] formulation inside the above equation we have:

$$[V_n] = [V_1] - [BCBV][BIBC][I] = [V_1] - [DLF][I] \quad \text{(C-39)}$$

As we have:

$$I_n^k = I_{n(V_n^k)}^{real} + jI_{n(V_n^k)}^{imag} = (\frac{P_n + jQ_n}{V_n^k})^* \quad \text{(C-40)}$$

Then,

$$V_n^{k+1} = [V_1] - [DLF][I_n^k] \quad \text{(C-41)}$$

As BFS technique does not need to calculate Jacobian and inverse admittance matrices, it decreases time-consuming computational calculations. Hence, BFS could be a better power flow solution for online applications.

In order to calculate transformer loss, load flow calculations has to be performed. When performing load flow calculation for transformer loss, an overhead line is defined using sequence impedance (Positive sequence: Z_1 and zero sequence: Z_0) based on the (C-42) and (C-43) formulations to convert impedances to phase domain.

$$Z_s = \frac{1}{3}(Z_0 + 2Z_1) \tag{C-42}$$

$$Z_m = \frac{1}{3}(Z_0 - Z_1) \tag{C-43}$$

Then, we construct the 3x3 matrix impedance (matrix Z) for phase domain calculation. For copper losses, it is possible to compute the total loss through the difference between the power at the input and the power at the output of transformer after computing the load flow:

$$P_{copper-loss} = (V_{\text{input}} - V_{\text{output}})\bar{I} \tag{C-44}$$

For transformer total loss, we can use:

$$P_{trans-loss} = \left|R(Z).I_{input}^2\right| \tag{C-45}$$

It is possible to use an equivalent shunt resistance for modeling no-load loss. Mostly, the no-load loss is given to the problem in kW. Hence, we need to transform this kW to an equivalent resistance base on nominal power of the transformer. For example, for a distribution center tap transformer, the no-load equivalent shunt resistant is located before series resistance and reactance of transformer primary side.

Typically, losses in transformers vary with load current, and may be expressed as "no-load" or "full-load" losses. Winding resistance creates load losses, and hysteresis and eddy current losses create over 99% of no-load loss. Transformer losses can be summarized into two losses: first loss is according to transformer windings or copper loss, and the other is in the magnetic circuit, called iron loss or core loss. Hence, the main losses in a transformer are: Dielectric loss, Hysteresis losses in the core, Eddy current (Foucault) losses in the core and resistive losses (copper loss) in the conductors. Dielectric loss occurs due to electrostatic stress of transformer insulation. It is typically proportional to the developed high voltage, the type and the thickness of insulation. It varies with frequency. Normally, it is very small in amount and is quite constant. Thus, this loss can be ignored in medium voltage transformers. Regarding the Hysteresis loss in the core, each time the magnetic field reverses (because of the AC current), a small amount of energy is lost due to hysteresis within the core. Hence, a considerable amount of no-load loss is hysteresis loss. Regarding eddy current (Foucault) losses in the core, it is possible to state that ferromagnetic materials are good conductors and a core made from such a material makes a single short-circuited turn throughout its length. Therefore, eddy currents circulate in the core and they can cause resistive heating of the material of the core. Eddy current losses can be reduced by insulating the core of a stack of plates

electrically from each other. That is the reason almost all transformers that are operating in low frequencies employ laminated cores.

Regarding resistive losses (copper loss) in transformer windings, these losses illustrate load dependent variable losses, that can be shown as I^2R. They vary by the square of the current in the windings and by D.C. resistance of winding. In turn, the resistance varies with the resistivity, the size of line/cable, and the temperature. In addition, these losses change with winding temperature. Hence, the loss can be different in different loading and different methods of cooling.

At CVR point of view, transformer loss highly depends on two main factors: imposed voltage to the transformer and transformer magnetizing characteristics which is related to the transformer magnetizing current. Assume that we reduce voltage of the customers using some voltage control devices on the secondary side of a transformer. This does not mean that the imposed voltage to the core is reduced because transformer effective voltage has to be imposed from its primary side. Thus, from Foucault loss viewpoint, there is no change at the core, but when the secondary voltage reduces the load behavior would then be the factor that can affect transformer current. This includes hysteresis loss of the transformer and it highly depends on the load characteristics. If the load be as a constant$cos\varphi$, by reducing the secondary voltage, the current will be reduced (almost, not always). Therefore, the transformer loss will be reduced too. Assume that we reduce voltage of the customers applying voltage control devices on the primary side of a pole-mounted transformer: $V^2 \propto Foucault\ Loss$. Thus, the transformer loss will be reduced. In conclusion, by increasing transformer voltage, the transformer loss will be increased too. It is possible to use the following formulation for calculating Foucault and eddy current losses:

$$P_f = \left(\frac{W^2}{12\ r\ N^2 S^2}\right) \times V^2 \qquad \text{(C-46)}$$

Where, *W* is Iron thickness of the core, *r* is resistivity of the core and *S* is core cross section. For Hysteresis loss model:

$$P_h = Vol\ (fe) \times f \times K_h \times {B_{max}}^{1.6} \qquad \text{(C-47)}$$

Where, *Vol (fe)* is the volume of the core, *f* is frequency, K_h is Hysteresis constant coefficient and$B_{max}$is magnetic field. Therefore:

$$P_{Transformer\ Core} = P_f + P_h \qquad \text{(C-48)}$$

For analyzing transformer core loss in more accurate way, the Frequency should be considered as well. If we manipulate the voltage in a way that we bring the core out of its linear area, the transformer will start to generate flickers and harmonics. At this time, the voltage frequency spectrum and the core current has to be studied. If we reduce the voltage, we will not have harmonic issue because, the core condition will improve but if we increase the voltage, then the harmonics can be generated (hysteresis has direct relation to the frequency). Based on the Ferranti effect, if the inductive loads of the network, reduce in some operating time (mostly at night) it leads to have more capacitive lines which increase the voltage at the end of line. In these times, the transformers operate

with a buzz-like sound. This sound shows that the transformer core loss becomes high in these operating times. Core loss profile for distribution transformers can be found in: http://www.powersystem.org/docs/publications/c1-triplett2010-[compatibility-mode].pdf
As stated, copper loss is related to the resistance of the windings and the square of transformer current based on (C-45). This loss depends on transformer loading. An increase in loading, either real or reactive, will result in an increase in current flow and a correspondingly greater amount of loss in the transformer. Total loss of transformer can be found by (C-49). Core loss profile of different distribution transformer can be found in: http://ecmweb.com/contractor/overcoming-transformer-losses

$$P_{Transformer\ Loss} = P_f + P_h + P_{cu} \qquad \text{(C-49)}$$

Appendix D.

List of Publications and Awards

The list of accepted/submitted journal papers is as follows:

1- M. Manbachi, M. Nasri, B. Shahabi, H. Farhangi, A. Palizban, S. Arzanpour, M. Moallem, D. Lee, "Real-Time Adaptive VVO/CVR Topology Using Multi Agent System and IEC 61850-Based Communication Protocol," *IEEE Transactions on Sustainable Energy*, vol. 5, no. 2, pp. 587-597, October 2013.
2- M. Manbachi, H. Farhangi, A. Palizban, S. Arzanpour, "Quasi Real-Time ZIP Load Modeling for Conservation Voltage Reduction of Smart Distribution Networks using Disaggregated AMI Data," *Accepted and Published Online in Sustainable Cities and Society Journal*, June 2015.
3- M. Manbachi, H. Farhangi, A. Palizban, S. Arzanpour, "Volt-VAR Optimization of Smart Distribution Networks utilizing Vehicle to Grid Dispatch," *Accepted and Published Online in International Journal of Electrical Power and Energy Systems*, July 2015.
4- M. Manbachi, H. Farhangi, A. Palizban, S. Arzanpour, "A Novel Approach for Maintenance Scheduling of Volt-VAR Control Assets in Smart Distribution Networks," *Accepted in Canadian Journal of Electrical and Computer Engineering*, March 2015.
5- M. Manbachi, H. Farhangi, A. Palizban, S. Arzanpour, "Smart Grid Adaptive Volt-VAR Optimization Engine utilizing Particle Swarm Optimization and Fuzzification," *submitted to Applied Energy Journal*, May 2015.
6- M. Manbachi, H. Farhangi, A. Palizban, S. Arzanpour, "Conservation Voltage Reduction Plans of the Future," *submitted to The Electricity Journal*, May 2015.
7- M. Manbachi, H. Farhangi, A. Palizban, S. Arzanpour, "Impact of Micro-CHP/PV Penetrations on Smart Grid Adaptive Volt-VAR Optimization of Distribution Networks using AMI data," *submitted to IEEE Transactions on Power Delivery*, June 2015.
8- M. Manbachi, A. Sadu, H. Farhangi, A. Monti, A. Palizban, F. Ponci, S. Arzanpour, "Real-Time Co-Simulation Monitoring and Control Platform for AMI-based Volt-VAR Optimization of Smart Distribution Networks," *submitted to IEEE Transactions on Power Delivery*, June 2015.
9- M. Manbachi, A. Sadu, H. Farhangi, A. Monti, A. Palizban, F. Ponci, S. Arzanpour, "Real Time Co-Simulation Platform for Smart Grid-based Volt-VAR Optimization using IEC 61850 MMS and GOOSE Messaging," *submitted to IEEE Transactions on Industrial Informatics*, June 2015.
10- M. Manbachi, H. Farhangi, A. Palizban, S. Arzanpour, "Impact of EV Penetration on Volt-VAR Optimization of Distribution Networks using Real-Time Co-Simulation Monitoring Platform," *submitted to Applied Energy Journal*, Aug. 2015.

The list of conference papers is as follows:

11- M. Manbachi, A. Sadu, H. Farhangi, A. Monti, A. Palizban, F. Ponci, S. Arzanpour, “Real-Time Communication Platform for Smart Grid Adaptive Volt-VAR Optimization of Distribution Networks,” *Accepted in IEEE International Conference on Smart Energy Grid Engineering*, May 2015.
12- M. Manbachi, A. Sadu, H. Farhangi, A. Monti, A. Palizban, F. Ponci, S. Arzanpour, “Real-Time Co-Simulated Platform for Novel Volt-VAR Optimization of Smart Distribution Network using AMI Data,” *Accepted in IEEE International Conference on Smart Energy Grid Engineering*, May 2015.
13- M. Manbachi, H. Farhangi, A. Palizban, S. Arzanpour, “Real-Time Co-Simulated Platform for Energy Conservation of Smart Distribution Network using AMI-based VVO Engine,” *Accepted in 2015 CIGRE Canada Conference*, April 2015.
14- M. Manbachi, H. Farhangi, A. Palizban, S. Arzanpour, A Novel Predictive Volt-VAR Optimization Engine for Smart Distribution Systems, in *Proc. 2014 CIGRÉ Canada Conference*, Toronto, Sept. 2014.
15- M. Manbachi, H. Farhangi, A. Palizban, S. Arzanpour, Predictive Algorithm for Volt/VAR Optimization of Distribution Networks Using Neural Networks, in *Proc. IEEE Canadian Conference on Electrical and Computer Engineering (CCECE2014)*, Toronto, Canada, May 2014.
16- M. Manbachi, H. Farhangi, A. Palizban, S. Arzanpour, “Impact of V2G on Real-time Adaptive Volt/VAr Optimization of Distribution Networks,” in *Proc. IEEE Electrical Power and Energy Conference (EPEC 2013)*, Halifax, Canada, August 2013.
17- M. Manbachi, B. Shahabi, H. Farhangi, A. Palizban, S. Arzanpour, D. C. Lee, “A Real-time Adaptive Volt-VAr Optimization Engine using Intelligent Agents and Narrow-Band Power Line Communication,” *accepted-poster at Utility Telecom Conference*, Vancouver, Canada, September 2012.
18- M. Manbachi, H. Farhangi, A. Palizban and S. Arzanpour, “Real-Time Adaptive Optimization Engine Algorithm for Integrated Volt/VAr Optimization and Conservation Voltage Reduction of Smart Microgrids,” in *Proc. CIGRÉ Canada Conference*, Montreal, Quebec, September 2012.

The list of awards is as follows:

1. Awarded 3rd best poster presentation at 3rd NSERC Smart Microgrid Annual General Meeting (AGM), Vancouver, BC, July 2013. Poster title: Smart Grid Adaptive Solution for Volt/VAR Optimization (VVO) of Distribution Networks Using VAR Dispatch.
2. Won best poster prize at 4th NSERC Smart Microgrid Annual General Meeting (AGM), Montreal, QC, September 2014. Poster title: A Novel Predictive Volt-VAR Optimization Engine for Smart Distribution Networks.
3. Best Student Paper Award at IEEE Smart Energy Grid Engineering Conference, Oshawa, ON, August 2015. Paper title: Real-Time Co-Simulated Platform for Novel Volt-VAR Optimization of Smart Distribution Network using AMI Data.